MRI Assessment of Neurovascular Changes in Idiopathic Parkinson's disease

A thesis submitted to
The University of Manchester
for the degree of
Doctor of Philosophy (PhD)
in the Faculty of Biology, Medicine and Health

2016

Sarah Al-Bachari

School of Biological Sciences

Neuroscience & Experimental Psychology

Contents

Final Word Count:

64351

List of Figures

List of Tables

Abbreviations

AAT – arterial arrival time

AD – Alzheimer's disease

AIF – arterial input function

AMB – aberrant motor behaviours

ASL – arterial spin labelling

BA - Brodmann area

BBB – blood-brain barrier

BG – basal ganglia

BOLD – blood oxygenation level dependent

CN – control negative

CNS – central nervous system

CO_2 - carbon dioxide

CP – control positive

CT - computer tomography

CV - cerebrovascular

CVD – cerebrovascular disease

CVR – cerebrovascular reactivity

CVR_{AAT} - cerebrovascular reactivity measures of arterial arrival time

CVR_{CBF} - cerebrovascular reactivity measures of cerebral blood flow

DA – dopamine

DCE MRI – dynamic contrast enhanced magnetic resonance imaging

DS - digit span

DSST - digit symbol substitution test

DTI - diffusion tensor imaging

DWMH - deep white matter hyperintensity

EPI - echo planar imaging

$ETCO_2$ – end-tidal carbon dioxide

FA - flip angle

FAS - (verbal) fluency assessment scale

FLAIR – fluid attenuation inversion recovery

fMRI - functional MRI

GM - grey matter

GML - gray matter lesion

HAM-D - Hamilton depression rating scale

Hct - haematocrit

H&Y – Hoehn and Yahr

IPD – idiopathic Parkinson's disease

k^{Tran} – transfer constant

LARS - Lille apathy rating scale

LB - Lewy body

L-dopa – levodopa

LEDD – levodopa equivilant score

LL - Look-Locker

LTH – Lancashire teaching hospitals

MAP – mean arterial pressure

MCA – middle cerebral artery

MCI - mild cognitive impairment

MDS – movement disorder society

MoCA - Montreal cognitive assessment

MPTP - 1-methyl-4-phenyl-1,2,3,6-tetrahydropyridine

MRI – magnetic resonance imaging

MRIF - University of Manchester MRI facility

NMS - non-motor symptoms

NO – nitric oxide

NPI - neuropsychiatric inventory

NVU - neurovascular unit

O_2 - oxygen

PD - Parkinson's disease

PDD - Parkinson's disease with dementia

PD-MCI - Parkinson's disease with mild cognitive impairment

PET - positron emission tomography

PIGD - postural instability and gait disorder

PRAGE – magnetisation prepared rapid gradient echo

PRoBaND - Parkinson's repository of biosamples and network datasets

PVH - periventricular hyperintensity

QUIPS - questionnaire for impulsive-compulsive disorders in Parkinson's

RF - risk factor

ROI - region of interest

ROS - reactive oxygen species

SCOPA-AUT - scales for outcomes in Parkinson's disease – autonomic

SN – substantia nigra

SNpc - substantia nigra pars compacta

SPECT – single positron emission computed tomography

SPM – statistical parametric mapping

SRFT – Salford royal foundation trust

STAR - signal targeting with alternating radiofrequency

STN – subthalamic nucleus

STR - striatum

SVD - small vessel disease

TCD – transcranial doppler

TD – tremor dominant

TE - echo time

3T – 3 Tesla

TIA – transient ischaemic attack

TMT- B - trail making test B

TR - repetition time

UKPDS BB – United Kingdom Parkinson's Disease Society Brain Bank

UOM – University of Manchester

UPDRS - unified Parkinson's disease rating scale

VMR – vasomotor reactivity

VBM – volume based morphometry

Vp – blood volume

WAIS-R - Wechsler adult intelligence scale-revised

WML – white matter lesion

WMV – white matter volume

WTCRF - Wellcome Trust Clinical Research Facility

Abstract

Idiopathic Parkinson's disease (IPD) is the second most common neurodegenerative disease, yet effective disease modifying treatments are still lacking. Neurodegeneration involves multiple interacting pathological pathways. The extent to which neurovascular mechanisms are involved in IPD is not well defined. Indeed within the umbrella term of IPD great heterogeneity of motor (and non-motor) features exists, suggesting that different phenotypes may have differing underlying pathophysiologies. We aimed to determine whether novel magnetic resonance imaging (MRI) techniques can reveal changes in structural or physiological neurovascular measures, herein also referred to as 'altered neurovascular status (NVS)', in IPD.

Based on preliminary data from our initial exploratory study in a small IPD cohort, phenotypic differences in structural and physiological MRI measures of NVS were investigated in a larger study. The 3 Tesla (3T) MRI protocol included T2-weighted fluid-attenuated inversion recovery (FLAIR) imaging to assess white matter lesion (WML) burden, arterial spin labelling (ASL) measurements of cerebral blood flow (CBF) and arterial arrival time (AAT) and dynamic contrast enhanced (DCE) measures of blood-brain barrier (BBB) integrity. Analysis was undertaken of IPD clinical phenotypes, by comparison with two control groups.

In total, fifty-one patients with IPD (mean age 69.0 ± 7.7 years) (21 tremor dominant [TD], 24 postural instability and gait disorder [PIGD] and 6 intermediates) were compared with 2 control groups, the first comprising 18 control positive (CP) subjects with a history of clinical cerebrovascular disease (CVD) (mean age 70.1 ± 8.0 years) and the second comprising 34 control negative (CN) subjects without a history of clinical CVD (mean age 67.4 ± 7.6 years).

IPD patients showed diffuse regions of significantly prolonged AAT and lower CBF by comparison with CN subjects, and a few regions of prolonged AAT by comparison with CP subjects, despite significantly fewer vascular risk factors. TD patients showed regions of significantly prolonged AAT and lower WML volume by comparison with PIGD patients. IPD patients also showed increased leakiness of the BBB in basal ganglia regions compared to the CN group, with a similar pattern in both IPD phenotypes.These data provide evidence of altered NVS in IPD, with IPD phenotype specific differences.

Institution: The University of Manchester
Candidate: Sarah Al-Bachari
Degree Title: Doctor of Philosophy
Thesis Title: MRI Assessment of Neurovascular Changes in Idiopathic Parkinson's disease
Date: August 2016

Declaration

No portion of the work referred to in the thesis has been submitted in support of an application for another degree or qualification of this or any other university or other institute of learning.

Copyright Statement

Alternative Format Statement (Based on the University of Manchester research office graduate education team guidelines, June 2014)

The University of Manchester allows for the submission of theses in alternative format i.e. for '*a postgraduate doctoral .. student to incorporate sections that are in a format suitable for submission for publication in a peer-reviewed journal'*. '*The same standards are expected for that of a standard thesis'. 'Materials included are solely and/or partly authored by the student and can include already published or submitted work'. 'The thesis must remain an original contribution to the field of research'.' Permission must be sought'* (see page 16).

The alternative format was selected for this PhD as it allows the author to focus on publishing work from the PhD whilst still ensuring a '*coherent and continuous'* thesis, supplemented by the chapters 1 and 6, introduction and discussion, respectively. Each chapter begins with the contribution of the thesis author, highlighting the fact the author played a substantive role in the study design, data collection, analysis, interpretation and write up of the paper.

PERMISSION TO SUBMIT A PHD THESIS IN ALTERNATIVE FORMAT

(SUITABLE FOR PUBLICATION OR DISSEMINATION)

We confirm that the following student in the Faculty of Medical and Human Sciences, has been granted permission by his/her supervisor to submit a PhD thesis in alternative format approved under the regulations, including sections which are in a format suitable for submission for publication or dissemination.

Name: Sarah AL-BACHARI

Degree programme: PhD Medicine (PopHlth)

Registration Number: 5890493

School: Medicine

This form should be submitted with the thesis.

Signed: _____ Date: 22.01.16

Graduate Education Manager

Faculty of Medical and Human Sciences Graduate Office

Publications and Presentations

Publications and presentations related to work performed as part of the PhD are as follows:-

1. **Al-Bachari, S.**, Vidyasagar, R., Emsley, H.C.A., Parkes, L.M. 2016. Structural and Physiological Neurovascular Changes in Idiopathic Parkinson's Disease and its Clinical Phenotypes. J Cereb Blood Flow Metab. Submitted. (Full Paper).

2. Hanby, M.F., **Al-Bachari, S.**, Makin, F., Vidyasagar, R., Parkes, L.M., Emsley, H.C.A. 2015. Structural and physiological MRI correlates of occult cerebrovascular disease in late-onset epilepsy. Neuroimage Clinical. 20, 9:128-33. (Full Paper).

3. **Al-Bachari, S.**, Emsley, H.C.A., Vidyasagar, R., Parkes, L.M. 2015. An Arterial Spin Labelling Study Revealing Altered Neurovascular Status in Idiopathic Parkinson's Disease; Comparisons with Cerebrovascular Disease. June 2015. (Abstract). [E-poster presented at the *International Society for Magnetic Resonance in Medicine 23rd Annual Meeting in Toronto, Ontario, Canada* in June 2015, poster number 4295].

4. **Al-Bachari, S.**, Emsley, H.C.A, Vidyasagar, R., Parkes, L.M. Neurovascular status in idiopathic Parkinson's disease; an MRI study. June 2015. Movement Disorders 30, S568–S633. (Abstract). [Poster, presented at the *19th International Congress of Parkinson's Disease and Movement Disorders*, *San Diego*].

5. **Al-Bachari, S.**, Vidyasagar, R., Silverdale, M., Emsley, H.C.A., Parkes, L.M. Nov 2015. Similarities in Arterial Arrival Time Prolongation and Posterior Hypoperfusion in Patients with Idiopathic Parkinson's Disease and Stroke. J Neurol Neurosurg Psychiatry 86, 46. (Abstract). [Poster, presented at the *Association of British Neurologists [ABN] Annual Meeting*, 2015].

6. **Al-Bachari, S.**, Parkes, L.M., Vidyasagar, R., Hanby, M., Tharakan, V., Leroi, I., Emsley, H.C.A. 2014 Arterial Spin Labelling Reveals Prolonged Arterial Arrival Time in Idiopathic Parkinson's Disease. Neuroimage Clinical 6, 1-8. (Full Paper).

7. Gibson, L.M., Hanby, M.F., **Al-Bachari, S.**, Parkes, L.M., Allan, S., Emsley, H.C.A 2014. Late-onset epilepsy and occult cerebrovascular disease. J Cereb Blood Flow Metab. 34(4), 564-70. (Full Paper).

8. **Al-Bachari, S.**, Parkes, L.M., Vidyasagar, R., Hanby, M., Tharakan, V., Leroi I., Emsley, H.C.A. 2013. Clinical Phenotype-specific Differences in Cerebral Haemodynamics in Idiopathic Parkinson's Disease. J Neurol Neurosurg Psychiatry 84, 11. (Abstract). [Poster, presented at *the Association of British Neurologists (ABN) Annual Meeting*, May 2013].

9. Hanby, M., Fairclough, S., Makin, F., **Al–Bachari, S.**, Vidyasagar, R., Parkes, L.M., Emsley, H.C.A. Alterations in Structural and Haemodynamic Cerebrovascular Measures in Late Onset Epilepsy. 2012. J Neurol Neurosurg Psychiatry 84, 11. (Abstract). [Poster presented at the *ABN annual meeting*, May 2013].

10. **Al-Bachari, S.**, Parkes, L.M., Vidyasagar, R., Hanby, M., Tharakan, V., Leroi, I., Emsley, H.C.A. 2013. Cerebrovascular Mechanisms of Idiopathic Parkinson's Disease; an Arterial Spin Labelled Perfusion MRI Study of Cerebrovascular Dysfunction. (Abstract). [Poster, presented at the *International Society for Magnetic Resonance in Medicine 21st Annual Meeting in Salt Lake City (USA)* in April 2013 (Poster number 1142)].

Preface

The author graduated from the University of Liverpool in 2007 with an MBChB(Hons). Whilst at medical school, she embarked on many special study modules, receiving distinctions, at the Walton Centre for Neurology and Neurosurgery. This sparked her interest in Neurology leading to an intercalated degree, BSc(Hons) in Neuroscience at the University of Manchester, achieved in 2006. Dedicated to pursuing a career in Neurology she went on to complete her foundation and core medical training in the North West Deanery, whilst maintaining her research interests.

Soon after embarking on what was at the time an MPhil, she recognised the great pleasure she derived from the team's work into this exciting area and endeavored to secure funding for a PhD. Funding was secured via a joint MRC and Biomedical Imaging Institute fellowship and from the Sydney Driscoll Neuroscience Foundation. To continue her research interests and maintain momentum she is currently embarking on an academic clinical fellowship (ACF) in Neurology (at Lancaster University) and has completed her first year of neurology training. Her passion to become a clinical academic neurologist continues.

Acknowledgements

I would like to take this opportunity to extend my sincere gratitude to all that made this PhD work a possibility, with particular recognition of:-

- My supervisors, Drs Hedley Emsley and Laura Parkes, for recognising, encouraging and guiding any potential I may have had to make this PhD successful. For providing me with an opportunity to work with them as part of an effective and exciting research team. For their invaluable advice, support and teaching, with specific thanks to Dr Laura Parkes for her invaluable teaching and guidance on imaging methodology and analysis.
- To all the participants who without which this work and any insights gained would not have been a possibility. Thank you for your kindness and being such a joy to work with.
- The University of Manchester (UOM), the UOM Biomedical Imaging Institute and University of Manchester's MRI facility (MRIF), the MRC and to the Sydney Driscoll charity for the opportunity to perform and for providing funding towards the PhD.
- Drs Rishma Vidyasagar, Martha Hanby, Vivek Tharaken, Ira Leroi and Mr Matt Wright for their input and work towards the pilot study and initial study design.
- My advisor Professor Ollier, for his timely advice, support and encouragement.
- All the radiographers at SRFT and WTCRF for their expertise and support, with specific thanks to Mr Neal Sherratt for his enthusiasm towards this study and often going above and beyond.
- Dr Josephine Naish and Professor Parker for input towards the MRI DCE data, help with devising the MATLAB codes and set-up of the imaging protocol.
- All the team at ISBE for being an inspiration with specific thanks to the IT support team, Dr Dan Cox for his help and support with various aspects of this work including recruitment, sharing of ideas, computer support etc., Helen Beaumont and Wenge Wu for their work towards the ASL and WML imaging protocols respectively.
- For all who helped with recruitment in particular the PD nurses at LTHTR, Dr Silverdale and other consultants at SRFT.
- Dr Laura Howell for statistics teaching and support.
- A personal thanks to Dr Claudia Lindner for being an inspirational PhD student before me and remaining a supportive role model.

- Ultimately to my family, in particular my parents, who have shown me unconditional support and pride, despite my passion for research remaining an enigma to them!

  I am of course grateful for everyone else who has had any involvement in this PhD as inevitably this list is non-exhaustive.

Chapter 1: Introduction

1.1 Defining Idiopathic Parkinson's disease

James Parkinson first reported Parkinson's disease in 1817 as "the shaking palsy". Idiopathic Parkinson's disease (IPD) is now known to be the second most common neurodegenerative disease after Alzheimer's disease (AD), affecting 1–2% of the population over the age of 65 with its incidence increasing steeply with age (Van Den Eeden et al., 2003). It is a chronic movement disorder characterised by slowness of movement (bradykinesia), with at least one other feature of resting tremor, postural instability and rigidity. Progression is variable and difficult to predict, but is often associated with significant disability.

Treatment for IPD remains purely symptomatic, with a complete absence of effective disease modifying or neuroprotective agents. This is at least in part due to our current, arguably poor, understanding of the neurodegenerative process. Nonetheless recent molecular and imaging studies have resulted in exciting advances in our understanding of the pathophysiology of neurodegeneration (Sulzer, 2007; Tansey and Goldberg, 2010; Zlokovic, 2008). Indeed, neurodegenerative pathophysiology is now believed to be multifactorial with many key factors, acting and interacting, leading to the vicious circle of neuronal death (Collins et al., 2012; Sulzer, 2007).
What follows is an attempt to explore our current understanding of IPD pathophysiology and the multiple factors implicated in this neurodegenerative process.

This will lead on to a more focused, in depth, exploration of neurovascular mechanisms, critiquing current evidence and postulating more refined approaches to aid our understanding of neurovascular status (NVS) in IPD, on the path to effective disease modifying/neuroprotective treatments. Herein we have used the term 'neurovascular status' (NVS) to encompass the various structural and physiological neurovascular markers.

1.2 Current Understanding of IPD Pathophysiology

1.21 IPD-A Neurodegenerative Disorder

> *'Defining neurodegenerative diseases is like defining the continent of Europe: part history, part science, part politics, and to cap it, both could have an effect on health and prosperity'* (Williams, 2002).

Neurodegeneration is a curious term, arguably not clearly defined, with no clearly known definitive cause and understandably no viable therapeutic options for the diseases it leads to. It encompasses a range of conditions, hundreds, AD and IPD being the first and second most common respectively (Przedborski et al., 2003). All are believed to be the result of progressive and selective loss, or at least dysfunction, of neurons. The site-specific population of neurons affected determines the clinical picture and therefore defines the condition (Wijsman et al., 2005). The preferential involvement of certain pathways, the mediators of damage, and indeed the nature of the damage in neurodegeneration all continue to provoke substantial debate.

1.22 IPD-The Final Outcome of the Neurodegenerative Process

The pathological hallmark of IPD is the specific and progressive degeneration of dopaminergic (DA) neurons in the substantia nigra pars compacta (SNpc) of the basal ganglia (BG) and depletion of dopamine in the striatum (STR) (Savitt et al., 2006). This is associated with the widespread occurrence of intracytoplasmic α-synuclein positive inclusion bodies known as Lewy bodies (LB) and Lewy neurites of neuronal cells (Choonara et al., 2009). It is well known that α-synuclein is expressed in the brain, where it interacts with membranes, vesicular structures, and a variety of other proteins. LBs are abnormal, post-translationally modified, and aggregated forms of α-synuclein.

As the term idiopathic implies, why this abnormal protein accumulation in selective neuronal pathways occurs, remains mostly unknown, but the likely contributing factors will be discussed in section 1.23. Braak et al., using pathological staining studies discovered a temporal pattern of LB distribution, and staged IPD progression histologically (Braak et al., 2003; Goedert et al., 2013). Stages 1 and 2 begin at the medulla oblongata/pontine tegmentum and olfactory bulb, with these patients usually being pre-symptomatic. Then the substantia nigra, areas of the midbrain and basal forebrain become involved as the disease advances to Braak stages 3 and 4. By stages 5 and 6 the pathological changes appear in the neocortex.

Over recent years the apparent 'prion like transmission' of α-synuclein has attracted much interest. This occurred as studies revealed the ability of α-synuclein to pass between neurons (Foltynie and Kahan, 2013; Luk et al., 2012; Volpicelli-Daley et al., 2011). Whilst an interesting concept, this leaves our understanding incomplete, as this does not for instance account for the initial steps leading to proteinopathy. What follows is an account of our current understanding of the initial steps in neurodegeneration, particularly in the context of IPD.

1.23 IPD- The Initial Steps Leading to the Neurodegenerative Process

The factors which initiate the protein misfolding process, its mechanisms and importantly how an accumulation of particular proteins directly results in neuronal death are questions still open to discussion. What follows is an attempt to disentangle the key players in the neurodegenerative process; starting with the traditional concepts and moving on to the more contemporary.

1.231 Aging

Traditionally it has been argued that the most consistent risk factor for developing a neurodegenerative disorder, especially AD or IPD, is increasing age (Farooqui and Farooqui, 2009). The natural process of aging has been defined as '*a progressive deterioration of biological functions after the organism has attained its maximal reproductive competence'* (Harman, 1981).

This process has been attributed to different theories, such as the oxidative stress theory, proteinopathies, DNA damage and lack of repair and altered gene expression (Harley, 1991; Harman, 1981; Levine and Stadtman, 2001). It remains however that the biological mechanisms which underlie aging are still unknown and despite genomic analysis and modifying environmental factors such as diet, the inevitability of aging ensues, so more modifiable risk factors should be sought. Equally the role aging *per se* plays in the pathophysiology of IPD has come under scrutiny, indeed Kish et al., indicated that the regional and sub regional pattern of striatal dopamine loss in normal aging differs substantially from the pattern typically observed in IPD; arguing the cause of IPD cannot be primarily an age-dependent process (Darbin, 2012; Kish et al., 1992).

1.232 Faulty Genes

Only around 10% of cases of IPD have a clear genetic origin (Lesage and Brice, 2009). At least 16 Parkinson's disease-related genetic loci (the PARK loci) and 11 genes associated with these PARK loci have been identified (Lesage and Brice, 2009; Lill et al., 2012). These rare familial cases show an autosomal dominant or recessive mode of inheritance and several causative genes have been identified e.g. *SNCA*, *LRRK2*, *PARK2*, *PINK1, VPS35* and *EIF4G1*. Genetic work has now turned to non-Mendelian forms of IPD, which are likely caused by the combined effects of genetic and environmental factors, but their implication in IPD is not always certain. The α-synuclein gene has been identified in genome wide association studies (GWAS) and has been quoted to be '*the largest single genetic risk factor for the apparently sporadic forms of the disease'* (Foltynie and Kahan, 2013; Nalls et al., 2011). Yet even these studies admit that understanding of how LBs cause neuronal death is largely unknown. Many, in fact around 800, genetic association studies in IPD have been performed over the past 20 years yet little focus has been placed on the link between genetic findings and disease biology (Lill et al., 2012).

1.233 Mitochondrial Dysfunction

The mitochondrial hypothesis of neurodegeneration postulates that defects in mitochondrial metabolism leads to mitochondrial dysfunction, reduction in adenosine triphosphate (ATP) mediated cellular activity, and therefore ion dysregulation and neurotoxicity. This is believed to be involved in IPD pathology as mitochondrial toxins can cause parkinsonism and conversely mitochondrial dysfunction is noted in IPD (Golpich et al., 2016; Kuter et al., 2016; Melo et al., 2016; Onyango et al., 2017). Recent studies however show that the causes remain mostly unknown and the position within the neurodegenerative cascade uncertain, so there are unanswered questions in respect of the role of mitochondrial dysfunction (Lezi and Swerdlow, 2012).

1.234 Oxidative Stress

The attributes of dopaminergic nigrostriatal cells, specifically their reduced level of the anti-oxidant glutathione and increased nigral iron content make them particularly vulnerable to oxidative stress (Fahn and Cohen, 1992). Oxidative stress is caused by an

imbalance between the production and destruction of reactive oxygen species (ROS) and reactive nitrogen species (RNS). Oxidative stress has been implicated in neuronal dysfunction and death via release of peroxide, which damages all components of the neuron. What stimulates oxidative stress and the precise mechanisms of neurodegeneration remain mostly speculative (Freeman and Keller, 2012). Oxidative stress damages mitochondria, as mitochondria produce large amounts of nitric oxide (NO), dysfunctional mitochondria can itself lead to increase NO levels (Di Marco et al., 2015).

1.235 Neuroinflammation and Glial Activation

Microglia are the resident immune cells in the central nervous system (CNS) and constitute about 5-20% of glial cells (Chung et al., 2010). They mediate innate immune responses to invading pathogens by secreting an array of cytokines, chemokines, prostaglandins, reactive oxygen and nitrogen species and growth factors. They are physiologically neuroprotective but prolonged overactivation of microglia has been implicated in leading to oxidative stress, mitochondrial dysfunction and to trigger apoptotic cascades (particularly cytokine and adaptive immune responses) in neurons (Arai et al., 2006).

In a post mortem study over 20 years ago, McGeer et al., demonstrated the presence of activated microglia in the substantia nigra (SN) of a PD patient's brain (McGeer et al., 1988). Subsequently animal models using potent inducers of inflammation such as 1-methyl-4-phenyl-1, 2, 3, 6-tetrahydropyridine (MPTP) have shown how microglial cells contribute to neurotoxicity in the CNS. The SN is particularly sensitive to this process, leading to selective DA degeneration, especially in the aging brain (L'Episcopo et al., 2011; Machado et al., 2011; Meredith et al., 2008; Sawada et al., 2007). Epidemiological studies have demonstrated the sensitivity of the midbrain DA neurons to cytokines (Freeman and Keller, 2012). Positron emission tomography (PET) studies, labelling and imaging microglial activation, and molecular studies, have implicated precise inflammatory pathways. Thanks to this surge of research over the past 15 years, '*an overwhelming number of proof-of-principle studies strongly implicate inflammatory processes in the progressive loss of nigral DA neurons*' in PD (Chung et al., 2010). In particular the role of chronic inflammation is implicated, which predates the initial insult.

So what are the factors that lead to the chronic inflammatory process? Indeed all the effects of neuroinflammation (cytokine release, oxidative stress, mitochondrial dysfunction) have themselves been implicated in at least the perpetuation of the chronic

immune response (Collins et al., 2012). Thus the '*two-hit hypothesis*' has emerged, which suggests that neurodegenerative disorders such as PD are multifactorial, and possibly a consequence of '*multiple-hits'* involving a variety of factors (Chen and Liu, 2012) e.g. ischaemia could be the first hit, 'priming' the brain for a more exaggerated chronic inflammatory response to subsequent hits. This leads on to a vicious circle of inflammation, CNS damage e.g. breakdown of the blood brain barrier (BBB), further cytokine release, further inflammation etc. leading to eventual death of vulnerable neuronal populations. Specific triggers and the pivotal role the BBB plays in this process will be discussed in the next section dedicated to the vascular pathophysiology of neurodegeneration.

1.3 The Neurovascular Model of Neurodegeneration

The neurovascular (NV) model of neurodegeneration is rapidly evolving; indeed over the few years this PhD was performed the insights into this theory have become more sophisticated. As the name suggests, alterations in the cerebral vasculature, whether causal in, or an effect of, the neurodegenerative process, are thought to play a central role in the vicious circle of neurodegeneration. Indeed vascular changes have been noted even before neuronal dysfunction and loss and are present in the prodromal period.

Our understanding of the NV model of neurodegeneration originates from preclinical; mainly laboratory based molecular and pathological studies, where 'a proof of principle' has been argued. Knowledge in this area has developed further with the evolution of imaging techniques to provide *in vivo* insights. Arguably our understanding has been somewhat confused by conflicting findings, at times, from epidemiological and pathological studies. Therefore what follows is a breakdown of our understanding of this process from bench to clinical studies. To set the scene, there is a brief explanation of our current understanding of the cerebral microvascular system. Therein follows an explanation of the vascular model of neurodegeneration through preclinical, predominantly *in vitro*, studies. This is followed by a summary outlining the contribution of clinical studies, among which neuroimaging studies are arguably at the forefront.

1.31 The Cerebrovascular System

1.311 Structure

'*Nearly every neuron in the brain has its own capillary*' (Zlokovic, 2005)

The brain is a remarkable organ; despite only accounting for 2% of the body's total mass it consumes 20% of the energy produced in the resting state (Attwell et al., 2010). It demands an almost constant blood supply to nourish the neurons and glial cells and so the brain is a densely vascular organ. Even a reduction or short interruption to the blood supply can cause neurons and glial cells to dysfunction and die. To this end the brain has a highly adapted vascular system resulting in a relatively constant blood supply which is able to adjust to the demands of the brain (Farkas et al., 2000b).

The large vessels are the point of entry of blood to the brain and branch into progressively narrower vessels to form pial vessels on the surface of the brain and penetrating arterioles to supply deeper structures forming parenchymal arterioles. These arterioles eventually lead to the capillaries, with the brain capillary endothelium forming the BBB (http://www.ncbi.nlm.nih.gov/books/NBK53081/). Unlike pial cells that form collateral networks, penetrating and parenchymal arterioles are long and largely unbranched such that occlusion of an individual arteriole results in significant reductions in flow and damage (infarction) to the surrounding local tissue (Nishimura et al., 2007). The capillaries, which are the only site of oxygen and nutrient transfer (and where removal of waste products occurs), have formed a highly developed system of control which has attracted much attention over the past 2 decades. This has led to the term the 'neurovascular unit' (NVU), which will be given further attention in section 1.32.

1.312 Perfusion

Cerebral perfusion refers to the delivery of blood flow in the brain, cerebral blood flow (CBF), and is quantified as units of mL/g/min i.e. the volume of blood flow per unit brain mass per minute (Wolf and Detre, 2007). Cerebral autoregulation refers to the brain's ability to maintain its own blood flow based on demand, and despite changes in systemic arterial pressures and other physiological parameters[1]. Beyond these limits autoregulation is lost and flow depends on mean arterial pressure (http://www.ncbi.nlm.nih.gov/books/NBK53081/). It is at this point that oxygen

[1] Including cerebral metabolism, neurohumeral factors, partial pressures of carbon dioxide and oxygen.

extraction becomes additionally important, as increased oxygen extraction from the blood attempts to compensate for the reduced perfusion. Once the decrease in perfusion can no longer be compensated for by increased oxygen extraction then ischaemia and its consequences ensue (Ostergaard et al., 2013).

Indeed the metabolic needs of neuronal activity and all the cellular elements of the NVU must be matched or 'coupled' by an adequate blood flow, which involves tight coordination between neuronal activity and blood flow within the brain parenchyma, termed 'neurovascular coupling', the usual response of which is termed hyperaemia (Attwell et al., 2010). Recent studies have shown that properties of the small arterioles via astrocytes contribute to neurovascular coupling (Anderson and Nedergaard, 2003; Iadecola, 2004). This is demonstrated by the local increase in blood flow seen in response to increased neural activity (Drake and Iadecola, 2007).

Certain hemodynamic factors dominate cerebral perfusion. Based on Poiseuille's Law (Equation 1), CBF is dependent upon vessel length L, cerebral perfusion pressure ΔP, vessel radius r, and viscosity of blood η (Hurn and Traystman, 1997).

$$CBF = \frac{\pi r^4 \Delta P}{8\eta L} \qquad [1]$$

It can be seen that CBF is very sensitive to changes in vessel radius (to the power of 4), and it is principally by alterations to vessel diameter that CBF is controlled. Although the larger vessels influence perfusion pressures, it is the microvasculature, predominantly the arterioles, that alter in diameter to meet the variable needs of the brain and it is these arterioles that are most narrow and thus provide the greatest resistance. More recent studies have also highlighted the contribution of capillaries (Attwell et al., 2010).

Although the autoregulatory mechanisms are not fully understood, it is felt that a combination of myogenic, neurogenic and endothelial factors contribute to the regulation of CBF. Within certain perfusion pressure parameters, local mechanisms suffice, but beyond these, local mechanisms are exhausted. The myogenic component is defined as the intrinsic capacity of vascular smooth muscle cells to contract in response to mechanical stress such as increase in transmural pressure (Farkas and Luiten, 2001; Ursino, 1991), with increased vascular tone leading to decreased lumen diameter - in other words stretch dependent vasoconstriction. This phenomenon invariably depends upon the intact vasculature to function normally. Endothelial cells play an important role in the regulation of vascular tone by releasing potent vasoactive factors, such as NO, free

radicals, prostacyclin, endothelium-derived hyperpolarizing factor, and endothelin (Girouard and Iadecola, 2006). Neurogenic factors also come into play, such as release of certain neurotransmitters e.g. noradrenaline which is a potent vasodilator.

All these processes are geared towards ensuring adequate perfusion to the brain capillaries, which form the BBB, a key part of the NVU, and the site where neuronal needs are met. Thus it is essential that the capillary system and flow patterns are also understood. The brain capillaries are extensive, with a total length of over 400 miles (http://www.ncbi.nlm.nih.gov/books/NBK53081/). The net extraction of diffusible substances is thought to be limited by (i) regional CBF; (ii) capillary permeability; and (iii) the capillary surface area. Capillary surface area is determined by capillary density, length, and blood volume per unit volume (Ostergaard et al., 2013). Apart from CBF which we have discussed, these factors under normal conditions remain static. However if the structural components are affected, such as through neurodegeneration, this would lead to decreased oxygen supply and its consequences. Interesting work centering around capillary dysfunction and flow patterns affecting net oxygen extraction with compensatory CBF reduction to reduce functional shunting is underway (Ostergaard et al., 2013; Ostergaard et al., 2016).

This brief overview illustrates the importance of an intact microvascular system to ensure adequate perfusion, autoregulation and neurovascular coupling in the brain. If these systems are abnormal e.g. reduced capillary number or altered structure and therefore functioning of the arterioles, then neuronal and glial dysfunction will ensue. To put this in a context relevant to IPD, a brief summary of the basal ganglia circulation follows.

1.313 Particular Insights into Basal Ganglia circulation

The basal nuclei are supplied by perforating branches of the anterior cerebral artery (ACA), Heubner's artery, middle cerebral artery (MCA)and anterior choroidal artery (AChA) (Vitosevic et al., 2005). Therefore by definition it is very much a border zone area i.e. region supplied by the most distal branches of large arteries. Border zone regions are the most sensitive to hypoperfusion as they are the least likely areas to receive adequate supply due to their distal location.

Perforating arteries can be described as '*small twigs'* that originate from main cerebral arteries at the base of the brain (Djulejic et al., 2015). They are thin walled; long

penetrating vessels that do not anastomose to form collaterals. Characteristically perforators are small vessels of less than 1 mm in diameter, except for certain lenticulostriate vessels and some Heubner arterioles which exceed 1 mm in size. The BG vascular supply highlights how the blood supply to the brain is not uniform, thus some regions such as deep white matter and BG structures are more vulnerable than others to chronic hypoperfusion (Brown and Thore, 2011; Moody et al., 1990).
Disrupted microvascular integrity and reduced cerebral blood flow are the cornerstones of the vascular hypothesis of neurodegeneration and will be discussed in some depth in the next two sections.

1.32 Introducing the Neurovascular Unit (NVU)

The Neurovascular Unit (NVU) is a complex network of cells and mechanisms intertwined with multiple networks of communications. It essentially consists of endothelial (capillary) cells supported at a basement membrane and by glial cells (i.e. microglia, oligodendroglia, and astrocyte end-feet), in close proximity to a neuron (Figure 1.1) (Stanimirovic and Friedman, 2012). The NVU controls BBB permeability and CBF, it also maintains the neuronal 'milieu' which is required for proper functioning of neuronal circuits (Zlokovic, 2011).

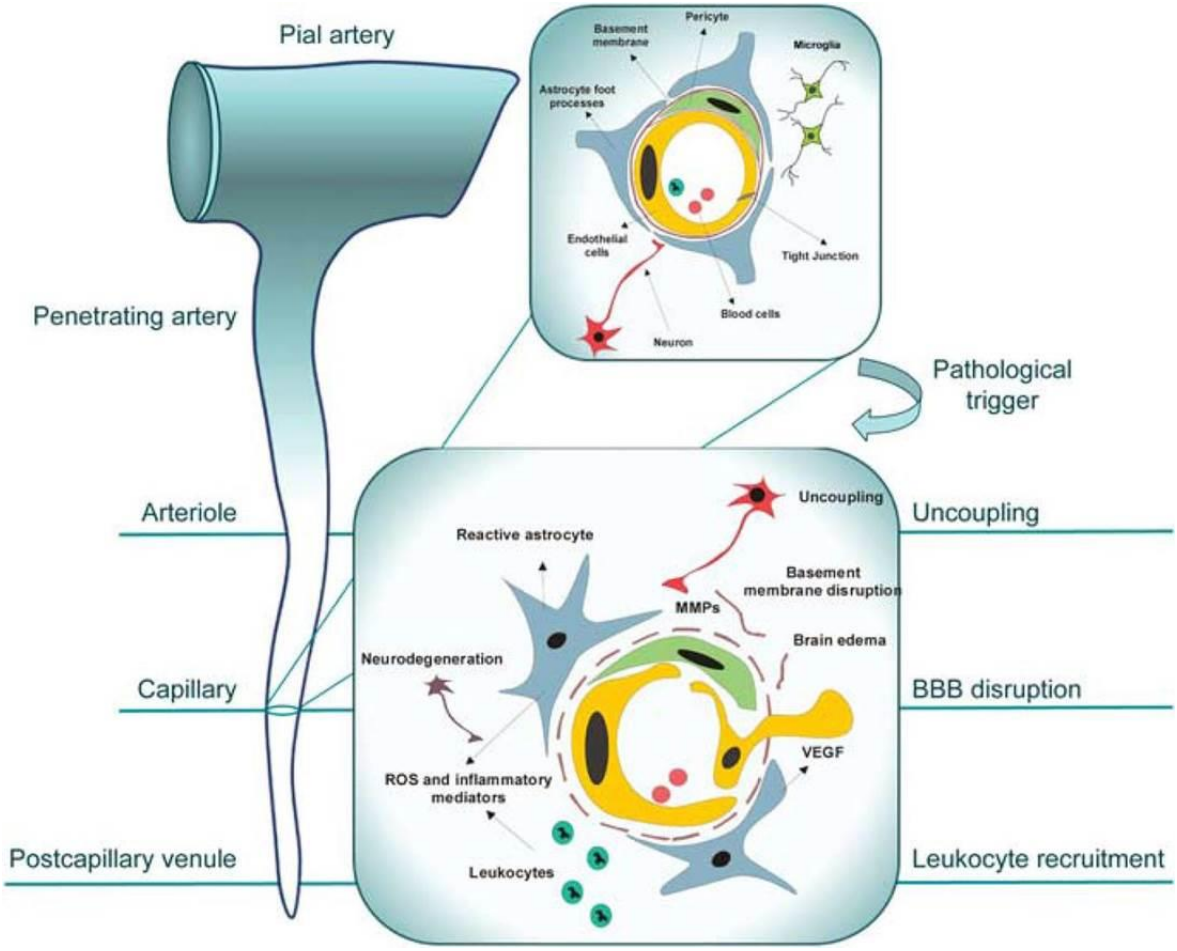

Figure 1.1: An illustration of the NVU (top square). Bottom square indicating pathology that can occur at and disrupt the NVU.

Reproduced with permission from the Journal of Cerebral Blood Flow and metabolism (Stanimirovic and Friedman, 2012).

The endothelium forms the capillaries and is the anatomical site of the BBB (Grammas et al., 2011). Initially believed to be a passive barrier, 'a sheet of nucleated cellophane' (Florey, 1966), the endothelial cells are now known to be highly specialised, metabolically active and synthetic. Tight junctions hold the endothelial cells together at junctional complexes, such as the adherens junctions, tight junctions and gap junctions, producing a selectively permeable, highly electrically resistant barrier to red blood cells, leukocytes, and plasma and water soluble components (Pardridge, 2005). Equally the junctions act as a point of communication between the endothelial cells and the encircling, structurally supportive, pericytes and astrocytes. The astrocytes, pericytes and endothelium maintain the basement membrane, a layer of extracellular matrix of structural proteins e.g. collagen. This contributes significantly to the barrier properties of the BBB. This communication between the glial cells and BBB helps to regulate microvascular

permeability, remodelling and angiogenesis via the secretion of various molecules including growth factors and angiogenic molecules (Dore-Duffy and LaManna, 2007). In addition, the astrocytes and pericytes collectively produce a range of enzymes to modify molecules that do manage to pass the physical barriers (Danbolt, 2001; Morale et al., 2006; Shimizu et al., 2007).

Collectively, the NVU orchestrates the maintenance of the brain 'milieu' that is the optimal physiological environment for neurons, neuronal circuits, synaptic transmission, synaptic remodelling, angiogenesis and neurogenesis (Zlokovic, 2008). Ions are transported via ATP dependent transporters to allow normal action potential production along the neurons (O'Kane et al., 2004). Neuroactive peptides and proteins are allowed to cross into neurons via 'receptor mediated transport systems' and are thus a route to drug delivery to the brain (Popescu et al., 2009). All these processes are highly metabolically demanding, which is reflected by the high number of mitochondria in endothelial cells (Zlokovic, 2011). BBB transport systems and cellular junctions have been comprehensively reviewed recently (Zhao et al., 2015). They also mediate immune responses particularly when activated. Astrocyte-derived neurotrophic factors have been shown to protect against neurotoxins (Sandhu et al., 2009).

The neural milieu is strictly separated from circulatory spaces by the BBB, which also protects and controls from circulatory products. With the explosion of molecular research over the past decade or so, the sophisticated interactions within the NVU are becoming better appreciated. It would go beyond the scope of this introduction to mention all the molecular interactions, yet general groups and relevant physiology have been mentioned above.

1.33 The Neurovascular Model of Neurodegeneration – When Things Go Wrong

After a couple of decades of intense research only quite recently has it come to light that the neurovascular (NV) model of neurodegeneration centres around two key events: i) disturbances in the morphology and function of the capillary wall with associated NVU dysfunction; and ii) disruption of normal CBF, predominantly at the level of the arterioles. These vascular processes are by no means independent and the chronology and degree to which they interact remains yet to be elucidated. What follows is an in-depth consideration of these two key changes and how the NV model fits in with more

conventional players in the neurodegenerative process culminating in what has recently been coined the '*two-hit vascular hypothesis of neurodegeneration*' (Sagare et al., 2012).

1.331 Evidence for BBB dysfunction in neurodegenerative states

Ultimately, dysfunctioning of the NVU leads to dysregulation of the normally tightly controlled and regulated matching of neuronal vascular and metabolic demands, culminating in neuronal dysfunction and neurodegenerative changes (Brown and Thore, 2011; Ostergaard et al., 2013; Winkler et al., 2014). Figure 1.1 illustrates potential NVU pathology (Stanimirovic and Friedman, 2012).

1.3311 Breakdown of the BBB

Increase in BBB permeability, leading to an infiltration of systemic inflammatory mediators into the brain, has been established in a range of neurodegenerative pathology models (Farkas et al., 2000b; Kortekaas et al., 2005). Capillary basement membrane thickening, collagen formation and local disruptions to the endothelial cell-pericyte-junction connections have been shown in PD (Bell and Zlokovic, 2009; Sagare et al., 2013a; Winkler et al., 2014). In fact dysfunction of the BBB transporter system, due to an underexpression of tight junction proteins can lead to the extravasations of small and large molecules in the brain (Faucheux et al., 1999). This can lead to brain oedema and suppression of capillary flow and hypoperfusion.

1.3312 Physiological Decline-Abnormality in the Metabolic and Synthetic Function of the NVU

It is not only the physical breakdown of the BBB, but also the loss of normal physiological function, which have been linked to neuronal death. NVU pericyte dysfunction has been attributed to release of angiogenic factors, vascular epithelial growth factor (VEGF) and pericyte epidermal growth factor (PEDF), which induce structural changes in blood vessels such as tortuous vessels and poor regulation of capillary diameter and blood flow (Winkler et al., 2011; Yasuda et al., 2007). The efflux pumps in the NVU have been found to operate insufficiently in PD patients (Farkas et al., 2000b). Enzymatic mechanisms

controlling the basement membrane and the extracellular matrix have been shown to decrease in activity, disrupting the BBB and allowing inflammatory invasion (Danbolt, 2001). Indeed the alterations in NVU metabolic functions have been shown to lead to the secretion of multiple neurotoxic and inflammatory factors (Di Marco et al., 2015; Glass et al., 2010; Sagare et al., 2012, 2013b; Winkler et al., 2014; Yasuda et al., 2007; Zlokovic, 2008, 2011). In addition, the breakdown of the BBB has been attributed to higher levels of BBB transporter dysfunction of nutrient transfer including ion pumps, ABC transporters etc., in AD and PD models, contributing to mitochondrial dysfunction (Armulik et al., 2010; Lipton, 2005). NVU malfunction has also been attributed to impaired clearance and increased production of Aβ in AD (Di Marco et al., 2015).

1.3313 Evidence for altered microvasculature in neurodegeneration proximal to and at the level of NVU

Numerous studies of microvascular pathology in AD have repeatedly reported altered morphology of the vessels, particularly capillaries. These pathologies have been reported so consistently that preclinical studies have stated certain neurodegenerative disorders such as AD to be '*vasculopathies*' (de la Torre, 2004). The key microvascular changes can be summarised as follows.

Decreased vascular density demonstrated by string vessel formation and loss of capillary vessels. String vessels are basement membrane remnants of capillaries that have lost their endothelium (Brown, 2010; Brown and Thore, 2011), they cannot transport blood and are believed to be a consequence of ischaemia. Signs of vessel regression are also detectable, and microvessels often seem fragmented, with fewer branches, and frequently present with a degenerated, atrophic endothelium and collapsed lumen. These alterations can understandably reduce local brain perfusion (Storkebaum et al., 2011). In addition reduced capillary density has been reported in both AD and IPD (Brown and Thore, 2011; Farkas et al., 2000b; Yang et al., 2015).

Other alterations in vascular structure namely tortuous vessels, venous collagenases and irregular basement membranes and precapillary fibrosis have also been reported. This pathology is more at the arteriole level. The arterioles supplying the deep white matter travel the longest course and become more twisted or tortuous with aging which increases the vessel length; with each loop there is a loss of kinetic energy and increased BP required to maintain flow (Farkas et al., 2000b; Moody et al., 1991). AD brains have been studied most and reveal increased burden, compared to normal aging, of this

tortuosity of the terminal arterioles and capillaries reflective of loss of smooth contour of the vessels and fibrosis, thickening of the BM and thinning of the endothelial cells (Kalaria, 1996). The thickened BM is also considered to be a consequence of cerebral amyloid angiopathy (CAA) and Aβ accumulation in AD (Storkebaum et al., 2011). Atrophy and swelling of endothelial cells and loss of endothelial mitochondria have also been noted (Di Marco et al., 2015; Farkas and Luiten, 2001; Sagare et al., 2012). Although AD studies predominate, some recent studies comparing IPD microvascular pathology to that seen in AD showed similar changes in both disorders (Farkas et al., 2000b; Sarkar et al., 2014; Yang et al., 2015).

1.332 The NV Model of Neurodegeneration – Cerebral Hypoperfusion

From our basic understanding of physiological CBF control it would seem reasonable to think the alterations in arteriolar and capillary morphology would contribute to a loss of regulatory capacity (e.g. reduced myogenic, endothelial and neurogenic control of vascular diameter). This would impair compensatory mechanisms and lower CBF i.e. damage to resistant blood vessels that leads to insufficient cerebral blood flow (Farkas and Luiten, 2001).

Indeed regional cerebral hypoperfusion is becoming a recurrent theme in studies of AD and IPD. The patterns of hypoperfusion seem to be disease specific i.e. AD differs from IPD, with posterior hypoperfusion predominating in IPD. It has been postulated that this may be a consequence of inhibited flow through tortuous vessels, misery flow due to capillary loss and inefficient flow due to endothelial dysfunction (Brown, 2010; Ostergaard et al., 2013), but will be discussed further in the final paragraph of this section. Many studies have demonstrated hypoperfusion (and metabolism) to be present in the prodromal stages of AD and IPD and at the point of diagnosis suggesting a role of altered NVS in the pathogenesis (Ostergaard et al., 2013).

Though altered vasculature would impair NVU function the converse is true also i.e. that cerebral hypoperfusion leads to vascular morphology and NVU dysfunction. As previously described, the brain is very sensitive to reductions in CBF due to its high metabolic demand and lack of reserve. Not surprisingly in this context hypoperfusion, in particular its consequent glucose and oxygen deprivation, may lead to direct damage to parenchymal cells and the BBB. This occurs as hypoperfusion can reduce the efficacy of the multiple energy dependent ion pumps, disrupts ATP synthesis and the ability to

produce action potentials, in turn lowering the pH of the neuronal milieu, with accumulation of glutamate and proteinous toxins (Glass et al., 2010) and contribute to mitochondrial dysfunction and increased oxidative stress (Farkas et al., 2007; Grammas et al., 2011; Kelleher and Soiza, 2013; Perry et al., 2000; Shah et al., 2012; Yamagata et al., 2004). In addition, hypoperfusion has been associated with altered levels of endothelial angiogenic proteins including VEGF (Di Marco et al., 2015).

1.34 Summarising the role of the Neurovascular Unit in Neurodegeneration

Inevitably if the path of blood flow becomes an arduous inefficient journey as a consequence of vessel tortuosity, stenosis, increased path length and endothelial dysfunction, then CBF will be compromised. Therefore integrity of the vascular endothelium will have a direct consequence on CBF (de la Torre, 2012). Poiseuille's law demonstrates how only minor changes in vascular morphology can have a major impact on CBF. Cerebral hypoperfusion in turn will compromise the highly metabolic activities of the NVU, leading to NVU dysfunction, with potential deleterious effects on neuronal function. Morphological changes of the microvasculature e.g. basement membrane thickening, physically hinder BBB functioning including nutrient transport, transport of toxic waste and other important carrier systems of the BBB (Farkas et al., 2000b). Thus NVU function and CBF are intimately interrelated.

Collectively, neurovascular changes, with downstream effects such as increased oxidative stress, inflammation and mitochondrial dysfunction, can be seen to be closely related to the neurodegenerative process. NVU dysfunction is associated with inflammatory activation and alterations in angiogenesis and direct damage to BBB integrity. Physical breakdown of the BBB allows the infiltration of lymphocytes, macrophages and other toxins into the brain parenchyma (Chung et al., 2010; Hemmer et al., 2004; Stolp and Dziegielewska, 2009). The endothelium is a rich source of NO which regulates vascular tone; capillary dysfunction results in NO dysregulation contributing to the vicious cycle of neurodegeneration (Di Marco et al., 2015).

1.35 Clinical Studies – Conflicted Evidence

Despite the consistency in results of preclinical studies, they mostly take an *in vitro*, highly reductionist approach in the non-human that although necessary, can be argued to be limited in relevance. Turning then to clinical studies, the main approach of epidemiological studies and pathological studies has been to view CVD in IPD as more of a comorbidity; i.e. by definition a coexisting, yet distinct, disease process from that of the index disease which has an effect, interaction and implication on the index disease (Feinstein, 1970). Thus attempts have been made to link IPD more with conventional large vessel CVD, such as large vessel infarcts and strokes. Consistently these have shown the prevalence of infarcts and stroke (typically large artery) in IPD to be equal to or less than controls (Ben-Shlomo and Marmot, 1995; Ghebremedhin et al., 2010; Jellinger, 2003; Mastaglia et al., 2002; Morley and Duda, 2012; Nataraj and Rajput, 2005; Struck et al., 1990). More recently a few pathological studies have focused specifically on SVD and revealed changes including basement membrane thickening, capillaries with fibrosis, fewer, shorter capillaries which were larger in diameter and less branched (Farkas et al., 2000a; Farkas et al., 2000b). This highlights how essential it is to select appropriate measures of CVD or neurovascular change.

Time and again cardiovascular risk factors have been linked to AD, the commonest neurodegenerative disorder; the same does not apply to IPD. Studies argue IPD patients have lower cardiovascular risk factors as incidence of tobacco smoking amongst the IPD population is usually lower with lower frequencies of hyperlipidaemia and obesity and levodopa is felt to have cardiovascular protective properties (Alves et al., 2004; Scigliano et al., 2008, 2009). Other studies argue that IPD patients have specific risk factors such as orthostatic hypotension and immobility (Hajjar et al., 2010; Nanhoe-Mahabier et al., 2009). Despite this lack of association with cardiovascular risk factors in IPD compared to AD, similar microvascular changes have been noted in both, patterns of hypoperfusion have been noted in both, as well as alterations in the NVU (Guan et al., 2013; Rektor et al., 2009). This would strongly suggest that even perhaps in AD it is not simply the coexistence of CVD in the conventionally understood use of the term or its risk factors that contribute to the neurodegenerative process but the interactions of various pathways that occur at the microvascular level (usually in the setting of the aging brain) that don't necessarily need larger vessel disease and its consequences to exist.

Of course both neurodegeneration and CVD are more prevalent in the aging population and therefore more likely to coexist and impact one another. So the logical question which follows is; is CVD merely a comorbidity or are alterations in vasculature, herein

referred to as alterations in neurovascular status (NVS), an intrinsic part of, or at least a player in, the neurodegenerative process itself? This question may remain unanswered, but what follows is an attempt to evaluate the role alterations in NVS play in IPD, taking a more precise approach, looking at subtle changes and small vessel pathology. Over recent years with advances in imaging technologies, more methods to assess NVS have been established. Therefore the next section is dedicated to exploring these imaging techniques and whether they help to establish an association of cerebrovascular dysfunction with IPD, first looking at physiological measures moving on structural measures.

1.36 Insights from Clinical Imaging Studies

Positron Emission Tomography (PET) allows accurate and quantitative *in vivo* regional measurements of cerebral circulation and cellular metabolism (Powers and Zazulia, 2010). As PET is considered an invasive imaging technique and has not been employed in our study the main focus of this section will be on MRI techniques.

1.361 Cerebral Perfusion Studies

Perfusion studies have allowed physiological measures of subtle alterations in NVS. These include exciting innovative MR techniques using arterial spin labelling (ASL) and functional MRI (fMRI) with blood oxygen level dependent (BOLD) signal to measure alterations in cerebral blood flow (CBF) and cerebrovascular reactivity. Multiple reviews argue their role in IPD yet studies implementing these measures are few (Schuff, 2009). Neurodegenerative diseases such as AD and IPD have recently been associated with region-specific alterations in perfusion. Here the principles of MRI techniques and key findings in IPD will be summarised.

1.3611 MRI with Arterial Spin Labelling (ASL)

ASL provides a robust method for quantifying absolute cerebral perfusion using magnetically labelled arterial blood water as an endogenous diffusible flow (Detre et al., 1998). In ASL studies, inflowing arterial blood water is magnetically labelled/tagged, using a specific radiofrequency pulse. Magnetically labelled arterial water decays with T1 relaxation, the T1 relaxation time of water in blood at 3T is approximately 1.6 seconds

(Wolf and Detre, 2007). Images are acquired after a post-labelling delay time, to allow magnetically labelled blood to flow into the microvasculature and tissue (Alsop and Detre, 1996). The presence of the labelled blood reduces the tissue magnetisation, which can be measured with a '*snapshot*' MRI imaging sequence such as echo-planar imaging and compared to an unlabelled '*control*' image (Wolk and Detre, 2012). Perfusion is proportional to the degree of signal reduction, which is determined by the pair-wise subtraction of images that are acquired with labelling and without (control). Absolute CBF can be estimated by modelling expected signal changes in the brain based on a number of fixed or estimated parameters including the T1 of blood. It is the average of multiple control-label pairs which allows the creation of high quality CBF maps, enabling quantification of whole brain or regional blood flow and also voxel based analysis.

In addition another parameter, named arterial arrival time (ATT), the time taken for blood to travel from the labelling slab to the voxel of interest can be measured. It is unclear exactly what compartment the blood will be in, but probably arterioles and capillaries, not having had sufficient time to diffuse into the tissue at the time of measurement. Labelled blood water eventually exchanges into the extravascular space and will diffuse back into the venous vessels, but the signal will be lost by then due to T1 relaxation, therefore the resultant signal is largely from the arterioles and capillaries. Explanations for prolonged AAT mainly centre around structural vascular changes such as changes in tortuosity of vessels (including large carotid vessels and arterioles) which increase the path length and thus prolong transit time (Chen et al., 2012; Liu et al., 2012). Equally studies have revealed substantially prolonged AAT in patients with CVD because of collateral circulation (Wolf et al., 2003).

ASL MRI have been used in the context of acute and chronic CVD with promising results. It is completely non-invasive; it can be repeated rapidly and in principle indefinitely, offering a clear advantage over the more common approach of injection of an exogenous contrast agent. It also offers high reliability in both young and elderly subjects (Dai et al., 2009).

CBF measured by ASL should be a close indicator of glucose metabolism as measured by PET. Only quite recently have studies utilised ASL to assess perfusion patterns in neurodegenerative disorders. To date such perfusion studies have shown regional reductions in CBF in multiple AD studies (Chao et al., 2010; Chen et al., 2011; Johnson et al., 2005) with areas of hypoperfusion that overlap considerably with hypometabolism frequently reported with PET (Mai and Berr, 1999). Interestingly some studies have also noted increased regional CBF (hyperperfusion) of patients with prodromal and early stage

AD, which may have implications for pathophysiology and the role of compensatory responses to neurodegeneration (Wolk and Detre, 2012). In a similar manner, even in early to moderate PD similar perfusion defects have been observed, with the perfusion deficit being more extensive than the loss of gray matter, suggesting that structural changes may follow functional change (Fernandez-Seara et al., 2012; Melzer et al., 2011). Of note PET measures of metabolism reveal a distinct PD-related metabolic covariance pattern affecting similar areas to that of perfusion (posterior hypometabolism and increased metabolism in the BG), with high correlation between metabolism and perfusion (Ma et al., 2010). However a recent study revealed a larger perfusion decrease in the PD-related pattern in cortical regions including the insula than in the metabolic brain pattern (Teune et al., 2014). Interestingly PET studies have revealed metabolic changes preceding motor abnormalities and progressing with disease progression which perhaps sheds some light on the pathophysiology of the disease (Tang et al., 2010). Hypoperfusion in neurodegenerative states has previously been attributed to direct tissue loss or the result of loss of functional connectivity (Borghammer et al., 2010).

It remains difficult, yet essential, to tease out the chronology of the changes to really know whether hypoperfusion is a cause or effect of the neurodegenerative process. To the author's knowledge although a handful of studies utilising ASL MRI in PD exist, they do not measure AAT and have not sought to understand alterations specifically in NVS (Fernandez-Seara et al., 2012; Melzer et al., 2011).

1.3612 fMRI using Blood Oxygenation Level Dependent Signal

fMRI using the BOLD signal is sensitive to the paramagnetic properties of deoxyhaemoglobin in the blood. Deoxyhaemoglobin causes local magnetic field disturbances, causing the water protons to resonate at different frequencies, which in turn cause the net signal to decay (and reduce T2*) more quickly. The higher the concentration of deoxyhaemoglobin the stronger the decay and the lower the MRI signal. A local increase in blood flow will reduce the concentration of deoxyhaemoglobin and increase the BOLD signal. Thus, the BOLD signal can be considered as a marker of CBF change (Derejko et al., 2006; Ogawa et al., 1990). BOLD MRI signal reflects CBF, but also depends on cerebral blood volume, cerebral metabolic rate of oxygen, arterial oxygenation, and haematocrit level to a lesser extent (Pillai and Zaca, 2012).

1.3613 From Cerebral Blood Flow (CBF) Measurements to Cerebrovascular Reactivity (CVR)

ASL and BOLD MRI under carbon dioxide inhalation, to induce mild hypercapnia stimulating vasodilatation, can be used to measure cerebrovascular reactivity (CVR), i.e. the change in CBF or BOLD for a given change in end-tidal CO_2. The measure may reflect cerebral haemodynamic impairment (Hajjar et al., 2010). CVR reflects the capacity of blood vessels to dilate and is an important marker for brain vascular reserve, thus reflecting CV integrity (Yezhuvath et al., 2009). This method has been used in AD impairments in CVR in animals and humans (Cantin et al., 2011; Iadecola, 2004; Mueggler et al., 2002; Princz-Kranz et al., 2010).

These perfusion techniques are not without their limitations, in particular their individual confounding factors such as inter-subject and gender variations. In addition although CVR can be utilised as a measure of neurovascular integrity, many factors such as blood pressure and diabetes in addition to traditionally non vascular factors such as certain drugs and depression, can affect CVR (Kimura et al., 2006).

1.3614 DCE MRI

Dynamic contrast-enhanced (DCE) MRI specifically probes BBB integrity by measuring the leakage of contrast agent. A Gadolinium contrast agent is administered and a dynamic series of images are taken before and after injection. Gadolinium is an effective and widely used contrast agent and in its chelated forms has low toxicity. It works by shortening the T1 so increasing (enhancing) the signal. The kinetics of the passage of the bolus into the tissues can be measured by the MR signal change and modelled to estimate certain parameters such as the transfer constant, k^{Trans}, and the plasma volume, Vp (Tofts, PS. T1-weighted DCE Imaging Concepts: Modelling, Acquisition and Analysis. MAGNETOM Flash (Siemens) 2010; http://www.paul-tofts-phd.org.uk/DCE-MRI_siemens.pdf) (accessed 30 May 2016). k^{Trans} is a transfer constant that measures the combined effect of blood flow (through a capillary) and BBB permeability. In high flow systems with low permeability such as the brain, alterations in k^{Trans} can be presumed to represent alterations in BBB permeability. In order to estimate k^{Trans} and Vp the dynamic concentration of contrast agent in plasma, the so-called arterial input function (AIF) must be quantified (Lavini and Verhoeff, 2010). As measurements at the single capillary level

are not possible, this can be overcome by several means including acquiring the AIF from a large vein or venous sinus (Calamante, 2013).

Although traditionally DCE MRI has been used to study relatively high levels of BBB disruption, such as in tumours, a recent meta-analysis has revealed how more refined methods can be used to measure subtle BBB change (Heye et al., 2014; Heye et al., 2016). Indeed DCE MRI has been used in the setting of aging, mild cognitive impairment (MCI) and AD revealing focal areas of increased leakiness of the BBB (Heye et al., 2014). To the author's knowledge DCE MRI has not been used in the clinical setting of IPD.

1.362 Structural Markers of CV dysfunction - Introducing the Concept of Small Vessel Disease (SVD)

Cerebral SVD is a single term which describes diverse pathologies; all of which are believed to centre around disease affecting the perforating cerebral arterioles (in fact predominantly arteriolar dysfunction), capillaries and venules, with resulting damage to the cerebral white matter and grey matter (Wardlaw et al., 2013a). Clinically SVD presents as gait, cognitive, bladder instability and mood problems (O'Sullivan, 2008), in addition to stroke. Neuropathologically, the acclaimed studies by Miller Fisher have revealed typical changes of 'diffuse abnormality in the small deep vessel wall' which he referred to as 'segmental arteriolar disorganisation'; he also revealed fibrin deposition (Fisher, 1968, 2011). Since then, less compliant vessels with loss of smooth muscle autoregulation, vessel wall thickening and increased tortuosity and lumen restriction have been revealed (Knottnerus et al., 2009; Pantoni and Garcia, 1997; Stevenson et al., 2010; Wardlaw et al., 2013b). Indeed the '*small deep perforating vessels or lenticulostriate vessels branch like poplar trees rather than like oak trees*' each of which provide blood supply to a specific region without anastomosis (Wardlaw et al., 2009; Wardlaw et al., 2013b). At points between the cortical and ventricular surfaces they form internal border zone areas and so are particularly vulnerable to damage as a result of reduced CBF.

Though neuropathological studies are very helpful, arguably the greatest insights into SVD stem from neuroimaging work to the extent that SVD has been considered to be a neuroimaging term. Neuroimaging, predominantly MRI markers, measure the consequence of SVD. To date there are many markers of SVD including recent small subcortical infarcts, lacunes, white matter lesions (WML) also known as leukoaraiosis,

enlarged perivascular spaces, microbleeds and some would argue atrophy (Wardlaw et al., 2013c).

Although from an imaging perspective multiple endpoints for SVD have been identified, for the purpose of the thesis leukoaraiosis (WML) will be focused on in the next section.

1.3621 White Matter Lesions/Leukoaraiosis

In 1987 Hachinski et al. coined the term leukoaraiosis, derived from the Greek leuko=white; araiosis=rarefaction (Hachinski et al., 1987). They argued the importance of recognising the cause and aetiology of white matter lesions found on imaging. These lesions are characterised by areas with high signal intensities on T2 -weighted MRI (with or without FLuid Attenuated Inversion Recovery [FLAIR]) or as rounded areas with low attenuation on CT (O'Sullivan et al., 2005). The areas generally affected are the deep white matter (DWM), periventricular regions, BG, brainstem and pons, with such changes presumed to result from vascular pathology (Longstreth et al., 2000; Wardlaw et al., 2013c).

SVD has been strongly associated with risk factors for CVD (Wardlaw et al., 2015); though WML pathophysiology is not fully understood. WMLs also occur in the context of neuroinflammation and thus they are believed to be multifactorial (Wardlaw et al., 2013c). O'Sullivan writes '*in regions of leukoaraiosis the major pathological findings are myelin pallor, enlargement of perivascular spaces, gliosis and axonal loss*' (O'Sullivan, 2008). Fazekas et al., showed that heterogeneity of WMLs decreased as the size and extent of WML increased with vascular changes becoming more consistent (Fazekas et al., 1993). Indeed rating scales have been developed to help semi quantitatively measure the extent of the lesions from small punctate lesions to large confluent lesions (Fazekas et al., 1993; Wahlund et al., 2001). Imaging studies have revealed WMLs to have increased leakiness of BBB and have even associated WML with capillary loss (Bohnen et al., 2011; Pantoni and Garcia, 1997).

Measurements of leukoaraiosis in the context of IPD are conflicted and the table below helps to summarise some key studies. These results suggest a multimodal approach to WML burden, including not only numerical quantification but also lesion volume is required for a true reflection of SVD burden (O'Sullivan, 2008; Rost et al., 2014).

Study	Design	Population	Findings
Piccini et al., (Piccini et al., 1995)	Radiological MR study: prevalence and extent of WML. Hoehn and Yahr stage (Measure of PD severity). Phenotype using UPDRS scale.	102 nondemented patients with idiopathic PD and 68 sex- and age-matched healthy controls all screened for absence of cerebrovascular risk factors.	The frequency and the extent of periventricular hyperintensities were significantly higher in patients with PD than in healthy subjects. The patients who had periventricular hyperintensities had significantly shorter disease duration and greater disease severity, i.e. a higher disease progression index, than those who did not.
Sohn et al., (Sohn and Kim, 1998)	Radiological MR study: prevalence and extent of WML. Hoehn and Yahr stage (Measure of PD severity). Phenotype using UPDRS scale. Depression score also measured.	44 patients with PD on levodopa therapy. MR scans taken 12 hours off medication.	13 patients (30%) had WMLs on MRI. Of the 13: they were significantly older and gait and posture scores higher than the WML free group, with less levodopa-responsiveness to bradykinesia
Lee et al., (Lee et al., 2009)	Radiological MR study: Hoehn and Yahr stage (Measure of PD severity). Phenotype using UPDRS scale.	141 patients with IPD, divided into 2 phenotypes - tremor or postural instability and gait difficulty (PIGD)-dominant groups.	Leukoaraiosis grade was independently associated with age, the PIGD motor phenotype of PD (rigidity, bradykinesia and axial symptoms) and disease severity. No association with tremor or disease duration.
Bohnen et al., (Bohnen et al., 2011)	Radiological PET and MRI measurements of metabolic activity and of leukoaraiosis respectively: and Clinical Hoehn and Yahr stage (Measure of PD severity). Phenotype using UPDRS scale. Dementia Rating Scale score.	73 PD patients, dopaminergic drugs withheld overnight and patients imaged in morning	Comorbid leukoaraiosis with a significant association with axial motor dysfunction, borderline association with bradykinesia and gait. No association of WML with tremor and rigidity NB axial symptoms can be considered as part of the PIGD.
Herman et al., (Herman et al., 2013)	Radiological MR study: Hoehn and Yahr stage (Measure of PD severity) Phenotype using UPDRS scale	104 PD patients (62 PIGD and 42 TD)	This study did not demonstrate any association between WMHs and the PIGD or TD motor sub-types in patients with PD

Table 1.1: Studies examining the WML burden in various IPD motor phenotypes

Studies of leukoaraiosis *per se* (independent of the presence of IPD or not) have revealed as many as 80% of people with WMLs had some degree of gait disorder, likewise deterioration in gait is associated with progression of leukoaraiosis (Schmidt et al., 2012b). Physiological measures of CV dysfunction in specific IPD subgroups are lacking.

1.4 Phenotyping IPD - A More Refined Approach

As alluded to in the above sections, even with exciting advances in measurements of subtle CVD, the heterogeneity of clinical features within IPD itself demands a more precise approach to investigating any potential associations. It is now increasingly recognised that within the umbrella term of IPD great heterogeneity in non-motor and motor clinical features exists. This has led to multiple, large national studies including PRoBaND, CamPaIGN and the Oxford discovery to help define these differences into phenotypes (Iadecola, 2004; Malek et al., 2015; Williams-Gray et al., 2009).Over 2 decades ago Jankovic et al., analysed a large 'DATATOP' database of 800 patients in early non treated Parkinson's disease to explore the clinical heterogeneity that exists within IPD (Jankovic et al., 1990). Their findings led to the emergence of 2 key motor clinical phenotypes; the postural instability and gait disorder (PIGD) and tremor dominant (TD) phenotypes.

The TD phenotype is generally considered to have more of a benign course, less associated with non-motor features of IPD and more responsive to L-dopa treatment (Thenganatt and Jankovic, 2014). Conversely the PIGD phenotype, for which gait and postural instability dysfunction predominate, are associated with more cognitive, neuropsychiatric and other non-motor symptoms and is generally considered less responsive to L-dopa treatment and felt to reflect non dopaminergic pathways (de Lau et al., 2014; van Rooden et al., 2011). Due to the great heterogeneity of motor features between the two motor groups the concept that they have differing underlying pathophysiologies is rapidly emerging (Lawton et al., 2015; Williams-Gray et al., 2013). As Table 1.1 demonstrates the PIGD group is mostly associated with increased WML burden and studies of perfusion and metabolism in specific phenotypes is generally lacking.

Phenotypes can be assessed using the unified Parkinson's disease rating scale (UPDRS) and Jankovic's method (Jankovic et al., 1990). Subtype classification is based on the ratio of the average of UPDRS 'tremor' items (items 16, 20 and 21) divided by the average of 'postural instability and gait difficulty' items (13–15, 29 and 30). Patients were

categorised as having tremor-dominant IPD if the ratio of the mean tremor score to the mean PIGD score was 1.5 or higher and as PIGD dominant if the ratio was 1 or lower, and as intermediate with a score of greater than one and less than 1.5 (Jankovic et al., 1990; Stebbins et al., 2013).

This heterogeneity in clinical features can also be seen in IPD's non motor features (Hu et al., 2014b).Non-motor features of IPD, though they are many, can be divided into autonomic dysfunction, sleep disturbances, a range of neuropsychiatric symptoms and cognitive decline; all of which are more greatly associated with the PIGD phenotype (Aarsland et al., 1999).

1.41 Cognitive Decline

IPD is associated with mild cognitive impairment and dementia. Older people with IPD are at a six fold increased risk of developing dementia, when compared with age matched controls (Aarsland and Kurz, 2010). Dementia is believed to develop in around 80% of the IPD patients by 20 years of diagnosis (Reid et al., 2011).Current literature suggests that cognitive dysfunction (as measured by various scales including the Montreal cognitive assessment tool [MoCA]) is attributed to patterns of cerebral hypoperfusion which are disease specific and not related to the cognitive score *per se* but rather the underlying disease process e.g. pattern of correlation of perfusion with cognitive scores differs between IPD, AD and dementia with Lewy bodies (Chao et al., 2010; Firbank et al., 2003; Mito et al., 2005; Nobili et al., 2008). Perfusion studies in IPD patients with and without dementia have revealed widespread cortical hypoperfusion and in particular hypoperfusion in the posterior cortex, parietal regions, precuneus and cuneus in PD and PDD when compared with controls (Fernandez-Seara et al., 2012; Kamagata et al., 2011; Ochudlo et al., 2003).

1.42IPD and Neuropsychiatric Conditions

A wide variety of neuropsychiatric disturbances occurs in the context of IPD including depression, anxiety, psychosis, impulsivity and apathy. These symptoms can even predate the motor manifestations of IPD. They understandably have a significant impact on quality of life (Aarsland et al., 2007). In fact in a recent meta-analysis of 126 functional neuroimaging studies, Postuma and Dagher found evidence for a model of the basal ganglia connectivity which divides the basal ganglia into motor, associative, and

limbic areas, supporting previous work in this area (Postuma and Dagher, 2006). As the limbic area is implicated in emotion this provides evidence for a neurodegenerative mechanistic cause of depression in IPD.

1.5 Conclusion

IPD remains a progressive neurodegenerative disorder, yet recent molecular and imaging studies have resulted in exciting advances in our understanding of this process. Indeed neurodegenerative disorders are now believed to be multi-factorial with many key factors leading to the vicious circle of neuronal death. This has led to the 'neurovascular model' of neurodegeneration, which challenges the purely neurocentric model and argues the key role vascular mechanisms play in this process. Indeed damage to the NVU; a complex, metabolically active system of endothelial cells and glial cells in close proximity to a neuron has been attributed to neuronal death. Recognition of NV dysfunction and an improved understanding of associated changes such as cerebral perfusion, CVR and BBB dysfunction (and the impact of frequently used treatments) in IPD may have prognostic implications. These would include treatment to arrest CVD progression and modify the potential contribution of CVD to the neurodegenerative process.

Current IPD treatment remains only symptomatic. This has highlighted many 'critical unmet clinical needs' relating to the management of IPD (Meissner et al., 2011). Aside from tremor, rigidity and bradykinesia other motor features of IPD are often somewhat neglected. These include freezing of gait, postural instabilities and abnormal postures which cause significant disability yet respond little to current IPD treatments, which is probably reflective of their understudied and poorly understood pathophysiology (Hely et al., 2008). This has led to a movement towards the classification of the predominant motor symptoms based on the UPDRS. Equally the non-motor features of IPD which include cognitive decline and neuropsychiatric symptoms of depression, anxiety, apathy and psychosis are poorly understood and targeted, despite their prevalence.

The evidence for NV dysfunction in IPD has been summarised in Table 1.2. Bearing in mind the overwhelming majority of molecular studies of NVU dysfunction in neurodegeneration have been performed in AD, the data in IPD is still rapidly accumulating. Clinical epidemiological studies remain equivocal, probably due to the variable end points and surrogate markers of CVD and the failure to recognise the potential difference in pathophysiologies of varying IPD clinical phenotypes.

It remains unclear whether progression from bench to bedside will be made with the discrepancies in clinical studies acting as a stumbling block. The development and application of multimodal imaging techniques are likely to be important. A more focused approach, realising the pattern of altered NVS in IPD phenotypes, using and developing more sensitive imaging techniques is required, so that attention can be focused on finding disease modifying agents for this disabling disorder.

Type of Study	**Key Findings**	**References**
Preclinical Molecular	BBB P-gp transporter abnormalities leading to PD pathogenesis	(Bartels, 2011; Funke et al., 2009; Lee et al., 2004)
	Alterations in BBB in IPD – structural +/- physiological	(Armulik et al., 2010; Carvey et al., 2005; Chao et al., 2009; Chen et al., 2008; Desai Bradaric et al., 2012; Jangula and Murphy, 2013; Patel et al., 2011a; Sarkar et al., 2014; Zhao et al., 2007)
	Vascular remodelling and altered vasculature	(Barcia et al., 2005; Wada et al., 2006)
Pathological	Capillary abnormalities – loss of capillaries, alteration in calibre of capillaries, basement membrane thickening	(Brown and Thore, 2011; Farkas et al., 2000a; Farkas et al., 2000b; Guan et al., 2013; Sarkar et al., 2014)
	Amyloid angiopathy in IPD	(Bertrand et al., 2008)
	In vitro evidence of BBB disruption during PD development (in striatum and SNpc)	(Gray and Woulfe, 2015; Jangula and Murphy, 2013; Kortekaas et al., 2005)
	Enhanced angiogenesis resulting in abnormal vascular permeability in PD	(Desai Bradaric et al., 2012; Yasuda et al., 2007)
	SVD in autopsy proven IPD (variable changes between IPD and controls)	(Schwartz et al., 2012)
	No increased burden of CV lesions or stroke in PD	(Ghebremedhin et al., 2010; Jellinger, 2003; Mastaglia et al., 2002)
Epidemiological/Other clinical	An increased risk of CVD in PD	(Ben-Shlomo and Marmot, 1995; Gorell et al., 1994)
	A reduced risk of CVD in PD	(Nataraj and Rajput, 2005; Struck et al., 1990,)

	No clear relationship between CVD and IPD	(Levine et al., 1992)
	Increased CSF markers of angiogenesis in PD	(Janelidze et al., 2015, (Pisani et al., 2012))
Imaging	BBB disruption in PD patients	(Hirano et al., 2008)
	Altered perfusion pattern in IPD	(Borghammer et al., 2010; Fernandez-Seara et al., 2012; Kamagata et al., 2011; Le Heron et al., 2014; Ma et al., 2010; Madhyastha et al., 2015; Melzer et al., 2011; (Tang et al., 2010) Teune et al., 2014)
	Other MRI measures of altered vasculature	(Rektor et al., 2009)

Table 1.2: **Summary of the data pertaining to the neurovascular hypothesis in IPD (WML data presented separately in Table 1.1)**

1.6 The Study

1.61 The Hypotheses:

MRI techniques can be utilised as feasible structural and physiological measures of NVS. The physiological markers of NVS include cerebral perfusion (CBF and AAT), cerebrovascular reactivity (CVR) and DCE MRI measures of subtle BBB dysfunction.

Differences in structural and physiological measures of NVS exist between IPD patients and controls.

NVS varies according to the clinical phenotype of IPD and may modify the clinical features including non-motor features.

1.62 Methodology:

Preliminary pilot work began with 14 IPD patients and 14 age matched healthy controls. Recruitment of subjects with IPD was from the database of patients managed by the regional neurosciences centre based at Royal Preston Hospital. Participants underwent an MRI protocol incorporating a range of imaging techniques including T2-weighted FLAIR,

ASL and DCE. In addition a hypercapnic challenge was administered during ASL acquisition to probe cerebrovascular reactivity (CVR). This resulted in an MRI protocol lasting just over one hour. Imaging was undertaken on the 3T MRI scanner at Salford Royal Hospital (University of Manchester MRI Facility, MRIF).
This work formed the basis of the larger study. The imaging protocol was adapted and the hypercapnic challenge removed due to various issues discussed in Chapter 4. For the main study the aim was to recruit 20 subjects in each of the IPD TD and PIGD subgroups and up to 40 age matched controls (up to 20 without CVD, up to 20 with CVD). Some data from preliminary experiments were used. Recruitment of patients with IPD was through the regional neurosciences centres based at Lancashire Teaching Hospitals NHS Foundation Trust and Salford Royal Hospital NHS Foundation Trust. Patients were approached by phone and by letter. All travel costs were reimbursed.
Imaging was undertaken on the 3T Scanner at the Wellcome Trust Clinical Research Facility, based on the Central Manchester & Manchester Children's University NHS Foundation Trust hospital site. During this visit routine clinical baseline data (including medical history, clinical presentation, duration and severity of IPD) and all current medications were recorded. The phenotype of IPD was determined using the UPDRS. Also a blood sample, 5-10 ml of whole blood, was taken during cannulation or via venepuncture, at the time of imaging, for quantification of peripheral blood markers of inflammation and endothelial activation/dysfunction, to be reported separately.

Of note the imaging protocol was developed to provide a comprehensive multimodal approach in order to thoroughly address the question of potential NV changes in IPD. However it was not possible to analyse and demonstrate all the data in this time, so the areas that are outside the scope of the thesis have been highlighted in italics (to be reported separately) and the remainder reported and discussed further in subsequent chapters.

The Imaging Protocol (Main Study)

The imaging protocol (approximately 1 hour), was as outlined below:

Structural imaging:

T1-weighted MPRAGE with 1mm isotropic resolution. Voxel-based morphometry was used to assess group differences in grey matter volume.

.

T2-weighted FLAIR. Estimates of the volume of white matter lesions, which was compared between the groups.

T2-weighted gradient echo (microbleeds), to enable counting of the number of microbleeds, for comparison between the groups.*

MR angiography (to exclude major artery narrowing)

Physiological Imaging:

Arterial Spin Labelling with STAR labelling and Look-Locker read-out (Edelman et al., 1994; Gunther et al., 2001). Quantitative maps of CBF and arterial arrival time were produced and whole brain values extracted. Voxel-based analysis was used to determine group differences in CBF and AAT.

Dynamic Contrast Enhanced MRI over 20 minutes following Gadolinium injection to assess subtle BBB alterations. Quantitative maps of k^{Trans} and Vp were produced and regional values extracted for comparison between the groups.

Diffusion weighted MRI for quantification of tissue microstructure.

Inflammatory Markers

Plasma samples will be analysed using specific immunoassays for determination of concentrations of a number of markers of inflammation (CRP, IL-6) and endothelial activation/dysfunction (ICAM-1, VCAM-1, Endothelin-1, E-Selectin, von Willebrand Factor).

The Clinical Scales

Clinical scales were also administered during the attendance at the Wellcome research facility (with the option of these being undertaken during a home visit). The clinical scales covered non-motor features of IPD, as outlined below:

Montreal Cognitive Assessment Tool (MoCA) - for mild cognitive impairment

Brief cognitive assessment for patients with cerebral small vessel disease (O'Sullivan et al., 2005)

Questionnaire for impulsive-compulsive disorders (in IPD) (QUIPS) (Weintraub et al., 2012)

SCOPA-AUT: assessment for autonomic dysfunction in IPD (Visser et al., 2004)

The Neuropsychiatric Inventory (NPI) (Cummings et al., 1994)

Note in the preliminary work the QUIPS, SCOPA-AUT and NPI were not administered, but other scales to measure psychiatric features were implemented as outlined in Chapter 3, section 3.21.

Statistics:

The preliminary work allowed sample sizes to be determined for the main study. One key component of the work concerns the regional comparisons of CBF images between groups. Previous work has found significant group differences with patient groups of size 25 (Fernandez-Seara et al., 2012). One study addressing precisely this issue of appropriate sample sizes for regional analysis of CBF images, suggests that 20 participants are required in each group to detect 15% differences in grey matter CBF in a between-groups comparison. In the pilot work, mean grey matter CBF was estimated to be 35 ml/min/100ml with a standard deviation of 6 ml/min/100ml (16% of the mean value), which is a similar ratio of SD to mean as in the Murphy *et al.* paper, giving therefore a similar sample size calculation (Murphy et al., 2011). One other key measurement is grey matter arterial transit time. The pilot work for this thesis showed this to have a mean value of 1530 ms with an SD of 140 ms (9% of the mean value), requiring fewer subjects to detect a 15% difference between groups. Hence, the aim to image 20 participants in each group of interest in the main study.

Critique of Study Design:

A case-control study was felt desirable to identify differences between IPD and controls bearing in mind the time and resources available. What follows is an overview and critique of case-control studies.

Case-control studies are a type of observational study that 'work backwards', identifying a particular outcome e.g. a disease such as IPD and taking a look back retrospectively to an exposure which might have caused that outcome (Grimes and Schulz, 2002, 2005; Schulz and Grimes; Schulz and Grimes, 2002). The main advantage is that outcomes that may take a long time to develop e.g. cardiovascular disease can be identified more rapidly than other methods. It is however paramount that an appropriate case and control group are selected in order to ensure all important factors are similar, so that any differences in outcome measure can be attributed to the disease and not other confounding variables. In this study matching for the number of cerebrovascular risk factors in the non CVD group was deemed necessary so that alterations in NVS could be attributed to the IPD disease process and not simply CV risk factors. Although, in retrospect, it was felt that attempts to match each individual RF may have been a more preferable approach (this is discussed further in Chapter 6). Age is also associated with CVD therefore the groups were matched for age. Other factors that could potentially influence the certain results such as gender, mean arterial pressures, disease duration were taken out as covariates during the analysis to avoid potential bias. In addition in the case of certain variables such as gender, a sub analysis with a gender matched control group was performed,

In order to avoid selection bias (a systematic error in the design, recruitment, data collection or analysis) recruitment of controls was in the most part spouses/relatives of the IPD or CVD group thus having similar exposures and background to that of the disease groups. Some controls (8 out of 34) were taken from volunteers interested in participating in research thus potentially more motivated and therefore their health maybe better. The clinical MRI imaging approach meant that objective outcome measures could be achieved. Analyses of data between groups were identical to avoid any bias; however a limitation was that the observer of the scan findings was not blinded to either control-case status or the study hypothesis.

1.7 Outline of Thesis

The importance of addressing the heterogeneity that exists within IPD has been outlined above and therefore chapter 2 is dedicated to a description of the non-motor features of the entire IPD population studied for this thesis. The chapters have been written in paper format as an alternative format thesis was deemed most suitable in order to facilitate publications. The presentation of the key findings from the pilot work follows in chapter 3. This has been published in the peer reviewed journal Neuroimage:Clinical and, apart from

some formatting changes to ensure consistency throughout the thesis, the paper has been unchanged. The key findings of the main study follow in the two subsequent chapters, with chapter 4 presenting ASL data and chapter 5 presenting the DCE data. Again both have been written in paper format, and chapter 4 has been submitted to the Journal of Cerebral Blood Flow and Metabolism. Chapter 5 is also drafted for journal submission. To complete the thesis chapter 6 provides an overarching discussion of the thesis, summarising key findings, conclusions and future perspectives.

References

Aarsland, D., Bronnick, K., Ehrt, U., De Deyn, P.P., Tekin, S., Emre, M., Cummings, J.L., 2007. Neuropsychiatric symptoms in patients with Parkinson's disease and dementia: frequency, profile and associated care giver stress. J Neurol Neurosurg Psychiatry 78, 36-42.

Aarsland, D., Kurz, M.W., 2010. The epidemiology of dementia associated with Parkinson disease. J Neurol Sci 289, 18-22.

Aarsland, D., Larsen, J.P., Lim, N.G., Janvin, C., Karlsen, K., Tandberg, E., Cummings, J.L., 1999. Range of neuropsychiatric disturbances in patients with Parkinson's disease. J Neurol Neurosurg Psychiatry 67, 492-496.

Abramov, A.Y., Gegg, M., Grunewald, A., Wood, N.W., Klein, C., Schapira, A.H., 2011. Bioenergetic consequences of PINK1 mutations in Parkinson disease. PLoS One 6, e25622.

Alsop, D.C., Detre, J.A., 1996. Reduced transit-time sensitivity in noninvasive magnetic resonance imaging of human cerebral blood flow. J Cereb Blood Flow Metab 16, 1236-1249.

Alves, G., Kurz, M., Lie, S.A., Larsen, J.P., 2004. Cigarette smoking in Parkinson's disease: influence on disease progression. Mov Disord 19, 1087-1092.

Anderson, C.M., Nedergaard, M., 2003. Astrocyte-mediated control of cerebral microcirculation. Trends Neurosci 26, 340-344; author reply 344-345.

Arai, H., Furuya, T., Mizuno, Y., Mochizuki, H., 2006. Inflammation and infection in Parkinson's disease. Histol Histopathol 21, 673-678.

Armulik, A., Genove, G., Mae, M., Nisancioglu, M.H., Wallgard, E., Niaudet, C., He, L., Norlin, J., Lindblom, P., Strittmatter, K., Johansson, B.R., Betsholtz, C., 2010. Pericytes regulate the blood-brain barrier. Nature 468, 557-561.

Attwell, D., Buchan, A.M., Charpak, S., Lauritzen, M., Macvicar, B.A., Newman, E.A., 2010. Glial and neuronal control of brain blood flow. Nature 468, 232-243.

Bell, R.D., Zlokovic, B.V., 2009. Neurovascular mechanisms and blood-brain barrier disorder in Alzheimer's disease. Acta Neuropathol 118, 103-113.

Ben-Shlomo, Y., Marmot, M.G., 1995. Survival and cause of death in a cohort of patients with parkinsonism: possible clues to aetiology? J Neurol Neurosurg Psychiatry 58, 293-299.

Bohnen, N.I., Muller, M.L., Zarzhevsky, N., Koeppe, R.A., Bogan, C.W., Kilbourn, M.R., Frey, K.A., Albin, R.L., 2011. Leucoaraiosis, nigrostriatal denervation and motor symptoms in Parkinson's disease. Brain 134, 2358-2365.

Borghammer, P., Chakravarty, M., Jonsdottir, K.Y., Sato, N., Matsuda, H., Ito, K., Arahata, Y., Kato, T., Gjedde, A., 2010. Cortical hypometabolism and hypoperfusion in Parkinson's disease is extensive: probably even at early disease stages. Brain Struct Funct 214, 303-317.

Braak, H., Del Tredici, K., Rub, U., de Vos, R.A., Jansen Steur, E.N., Braak, E., 2003. Staging of brain pathology related to sporadic Parkinson's disease. Neurobiol Aging 24, 197-211.

Brown, W.R., 2010. A review of string vessels or collapsed, empty basement membrane tubes. J Alzheimers Dis 21, 725-739.

Brown, W.R., Thore, C.R., 2011. Review: cerebral microvascular pathology in ageing and neurodegeneration. Neuropathol Appl Neurobiol 37, 56-74.

Calamante, F., 2013. Arterial input function in perfusion MRI: a comprehensive review. Prog Nucl Magn Reson Spectrosc 74, 1-32.

Cantin, S., Villien, M., Moreaud, O., Tropres, I., Keignart, S., Chipon, E., Le Bas, J.F., Warnking, J., Krainik, A., 2011. Impaired cerebral vasoreactivity to CO2 in Alzheimer's disease using BOLD fMRI. NeuroImage 58, 579-587.

Chao, L.L., Buckley, S.T., Kornak, J., Schuff, N., Madison, C., Yaffe, K., Miller, B.L., Kramer, J.H., Weiner, M.W., 2010. ASL perfusion MRI predicts cognitive decline and conversion from MCI to dementia. Alzheimer Dis Assoc Disord 24, 19-27.

Chen, Y., Liu, L., 2012. Modern methods for delivery of drugs across the blood-brain barrier. Adv Drug Deliv Rev 64, 640-665.

Chen, Y., Wang, D.J., Detre, J.A., 2012. Comparison of arterial transit times estimated using arterial spin labeling. MAGMA 25, 135-144.

Chen, Y., Wolk, D.A., Reddin, J.S., Korczykowski, M., Martinez, P.M., Musiek, E.S., Newberg, A.B., Julin, P., Arnold, S.E., Greenberg, J.H., Detre, J.A., 2011. Voxel-level comparison of arterial spin-labeled perfusion MRI and FDG-PET in Alzheimer disease. Neurology 77, 1977-1985.

Choonara, Y.E., Pillay, V., du Toit, L.C., Modi, G., Naidoo, D., Ndesendo, V.M., Sibambo, S.R., 2009. Trends in the molecular pathogenesis and clinical therapeutics of common neurodegenerative disorders. Int J Mol Sci 10, 2510-2557.

Chung, Y.C., Ko, H.W., Bok, E., Park, E.S., Huh, S.H., Nam, J.H., Jin, B.K., 2010. The role of neuroinflammation on the pathogenesis of Parkinson's disease. BMB Rep 43, 225-232.

Collins, L.M., Toulouse, A., Connor, T.J., Nolan, Y.M., 2012. Contributions of central and systemic inflammation to the pathophysiology of Parkinson's disease. Neuropharmacology 62, 2154-2168.

Cummings, J.L., Mega, M., Gray, K., Rosenberg-Thompson, S., Carusi, D.A., Gornbein, J., 1994. The Neuropsychiatric Inventory: comprehensive assessment of psychopathology in dementia. Neurology 44, 2308-2314.

Dai, W., Lopez, O.L., Carmichael, O.T., Becker, J.T., Kuller, L.H., Gach, H.M., 2009. Mild cognitive impairment and alzheimer disease: patterns of altered cerebral blood flow at MR imaging. Radiology 250, 856-866.

Danbolt, N.C., 2001. Glutamate uptake. Prog Neurobiol 65, 1-105.

de la Torre, J.C., 2004. Alzheimer's disease is a vasocognopathy: a new term to describe its nature. Neurol Res 26, 517-524.

de la Torre, J.C., 2012. Cerebral hemodynamics and vascular risk factors: setting the stage for Alzheimer's disease. J Alzheimers Dis 32, 553-567.

de Lau, L.M., Verbaan, D., van Rooden, S.M., Marinus, J., van Hilten, J.J., 2014. Relation of clinical subtypes in Parkinson's disease with survival. Mov Disord 29, 150-151.

Derejko, M., Slawek, J., Wieczorek, D., Brockhuis, B., Dubaniewicz, M., Lass, P., 2006. Regional cerebral blood flow in Parkinson's disease as an indicator of cognitive impairment. Nucl Med Commun 27, 945-951.

Detre, J.A., Alsop, D.C., Vives, L.R., Maccotta, L., Teener, J.W., Raps, E.C., 1998. Noninvasive MRI evaluation of cerebral blood flow in cerebrovascular disease. Neurology 50, 633-641.

Di Marco, L.Y., Venneri, A., Farkas, E., Evans, P.C., Marzo, A., Frangi, A.F., 2015. Vascular dysfunction in the pathogenesis of Alzheimer's disease--A review of endothelium-mediated mechanisms and ensuing vicious circles. Neurobiol Dis 82, 593-606.

Djulejic, V., Marinkovic, S., Milic, V., Georgievski, B., Rasic, M., Aksic, M., Puskas, L., 2015. Common features of the cerebral perforating arteries and their clinical significance. Acta Neurochir (Wien) 157, 1393.

Dore-Duffy, P., LaManna, J.C., 2007. Physiologic angiodynamics in the brain. Antioxid Redox Signal 9, 1363-1371.

Drake, C.T., Iadecola, C., 2007. The role of neuronal signaling in controlling cerebral blood flow. Brain Lang 102, 141-152.

Edelman, R.R., Siewert, B., Darby, D.G., Thangaraj, V., Nobre, A.C., Mesulam, M.M., Warach, S., 1994. Qualitative mapping of cerebral blood flow and functional localization with echo-planar MR imaging and signal targeting with alternating radio frequency. Radiology 192, 513-520.

Fahn, S., Cohen, G., 1992. The oxidant stress hypothesis in Parkinson's disease: evidence supporting it. Ann Neurol 32, 804-812.

Farkas, E., De Jong, G.I., Apro, E., De Vos, R.A., Steur, E.N., Luiten, P.G., 2000a. Similar ultrastructural breakdown of cerebrocortical capillaries in Alzheimer's disease, Parkinson's disease, and experimental hypertension. What is the functional link? Ann N Y Acad Sci 903, 72-82.

Farkas, E., De Jong, G.I., de Vos, R.A., Jansen Steur, E.N., Luiten, P.G., 2000b. Pathological features of cerebral cortical capillaries are doubled in Alzheimer's disease and Parkinson's disease. Acta Neuropathol 100, 395-402.

Farkas, E., Luiten, P.G., 2001. Cerebral microvascular pathology in aging and Alzheimer's disease. Prog Neurobiol 64, 575-611.

Farkas, E., Luiten, P.G., Bari, F., 2007. Permanent, bilateral common carotid artery occlusion in the rat: a model for chronic cerebral hypoperfusion-related neurodegenerative diseases. Brain Res Rev 54, 162-180.

Farooqui, T., Farooqui, A.A., 2009. Aging: an important factor for the pathogenesis of neurodegenerative diseases. Mech Ageing Dev 130, 203-215.

Faucheux, B.A., Bonnet, A.M., Agid, Y., Hirsch, E.C., 1999. Blood vessels change in the mesencephalon of patients with Parkinson's disease. Lancet 353, 981-982.

Fazekas, F., Kleinert, R., Offenbacher, H., Schmidt, R., Kleinert, G., Payer, F., Radner, H., Lechner, H., 1993. Pathologic correlates of incidental MRI white matter signal hyperintensities. Neurology 43, 1683-1689.

Feinstein, A.R., 1970. The pre-therapeutic classification of co-morbidity in chronic disease. Journal of Chronic Diseases 23, 455-468.

Fernandez-Seara, M.A., Mengual, E., Vidorreta, M., Aznarez-Sanado, M., Loayza, F.R., Villagra, F., Irigoyen, J., Pastor, M.A., 2012. Cortical hypoperfusion in Parkinson's disease assessed using arterial spin labeled perfusion MRI. NeuroImage 59, 2743-2750.

Firbank, M.J., Colloby, S.J., Burn, D.J., McKeith, I.G., O'Brien, J.T., 2003. Regional cerebral blood flow in Parkinson's disease with and without dementia. NeuroImage 20, 1309-1319.

Fisher, C.M., 1968. The arterial lesions underlying lacunes. Acta Neuropathol 12, 1-15.

Fisher, C.M., 2011. Lacunes: Small, deep cerebral infarcts. Neurology 77, 2104.

Florey, 1966. The endothelial cell. Br Med J 2, 487-490.

Foltynie, T., Kahan, J., 2013. Parkinson's disease: an update on pathogenesis and treatment. Journal of Neurology 260, 1433-1440.

Freeman, L.R., Keller, J.N., 2012. Oxidative stress and cerebral endothelial cells: regulation of the blood-brain-barrier and antioxidant based interventions. Biochim Biophys Acta 1822, 822-829.

Ghebremedhin, E., Rosenberger, A., Rub, U., Vuksic, M., Berhe, T., Bickeboller, H., de Vos, R.A., Thal, D.R., Deller, T., 2010. Inverse relationship between cerebrovascular lesions and severity of lewy body pathology in patients with lewy body diseases. J Neuropathol Exp Neurol 69, 442-448.

Girouard, H., Iadecola, C., 2006. Neurovascular coupling in the normal brain and in hypertension, stroke, and Alzheimer disease. J Appl Physiol (1985) 100, 328-335.

Glass, C.K., Saijo, K., Winner, B., Marchetto, M.C., Gage, F.H., 2010. Mechanisms underlying inflammation in neurodegeneration. Cell 140, 918-934.

Goedert, M., Spillantini, M.G., Del Tredici, K., Braak, H., 2013. 100 years of Lewy pathology. Nat Rev Neurol 9, 13-24.

Grammas, P., Martinez, J., Miller, B., 2011. Cerebral microvascular endothelium and the pathogenesis of neurodegenerative diseases. Expert Rev Mol Med 13, e19.

Guan, J., Pavlovic, D., Dalkie, N., Waldvogel, H.J., O'Carroll, S.J., Green, C.R., Nicholson, L.F., 2013. Vascular degeneration in Parkinson's disease. Brain Pathol 23, 154-164.

Gunther, M., Bock, M., Schad, L.R., 2001. Arterial spin labeling in combination with a look-locker sampling strategy: inflow turbo-sampling EPI-FAIR (ITS-FAIR). Magn Reson Med 46, 974-984.

Hajjar, I., Zhao, P., Alsop, D., Novak, V., 2010. Hypertension and cerebral vasoreactivity: a continuous arterial spin labeling magnetic resonance imaging study. Hypertension 56, 859-864.

Harley, C.B., 1991. Telomere loss: mitotic clock or genetic time bomb? Mutat Res 256, 271-282.

Harman, D., 1981. The aging process. Proc Natl Acad Sci U S A 78, 7124-7128.

Hely, M.A., Reid, W.G., Adena, M.A., Halliday, G.M., Morris, J.G., 2008. The Sydney multicenter study of Parkinson's disease: the inevitability of dementia at 20 years. Mov Disord 23, 837-844.

Hemmer, B., Cepok, S., Zhou, D., Sommer, N., 2004. Multiple sclerosis -- a coordinated immune attack across the blood brain barrier. Curr Neurovasc Res 1, 141-150.

Herman, T., Rosenberg-Katz, K., Jacob, Y., Auriel, E., Gurevich, T., Giladi, N., Hausdorff, J.M., 2013. White matter hyperintensities in Parkinson's disease: do they explain the disparity between the postural instability gait difficulty and tremor dominant subtypes? PLoS One 8, e55193.

Heye, A.K., Culling, R.D., Valdes Hernandez Mdel, C., Thrippleton, M.J., Wardlaw, J.M., 2014. Assessment of blood-brain barrier disruption using dynamic contrast-enhanced MRI. A systematic review. Neuroimage Clin 6, 262-274.

Heye, A.K., Thrippleton, M.J., Armitage, P.A., Valdes Hernandez Mdel, C., Makin, S.D., Glatz, A., Sakka, E., Wardlaw, J.M., 2016. Tracer kinetic modelling for DCE-MRI quantification of subtle blood-brain barrier permeability. NeuroImage 125, 446-455.

Hu, M.T., Szewczyk-Krolikowski, K., Tomlinson, P., Nithi, K., Rolinski, M., Murray, C., Talbot, K., Ebmeier, K.P., Mackay, C.E., Ben-Shlomo, Y., 2014. Predictors of cognitive impairment in an early stage Parkinson's disease cohort. Mov Disord 29, 351-359.

Hurn, P.D., Traystman, R.J., 1997. Overview of cerebrovascular hemodynamics. Primer on Cardiovascular Diseases, 42-44.

Iadecola, C., 2004. Neurovascular regulation in the normal brain and in Alzheimer's disease. Nat Rev Neurosci 5, 347-360.

Jankovic, J., McDermott, M., Carter, J., Gauthier, S., Goetz, C., Golbe, L., Huber, S., Koller, W., Olanow, C., Shoulson, I., et al., 1990. Variable expression of Parkinson's disease: a base-line analysis of the DATATOP cohort. The Parkinson Study Group. Neurology 40, 1529-1534.

Jellinger, K.A., 2003. Prevalence of cerebrovascular lesions in Parkinson's disease. A postmortem study. Acta Neuropathol 105, 415-419.

Johnson, N.A., Jahng, G.H., Weiner, M.W., Miller, B.L., Chui, H.C., Jagust, W.J., Gorno-Tempini, M.L., Schuff, N., 2005. Pattern of cerebral hypoperfusion in Alzheimer disease and mild cognitive impairment measured with arterial spin-labeling MR imaging: initial experience. Radiology 234, 851-859.

Kalaria, R.N., 1996. Cerebral vessels in ageing and Alzheimer's disease. Pharmacol Ther 72, 193-214.

Kamagata, K., Motoi, Y., Hori, M., Suzuki, M., Nakanishi, A., Shimoji, K., Kyougoku, S., Kuwatsuru, R., Sasai, K., Abe, O., Mizuno, Y., Aoki, S., Hattori, N., 2011. Posterior hypoperfusion in Parkinson's disease with and without dementia measured with arterial spin labeling MRI. J Magn Reson Imaging 33, 803-807.

Kelleher, R.J., Soiza, R.L., 2013. Evidence of endothelial dysfunction in the development of Alzheimer's disease: Is Alzheimer's a vascular disorder? Am J Cardiovasc Dis 3, 197-226.

Kimura, Y., Oku, N., Kajimoto, K., Katoh, H., Tanaka, M.R., Takasawa, M., Imaizumi, M., Kitagawa, K., Hori, M., Hatazawa, J., 2006. Diastolic blood pressure influences cerebrovascular reactivity measured by means of 123I-iodoamphetamine brain single photon emission computed tomography in medically treated patients with occlusive carotid or middle cerebral artery disease. Ann Nucl Med 20, 209-215.

Kish, S.J., Shannak, K., Rajput, A., Deck, J.H., Hornykiewicz, O., 1992. Aging produces a specific pattern of striatal dopamine loss: implications for the etiology of idiopathic Parkinson's disease. J Neurochem 58, 642-648.

Knottnerus, I.L., Ten Cate, H., Lodder, J., Kessels, F., van Oostenbrugge, R.J., 2009. Endothelial dysfunction in lacunar stroke: a systematic review. Cerebrovasc Dis 27, 519-526.

Kortekaas, R., Leenders, K.L., van Oostrom, J.C., Vaalburg, W., Bart, J., Willemsen, A.T., Hendrikse, N.H., 2005. Blood-brain barrier dysfunction in parkinsonian midbrain in vivo. Ann Neurol 57, 176-179.

L'Episcopo, F., Tirolo, C., Testa, N., Caniglia, S., Morale, M.C., Impagnatiello, F., Marchetti, B., 2011. Switching the microglial harmful phenotype promotes lifelong restoration of subtantia nigra dopaminergic neurons from inflammatory neurodegeneration in aged mice. Rejuvenation Res 14, 411-424.

Lavini, C., Verhoeff, J.J., 2010. Reproducibility of the gadolinium concentration measurements and of the fitting parameters of the vascular input function in the superior sagittal sinus in a patient population. Magn Reson Imaging 28, 1420-1430.

Lee, S.J., Kim, J.S., Lee, K.S., An, J.Y., Kim, W., Kim, Y.I., Kim, B.S., Jung, S.L., 2009. The severity of leukoaraiosis correlates with the clinical phenotype of Parkinson's disease. Arch Gerontol Geriatr 49, 255-259.

Lesage, S., Brice, A., 2009. Parkinson's disease: from monogenic forms to genetic susceptibility factors. Hum Mol Genet 18, R48-59.

Levine, R.L., Stadtman, E.R., 2001. Oxidative modification of proteins during aging. Exp Gerontol 36, 1495-1502.

Lezi, E., Swerdlow, R.H., 2012. Mitochondria in neurodegeneration. Adv Exp Med Biol 942, 269-286.

Lill, C.M., Roehr, J.T., McQueen, M.B., Kavvoura, F.K., Bagade, S., Schjeide, B.M., Schjeide, L.M., Meissner, E., Zauft, U., Allen, N.C., Liu, T., Schilling, M., Anderson, K.J., Beecham, G., Berg, D., Biernacka, J.M., Brice, A., DeStefano, A.L., Do, C.B., Eriksson, N., Factor, S.A., Farrer, M.J., Foroud, T., Gasser, T., Hamza, T., Hardy, J.A., Heutink, P., Hill-Burns, E.M., Klein, C., Latourelle, J.C., Maraganore, D.M., Martin, E.R., Martinez, M., Myers, R.H., Nalls, M.A., Pankratz, N., Payami, H., Satake, W., Scott, W.K., Sharma, M., Singleton, A.B., Stefansson, K., Toda, T., Tung, J.Y., Vance, J., Wood, N.W., Zabetian, C.P., Young, P., Tanzi, R.E., Khoury, M.J., Zipp, F., Lehrach, H., Ioannidis, J.P., Bertram, L., 2012. Comprehensive research synopsis and systematic meta-analyses in Parkinson's disease genetics: The PDGene database. PLoS Genet 8, e1002548.

Lipton, S.A., 2005. The molecular basis of memantine action in Alzheimer's disease and other neurologic disorders: low-affinity, uncompetitive antagonism. Curr Alzheimer Res 2, 155-165.

Liu, Y., Zhu, X., Feinberg, D., Guenther, M., Gregori, J., Weiner, M.W., Schuff, N., 2012. Arterial spin labeling MRI study of age and gender effects on brain perfusion hemodynamics. Magn Reson Med 68, 912-922.

Longstreth, W.T., Jr., Arnold, A.M., Manolio, T.A., Burke, G.L., Bryan, N., Jungreis, C.A., O'Leary, D., Enright, P.L., Fried, L., 2000. Clinical correlates of ventricular and sulcal size on cranial magnetic resonance imaging of 3,301 elderly people. The Cardiovascular Health Study. Collaborative Research Group. Neuroepidemiology 19, 30-42.

Luk, K.C., Kehm, V., Carroll, J., Zhang, B., O'Brien, P., Trojanowski, J.Q., Lee, V.M., 2012. Pathological alpha-synuclein transmission initiates Parkinson-like neurodegeneration in nontransgenic mice. Science 338, 949-953.

Ma, Y., Huang, C., Dyke, J.P., Pan, H., Alsop, D., Feigin, A., Eidelberg, D., 2010. Parkinson's disease spatial covariance pattern: noninvasive quantification with perfusion MRI. J Cereb Blood Flow Metab 30, 505-509.

Machado, A., Herrera, A.J., Venero, J.L., Santiago, M., de Pablos, R.M., Villaran, R.F., Espinosa-Oliva, A.M., Arguelles, S., Sarmiento, M., Delgado-Cortes, M.J., Maurino, R., Cano, J., 2011. Inflammatory Animal Model for Parkinson's Disease: The Intranigral Injection of LPS Induced the Inflammatory Process along with the Selective Degeneration of Nigrostriatal Dopaminergic Neurons. ISRN Neurol 2011, 476158.

Mai, V.M., Berr, S.S., 1999. MR perfusion imaging of pulmonary parenchyma using pulsed arterial spin labeling techniques: FAIRER and FAIR. J Magn Reson Imaging 9, 483-487.

Malek, N., Swallow, D.M., Grosset, K.A., Lawton, M.A., Marrinan, S.L., Lehn, A.C., Bresner, C., Bajaj, N., Barker, R.A., Ben-Shlomo, Y., Burn, D.J., Foltynie, T., Hardy, J., Morris, H.R., Williams, N.M., Wood, N., Grosset, D.G., 2015. Tracking Parkinson's: Study Design and Baseline Patient Data. J Parkinsons Dis 5, 947-959.

Mastaglia, F.L., Johnsen, R.D., Kakulas, B.A., 2002. Prevalence of stroke in Parkinson's disease: a postmortem study. Mov Disord 17, 772-774.

McGeer, P.L., Itagaki, S., Boyes, B.E., McGeer, E.G., 1988. Reactive microglia are positive for HLA-DR in the substantia nigra of Parkinson's and Alzheimer's disease brains. Neurology 38, 1285-1291.

Meissner, W.G., Frasier, M., Gasser, T., Goetz, C.G., Lozano, A., Piccini, P., Obeso, J.A., Rascol, O., Schapira, A., Voon, V., Weiner, D.M., Tison, F., Bezard, E., 2011. Priorities in Parkinson's disease research. Nat Rev Drug Discov 10, 377-393.

Melzer, T.R., Watts, R., MacAskill, M.R., Pearson, J.F., Rueger, S., Pitcher, T.L., Livingston, L., Graham, C., Keenan, R., Shankaranarayanan, A., Alsop, D.C., Dalrymple-Alford, J.C., Anderson, T.J., 2011. Arterial spin labelling reveals an abnormal cerebral perfusion pattern in Parkinson's disease. Brain 134, 845-855.

Meredith, G.E., Sonsalla, P.K., Chesselet, M.F., 2008. Animal models of Parkinson's disease progression. Acta Neuropathol 115, 385-398.

Mito, Y., Yoshida, K., Yabe, I., Makino, K., Hirotani, M., Tashiro, K., Kikuchi, S., Sasaki, H., 2005. Brain 3D-SSP SPECT analysis in dementia with Lewy bodies, Parkinson's disease with and without dementia, and Alzheimer's disease. Clin Neurol Neurosurg 107, 396-403.

Moody, D.M., Bell, M.A., Challa, V.R., 1990. Features of the cerebral vascular pattern that predict vulnerability to perfusion or oxygenation deficiency: an anatomic study. AJNR Am J Neuroradiol 11, 431-439.

Moody, D.M., Santamore, W.P., Bell, M.A., 1991. Does tortuosity in cerebral arterioles impair down-autoregulation in hypertensives and elderly normotensives? A hypothesis and computer model. Clin Neurosurg 37, 372-387.

Morale, M.C., Serra, P.A., L'Episcopo, F., Tirolo, C., Caniglia, S., Testa, N., Gennuso, F., Giaquinta, G., Rocchitta, G., Desole, M.S., Miele, E., Marchetti, B., 2006. Estrogen, neuroinflammation and neuroprotection in Parkinson's disease: glia dictates resistance versus vulnerability to neurodegeneration. Neuroscience 138, 869-878.

Morley, J.F., Duda, J.E., 2012. Parkinson's disease and the risk of cerebrovascular pathology. Mov Disord 27, 1471-1472.

Mueggler, T., Sturchler-Pierrat, C., Baumann, D., Rausch, M., Staufenbiel, M., Rudin, M., 2002. Compromised hemodynamic response in amyloid precursor protein transgenic mice. J Neurosci 22, 7218-7224.

Muftuoglu, M., Elibol, B., Dalmizrak, O., Ercan, A., Kulaksiz, G., Ogus, H., Dalkara, T., Ozer, N., 2004. Mitochondrial complex I and IV activities in leukocytes from patients with parkin mutations. Mov Disord 19, 544-548.

Murphy, K., Harris, A.D., Diukova, A., Evans, C.J., Lythgoe, D.J., Zelaya, F., Wise, R.G., 2011. Pulsed arterial spin labeling perfusion imaging at 3 T: estimating the number of subjects required in common designs of clinical trials. Magn Reson Imaging 29, 1382-1389.

Nalls, M.A., Plagnol, V., Hernandez, D.G., Sharma, M., Sheerin, U.M., Saad, M., Simon-Sanchez, J., Schulte, C., Lesage, S., Sveinbjornsdottir, S., Stefansson, K., Martinez, M., Hardy, J., Heutink, P., Brice, A., Gasser, T., Singleton, A.B., Wood, N.W., 2011. Imputation of sequence variants for identification of genetic risks for Parkinson's disease: a meta-analysis of genome-wide association studies. Lancet 377, 641-649.

Nanhoe-Mahabier, W., de Laat, K.F., Visser, J.E., Zijlmans, J., de Leeuw, F.E., Bloem, B.R., 2009. Parkinson disease and comorbid cerebrovascular disease. Nat Rev Neurol 5, 533-541.

Nataraj, A., Rajput, A.H., 2005. Parkinson's disease, stroke, and related epidemiology. Mov Disord 20, 1476-1480.

Nishimura, N., Schaffer, C.B., Friedman, B., Lyden, P.D., Kleinfeld, D., 2007. Penetrating arterioles are a bottleneck in the perfusion of neocortex. Proc Natl Acad Sci U S A 104, 365-370.

Nobili, F., Frisoni, G., Portet, F., Verhey, F., Rodriguez, G., Caroli, A., Touchon, J., Calvini, P., Morbelli, S., Carli, F., Guerra, U., Pol, L., Visser, P.-J., 2008. Brain SPECT in subtypes of mild cognitive impairment. Journal of Neurology 255, 1344-1353.

O'Kane, R.L., Vina, J.R., Simpson, I., Hawkins, R.A., 2004. Na+ -dependent neutral amino acid transporters A, ASC, and N of the blood-brain barrier: mechanisms for neutral amino acid removal. Am J Physiol Endocrinol Metab 287, E622-629.

O'Sullivan, M., Morris, R.G., Markus, H.S., 2005. Brief cognitive assessment for patients with cerebral small vessel disease. J Neurol Neurosurg Psychiatry 76, 1140-1145.

O'Sullivan, M., 2008. Leukoaraiosis. Practical Neurology 8, 26-38.

Ochudlo, S., Opala, G., Jasinska-Myga, B., Siuda, J., Nowak, S., 2003. [Inferior frontal region hypoperfusion in Parkinson disease with dementia]. Neurol Neurochir Pol 37 Suppl 5, 133-144.

Ogawa, S., Lee, T.M., Nayak, A.S., Glynn, P., 1990. Oxygenation-sensitive contrast in magnetic resonance image of rodent brain at high magnetic fields. Magn Reson Med 14, 68-78.

Ostergaard, L., Aamand, R., Gutierrez-Jimenez, E., Ho, Y.C., Blicher, J.U., Madsen, S.M., Nagenthiraja, K., Dalby, R.B., Drasbek, K.R., Moller, A., Braendgaard, H., Mouridsen, K., Jespersen, S.N., Jensen, M.S., West, M.J., 2013. The capillary dysfunction hypothesis of Alzheimer's disease. Neurobiol Aging 34, 1018-1031.

Ostergaard, L., Engedal, T.S., Moreton, F., Hansen, M.B., Wardlaw, J.M., Dalkara, T., Markus, H.S., Muir, K.W., 2016. Cerebral small vessel disease: Capillary pathways to stroke and cognitive decline. J Cereb Blood Flow Metab 36, 302-325.

Pantoni, L., Garcia, J.H., 1997. Pathogenesis of leukoaraiosis: a review. Stroke 28, 652-659.

Pardridge, W.M., 2005. Molecular biology of the blood-brain barrier. Mol Biotechnol 30, 57-70.

Perry, G., Nunomura, A., Hirai, K., Takeda, A., Aliev, G., Smith, M.A., 2000. Oxidative damage in Alzheimer's disease: the metabolic dimension. Int J Dev Neurosci 18, 417-421.

Piccini, P., Pavese, N., Canapicchi, R., Paoli, C., Del Dotto, P., Puglioli, M., Rossi, G., Bonuccelli, U., 1995. White matter hyperintensities in Parkinson's disease. Clinical correlations. Arch Neurol 52, 191-194.

Pillai, J.J., Zaca, D., 2012. Comparison of BOLD cerebrovascular reactivity mapping and DSC MR perfusion imaging for prediction of neurovascular uncoupling potential in brain tumors. Technol Cancer Res Treat 11, 361-374.

Popescu, B.O., Toescu, E.C., Popescu, L.M., Bajenaru, O., Muresanu, D.F., Schultzberg, M., Bogdanovic, N., 2009. Blood-brain barrier alterations in ageing and dementia. J Neurol Sci 283, 99-106.

Postuma, R.B., Dagher, A., 2006. Basal ganglia functional connectivity based on a meta-analysis of 126 positron emission tomography and functional magnetic resonance imaging publications. Cereb Cortex 16, 1508-1521.

Powers, W.J., Zazulia, A.R., 2010. PET in Cerebrovascular Disease. PET Clin 5, 83106.

Princz-Kranz, F.L., Mueggler, T., Knobloch, M., Nitsch, R.M., Rudin, M., 2010. Vascular response to acetazolamide decreases as a function of age in the arcA beta mouse model of cerebral amyloidosis. Neurobiol Dis 40, 284-292.

Przedborski, S., Vila, M., Jackson-Lewis, V., 2003. Neurodegeneration: what is it and where are we? J Clin Invest 111, 3-10.

Rektor, I., Goldemund, D., Sheardova, K., Rektorova, I., Michalkova, Z., Dufek, M., 2009. Vascular pathology in patients with idiopathic Parkinson's disease. Parkinsonism Relat Disord 15, 24-29.

Rost, N.S., Sadaghiani, S., Biffi, A., Fitzpatrick, K.M., Cloonan, L., Rosand, J., Shibata, D.K., Mosley, T.H., Jr., 2014. Setting a gold standard for quantification of leukoaraiosis burden in patients with ischemic stroke: the Atherosclerosis Risk in Communities Study. J Neurosci Methods 221, 196-201.

Sagare, A.P., Bell, R.D., Zhao, Z., Ma, Q., Winkler, E.A., Ramanathan, A., Zlokovic, B.V., 2013a. Pericyte loss influences Alzheimer-like neurodegeneration in mice. Nat Commun 4, 2932.

Sagare, A.P., Bell, R.D., Zlokovic, B.V., 2012. Neurovascular dysfunction and faulty amyloid beta-peptide clearance in Alzheimer disease. Cold Spring Harb Perspect Med 2.

Sagare, A.P., Bell, R.D., Zlokovic, B.V., 2013b. Neurovascular defects and faulty amyloid-beta vascular clearance in Alzheimer's disease. J Alzheimers Dis 33 Suppl 1, S87-100.

Sandhu, J.K., Gardaneh, M., Iwasiow, R., Lanthier, P., Gangaraju, S., Ribecco-Lutkiewicz, M., Tremblay, R., Kiuchi, K., Sikorska, M., 2009. Astrocyte-secreted GDNF and glutathione antioxidant system protect neurons against 6OHDA cytotoxicity. Neurobiol Dis 33, 405-414.

Sarkar, S., Raymick, J., Mann, D., Bowyer, J.F., Hanig, J.P., Schmued, L.C., Paule, M.G., Chigurupati, S., 2014. Neurovascular changes in acute, sub-acute and chronic mouse models of Parkinson's disease. Curr Neurovasc Res 11, 48-61.

Savitt, J.M., Dawson, V.L., Dawson, T.M., 2006. Diagnosis and treatment of Parkinson disease: molecules to medicine. J Clin Invest 116, 1744-1754.

Sawada, H., Hishida, R., Hirata, Y., Ono, K., Suzuki, H., Muramatsu, S., Nakano, I., Nagatsu, T., Sawada, M., 2007. Activated microglia affect the nigro-striatal dopamine neurons differently in neonatal and aged mice treated with 1-methyl-4-phenyl-1,2,3,6-tetrahydropyridine. J Neurosci Res 85, 1752-1761.

Schmidt, R., Berghold, A., Jokinen, H., Gouw, A.A., van der Flier, W.M., Barkhof, F., Scheltens, P., Petrovic, K., Madureira, S., Verdelho, A., Ferro, J.M., Waldemar, G., Wallin, A., Wahlund, L.O., Poggesi, A., Pantoni, L., Inzitari, D., Fazekas, F., Erkinjuntti, T., 2012. White matter lesion progression in LADIS: frequency, clinical effects, and sample size calculations. Stroke 43, 2643-2647.

Schuff, N., 2009. Potential role of high-field MRI for studies in Parkinson's disease. Mov Disord 24 Suppl 2, S684-690.

Scigliano, G., Ronchetti, G., Girotti, F., Musicco, M., 2008. Levodopa reduces risk factors for vascular disease in parkinsonian patients. Journal of Neurology 255, 1266-1267.

Scigliano, G., Ronchetti, G., Girotti, F., Musicco, M., 2009. Sympathetic modulation by levodopa reduces vascular risk factors in Parkinson disease. Parkinsonism Relat Disord 15, 138-143.

Shah, K., Desilva, S., Abbruscato, T., 2012. The role of glucose transporters in brain disease: diabetes and Alzheimer's Disease. Int J Mol Sci 13, 12629-12655.

Shimizu, H., Watanabe, E., Hiyama, T.Y., Nagakura, A., Fujikawa, A., Okado, H., Yanagawa, Y., Obata, K., Noda, M., 2007. Glial Nax channels control lactate signaling to neurons for brain [Na+] sensing. Neuron 54, 59-72.

Sohn, Y.H., Kim, J.S., 1998. The influence of white matter hyperintensities on the clinical features of Parkinson's disease. Yonsei Med J 39, 50-55.

Stanimirovic, D.B., Friedman, A., 2012. Pathophysiology of the neurovascular unit: disease cause or consequence? J Cereb Blood Flow Metab 32, 1207-1221.

Stevenson, S.F., Doubal, F.N., Shuler, K., Wardlaw, J.M., 2010. A systematic review of dynamic cerebral and peripheral endothelial function in lacunar stroke versus controls. Stroke 41, e434-442.

Stolp, H.B., Dziegielewska, K.M., 2009. Review: Role of developmental inflammation and blood-brain barrier dysfunction in neurodevelopmental and neurodegenerative diseases. Neuropathol Appl Neurobiol 35, 132-146.

Storkebaum, E., Quaegebeur, A., Vikkula, M., Carmeliet, P., 2011. Cerebrovascular disorders: molecular insights and therapeutic opportunities. Nat Neurosci 14, 1390-1397.

Struck, L.K., Rodnitzky, R.L., Dobson, J.K., 1990. Stroke and its modification in Parkinson's disease. Stroke 21, 1395-1399.

Sulzer, D., 2007. Multiple hit hypotheses for dopamine neuron loss in Parkinson's disease. Trends Neurosci 30, 244-250.

Tang, C.C., Poston, K.L., Dhawan, V., Eidelberg, D., 2010. Abnormalities in metabolic network activity precede the onset of motor symptoms in Parkinson's disease. J Neurosci 30, 1049-1056.

Tansey, M.G., Goldberg, M.S., 2010. Neuroinflammation in Parkinson's disease: its role in neuronal death and implications for therapeutic intervention. Neurobiol Dis 37, 510-518.

Teune, L.K., Renken, R.J., de Jong, B.M., Willemsen, A.T., van Osch, M.J., Roerdink, J.B., Dierckx, R.A., Leenders, K.L., 2014. Parkinson's disease-related perfusion and glucose metabolic brain patterns identified with PCASL-MRI and FDG-PET imaging. Neuroimage Clin 5, 240-244.

Thenganatt, M.A., Jankovic, J., 2014. Parkinson disease subtypes. JAMA Neurol 71, 499-504.

Ursino, M., 1991. Mechanisms of cerebral blood flow regulation. Crit Rev Biomed Eng 18, 255-288.

Van Den Eeden, S.K., Tanner, C.M., Bernstein, A.L., Fross, R.D., Leimpeter, A., Bloch, D.A., Nelson, L.M., 2003. Incidence of Parkinson's disease: variation by age, gender, and race/ethnicity. Am J Epidemiol 157, 1015-1022.

van Rooden, S.M., Colas, F., Martinez-Martin, P., Visser, M., Verbaan, D., Marinus, J., Chaudhuri, R.K., Kok, J.N., van Hilten, J.J., 2011. Clinical subtypes of Parkinson's disease. Mov Disord 26, 51-58.

Visser, M., Marinus, J., Stiggelbout, A.M., Van Hilten, J.J., 2004. Assessment of autonomic dysfunction in Parkinson's disease: the SCOPA-AUT. Mov Disord 19, 1306-1312.

Vitosevic, Z., Cetkovic, M., Vitosevic, B., Jovic, D., Rajkovic, N., Millisavljevic, M., 2005. [Blood supply of the internal capsule and basal nuclei]. Srp Arh Celok Lek 133, 41-45.

Volpicelli-Daley, L.A., Luk, K.C., Patel, T.P., Tanik, S.A., Riddle, D.M., Stieber, A., Meaney, D.F., Trojanowski, J.Q., Lee, V.M., 2011. Exogenous alpha-synuclein fibrils induce Lewy body pathology leading to synaptic dysfunction and neuron death. Neuron 72, 57-71.

Wahlund, L.O., Barkhof, F., Fazekas, F., Bronge, L., Augustin, M., Sjogren, M., Wallin, A., Ader, H., Leys, D., Pantoni, L., Pasquier, F., Erkinjuntti, T., Scheltens, P., 2001. A new rating scale for age-related white matter changes applicable to MRI and CT. Stroke 32, 1318-1322.

Wardlaw, J.M., Doubal, F., Armitage, P., Chappell, F., Carpenter, T., Munoz Maniega, S., Farrall, A., Sudlow, C., Dennis, M., Dhillon, B., 2009. Lacunar stroke is associated with diffuse blood-brain barrier dysfunction. Ann Neurol 65, 194-202.

Wardlaw, J.M., Doubal, F.N., Valdes-Hernandez, M., Wang, X., Chappell, F.M., Shuler, K., Armitage, P.A., Carpenter, T.C., Dennis, M.S., 2013a. Blood-brain barrier permeability and long-term clinical and imaging outcomes in cerebral small vessel disease. Stroke 44, 525-527.

Wardlaw, J.M., Smith, C., Dichgans, M., 2013b. Mechanisms of sporadic cerebral small vessel disease: insights from neuroimaging. Lancet Neurol 12, 483-497.

Wardlaw, J.M., Smith, E.E., Biessels, G.J., Cordonnier, C., Fazekas, F., Frayne, R., Lindley, R.I., O'Brien, J.T., Barkhof, F., Benavente, O.R., Black, S.E., Brayne, C., Breteler, M., Chabriat, H., Decarli, C., de Leeuw, F.E., Doubal, F., Duering, M., Fox, N.C., Greenberg, S., Hachinski, V., Kilimann, I., Mok, V., Oostenbrugge, R., Pantoni, L., Speck, O., Stephan, B.C., Teipel, S., Viswanathan, A., Werring, D., Chen, C., Smith, C., van Buchem, M., Norrving, B., Gorelick, P.B., Dichgans, M., 2013c. Neuroimaging standards for research into small vessel disease and its contribution to ageing and neurodegeneration. Lancet Neurol 12, 822-838.

Wardlaw, J.M., Valdes Hernandez, M.C., Munoz-Maniega, S., 2015. What are white matter hyperintensities made of? Relevance to vascular cognitive impairment. J Am Heart Assoc 4, 001140.

Weintraub, D., Mamikonyan, E., Papay, K., Shea, J.A., Xie, S.X., Siderowf, A., 2012. Questionnaire for Impulsive-Compulsive Disorders in Parkinson's Disease-Rating Scale. Mov Disord 27, 242-247.

Wijsman, E.M., Daw, E.W., Yu, X., Steinbart, E.J., Nochlin, D., Bird, T.D., Schellenberg, G.D., 2005. APOE and other loci affect age-at-onset in Alzheimer's disease families with PS2 mutation. Am J Med Genet B Neuropsychiatr Genet 132B, 14-20.

Williams-Gray, C.H., Evans, J.R., Goris, A., Foltynie, T., Ban, M., Robbins, T.W., Brayne, C., Kolachana, B.S., Weinberger, D.R., Sawcer, S.J., Barker, R.A., 2009. The distinct cognitive syndromes of Parkinson's disease: 5 year follow-up of the CamPaIGN cohort. Brain 132, 2958-2969.

Williams, A., 2002. Defining neurodegenerative diseases. BMJ 324, 1465-1466.

Winkler, E.A., Bell, R.D., Zlokovic, B.V., 2011. Central nervous system pericytes in health and disease. Nat Neurosci 14, 1398-1405.

Winkler, E.A., Sagare, A.P., Zlokovic, B.V., 2014. The pericyte: a forgotten cell type with important implications for Alzheimer's disease? Brain Pathol 24, 371-386.

Wolf, R.L., Alsop, D.C., McGarvey, M.L., Maldjian, J.A., Wang, J., Detre, J.A., 2003. Susceptibility contrast and arterial spin labeled perfusion MRI in cerebrovascular disease. J Neuroimaging 13, 17-27.

Wolf, R.L., Detre, J.A., 2007. Clinical neuroimaging using arterial spin-labeled perfusion magnetic resonance imaging. Neurotherapeutics 4, 346-359.

Wolk, D.A., Detre, J.A., 2012. Arterial spin labeling MRI: an emerging biomarker for Alzheimer's disease and other neurodegenerative conditions. Curr Opin Neurol 25, 421-428.

Yamagata, K., Tagami, M., Takenaga, F., Yamori, Y., Itoh, S., 2004. Hypoxia-induced changes in tight junction permeability of brain capillary endothelial cells are associated with IL-1beta and nitric oxide. Neurobiol Dis 17, 491-499.

Yang, P., Pavlovic, D., Waldvogel, H., Dragunow, M., Synek, B., Turner, C., Faull, R., Guan, J., 2015. String Vessel Formation is Increased in the Brain of Parkinson Disease. J Parkinsons Dis 5, 821-836.

Yasuda, T., Fukuda-Tani, M., Nihira, T., Wada, K., Hattori, N., Mizuno, Y., Mochizuki, H., 2007. Correlation between levels of pigment epithelium-derived factor and vascular endothelial growth factor in the striatum of patients with Parkinson's disease. Exp Neurol 206, 308-317.

Yezhuvath, U.S., Lewis-Amezcua, K., Varghese, R., Xiao, G., Lu, H., 2009. On the assessment of cerebrovascular reactivity using hypercapnia BOLD MRI. NMR Biomed 22, 779-786.

Zhang, L., Shimoji, M., Thomas, B., Moore, D.J., Yu, S.W., Marupudi, N.I., Torp, R., Torgner, I.A., Ottersen, O.P., Dawson, T.M., Dawson, V.L., 2005. Mitochondrial localization of the Parkinson's disease related protein DJ-1: implications for pathogenesis. Hum Mol Genet 14, 2063-2073.

Zhao, Z., Nelson, A.R., Betsholtz, C., Zlokovic, B.V., 2015. Establishment and Dysfunction of the Blood-Brain Barrier. Cell 163, 1064-1078.

Zlokovic, B.V., 2005. Neurovascular mechanisms of Alzheimer's neurodegeneration. Trends Neurosci 28, 202-208.

Zlokovic, B.V., 2008. The blood-brain barrier in health and chronic neurodegenerative disorders. Neuron 57, 178-201.

Zlokovic, B.V., 2011. Neurovascular pathways to neurodegeneration in Alzheimer's disease and other disorders. Nat Rev Neurosci 12, 723-738.

Chapter 2

The aim of this chapter is to establish the clinical characteristics of the entire IPD study population. This chapter is written in paper format, in keeping with the rest of the thesis yet it is simply a description of the cohort rather than hypothesis-driven research. To set the scene, a brief description of the methodology for the work will be described below. More specific methods are reported in the relevant subsequent chapters.

Location, regional neurosciences services and regional population characteristics

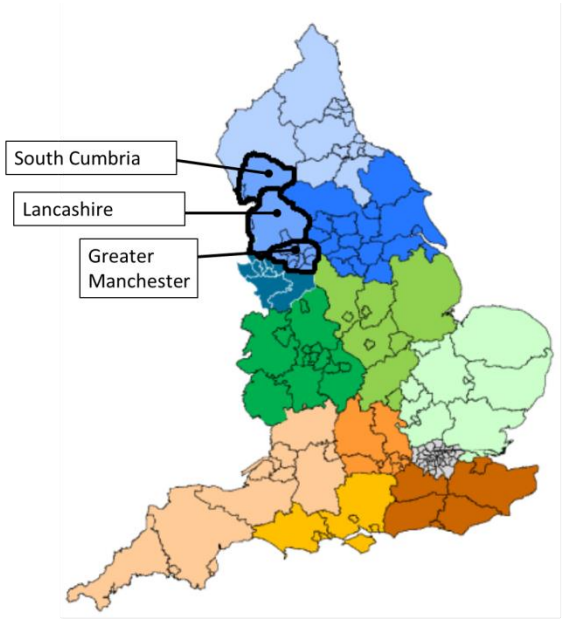

Figure 2.1 (modified from an image depicting the previous Department of Health Strategic Clinical Network footprints [until 2014])

Catchment areas for the regional neurosciences centres in Preston (Lancashire & South Cumbria) and Greater Manchester

Patient recruitment (described later) was from neurosciences services based at the regional neurosciences centres in Preston (at Lancashire Teaching Hospitals NHS Foundation Trust) (covering Lancashire & South Cumbria) and Greater Manchester (at Salford Royal Hospitals NHS Foundation Trust), corresponding to the previous Greater Manchester, Lancashire and South Cumbria Strategic Clinical Network footprint (prior to reconfiguration in 2016), as shown in Figure 2.1.

Lancashire Teaching Hospitals (LTH) NHS Foundation Trust, whose hospital sites include the Royal Preston Hospital (RPH) and the Chorley & South Ribble District General Hospital, provides general hospital services to approximately 390,000 people, and

regional services including neurosciences to a 1.6 million population in Lancashire and South Cumbria.

Salford Royal Hospitals NHS Foundation Trust (SRFT) runs Salford Royal Hospital, which provides general hospital services to approximately 250,000 people, and a number of regional services, including the Greater Manchester Neurosciences Centre which serves approximately 3.2 million people, principally within Greater Manchester.

Lancashire, South Cumbria and Greater Manchester together constitute approximately two-thirds of the total population of North West England, which is a very diverse region with rural and urban populations. Manchester is one of the most diverse cities in Europe. Overall the North West has above average deprivation, but has very affluent areas such as rural Lancashire and South Cumbria.

Clinical services

The neurology department at LTH has 11 consultant neurologists. There is an 18-bedded acute neurology ward and a day treatment centre.

The neurology department of the Greater Manchester Neurosciences Centre has approximately 30 consultant neurologists. There is a 26-bedded acute neurology unit and a 25-bedded neurology 5-day ward.

In both services a number of specialist nurses, including Parkinson's disease specialist nurses, working alongside the consultant neurologists.

Outpatient services for the two regional neurosciences services, include general neurology clinics and subspecialty (such as movement disorders) clinics, which are delivered at the RPH site and around Lancashire in Chorley, Blackpool, Lancaster, Blackburn and Burnley, and at the SRFT site and around the Greater Manchester region in central, north and south Manchester, Tameside, Stockport, Macclesfield, Trafford, Bolton, Leigh and Wigan.

Patient recruitment

The overwhelming majority of patient recruitment was from the LTH IPD population. This was made possible through the support of the PD nurses based as LTH who helped to identify suitable patients from their database of over 600 patients. In terms of recruitment from SRFT the PD nurse based at Macclesfield and three consultants based at SRFT helped identify potential patients. The clinical phenotype was judged based on clinical letters, and formally assessed during the visit (in 6 cases the patients were classified as 'intermediate' as opposed to either the PIGD or TD phenotype). Suitable patients identified were contacted by telephone. The study was explained, if interest

expressed a patient information sheet was sent and the patient subsequently contacted on a further occasion. If interested and able to participate in the study, arrangements were made to attend either SRFT for the preliminary work or WTCRF for the main study to complete the assessments and imaging. For those selected, if it was felt both the clinical assessments and imaging would be too burdensome on the same day, a home visit was arranged to complete the clinical assessments but this was very rarely needed.

Inclusion/Exclusion Criteria

For IPD patients a clinical diagnosis of IPD fulfilling UK Parkinson's disease society (UKPDS) Brain Bank (BB) criteria was required. This required the presence of bradykinesia, plus at least one of 4-6 Hz tremor, muscular rigidity and postural instability. For CP subjects the requirements included: being aged 50 or over with evidence of symptomatic CVD (TIA/stroke), over 6 months since onset, without evidence of parkinsonism, providing written informed consent. For CN subjects, age over 50 without known CVD or Parkinsonism was the requirement.

Exclusion criteria were:-

- features suggesting vascular parkinsonism (past history of repeated strokes leading to stepwise progression of parkinsonian features early symmetrical lower body involvement and failure to respond to dopaminergic therapy)
- History of TIA or stroke (apart from the CP group).
- Focal neurological signs (other than those due to IPD).
- Cognitive dysfunction sufficient to interfere with daily activities.
- Any other active significant medical condition likely to prevent completion of procedures.
- Evidence of infection within the previous 6 weeks
- Presence of a concomitant inflammatory condition (e.g. inflammatory arthritis, colitis, psoriasis)

In addition to the above exclusion criteria, only potential participants whom were felt to withstand the logistics of an hour long MRI protocol were recruited (i.e. not claustrophobic/significant anxiety, able to lie flat with head still etc.). Unfortunately due to the strict inclusion/exclusion criteria and logistics of having an MRI scan many patients who expressed interest were unable to participate.

After this brief introduction of the patient population and recruitment, what follows is the main chapter dedicated to a description of the clinical characteristics of the non-motor

features of, where possible, the entire IPD population studied for this thesis (i.e. preliminary and main study). As the study design was modified and the team changed throughout the process, a small amount of data from the preliminary work is missing. The clinical scales for the preliminary work were administered by a psychiatrist trainee Dr Vivek Tharaken and for the main study by the author. The author analysed and interpreted the data and drafted and revised the paper, with guidance from Drs Emsley and Parkes.

Non-motor Symptoms of IPD Phenotypes – Comparisons with Cerebrovascular Disease

Title page:

Non-motor Symptoms of IPD Phenotypes – Comparisons with CVD

Sarah Al-Bachari[1,2]

Iracema Leroi[3]

Laura M Parkes[2]

Hedley CA Emsley[4,5]

[1]Department of Neurology, Salford Royal NHS Foundation Trust, Salford , UK; [2] Centre for Imaging Science, Institute of Population Health, University of Manchester, UK; [3] Institute of Brain, Behaviour and Mental Health, University of Manchester, UK; [4]Faculty of Medical and Human Sciences, University of Manchester, UK; [5]Department of Neurology, Royal Preston Hospital, Preston, UK;

Corresponding author: Dr Sarah Al-Bachari

Address: Imaging and Data Sciences, University of Manchester, Stopford Building, Oxford Road, Manchester M13 9PT

Telephone: 0161 306 6000 Email: sarahalbachari@yahoo.co.uk

Support:

Sydney Driscoll Neuroscience Foundation; University of Manchester (Biomedical Imaging Institute) and Medical Research Council Studentship; Lancashire Teaching Hospitals NHS Foundation Trust & Lancaster University.

Headline:

Non-motor Symptoms in IPD phenotypes show similarities to CVD

Abbreviations:

AMB – aberrant motor behaviours, CN – control negative, CP - control positive, CVD - cerebrovascular disease, DS – digit span, DSST – digit symbol substitution test, H&Y – Hoehn and Yahr, IPD - idiopathic Parkinson's disease, L-dopa - levodopa, LEDD - Levodopa equivalent dose, LTH – Lancashire teaching hospitals, MoCA- Montreal cognitive assessment, NMS - non-motor symptoms, NPI - neuropsychiatric inventory, PIGD - Postural instability and gait disorder, QUIPS- Questionnaire for impulsive-compulsive disorders in Parkinson's , ROI - region of interest, SCOPA-AUT - Scales for Outcomes in Parkinson's disease – Autonomic, SRFT- Salford Royal Foundation Trust, SVD – small vessel disease, TD - tremor dominant, TIA – transient ischaemic attach, TMT-B –trial making test B, UKPDS BB - United Kingdom Parkinson's Disease Society Brain Bank, UPDRS - Unified Parkinson's Disease Rating Scale, WTCRF - Wellcome Trust Clinical Research Facility

Abstract

Over recent years, the non-motor symptoms (NMS) of idiopathic Parkinson's disease (IPD) including cognitive, neuropsychiatric features and autonomic dysfunction have become increasingly recognised; the management of which is now considered to be an 'unmet need' in IPD. The postural instability and gait disorder (PIGD) phenotype has been associated with greater NMS, with postulations that varying pathophysiologies underlie the different phenotypes. Vascular changes are increasingly recognised as players in the pathophysiology of IPD.

48 IPD participants (24 [PIGD; mean ± SD age 70.0 ± 7.6 years], 18 tremor dominant [TD; mean ± SD age 68.1 ± 7.2 years] and 6 intermediates), 32 control negative (CN; mean ± SD age 66.8 ± 7.2 years) without CVD and 18 control positive (CP; mean ± SD age 70.1 ± 8.0 years) with CVD underwent a battery of clinical scales. All groups were matched for age.

Results revealed a similar pattern of cognitive dysfunction in the IPD and CP groups with deficits in executive function compared to CN, with the PIGD group being the most affected. This highlights the potential differences in NMS within IPD phenotypes with a similar pattern to patients with CVD.

Five key words:
NMS, IPD phenotypes, CVD, cognition

2.1 Introduction

It has become increasingly recognised that within the umbrella term of IPD a wide range of motor and non-motor features exist (Chaudhuri et al., 2006). The non-motor symptoms (NMS) of IPD encompass a range of conditions from mild cognitive impairment (MCI) and dementia to anxiety and apathy to autonomic features and sleep disturbance (Aarsland et al., 2007; Aarsland et al., 1999; Leroi et al., 2012; Malek et al., 2015). Patterns of MCI and dementia are felt to be IPD specific, often present at diagnosis and are rather heterogeneous (Williams-Gray et al., 2009). A range of neuropsychiatric and autonomic symptoms are important markers of prognosis and important defining features of IPD motor sub-types (Marras and Chaudhuri, 2016). NMS are recognised to have a significant impact on quality of life and distress in IPD and have thus been highlighted as a '*clinically unmet need in IPD'*, demanding further research to aid understanding of the nature of the beast (Todorova et al., 2014).

This has led to multiple large national longitudinal studies to help define, explain the pathophysiology and understand these variations (Hu et al., 2014a; Malek et al., 2015; Williams-Gray et al., 2013). With such insight, it has become clearly apparent that neuroimaging studies are needed to help explain and track the pathogenesis of IPD and identify pathological differences particularly between phenotypic subgroups (Malek et al., 2015).

Both clinical and preclinical studies alike recognise the multifactorial nature of neurodegeneration, with evolving emphasis on the contribution of vascular dysfunction (Foltynie and Kahan, 2013; Grammas et al., 2011; Riess and Kruger, 1999). The Tracking Parkinson's study has observed a relationship between vascular risk factors and IPD postulating a potentially genome wide association of IPD and stroke, linking vascular risk factors to oxidative stress (Becker et al., 2010; Malek et al., 2015). This only adds further weight to the emerging '*vascular hypothesis'* of neurodegeneration which preclinical studies have provided (Nelson et al., 2015; Zlokovic, 2011).

In this study a battery of clinical assessments have been performed on the two major IPD motor phenotypes, tremor dominant (TD) and postural instability and gait disorder (PIGD) groups and comparisons have been made with a control negative (CN) and control positive (CP) group with and without known cerebrovascular disease (CVD) respectively. The purpose of which is to establish the clinical characteristics of this study group.

2.2 Methods

2.21 Participants

Relevant approvals were obtained including ethics (North West – Preston Research Ethics Committee), research governance and local university approvals**.** Recruitment of IPD patients was from Lancashire Teaching Hospitals (LTH) and Salford Royal Foundation Trust (SRFT). Eligibility criteria for IPD participants were a clinical diagnosis of IPD fulfilling UK Parkinson's disease society (UKPDS) brain bank (BB) criteria (http://www.ncbi.nlm.nih.gov/projects) without known clinical CVD (no history of TIA or stroke) or dementia (Emre et al., 2007). All IPD patients were selected based on a diagnosis of IPD without a diagnosis of dementia, they were screened and selected only if any deficit they had was not sufficient to interfere significantly with functional independence, although subtle difficulties on complex functional tasks were allowed (Litvan et al., 2011). Participants with CVD, the control positive (CP) group were recruited from patients at LTH with a diagnosis of stroke or transient ischaemic attack (TIA) within the previous 2 years (at least 3 months prior to recruitment). Controls without a history of either IPD or clinical CVD, the control negative (CN) group were also recruited. All groups were matched for age. All participants were required to provide written informed consent and had capacity to do so. IPD phenotype was assessed using the Unified Parkinson's Disease Rating Scale (UPDRS) (http://www.mdvu.org/library/ratingscales/pd/updrs.pdf). Participants were further classified into three subtypes (TD, PIGD, intermediate) by Jankovic's method (Jankovic et al., 1990). Disease severity was measured using the Hoehn and Yahr rating scale (Hoehn and Yahr, 1967). Routine clinical baseline data were also recorded and the levodopa equivalent doses (LEDD) calculated (Tomlinson et al., 2010).

A battery of standardised previously validated clinical scales were administered, these included the Montreal Cognitive Assessment (MoCA) tool (www.MoCAtest.org). A MoCA score less than 26, in addition to level 1 criteria of the PD-MCI criteria was considered as mild cognitive impairment (MCI) (Litvan et al., 2011). In order to identify MCI secondary to small vessel disease (SVD), a brief cognitive assessment tool for patients with cerebral SVD was applied (O'Sullivan et al., 2005). This tool is sensitive to executive/attentional deficits and attempts to discriminate from cognitive effects of healthy aging or large vessel disease. The elements which were assessed included the:- trail making test B (TMT-B), a test of working memory; phonemic fluency for words starting with the letters F, A and S (FAS) for 1 minute (each felt to be strongly reflective of executive function and memory retrieval); digit span (DS) test, reflective of executive function (Owen et al.,

1992; Whiteside et al., 2016) and WAIS-R digit symbol substitution test (DSST) a test of IQ and executive function. Apart from TMT-B, scaled scores were used. An ad hoc sub analysis of cube copying and clock drawing test (taken from MoCA scales) was performed, to help to tease out potential posteriorly based cognitive dysfunction (cube copying) from the more anterior dysfunction (clock drawing test) (Paula et al., 2013).

To demonstrate the profile of neuropsychiatric symptoms in IPD the 12-item Neuropsychiatric Inventory (NPI) was administered to all participants, as no participants had carers the questions were directed at the participant often with a family member present (Cummings, 1997). The mean scores were calculated as outlined in previous studies (Aarsland et al., 2007).

Autonomic function was measured using the scales for outcomes in Parkinson's disease - autonomic (SCOPA-AUT) questionnaire; a 23 part questionnaire divided into six domains (Visser et al., 2004). Impulsivity was measured using the Questionnaire for Impulsive-Compulsive Disorders in Parkinson's Disease-Rating Scale (QUIP-RS); a rating scale designed to measure severity of symptoms and support a diagnosis of impulse control disorders and related disorders in IPD (Weintraub et al., 2012).

Some patients (14 IPD and 14 controls) were taken from a similar pilot study, yet only overall MoCA scores and all components of the brief cognitive assessment tool were available for this group.

2.22 Data Analysis

All analyses of the demographic and cognitive scales were performed to consider differences between the IPD group as a whole and the CN and CP groups respectively and between the PIGD and TD groups. Analysis was using unpaired Student t-test with p-value set at < 0.05. For binary results, Pearson's Chi Squared test was employed again with p-value < 0.05.

2.3 Results

Forty eight IPD subjects were recruited (18 TD, 24 PIGD and 6 intermediates), 18 CP subjects with CVD (mean time, in years, since diagnosis 1.1±0.7) and 32 CN (table 2.1).

All groups were matched for age; a difference in genders between the CN group and the other groups was observed. IPD severity (as measured by H+Y but not UPDRS motor score) and LEDD score varied between the IPD phenotypes, as expected and provides validation of the clinical phenotype. CVD risk factors were statistically higher in the CVD group when compared to CN and IPD.

	CN (n=32)	CP (n=18)	All IPD (n=48)	p value (IPD Vs. CN)	p value (IPD Vs. CP)	PIGD (n=24)	TD (n=18)	p value (PIGD Vs. TD)
n (F:M)	17:15	4:14	12:36	n/a	n/a	5:19	7:13	n/a
Age: years: mean (SD) [range]	66.8 (7.2); [52-85]	70.1 (8.0); [53-84]	69.1 (7.9); [52-85]	0.46	0.5	70.0 (7.6); [58-89]	68.1 (7.2); [52-80]	0.39
No. of CV RF: mean (SD)	1.5 (1.1)	3.1 (1.1)	1.6 (1.5)	0.38	0.0001	1.6 (1.4)	1.6 (1.6)	0.9
Disease Duration: years mean (SD)	n/a	1.1 (0.7)	7.4 (4.4)	n/a	n/a	9.1 (4.5)	5.29 (3.5)	0.003
Hoehn & Yahr Score: mean (SD)	n/a	n/a	2.6 (1.0)	n/a	n/a	3.2 (0.8)	1.8 (0.7)	<0.0001
UPDRS 111 Score: mean (SD)	n/a	n/a	30.2 (11.8)	n/a	n/a	29.9 (21.1)	27.1 (10.3)	0.09
PIGD Score: mean (SD)	n/a	n/a	6.7 (4.8)	n/a	n/a	9.2 (4.6)	1.8 (1.5)	n/a
Tremor Score: mean (SD)	n/a	n/a	6.0 (5.2)	n/a	n/a	2.8 (3.0)	9.2 (4.6)	n/a
LEDD Score (mg): mean (SD)	n/a	n/a	593.0 (342)	n/a	n/a	785.9 (310.1)	370.0 (247.8)	<0.0001
MoCA: mean (SD)	28 (2.2)	25.4 (3.3)	25.2 (3.8)	<0.0001	0.85	23.8 (3.8)	27 (2.7)	0.002
MCI (%)	2 (6.3)	9 (50)	19 (39)	0.001	0.396	16 (66.7)	3 (16.7)	0
Phonemic Fluency (FAS): mean (SD)	61.1 (28.8)	39.2 (31.1)	40.4 (26.7)	0.002	0.89	31.1 (28.3)	53.2 (20.0)	0.005
DSST: mean (SD)	11.5 (2.6)	8.5 (3.2)	7.2 (3.5)	<0.0001	0.48	6.25 (3.5)	9.3 (2.3)	0.002
DS total score: mean (SD)	12.3 (3.1)	11.1 (3.4)	11.8 (2.6)	0.5	0.38	10.9 (2.6)	12.8 (2.4)	0.4
Trail Making B: mean (SD)	89.7 (47.6) 3 U	130.3 (70.0)	137.6 (76.4) 10 U	0.002	0.73	146.8 (61.6) 7 U	137.4 (95.1) 3 U	0.74
Cube copying score : mean (SD)	0.87 (0.35) n=30	0.67 (0.49) n=18	0.60 (0.48) n=42	0.017	0.216	0.47 (0.51) n=19	0.80 (0.38) n=15	0.035
Clock drawing score[2]: mean (SD)	2.97 (0.18)	2.89 (0.32)	2.46 (0.87)	0.021	0.09	2.37 (1.0)	2.7 (073)	0.269

Table 2.1: Demographics and clinical characteristics of the study group. DS – digit span; DSST – digit symbol substitution test; LEDD - levodopa equivalent daily dose; MoCA- Montreal cognitive assessment tool; MCI – mild cognitive impairment (based on level 1 MDS criteria); TMT-B; trial making test part B; U- unable to complete TMT-B; UPDRS 111 –unified Parkinson's disease rating scale motor score. Analysis using Student's t test apart from the MCI comparisons, cube copying score and clock drawing score for which Pearson's Chi Squared test was used.

[2] Same numbers per group as for cube copying score

2.31 Cognitive Scales

Two (6.3 %) CN participants fulfilled criteria for MCI compared to 19 (39.6%) IPD; 16 (67%) of whom were of the PIGD subgroup and 3 (16.6%) in the TD subgroup. Nine of the 18 (50%) CP participants fulfilled MCI criteria. The IPD group had significantly more deficits in all the cognitive scales apart from DS total score, compared to CN. There were no significant differences between the scores of the IPD and CP groups, although differences in the clock drawing test neared significance. There were significant subgroup differences in the FAS VF, cube copying (but not clock drawing) and DSST scores with poorer performance in the PIGD compared to the TD group.

Due to the differences in disease duration and LEDD score, the PIGD patients with longer than 10 years' disease duration were removed. This resulted in 17 PIGD patients compared to 18 TD. They remained matched for age, gender, cerebrovascular risk factors and were matched for LEDD score ($p = 0.81$), disease duration ($p = 0.91$) and UPDRS score ($p = 0.39$). Again no differences in DS total score were identified ($p = 0.07$), but differences in MoCA ($p = 0.002$), DSST ($p = 0.008$) and cube copying ($n=14$ per group, $p < 0.0001$) remained in this analysis of matched groups, in a similar pattern to the analysis of unmatched groups. Differences in VF and TMT B no longer reached significance ($p = 0.19$ and $p = 0.81$ respectively), although there were 6 PIGD compared to 3 TD who were unable to complete the TMT B task.

2.32 NPI

Within the IPD group, 13 patients (35.1%) scored on the NPI (mean disease duration of 7.62 years and mean LEDD score 704.9). Nine (52.9%) were of the PIGD compared to only 2 TD (13.3%) patients and 2 intermediates (Table 2.2). Sleep disturbance was the most commonly reported complaint (in over 50% of the PIGD group), followed by depression (21.6%), apathy (16.2%), anxiety (13.6%), irritability (13.6%) and disinhibition (5.4%). Eight CP (44.4%) patients scored positively in the NPI, with generally lower scores being reported in the CP group apart from apathy which had an equal distribution. Only 3 (15%) of the CN group scored positively on the NPI.

	CN (n=20)	CP (n=18)	All IPD (n=37)	PIGD (n=17)	TD (n=15)	Intermediate (n=4)
Delusions >0 n (%) >/= 4 n (%)	0	0	0	0	0	0
Hallucinations >0 n (%) ≥4 n (%)	0	0	6 (16.2) 2 (5.4)	4 (22.2) 2 (11.1)	0 0	2 (50) 0
Agitation/aggression >0 n (%) ≥4 n (%)	0	1 (5.6) 0	5 (13.6) 1 (2.7)	4 (22.2) 0	0	1 (25) 0
Depression >0 n (%) ≥4 n (%)	1 1 (5)	3 (16.7) 1 (5.6)	8 (21.6) 3 (8.1)	6 (33.3) 3 (16.7)	0 0	2 (50) 0
Anxiety >0 n (%) ≥4 n (%)	2 (10) 0	2 (11.1) 1 (5.6)	5 (13.6) 4 (10.8)	5 (27.8) 4 (22.2)	0 0	0 0
Euphoria >0 n (%) ≥4 n (%)	0	0	0	0	0	0
Apathy >0 n (%) ≥4 n (%)	3 (15) 2 (10)	3 (16.7) 3 (16.7)	6 (16.2) 5 (13.6)	5 (27.8) 4 (22.2)	0 0	1 (25) 1 (25)
Disinhibition >0 n (%) ≥4 n (%)	0	0	2 (5.4) 0	2 (11.1) 0	0	0
Irritability/lability >0 n (%) ≥4 n (%)	1 (5) 0	3 (16.7) 1	5 (13.6) 2 (5.4)	3 (16.7) 1 (5.6)	0 0	2 (50) 0
AMB >0 n (%) ≥4 n (%)	0	0	1 (2.7) 0	1 (5.6) 0	0	0
Sleep >0 n (%) ≥4 n (%)	2 (10) 1 (5)	5 (27.8) 4 (22.2)	13 (35.1) 8 (21.6)	10 (55.6) 6 (33.3)	1 (6.7) 0	2 (50) 2 (50)
Appetite >0 n (%) ≥4 n (%)	1 (5) 1 (5)	2 (11.1) 2 (11.1)	5 (13.6) 2 (5.4)	3 (16.7) 1 (5.6)	3 (20) 1 (6.7)	2 (50) 2 (50)
Total NPI Mean (SD)	2.1 (5.0)	4.7 (7.1)	6.7 (8.4)	10.4 (10.5)	n/a (only 1 patient)	5.3

Table 2.2: Neuropsychiatric Inventory item scores in the total group. Mean domain scores (frequency x severity) of the NPI items. >0 n (%) indicates the proportion with non-zero score, ≥4 n (%) indicates the proportion with score ≥4. AMB - aberrant motor behaviour.

2.33 QUIPS and SCOPA-AUT

Five PIGD compared to 1 TD patient had features of impulsivity, as measured by QUIPS, with the majority of the impulsivity features being increased interest in sex, hobbyism and punding (Table 2.3). No CP patients and one CN subject displayed features of impulsivity. Two of the 6 IPD patients exhibiting features of impulsivity had LEDD scores above the mean for that phenotype.

The PIGD group exhibited the highest scores in all domains of the SCOPA-AUT compared to the other groups, with similar distributions of features between all the groups.

Variable n (%)	**CN (n=20)**	**CP (n=18)**	**All IPD (n=37)**	**PIGD (n=18)**	**TD (n=15)**
Impulsivity					
Gambling	0	0	1 (2.7)	1 (5.6)	0
Sex	0	0	4 (10.8)	4 (22.2)	0
Buying	1 (5)	0	1 (2.7)	1 (5.6)	0
Eating	0	0	2 (5.4)	1 (5.6)	1 (6.7)
Medication	0	0	0	0	0
Hobbyism	0	0	4 (10.8)	3 (16.7)	1 (6.7)
Punding	0	0	3 (8.1)	3 (16.7)	0
Walkabout	0	0	0	0	0
One or more	1	0	6 (16.2)	5 (27.8)	1 (6.7)
SCOPA-AUT					
Gastrointestinal	0.8 (1.2)	1.2 (1.8)	4.5 (3.4)	5.8 (3.4)	2.6 (2.7)
Urinary	3.4 (2.3)	4.4 (3.4)	6.3 (3.9)	7.3 (4.4)	3.6 (6.2)
Cardiovascular	0.2 (0.4)	0.9 (1.1)	0.6 (1.1)	1.1 (1.2)	0.8 (0.8)
Thermoregulatory	0.9 (1.2)	0.9 (1.3)	1.2 (1.4)	1.5 (1.5)	0.7 (1.0)
Pupillomotor	0.3 (0.8)	0.3 (0.8)	0.5 (0.6)	0.4 (0.5)	0.3 (0.5)
Sexual	0.5 (1.5)	1.1 (2.0)	2.4 (2.5)	3.4 (2.8)	1.2 (2.0)
Constipation	0.3 (0.8)	0.6 (1.1)	2.6 (2.3)	3.4 (2.4)	1.1 (1.1)
Total Autonomic Score	5.6 (4.1)	8.2 (5.0)	14.9 (8.6)	18.6 (7.4)	9.7 (8.0)

Table 2.3: Impulsivity and autonomic features in each group. Quips scale for impulsivity and SCOPA-AUT for autonomic dysfunction (Visser et al., 2004). SCOPA-AUT based on mean (SD) of total scores for each domain.

2.4 Discussion

The results highlight the cognitive, neuropsychiatric and autonomic morbidity in IPD, with the greatest burden appearing in the PIGD group. This chapter simply provides a description of the study cohort with numbers being too small for any epidemiological associations to be hypothesised.A difference in executive function between the IPD and CN groups has been demonstrated with no significant difference between IPD and the CP group in any of the cognitive domains. This suggests the cognitive pattern observed in IPD is at least comparable to that of cerebrovascular disease. As there was significantly greater burden globally on most of the cognitive scales in the PIGD by comparison with the TD groups, it would suggest that there is greater similarity in pattern of cognitive dysfunction between the PIGD and CP groups than between the PIGD and TD groups.

Large longitudinal studies have teased out two main cognitive deficits in IPD, the more common 'frontostriatal' (executive) deficit and a 'posterior-cortical' deficit (which is more likely to lead to global cognitive decline) with 'posterior-cortical' cognitive deficit felt to probably reflect non dopaminergic cortical Lewy body disease and more associated with the PIGD group (Williams-Gray et al., 2009). We used cube copying as a means of measuring posterior cognitive function, and there was a clear increased burden in the PIGD compared to the TD group, with results again comparable to the CP group. Unfortunately, as only cube copying was used as a measure of posterior cognitive deficit the burden of posterior cognitive decline may not be fully appreciated in this study and further, perhaps prospective, data with a battery of scales measuring posterior cognitive function is warranted. In addition it has recently become recognised that cognitive decline associated with SVD is also quite heterogeneous and more global than previously appreciated, warranting a more comprehensive battery of scales (Kloppenborg et al., 2014; O'Sullivan, 2010). Nonetheless, these data have demonstrated the burden of executive dysfunction in the PIGD group which is similar to that of known CVD (the CP group).

The NPI scores across a range of neuropsychiatric symptoms were overwhelmingly higher in the PIGD group, although it is difficult to unpick the influence of LEDD scores and disease duration which were generally higher than that of the TD group. A recent meta-analysis of neuropsychiatric symptoms in IPD revealed depression (median prevalence: 29.8%; range: 6.8–63.3%), sleep disturbances (median prevalence: 18.3%; range: 7.9–49.0%), and apathy (median prevalence: 15.2%; range: 2.3–18.5%); a not dissimilar profile to this study. Our study found sleep disturbances to be the most common neuropsychiatric complaint, in keeping with other studies (Kohler et al., 2016).

Despite the steady increase in data pertaining to neuropsychiatric symptoms in IPD a motor phenotype approach appears to be lacking with studies generally clustering certain neuropsychiatric features, but not looking at motor phenotype (Aarsland et al., 2007; Aarsland et al., 1999; Cooney and Stacy, 2016; Leroi et al., 2012). NPI scores in the CP group were generally lower than in the IPD group, but also lower than the average scores in a recent review of neuropsychiatric sequelae after stroke which would suggest perhaps a similar pattern of NPI features are observed in IPD and cerebrovascular disease (Ferro et al., 2016). What remains clear is that larger, longitudinal studies looking at neuropsychiatric features in motor phenotypes, taking account of CVD, are required as predominance in PIGD is certainly suggested in this study and the associations with vascular pathology has not yet been thoroughly investigated.

Our SCOPA-AUT and QUIPS scores, despite our small sample size and the differences in duration of disease length and LEDD scores, seem to fall within results of similar studies (Kurtis et al., 2013; Malek et al., 2015; Marras and Chaudhuri, 2016). Of note only a third of the patients reporting features of impulsivity had LEDD scores above the mean.

2.5 Limitations

Ultimately the pattern and distribution of non-motor symptoms in IPD can only be understood in larger, perhaps longitudinal studies. There were inevitable differences in disease duration and IPD severity (as measured by H+Y but not UPDRS motor score) and LEDD score varied between the IPD phenotypes, as expected, but the nature of the cross sectional study makes it difficult to control for these factors.

2.6 Conclusions

What remains clear is that large studies of NMS of IPD are implicating a more severe non-TD dominant subtype, with greater association with non-motor features of IPD (Ba et al., 2016; Herman et al., 2015; Wu et al., 2016).. This data is in keeping with a greater burden of non-motor features in the PIGD compared to the TD group.

Due to the small sample sizes and limited neuropsychological tests used the question as to whether these findings are consistent with coexisting CVD in the context of IPD remains unanswered. Simply, an observation of a similarity in cognitive and neuropsychiatric features between the PIGD and CVD group has been made. As vascular factors remain modifiable and patterns of NMS in IPD, particularly the PIGD group are similar to that in CVD, it is imperative that the vascular contribution be better quantified and understood.

References

Aarsland, D., Bronnick, K., Ehrt, U., De Deyn, P.P., Tekin, S., Emre, M., Cummings, J.L., 2007. Neuropsychiatric symptoms in patients with Parkinson's disease and dementia: frequency, profile and associated care giver stress. J Neurol Neurosurg Psychiatry 78, 36-42.

Aarsland, D., Larsen, J.P., Lim, N.G., Janvin, C., Karlsen, K., Tandberg, E., Cummings, J.L., 1999. Range of neuropsychiatric disturbances in patients with Parkinson's disease. J Neurol Neurosurg Psychiatry 67, 492-496.

Ba, F., Obaid, M., Wieler, M., Camicioli, R., Martin, W.R., 2016. Parkinson Disease: The Relationship Between Non-motor Symptoms and Motor Phenotype. Can J Neurol Sci 43, 261-267.

Becker, C., Jick, S.S., Meier, C.R., 2010. Risk of stroke in patients with idiopathic Parkinson disease. Parkinsonism Relat Disord 16, 31-35.

Chaudhuri, K.R., Healy, D.G., Schapira, A.H., 2006. Non-motor symptoms of Parkinson's disease: diagnosis and management. Lancet Neurol 5, 235-245.

Cooney, J.W., Stacy, M., 2016. Neuropsychiatric Issues in Parkinson's Disease. Curr Neurol Neurosci Rep 16, 49.

Cummings, J.L., 1997. The Neuropsychiatric Inventory: assessing psychopathology in dementia patients. Neurology 48, S10-16.

Emre, M., Aarsland, D., Brown, R., Burn, D.J., Duyckaerts, C., Mizuno, Y., Broe, G.A., Cummings, J., Dickson, D.W., Gauthier, S., Goldman, J., Goetz, C., Korczyn, A., Lees, A., Levy, R., Litvan, I., McKeith, I., Olanow, W., Poewe, W., Quinn, N., Sampaio, C., Tolosa, E., Dubois, B., 2007. Clinical diagnostic criteria for dementia associated with Parkinson's disease. Mov Disord 22, 1689-1707; quiz 1837.

Ferro, J.M., Caeiro, L., Figueira, M.L., 2016. Neuropsychiatric sequelae of stroke. Nat Rev Neurol 12, 269-280.

Foltynie, T., Kahan, J., 2013. Parkinson's disease: an update on pathogenesis and treatment. Journal of Neurology 260, 1433-1440.

Grammas, P., Martinez, J., Miller, B., 2011. Cerebral microvascular endothelium and the pathogenesis of neurodegenerative diseases. Expert Rev Mol Med 13, e19.

Herman, T., Weiss, A., Brozgol, M., Wilf-Yarkoni, A., Giladi, N., Hausdorff, J.M., 2015. Cognitive function and other non-motor features in non-demented Parkinson's disease motor subtypes. J Neural Transm (Vienna) 122, 1115-1124.

Hoehn, M.M., Yahr, M.D., 1967. Parkinsonism: onset, progression and mortality. Neurology 17, 427-442.

Hu, M.T., Szewczyk-Krolikowski, K., Tomlinson, P., Nithi, K., Rolinski, M., Murray, C., Talbot, K., Ebmeier, K.P., Mackay, C.E., Ben-Shlomo, Y., 2014. Predictors of cognitive impairment in an early stage Parkinson's disease cohort. Mov Disord 29, 351-359.

Jankovic, J., McDermott, M., Carter, J., Gauthier, S., Goetz, C., Golbe, L., Huber, S., Koller, W., Olanow, C., Shoulson, I., et al., 1990. Variable expression of Parkinson's disease: a base-line analysis of the DATATOP cohort. The Parkinson Study Group. Neurology 40, 1529-1534.

Kloppenborg, R.P., Nederkoorn, P.J., Geerlings, M.I., van den Berg, E., 2014. Presence and progression of white matter hyperintensities and cognition: a meta-analysis. Neurology 82, 2127-2138.

Kohler, C.A., Magalhaes, T.F., Oliveira, J.M., Alves, G.S., Knochel, C., Oertel-Knochel, V., Pantel, J., Carvalho, A.F., 2016. Neuropsychiatric Disturbances in Mild Cognitive Impairment (MCI): a Systematic Review of Population-Based Studies. Curr Alzheimer Res.

Kurtis, M.M., Rodriguez-Blazquez, C., Martinez-Martin, P., 2013. Relationship between sleep disorders and other non-motor symptoms in Parkinson's disease. Parkinsonism Relat Disord 19, 1152-1155.

Leroi, I., Pantula, H., McDonald, K., Harbishettar, V., 2012. Neuropsychiatric symptoms in Parkinson's disease with mild cognitive impairment and dementia. Parkinsons Dis 2012, 308097.

Litvan, I., Aarsland, D., Adler, C.H., Goldman, J.G., Kulisevsky, J., Mollenhauer, B., Rodriguez-Oroz, M.C., Troster, A.I., Weintraub, D., 2011. MDS Task Force on mild cognitive impairment in Parkinson's disease: critical review of PD-MCI. Mov Disord 26, 1814-1824.

Malek, N., Swallow, D.M., Grosset, K.A., Lawton, M.A., Marrinan, S.L., Lehn, A.C., Bresner, C., Bajaj, N., Barker, R.A., Ben-Shlomo, Y., Burn, D.J., Foltynie, T., Hardy, J., Morris, H.R., Williams, N.M., Wood, N., Grosset, D.G., 2015. Tracking Parkinson's: Study Design and Baseline Patient Data. J Parkinsons Dis 5, 947-959.

Marras, C., Chaudhuri, K.R., 2016. Nonmotor features of Parkinson's disease subtypes. Mov Disord. 31, 1095-1102

Nelson, A.R., Sweeney, M.D., Sagare, A.P., Zlokovic, B.V., 2015. Neurovascular dysfunction and neurodegeneration in dementia and Alzheimer's disease. Biochim Biophys Acta. 1862, 887-900

O'Sullivan, M., 2010. Imaging small vessel disease: lesion topography, networks, and cognitive deficits investigated with MRI. Stroke 41, S154-158.

O'Sullivan, M., Morris, R.G., Markus, H.S., 2005. Brief cognitive assessment for patients with cerebral small vessel disease. J Neurol Neurosurg Psychiatry 76, 1140-1145.

Owen, A.M., James, M., Leigh, P.N., Summers, B.A., Marsden, C.D., Quinn, N.P., Lange, K.W., Robbins, T.W., 1992. Fronto-striatal cognitive deficits at different stages of Parkinson's disease. Brain 115 (Pt 6), 1727-1751.

Paula, J.J., Miranda, D.M., Moraes, E.N., Malloy-Diniz, L.F., 2013. Mapping the clockworks: what does the Clock Drawing Test assess in normal and pathological aging? Arq Neuropsiquiatr 71, 763-768.

Riess, O., Kruger, R., 1999. Parkinson's disease--a multifactorial neurodegenerative disorder. J Neural Transm Suppl 56, 113-125.

Todorova, A., Jenner, P., Ray Chaudhuri, K., 2014. Non-motor Parkinson's: integral to motor Parkinson's, yet often neglected. Practical Neurology 14, 310-322.

Tomlinson, C.L., Stowe, R., Patel, S., Rick, C., Gray, R., Clarke, C.E., 2010. Systematic review of levodopa dose equivalency reporting in Parkinson's disease. Mov Disord 25, 2649-2653.

Visser, M., Marinus, J., Stiggelbout, A.M., Van Hilten, J.J., 2004. Assessment of autonomic dysfunction in Parkinson's disease: the SCOPA-AUT. Mov Disord 19, 1306-1312.

Weintraub, D., Mamikonyan, E., Papay, K., Shea, J.A., Xie, S.X., Siderowf, A., 2012. Questionnaire for Impulsive-Compulsive Disorders in Parkinson's Disease-Rating Scale. Mov Disord 27, 242-247.

Whiteside, D.M., Kealey, T., Semla, M., Luu, H., Rice, L., Basso, M.R., Roper, B., 2016. Verbal Fluency: Language or Executive Function Measure? Appl Neuropsychol Adult 23, 29-34.

Williams-Gray, C.H., Evans, J.R., Goris, A., Foltynie, T., Ban, M., Robbins, T.W., Brayne, C., Kolachana, B.S., Weinberger, D.R., Sawcer, S.J., Barker, R.A., 2009. The distinct cognitive syndromes of Parkinson's disease: 5 year follow-up of the CamPaIGN cohort. Brain 132, 2958-2969.

Williams-Gray, C.H., Mason, S.L., Evans, J.R., Foltynie, T., Brayne, C., Robbins, T.W., Barker, R.A., 2013. The CamPaIGN study of Parkinson's disease: 10-year outlook in an incident population-based cohort. J Neurol Neurosurg Psychiatry 84, 1258-1264.

Wu, Y., Guo, X.Y., Wei, Q.Q., Ou, R.W., Song, W., Cao, B., Zhao, B., Shang, H.F., 2016. Non-motor symptoms and quality of life in tremor dominant vs postural instability gait disorder Parkinson's disease patients. Acta Neurol Scand 133, 330-337.

Zlokovic, B.V., 2011. Neurovascular pathways to neurodegeneration in Alzheimer's disease and other disorders. Nat Rev Neurosci 12, 723-738.

Chapter 3

Chapter 3 details the preliminary study, the aim of which was to assess the suitability of using novel quantitative MRI measures including ASL and DCE in the clinical setting to identify potential changes in NVS in IPD. This chapter is a published paper in Neuroimage Clinical and includes the study design, methodology, results and conclusions. The DCE data was combined with the main study findings and presented later in Chapter 5, leaving the focus of this chapter on insights from our MRI ASL preliminary work.

The initial study was designed by Drs Emsley and Parkes. Ethics was sought by Dr Emsley and myself. I recruited all the IPD patients, some of the control data was taken from a sister study investigating CVD in late onset epilepsy performed by Dr Martha Hanby and to a lesser extent myself. The imaging protocol was devised by Drs Parkes and Vidyasagar. I administered the UPDRS for all patients and coordinated the imaging sessions, but the clinical scales were administered during a home visit by a psychiatrist trainee Dr Vivek Tharaken. I analysed all the results under the supervision and guidance of, and using Matlab codes devised by, Dr Parkes. I wrote the majority of the paper with some help with methodology from Dr Laura Parkes and guidance from Dr Emsley.

Reference:-

Al-Bachari, S., Parkes, L.M., Vidyasagar, R., Hanby, M., Tharakan, V., Leroi, I., Emsley, H.C.A. 2014 Arterial Spin Labelling Reveals Prolonged Arterial Arrival Time in Idiopathic Parkinson's Disease. Neuroimage Clinical 6, 1-8

Arterial Spin Labelling Reveals Prolonged Arterial Arrival Time in Idiopathic Parkinson's Disease

Sarah Al-Bachari[1,2]

Laura M Parkes[2]

Rishma Vidyasagar[2]

Martha F Hanby[1]

Vivek Tharaken[3]

Iracema Leroi[3]

Hedley CA Emsley[1,4]

[1]Department of Neurology, Royal Preston Hospital, Preston, UK; [2]Centre for Imaging Science, Institute of Population Health, University of Manchester, UK; [3]Institute of Brain, Behaviour and Mental Health, University of Manchester, UK; [4]School of Medicine, University of Manchester, UK

Contact information for corresponding author:

Dr Hedley Emsley, Department of Neurology, Royal Preston Hospital, Preston PR2 9HT, UK

Tel: 00 44 1772 522558 Email: hedley.emsley@manchester.ac.uk

Running title:

Arterial spin labelling reveals prolonged arterial arrival time in idiopathic Parkinson's disease

Abbreviations:

ASL - arterial spin labelling, AAT - arterial arrival time, AD - Alzheimer's disease, CBF - cerebral blood flow, CO_2 - carbon dioxide, CV - cerebrovascular, CVD - cerebrovascular disease, CVR - cerebrovascular reactivity, CVR_{AAT} - cerebrovascular reactivity measures of arterial arrival time, CVR_{CBF} - cerebrovascular reactivity measures of cerebral blood flow, DS - digit span, DSST - digit symbol substitution test, DWMH - deep white matter hyperintensity, EPI - echo planar imaging, $ETCO_2$ - end-tidal carbon dioxide, FAS - (verbal) fluency assessment scale, FLAIR - fluid attenuation inversion recovery, fMRI - functional magnetic resonance imaging, HAM-D - Hamilton depression rating scale, IPD - idiopathic Parkinson's disease, LARS - Lille apathy rating scale, L-dopa - levodopa, LEDD - Levodopa equivalent dose, MCI - mild cognitive impairment, MoCA - Montreal cognitive assessment, MRI - magnetic resonance imaging, NPI - neuropsychiatric inventory, NVU - Neurovascular unit, O_2 - oxygen, PET - positron emission tomography, PIGD - Postural instability and gait disorder, PVH - peri ventricular hyperintensity, ROI - region of interest, SPECT - single positron emission computed tomography, SPM - statistical parametric mapping, STAR - signal targeting with alternating radiofrequency, TD - tremor dominant, TE - echo time, 3T - 3 Tesla, TMT-B - trail making test B, TR - repetition time, UKPDS BB - United Kingdom Parkinson's Disease Society Brain Bank, UPDRS - Unified Parkinson's Disease Rating Scale, WAIS-R - Wechsler adult intelligence scale-revised, WML - white matter lesion

Abstract

Idiopathic Parkinson's disease (IPD) is the second most common neurodegenerative disease, yet effective disease modifying treatments are still lacking. Neurodegeneration involves multiple interacting pathological pathways. The extent to which neurovascular mechanisms are involved is not well defined in IPD. We aimed to determine whether novel magnetic resonance imaging (MRI) techniques, including arterial spin labeling (ASL) quantification of cerebral perfusion, can reveal altered neurovascular status (NVS) in IPD.

Fourteen participants with IPD (mean ± SD age 65.1 ± 5.9 years) and 14 age and cardiovascular risk factor matched control participants (mean ± SD age 64.6 ± 4.2 years) underwent a 3T MRI scan protocol. ASL images were collected before, during and after a 6 min hypercapnic challenge. FLAIR images were used to determine white matter lesion score. Quantitative images of cerebral blood flow (CBF) and arterial arrival time (AAT) were calculated from the ASL data both at rest and during hypercapnia. Cerebrovascular reactivity (CVR) images were calculated, depicting the change in CBF and AAT relative to the change in end-tidal CO_2.

A significant ($p=0.005$) increase in whole brain averaged baseline AAT was observed in IPD participants (mean ± SD age 1532 ± 138 ms) compared to controls (mean ± SD age 1335 ± 165 ms). Voxel-wise analysis revealed this to be widespread across the brain. However, there were no statistically significant differences in white matter lesion score, CBF, or CVR between patients and controls. Regional CBF, but not AAT, in the IPD group was found to correlate positively with Montreal cognitive assessment (MoCA) scores. These findings provide further evidence of alterations in NVS in IPD.

Keywords

Arterial spin labelling, arterial arrival time, cerebral blood flow, Idiopathic Parkinson's disease, cerebrovascular reactivity, MoCA

Highlights

- Investigation of neurovascular status (NVS) in IPD using arterial spin labelling.
- Diffuse prolonged arterial arrival time in IPD compared to controls.
- Reduced regional CBF in the IPD group correlated with cognitive impairment.
- Clinical evidence of altered NVS in IPD warranting further research.

3.1 Introduction

Idiopathic Parkinson's disease (IPD) is the second most common neurodegenerative disorder, affecting 1–2% of the population over the age of 65, with the incidence increasing steeply with age (Van Den Eeden et al., 2003). Progression is variable and difficult to predict, but IPD is often associated with significant disability. Treatment remains symptomatic, with an absence of effective disease modifying or neuroprotective agents.

Alterations in neurovascular status (NVS) – including measures of cerebral haemodynamic function as well as more conventional clinical and radiological measures of cerebrovascular disease (CVD) – might be expected in IPD for two principal reasons. Firstly, neurodegeneration is considered to comprise multiple interacting pathological pathways (Collins et al., 2012). Recently there has been considerable interest in the disturbance of neurovascular unit (NVU) function and the 'neurovascular model' of neurodegeneration (Grammas et al., 2011; Zlokovic, 2008). The NVU is a complex, metabolically active system of endothelial cells and glial cells in close proximity to a neuron. Whether altered NVU function is primary or secondary to neurodegeneration, or even attributable to the effect of pharmacotherapy, remains unclear. Secondly, as IPD is strongly associated with ageing, an increased burden of comorbid CVD might be expected, but the evidence is somewhat conflicted probably on account of varying study designs and endpoints (Morley and Duda, 2012). Currently, the extent to which NVS is altered in IPD is poorly defined.

There is also substantial heterogeneity within IPD with respect to clinical phenotype, including motor and non-motor features and it is possible that differences in NVS might be influential in these differing phenotypes (Lee et al., 2009). Tremor dominant (TD) and postural instability and gait disorder (PIGD) phenotypes are recognised, based on the predominant motor features (Jankovic et al., 1990). Non-motor features (in particular neuropsychiatric and cognitive dysfunction) have been reported in a significant proportion of IPD patients; with cognitive decline being associated with worse motor and non-motor features (Aarsland et al., 1999; Hu et al., 2014b). Studies suggest distinct clinical courses and even variable involvement of the dopaminergic system and other pathways between phenotypes (Eggers et al., 2012; Mito et al., 2006) .

Magnetic resonance imaging (MRI) can provide valuable measures of NVS, such as white matter lesion (WML) burden and cerebral blood flow (CBF). Arterial spin labelling (ASL)

employs magnetically labelled endogenous arterial blood water to quantify cerebral perfusion. ASL can also measure arterial arrival time (AAT), the time taken for blood to travel from the labelling slab to the tissue of interest (Wang et al., 2003; Zappe et al., 2007). AAT is longest in distal branches, especially in border zone areas (Hendrikse et al., 2008; Petersen et al., 2006). Alterations in resting state AAT are considered likely to reflect chronic arteriolar vasodilatation or collateral flow (Derdeyn et al., 2002; Farkas and Luiten, 2001). Cerebrovascular reactivity (CVR) can be measured by combining ASL with a hypercapnic challenge. CVR reflects the capacity of blood vessels to dilate in response to a hypercapnic challenge and can be used as a measure of brain vascular reserve (Hajjar et al., 2010).

We hypothesize that NVS is altered in IPD. This was tested by comparing MRI measurements of NVS between a group of people with IPD and age and cardiovascular risk matched controls. In addition MRI images were correlated against cognitive and neuropsychiatric scores to determine any association between NVS measurements and such non-motor features of IPD.

3.2 Methods

3.21 Participants

Relevant approvals were obtained including ethics (North West – Preston Research Ethics Committee), research governance and local university approvals**.** Eligibility criteria for IPD participants were a clinical diagnosis of IPD fulfilling UK Parkinson's disease society (UKPDS) brain bank (BB) criteria (http://www.ncbi.nlm.nih.gov/projects) without known clinical CVD (no history of transient ischaemic attack or stroke) or dementia (Emre et al., 2007) or radiological evidence of large vessel cortical/subcortical infarct >1.5cm. Control participants (without IPD or above exclusion criteria), were matched for age and cardiovascular risk factors. All participants were required to provide written informed consent and had capacity to do so. All underwent a scan protocol on a 3T Philips Achieva MRI system using an 8 channel head coil at Salford Royal Hospital. Involuntary movements in participants were minimised using padding within the head coil. All participants were scanned 'ON' their medications. IPD phenotype was assessed using the Unified Parkinson's Disease Rating Scale (UPDRS) (http://www.mdvu.org/library/ratingscales/pd/updrs.pdf) during the scan visit. Participants were further classified into three subtypes (TD, PIGD, intermediate) by Jankovic's method (Jankovic et al., 1990). Disease severity was measured using the Hoehn and Yahr rating scale (Hoehn and Yahr, 1967). No alterations were made to the

participants' medications for the study protocol. Routine clinical baseline data were also recorded and the levodopa equivalent doses (LEDD) calculated (Tomlinson et al., 2010). A battery of clinical scales was administered, including the Montreal Cognitive Assessment (MoCA) (www.MoCAtest.org), the O'Sullivan brief cognitive assessment for participants with cerebral small vessel disease (O'Sullivan et al., 2005), the Lille apathy rating scale (LARS) (Sockeel et al., 2006), the Hamilton depression scale (HAM-D) (Muller and Dragicevic, 2003) and the neuropsychiatric inventory (NPI) psychosis subscale (Fernandez et al., 2008). Demographics and clinical data were compared between IPD and control participants using unpaired Student t-test with p-value set at < 0.05.

3.22 MRI protocol

A T2-weighted FLAIR image was acquired with the following parameters: TR 11s, TI 2.8s, TE 120 ms, in-plane resolution of 0.45mm, 30 axial slices of 4mm thickness with 1mm gap covering the whole brain. A Look-Locker ASL sequence was used (Gunther et al., 2001), with STAR labeling (Edelman et al., 1994) and 4 readout times of 800, 1400, 2000, 2600 ms, TR: 3500 ms; TE 22ms; flip angle 40 degrees; 3.5 x3.5 x 6 mm voxels with 1mm gap between slices; 15 slices covering the cerebrum but not the cerebellum with bipolar 'vascular crusher' gradients added to dephase fast flowing spins and so remove large vessel signal. The labeling slab was 15 cm with a 10 mm gap between labeling and imaging regions. 112 pairs of labeled and control images were collected, with scan duration approximately 13 minutes. To allow quantification of CBF an additional scan was acquired with TR = 10s and 15 read-out times (from 800 to 9200 ms) in order to estimate the equilibrium magnetisation of the brain. An additional echo planar image (EPI) was collected with the same slice positioning and the same voxel dimensions but with TE=35ms to give typical fMRI contrast for registration and normalisation purposes. A 3D T1-weighted image with 1mm isotropic resolution was also collected.

During the ASL acquisition a CO_2 (hypercapnic) challenge was carried out. After 5 mins of breathing room air (from which the baseline perfusion images were extracted) there followed 6 mins of hypercapnia, administered using a non-rebreathing circuit using the Fenn and Craig technique (Fenn and Craig, 1963) and a final 2 minutes of return to room air. This method involves a thin stream of gas (79% CO_2 balanced with 21% O_2) being delivered through larger tubing allowing it to mix with room air. This mixture then passes through a 3-way valve which directs it to a filter and a mouth piece (Vidyasagar et al., 2013). End-tidal CO_2 ($ETCO_2$) and O_2 were continuously monitored using Powerlab (LabChart7 V7.2.1, 2011) and the CO_2 flow-rate was altered to ensure all participants

reached an increased end tidal level approximately 1% above their baseline $ETCO_2$. Prior to each scanning session the gas analysers were calibrated using a canister of gas with known concentrations of 5.03% CO_2 and 21.0% O_2, each participant also had a trial session of inhaled gas to allow them to become accustomed to the apparatus, this also provided an opportunity to assess an appropriate flow rate required to induce a 1% change in $ETCO_2$.

3.23 Data analysis

WML burden was assessed semi-quantitatively using visual rating scales (Fazekas et al., 1993; Wahlund et al., 2001). Between group comparisons were made using student's unpaired t test analysis. ASL data were analysed using in-house MATLAB (Mathworks, MA, USA) routines using a single blood compartment model, adapted for Look-Locker readout (Parkes L.M., 2012). Further details of the ASL modeling are given in the appendix.

Baseline CBF and AAT maps were calculated using the first 5 mins of ASL data, during breathing of air. CVR maps were calculated using subtraction images of CBF and AAT between periods of air (5 mins) and hypercapnia (last 5 mins, omitting the first minute of hypercapnia to allow equilibrium to be reached) and dividing these by the value of $\Delta ETCO_2$ on an individual basis. Whole brain values for CBF, AAT, CVR_{CBF} (% CBF change/ $\Delta ETCO_2$) and CVR_{AAT} ($\Delta AAT / \Delta ETCO_2$) were calculated using a simple threshold mask based on the ASL control images on an individual basis. Differences between IPD and control participants for CBF, AAT and all CVR measures were tested using student t-tests in Excel. Differences between IPD and control participants for WML burden as measured by the visual rating scales were tested using Fisher's exact test in SPSS, taking into account the non parametric nature of the scales and small sample sizes. Linear regression was used to assess whether WML burden could predict CBF and AAT using WML burden as a categorical variable in regression.

Voxel-wise analysis was also performed using the SPM8 PET toolbox (http://www.fil.ion.ucl.ac.uk/spm/) to compare CBF, AAT and CVR maps between IPD and control participants (phenotype specific differences were not analysed due to the small sample sizes). Image pre-processing in SPM included (1) motion correction, (2) registration and normalisation of the EPI image to the EPI template within SPM, and application of this procedure to the perfusion maps, and (3) spatial smoothing of the normalised images using a 12mm full-width-half-maximum kernel. CBF maps were corrected for atrophy using the same method as Johnson et al., (Johnson et al., 2005)

according to the proportion of grey matter and white matter in each voxel, obtained from the segmented T1-weighted image. Voxel-wise comparisons of CBF, AAT, CVR_{CBF}, and CVR_{AAT} between the IPD and control groups were carried out using a two-sample unpaired t-test (unequal variances). Regions were considered significant at a p value of <0.001 uncorrected, with a minimum cluster size of 100 voxels (at the re-sampled voxel size of 2 mm isotropic), which was felt sufficient to avoid type II errors in view of the exploratory nature of the study (Lieberman and Cunningham, 2009) . Further analysis using Family-Wise Error (FWE) correction for multiple comparisons at the cluster level was performed (using Gaussian Radom Field Theory as employed in SPM8). In addition, voxel wise regression of CBF and AAT against MoCA and HAM-D scores were performed within both the IPD and control groups separately.

3.3 Results

3.31 Participants

Fourteen IPD participants (mean ± SD age 65.1 ± 5.9 years) and 14 control participants (mean ± SD age 64.6 ± 4.2 years) were enrolled into the study. Six IPD participants were assigned to the PIGD subgroup, 6 to the TD subgroup and 2 were intermediate (Table 3.1 and 3.2). Thirteen IPD and all 14 control participants completed the full scanning protocol (ASL data were lacking for 1 IPD participant due to difficulties tolerating the set-up of the gas apparatus in the scanner). All participants showed the expected increase in CBF and reduction in AAT with the hypercapnic challenge due to induced cerebrovasodilation (Hajjar et al., 2010). Two further IPD and 2 control participants were excluded from CVR analysis as the $\Delta ETCO_2$ gas response was outside the expected limits (4-12 mmHg). Twelve IPD and 13 control participants completed the clinical scales (6 PIGD, 6TD).

	Controls (n=14)	IPD (n=14)	p value (IPD vs control)	PIGD (n=6)	Tremor (n=6)
N (female: male)	4:10	6:9	n/a	4:2	0:6
Age, years: mean(SD);[range]	64.6(4.2); [58-71]	65.1 (5.9); [54-75]	0.7	65.5 (4.6); [61-72]	66.2 (0.6); [54-75]
No. of cardiovascular risk factors: mean (SD)	0.9 (1.0)	1.4 (1.4)	0.3	0.8 (1.0)	2 (1.5)
No. of other comorbidites: mean (SD)	0.43 (0.65)	0.9 (1.03)	0.2	1 (0.9)	0.8 (1.3)
Disease Duration, years: mean (SD)	n/a	9.2 (6.0)	n/a	10.8 (4.8)	5.2 (3.0)
Hoehn and Yahr Stage ON: mean (SD)	n/a	2.5 (1.1)	n/a	3.2 (1.1)	1.8 (0.6)
LEDD score: mean (SD)	n/a	638 (353)	n/a	750 (453)	488 (347)

Table 3.1: Demographics and clinical characteristics of the study group.

UPDRS Item	PIGD sub-score	TD sub-score
Bradykinesia mean (SD)	6.2 (3.7)	6.1 (0.2)
Tremor mean (SD)	1.8 (2.1)	11.5 (4.7)
Rigidity mean (SD)	8.5 (3.8)	8.2 (5.4)
PIGD Mean (SD)	12.5 (3.9)	1.5 (1.0)

Table 3.2: Key measurement items from the UPDRS. Scores: - bradykinesia (0-36), tremor (0-32), rigidity (0-20), PIGD (0-20)

3.32 Baseline CBF and AAT

Whole brain baseline CBF did not differ between the IPD and control groups (Table 3.3). The voxel-wise analysis did reveal one region of lower CBF in patients compared to controls (at $p<0.001$ minimum cluster size 100 voxels) in the right parietal lobe supramarginal gyrus near the angular gyrus (Talairach coordinates [16 -80 34], cluster size 231 voxels, peak t-value 3.8, peak p-value 0.0004). There were no regions of significant hyperperfusion in the IPD group compared to controls.

Whole brain baseline AAT was significantly prolonged in IPD participants compared to controls (Table 3.3). Voxel-wise analysis revealed widespread regions of significantly increased baseline AAT in the IPD group compared to controls, particularly in frontal and temporal regions at $p<0.001$ minimum cluster threshold 100 voxels (Figure 3.1b and Table 3.4). Two of these regions survive FWE correction (Figure 3.1c). There were no regions in the brain where AAT was significantly shorter in the IPD group than in the control group. A mean difference map of AAT between patients and controls was created to further shed light on the distribution of the prolonged AAT; this revealed bilateral, diffuse increases in AAT in the IPD group compared to controls (Figure 3.1a).

	Control group (n=14) mean ± SD	**IPD group (n=13) mean ± SD**	**p value (IPD Vs Controls)**
Baseline CBF (ml/min/100ml)	38.0 ± 9.3	35.3 ± 5.8	0.5
Baseline AAT (ms)	1335 ± 165	1532 ± 138	0.005
CVR_CBF (%/ΔmmHg)	2.2 ± 2.9	4.0 ± 2.9 (n=13)	0.2
CVR_AAT (Δms/ΔmmHg)	-21.5 ± 7.1	-15.3 ± 11.2 (n=13)	0.2

Table 3.3: Whole brain CBF, AAT and CVR measurements

Region	Cluster size	Cluster p(FWE-cor)	Peak t value	Peak p (uncor)	Peak MNI coordinates		
L inferior frontal gyrus extending to sub-gyral region	839	0.02	5.2	<0.0001	-32	38	10
			4.7	<0.0001	-34	24	8
			4.4	<0.0001	-32	16	14
L middle TL extending to large sub gyral region	2327	<0.0001	5.1	<0.0001	-42	-36	-2
			4.7	<0.0001	-42	-46	6
			4.7	<0.0001	-58	-6	-6
R middle temporal gyrus	110	0.8	4.6	<0.0001	64	-38	-8
L TL middle temporal gyrus	104	0.8	4.5	<0.0001	-66	-34	-12
L caudate body	101	0.8	4.5	<0.0001	-14	16	12
L cerebrum middle frontal gyrus	140	0.7	4.4	<0.0001	-32	56	-8
			3.9	0.0004	-40	52	-6
R inferior frontal gyrus	100	0.8	4.1	0.0002	-46	40	6
R TL superior to transverse T gyrus	119	0.8	4.0	0.0002	36	-34	10
			3.7	0.0005	50	-38	16
			3.7	0.0005	46	-34	6
R anterior cingulate	153	0.7	3.9	0.0003	14	40	10
			3.9	0.0003	8	46	6

Table 3.4: Regions of significantly longer AAT in the IPD group compared to controls at p<0.001, cluster size 100.

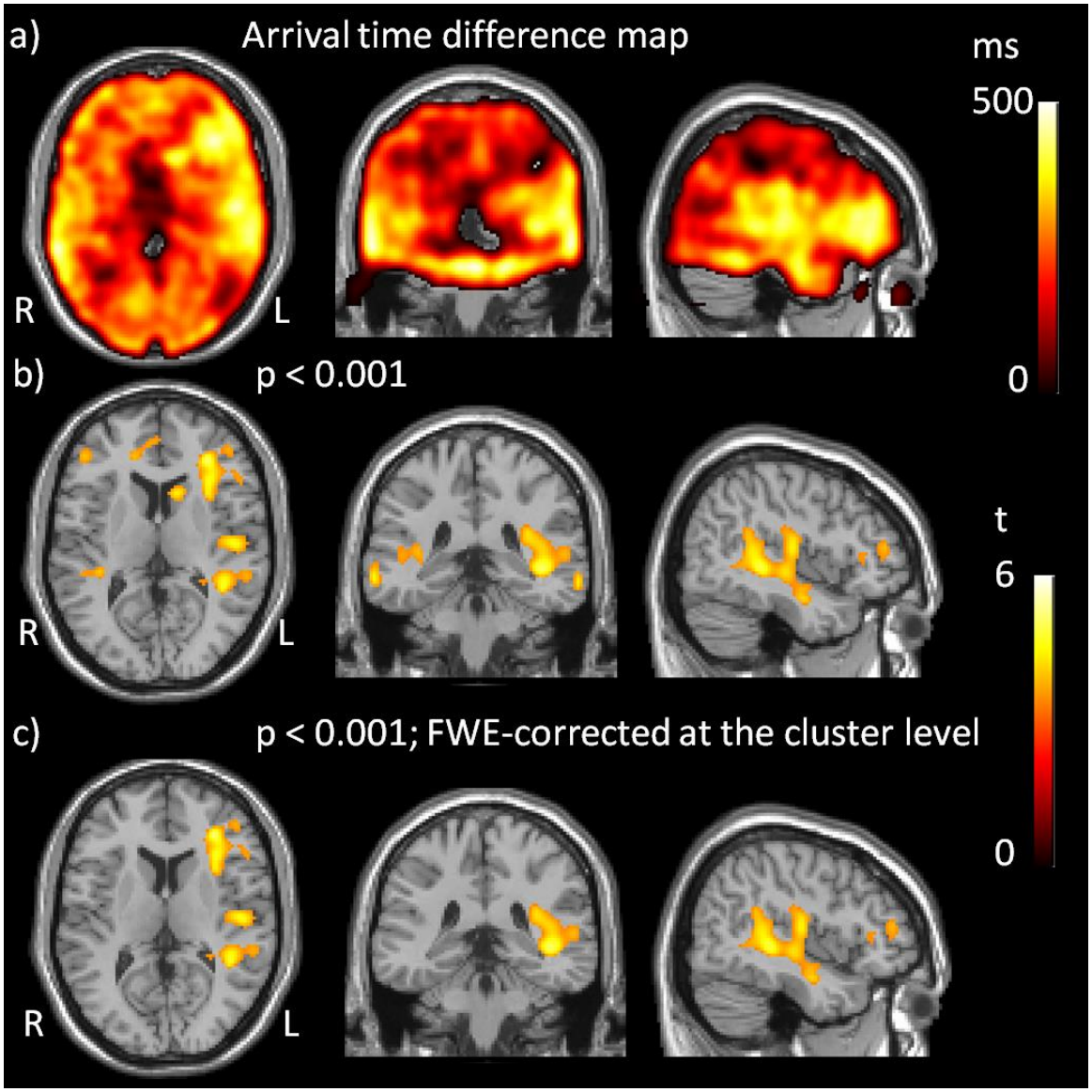

Figure 3.1: Regions of prolonged arrival time in IPD compared to controls.
a) Arrival time difference map created by subtraction of mean AAT in controls from mean AAT in patients. b) T statistic map obtained by comparison of AAT between the IPD group and controls thresholded to p<0.001 uncorrected, minimum cluster size 100 voxels and c) T statistic map thresholded at p<0.001 FWE-corrected with minimum cluster size 100 voxels. Thus displaying positive t values, representing increased AAT in the IPD group compared to controls (there were no regions of decreased AAT).

3.33 CVR measures

Whole brain measures of CVR_{CBF} or CVR_{AAT} did not differ between IPD and control participants. Voxel-wise analysis did not reveal any regions of statistically significant differences in these measurements between the groups.

3.34 WML burden

To test for differences in WML score the Fisher's Exact test was used, combining scores into categories (0-1) and 2 where appropriate since the majority of patients scored 1 or 2. The results showed no association between any of the WML scores and whether a participant has IPD, with p-values as given in Table 3.5. There were no statistically significant correlations between the WML burden (Wahlund scale) and CBF or AAT.

	Score	Control group (n=14) number (%)	IPD group (n=14) number (%)	p value (IPD Vs Controls)
Wahlund	0 or 1	12 (85.7%)	8 (57.1%)	0.2
	2	2 (14.3%)	6 (42.9%)	
Fazekas PVH	1	11(78.6%)	10 (71.4%)	1.0
	2	3 (21.4%)	4 (28.6%)	
Fazekas DWMH	0 or 1	12 (85.7%)	9 (65.3%)	0.4
	2	2 (14.3%)	5 (35.7%)	

Table 3.5: WML rating scales. PVH, Periventricular hyperintensity; DWMH, deep white matter hyperintensity

3.35 Clinical Scales

Results of the clinical scales are shown in Table 3.6. The IPD group (mean ± SD, score 8.5 ± 2.5) scored significantly lower than the control group (mean ± SD score 10.8 ± 2.7, $p = 0.03$) in the digit symbol substitution test (DSST). Six IPD participants (4 PIGD, 2 TD) but only one control participant met criteria for mild cognitive impairment as reflected by a score of ≤ 25 on the MoCA tool. Three IPD participants (2 PIGD, 1 intermediate) met the cut-off for 'mild depression' as measured by the Ham-D scale, whereas all control participants fell within the 'not depressed' range on this scale. All participants completed the trail making test part B (TMT-B) except for one IPD (PIGD

group) and one control participant. Neither group exhibited significant apathy or any features of psychosis as *per* the clinical scales.

	Controls (n=13)	**IPD (n=12)**	**p value (IPD vs control)**	**PIGD (n=6)**	**Tremor (n=5)**
Ham-D: mean (SD)	2.6 (2.4)	5.3 (5.4)	0.1	6.4 (4.2)	3.6 (7.0)
LARS: mean (SD)	-26.3 (5.2)	-25.3 (3.3)	0.6	-24.3 (3.7)	-26.8 (1.8)
DS: mean (SD)	9.5 (2.8)	11.4 (2.9)	0.1	10 (2.9)	13.4 (1.5)
DSST: mean (SD)	20.8 (2.7)	8.5 (2.5)	0.03	7.4 (1.6)	2.8 (0.6)
FAS VF: mean (SD)	52.3 (33.2)	49.0 (25.3)	0.8	39.7 (24.2)	62.0 (22.8)
TMT-B: mean (SD)	96.7 (40.8)	103.9 (40.8)	0.7	119.3 (43.7)	85.4 (31.4)
MoCA: mean (SD)	28.3 (3.0)	26.3 (3.0)	0.1	26.0 (3.3)	26.6 (2.7)

Table 3.6: Clinical scales and scores. Ham-D, Hamilton depression scale; LARS, Lille apathy rating scale; DS, digit span; DSST, digit symbol substitution test; FAS VF, verbal fluency; TMT-B, trial making test B; MoCA, Montreal cognitive assessment.

Voxel-wise analysis using linear regression was performed to identify potential regional correlations between MOCA and HAM-D scores, with both CBF and AAT. Reduced CBF mainly in parietal regions was found to correlate with reduced MoCA score (Table 3.7, Figure 3.2) in the IPD group only. To help verify the statistical threshold used, MoCA scores of the IPD participants were shuffled randomly and the voxel-wise regression analysis was repeated. No regions of significant correlation were found, confirming the validity of our findings. There were no regions of significant correlation of MoCA score and AAT in either of the two study groups. In addition Ham-D scores did not correlate with either CBF or AAT in either the IPD or control group.

Region	Cluster size	Cluster p (FWE-cor)	Peak t value	Peak p value uncorrected	Peak MNI coordinates
Left Superior parietal lobe extending into precuneus and angular gyrus	464	0.09	6.1 5.7 5.4	<0.0001	-30 -76 44 -40 -70 42 -48 -70 34
Left precuneus	112	0.6	5.7	<0.0001	-12 -72 48

Table 3.7: Regions of significant correlation between CBF and MoCA scores in the IPD group, thresholded to p<0.001 uncorrected and minimum cluster size 100 voxels.

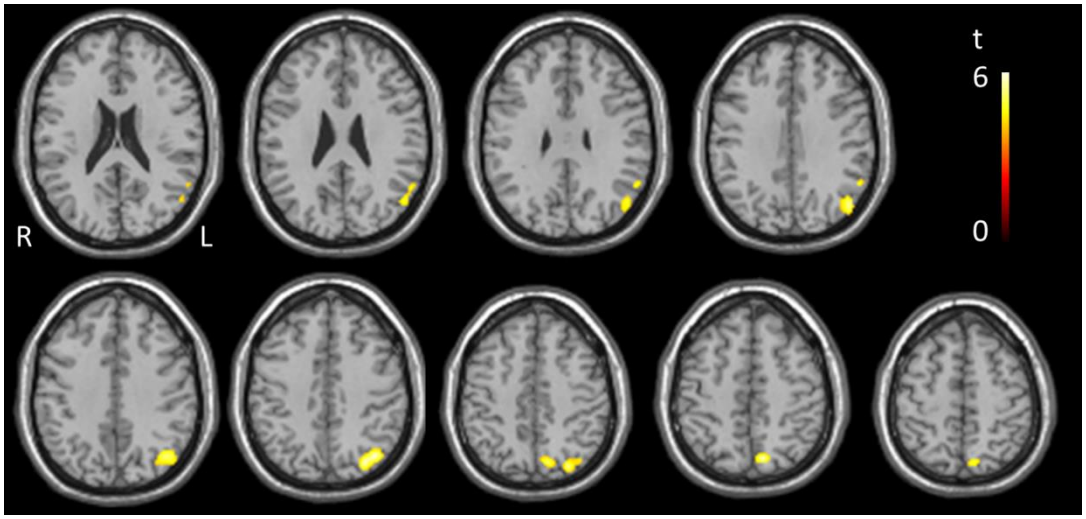

Figure 3.2: Regions of significant correlation between CBF and MoCA scores for the IPD group, thresholded to p<0.001 uncorrected and minimum cluster size 100 voxels.

3.4 Discussion

We hypothesised that NVS is altered in IPD, which may be a reflection of the neurodegenerative process or due to comorbid CVD. The two key findings of this study support this notion. We revealed diffuse AAT prolongation in the IPD group compared to healthy control participants and significant regional correlations between MoCA scores and CBF in the IPD group only.

To our knowledge, the prolonged AAT in the IPD group compared to controls has not been previously reported. Although the differences appear predominantly in the right hemisphere the mean difference maps suggest prolonged AAT is more diffuse (Figure 3.1). It is possible to attribute prolonged AAT to any factor which increases path length or decreases the velocity of flow i.e. diameter and resistance of vessels and characteristics of the circulating blood (Liu et al., 2012). Several other studies have reported on AAT in non-PD populations with various reasons proposed. For example, prolonged AAT has been noted in studies of ageing (Liu et al., 2012), presumably related to age driven structural cerebrovascular changes such as increased vessel tortuosity, increased rarefaction and arteriolar wall damage (Chen et al., 2012; Wolk and Detre, 2012). AAT prolongation in multiple sclerosis has been attributed to widespread inflammation or chronic vasodilation of the resistance vessels (Paling et al., 2013). A study in AD revealed prolonged AAT and hypoperfusion in the left inferior frontal and middle cingulate gyri (Mak et al., 2012). Lastly, stroke and TIA studies have attributed AAT prolongation to the recruitment of collateral pathways in large artery stenosis with, in some cases, preserved perfusion (Chalela et al., 2000; MacIntosh et al., 2010b; Zaharchuk, 2011).

We did not find differences in CBF between the IPD group and controls at the $p<0.001$, minimum cluster size 100 voxels, yet at the more lenient threshold of $p<0.005$, regions of hypoperfusion in the left cuneus in the IPD group were revealed. This perfusion deficit is in keeping with both ASL and positron emission tomography (PET) studies in IPD which have found a similar pattern of hypoperfusion and hypometabolism in IPD patients compared to healthy controls with significant correlation between PET and ASL perfusion patterns (Borghammer et al., 2010; Fernandez-Seara et al., 2012; Kamagata et al., 2011; Ma et al., 2010; Melzer et al., 2011). These studies consistently revealed bilateral hypoperfusion in the occipital lobe (including the cuneus) as well as posterior parietal regions, with variable patterns in the frontal lobe. Hypoperfusion in neurodegenerative states has previously been attributed to direct tissue loss or the result of loss of functional connectivity (Borghammer et al., 2010; Yoshiura et al., 2009). We feel that the small sample size may mean important differences between the 2 groups (such as

hypoperfusion) may be under-represented in this study. Our results show that AAT is a more sensitive marker of changes in NVS in IPD than CBF, and may be important to consider in future studies using ASL.

Despite diffuse baseline AAT prolongation in the IPD group, the global response of AAT and CBF to the hypercapnic challenge (CVR_{AAT} and CVR_{CBF}) did not differ significantly between the groups, suggesting vascular responsiveness is generally preserved. If the prolonged baseline AAT is indicative of chronic vasodilation then the AAT and CBF response in IPD group would be expected to be reduced (reduced capacity for further dilation). However, the variability of both CVR_{AAT} and CVR_{CBF} is large, so greater participant numbers are probably required to reliably test for these differences.

This study also revealed a positive correlation between CBF predominantly in posterior regions and total MoCA scores in the IPD group. This could mean that hypoperfusion in these regions contributes to cognitive impairment in IPD. Similarly cognitive scores including the mini mental state examination (MMSE) scores and MoCA have been noted to correlate with hypoperfusion in IPD and other diseases affecting cognition, with specific patterns of hypoperfusion dependent on the disease state (Chao et al., 2010; Firbank et al., 2003; Nobili et al., 2008; Yoon et al., 2012). However any potential causal relationship would need further study. We recognise that the relatively small sample size may potentially account for differences in other non-motor features not reaching statistical significance (Table 3.6) and further exploration of their pathophysiological underpinnings is warranted.

This study did not reveal differences in WML burden between the IPD group and controls; larger sample sizes would be needed to consider phenotype-specific differences. Due to time restrictions only WML rating scales were used whereas volume measurements of WML are possible and may help to tease out potential differences that exist between the groups (Rost et al., 2014).

Certain limitations of this exploratory study must be acknowledged. ASL techniques generally are limited by their low signal to noise ratio. However as it uses magnetically labeled arterial blood water as an endogenous tracer , it can be repeated multiple times within a session to improve signal-to-noise ratio producing comparable results to FDG PET (Ma et al., 2010).

We used only 4 post-labelling time-points for the ASL acquisition, which was necessary in order to cover the cerebrum with vascular crushing gradients enabled. More time points may have increased the precision of the AAT measurements.

Due to the exploratory nature of the study, uncorrected p-values have been displayed alongside FWE values, so a larger data set with FWE correction is required to verify the results. It is possible that differences in NVS might be influential in differing clinical phenotypes of IPD (Lee et al., 2009), however the small sample size in this study meant that phenotype-specific differences could not be explored. LEDD scores differed between participants, which may confound the results as previous studies have revealed regional blood flow increases with levodopa (Hershey et al., 2003; Kobari et al., 1995).

3.5 Conclusion

This exploratory work used MRI perfusion and structural measures to investigate NVS in IPD. In IPD we have identified prolonged baseline AAT, as well as regional posterior hypoperfusion with correlations with impaired cognition. Alterations in neurovascular parameters in IPD and their associations with clinical features and treatment, as well as the potential identification of targets for intervention, warrant further study. In addition with the great heterogeneity of motor features that exist within the umbrella term of IPD, a phenotypic approach should be explored in larger studies.

3.6 Appendix

ASL data were analysed using a single blood compartment model, adapted for Look-Locker readout (Parkes L.M., 2012). This model assumes that labelled water remains in the blood and that no labelled water leaves the voxel, an approach that has been shown to be reasonably accurate (Parkes and Tofts, 2002). With these assumptions, the signal in the difference image (control – label), ΔM, can be described by:

$$\frac{d\Delta M(t)}{dt} = -R_1 \Delta M(t) + f m_a(t) \qquad [1]$$

where R_1 is the apparent R_1 of blood during the Look-Locker readout and f is CBF. For STAR labelling the magnetisation of arterial blood, m_a, is given by:

$$m_a(t) = 2 m_a^0 \alpha \exp(-t R_{1b}) \qquad \text{for } t > t_a \text{ and } t < \tau \qquad [2]$$

and $m_a = 0$ at all other times. Here, t_a is the arrival time and τ is the bolus width. M_a^0 is the equilibrium magnetisation of arterial blood, α is the inversion efficiency (assumed to equal 1) and R_{1b} is the true R_1 of blood. According to (Gunther et al.,2001) $R_1=R_{1b}-\ln(\cos\theta)/TI_2$ where θ is the flip angle and TI_2 the spacing of the Look-Locker readout. The solution for ΔM is:

$$\Delta M(t) = \frac{2 f m_a^0 \alpha}{\Delta R} \exp(-tR_1)\left[\exp(t\Delta R) - \exp(t_a \Delta R)\right] \quad \text{for } t > t_a \text{ and } t < t_a + \tau \quad [3]$$

$$\Delta M(t) = \frac{2 f m_a^0 \alpha}{\Delta R} \exp(-tR_1) \exp(t_a \Delta R)\left[\exp(\tau \Delta R) - 1\right] \quad \text{for } t > t_a + \tau$$

Where $\Delta R = R_1 - R_{1b}$. The mean difference signal ΔM was fit on a voxel-wise basis to equation [3], extracting values for the 2 free parameters f (CBF) and t_a (AAT), with fixed values for τ = 1000ms (MacIntosh et al., 2010a), T_{1b} = 1600ms (Lu et al., 2004) (note $R_{1b}=1/T_{1b}$), and M^0. The calibration images were fit on a voxel-wise basis to a saturation recovery curve, producing maps of T_1 and M_0. M_a^0 was estimated from a whole brain estimate of M_0 divided by the blood-brain partition coefficient λ=0.9 (Roberts et al., 1996).

Acknowledgements

We would like to sincerely thank all the participants for their kind participation in the study. In addition, the radiographers at Salford Royal for their support and expertise and Mr Matthew Wright for his support and input whilst performing the scans. We'd also like to thank the University of Manchester's MRI facility (MRIF) for their financial contribution towards the scanning costs and the Biomedical Imaging Institute (BII) for their support and financial contribution towards analysis and writing.

References

Aarsland, D., Larsen, J.P., Lim, N.G., Janvin, C., Karlsen, K., Tandberg, E., Cummings, J.L., 1999. Range of neuropsychiatric disturbances in patients with Parkinson's disease. J Neurol Neurosurg Psychiatry 67, 492-496.

Borghammer, P., Chakravarty, M., Jonsdottir, K.Y., Sato, N., Matsuda, H., Ito, K., Arahata, Y., Kato, T., Gjedde, A., 2010. Cortical hypometabolism and hypoperfusion in Parkinson's disease is extensive: probably even at early disease stages. Brain Struct Funct 214, 303-317.

Chalela, J.A., Alsop, D.C., Gonzalez-Atavales, J.B., Maldjian, J.A., Kasner, S.E., Detre, J.A., 2000. Magnetic resonance perfusion imaging in acute ischemic stroke using continuous arterial spin labeling. Stroke 31, 680-687.

Chao, L.L., Buckley, S.T., Kornak, J., Schuff, N., Madison, C., Yaffe, K., Miller, B.L., Kramer, J.H., Weiner, M.W., 2010. ASL perfusion MRI predicts cognitive decline and conversion from MCI to dementia. Alzheimer Dis Assoc Disord 24, 19-27.

Chen, Y., Wang, D.J., Detre, J.A., 2012. Comparison of arterial transit times estimated using arterial spin labeling. MAGMA 25, 135-144.

Collins, L.M., Toulouse, A., Connor, T.J., Nolan, Y.M., 2012. Contributions of central and systemic inflammation to the pathophysiology of Parkinson's disease. Neuropharmacology 62, 2154-2168.

Derdeyn, C.P., Videen, T.O., Yundt, K.D., Fritsch, S.M., Carpenter, D.A., Grubb, R.L., Powers, W.J., 2002. Variability of cerebral blood volume and oxygen extraction: stages of cerebral haemodynamic impairment revisited. Brain 125, 595-607.

Edelman, R.R., Siewert, B., Darby, D.G., Thangaraj, V., Nobre, A.C., Mesulam, M.M., Warach, S., 1994. Qualitative mapping of cerebral blood flow and functional localization with echo-planar MR imaging and signal targeting with alternating radio frequency. Radiology 192, 513-520.

Eggers, C., Pedrosa, D.J., Kahraman, D., Maier, F., Lewis, C.J., Fink, G.R., Schmidt, M., Timmermann, L., 2012. Parkinson subtypes progress differently in clinical course and imaging pattern. PLoS One 7, e46813.

Emre, M., Aarsland, D., Brown, R., Burn, D.J., Duyckaerts, C., Mizuno, Y., Broe, G.A., Cummings, J., Dickson, D.W., Gauthier, S., Goldman, J., Goetz, C., Korczyn, A., Lees, A., Levy, R., Litvan, I., McKeith, I., Olanow, W., Poewe, W., Quinn, N., Sampaio, C., Tolosa, E., Dubois, B., 2007. Clinical diagnostic criteria for dementia associated with Parkinson's disease. Mov Disord 22, 1689-1707; quiz 1837.

Farkas, E., Luiten, P.G., 2001. Cerebral microvascular pathology in aging and Alzheimer's disease. Prog Neurobiol 64, 575-611.

Fazekas, F., Kleinert, R., Offenbacher, H., Schmidt, R., Kleinert, G., Payer, F., Radner, H., Lechner, H., 1993. Pathologic correlates of incidental MRI white matter signal hyperintensities. Neurology 43, 1683-1689.

Fenn, W.O., Craig, A.B., Jr., 1963. Effect of CO2 on respiration using a new method of administering CO2. J Appl Physiol 18, 1023-1024.

Fernandez-Seara, M.A., Mengual, E., Vidorreta, M., Aznarez-Sanado, M., Loayza, F.R., Villagra, F., Irigoyen, J., Pastor, M.A., 2012. Cortical hypoperfusion in Parkinson's disease assessed using arterial spin labeled perfusion MRI. NeuroImage 59, 2743-2750.

Fernandez, H.H., Aarsland, D., Fenelon, G., Friedman, J.H., Marsh, L., Troster, A.I., Poewe, W., Rascol, O., Sampaio, C., Stebbins, G.T., Goetz, C.G., 2008. Scales to assess psychosis in Parkinson's disease: Critique and recommendations. Mov Disord 23, 484-500.

Firbank, M.J., Colloby, S.J., Burn, D.J., McKeith, I.G., O'Brien, J.T., 2003. Regional cerebral blood flow in Parkinson's disease with and without dementia. NeuroImage 20, 1309-1319.

Grammas, P., Martinez, J., Miller, B., 2011. Cerebral microvascular endothelium and the pathogenesis of neurodegenerative diseases. Expert Rev Mol Med 13, e19.

Gunther, M., Bock, M., Schad, L.R., 2001. Arterial spin labeling in combination with a look-locker sampling strategy: inflow turbo-sampling EPI-FAIR (ITS-FAIR). Magn Reson Med 46, 974-984.

Hajjar, I., Zhao, P., Alsop, D., Novak, V., 2010. Hypertension and cerebral vasoreactivity: a continuous arterial spin labeling magnetic resonance imaging study. Hypertension 56, 859-864.

Hendrikse, J., Petersen, E.T., van Laar, P.J., Golay, X., 2008. Cerebral border zones between distal end branches of intracranial arteries: MR imaging. Radiology 246, 572-580.

Hershey, T., Black, K.J., Carl, J.L., McGee-Minnich, L., Snyder, A.Z., Perlmutter, J.S., 2003. Long term treatment and disease severity change brain responses to levodopa in Parkinson's disease. J Neurol Neurosurg Psychiatry 74, 844-851.

Hoehn, M.M., Yahr, M.D., 1967. Parkinsonism: onset, progression and mortality. Neurology 17, 427-442.

Hu, M.T., Szewczyk-Krolikowski, K., Tomlinson, P., Nithi, K., Rolinski, M., Murray, C., Talbot, K., Ebmeier, K.P., Mackay, C.E., Ben-Shlomo, Y., 2014. Predictors of cognitive impairment in an early stage Parkinson's disease cohort. Mov Disord.

Jankovic, J., McDermott, M., Carter, J., Gauthier, S., Goetz, C., Golbe, L., Huber, S., Koller, W., Olanow, C., Shoulson, I., et al., 1990. Variable expression of Parkinson's disease: a base-line analysis of the DATATOP cohort. The Parkinson Study Group. Neurology 40, 1529-1534.

Johnson, N.A., Jahng, G.H., Weiner, M.W., Miller, B.L., Chui, H.C., Jagust, W.J., Gorno-Tempini, M.L., Schuff, N., 2005. Pattern of cerebral hypoperfusion in Alzheimer disease and mild cognitive impairment measured with arterial spin-labeling MR imaging: initial experience. Radiology 234, 851-859.

Kamagata, K., Motoi, Y., Hori, M., Suzuki, M., Nakanishi, A., Shimoji, K., Kyougoku, S., Kuwatsuru, R., Sasai, K., Abe, O., Mizuno, Y., Aoki, S., Hattori, N., 2011. Posterior hypoperfusion in Parkinson's disease with and without dementia measured with arterial spin labeling MRI. J Magn Reson Imaging 33, 803-807.

Kobari, M., Fukuuchi, Y., Shinohara, T., Obara, K., Nogawa, S., 1995. Levodopa-induced local cerebral blood flow changes in Parkinson's disease and related disorders. J Neurol Sci 128, 212-218.

Lee, S.J., Kim, J.S., Lee, K.S., An, J.Y., Kim, W., Kim, Y.I., Kim, B.S., Jung, S.L., 2009. The severity of leukoaraiosis correlates with the clinical phenotype of Parkinson's disease. Arch Gerontol Geriatr 49, 255-259.

Lieberman, M.D., Cunningham, W.A., 2009. Type I and Type II error concerns in fMRI research: re-balancing the scale. Soc Cogn Affect Neurosci 4, 423-428.

Liu, Y., Zhu, X., Feinberg, D., Guenther, M., Gregori, J., Weiner, M.W., Schuff, N., 2012. Arterial spin labeling MRI study of age and gender effects on brain perfusion hemodynamics. Magn Reson Med 68, 912-922.

Lu, H.Z., Clingman, C., Golay, X., van Zijl, P.C.M., 2004. Determining the longitudinal relaxation time (T-1) of blood at 3.0 tesla. Magnetic Resonance in Medicine 52, 679-682.

Ma, Y., Huang, C., Dyke, J.P., Pan, H., Alsop, D., Feigin, A., Eidelberg, D., 2010. Parkinson's disease spatial covariance pattern: noninvasive quantification with perfusion MRI. J Cereb Blood Flow Metab 30, 505-509.

MacIntosh, B.J., Filippini, N., Chappell, M.A., Woolrich, M.W., Mackay, C.E., Jezzard, P., 2010a. Assessment of arterial arrival times derived from multiple inversion time pulsed arterial spin labeling MRI. Magn Reson Med 63, 641-647.

MacIntosh, B.J., Lindsay, A.C., Kylintireas, I., Kuker, W., Gunther, M., Robson, M.D., Kennedy, J., Choudhury, R.P., Jezzard, P., 2010b. Multiple inflow pulsed arterial spin-labeling reveals delays in the arterial arrival time in minor stroke and transient ischemic attack. AJNR Am J Neuroradiol 31, 1892-1894.

Mak, H.K., Chan, Q., Zhang, Z., Petersen, E.T., Qiu, D., Zhang, L., Yau, K.K., Chu, L.W., Golay, X., 2012. Quantitative assessment of cerebral hemodynamic parameters by QUASAR arterial spin labeling in Alzheimer's disease and cognitively normal Elderly adults at 3-tesla. J Alzheimers Dis 31, 33-44.

Melzer, T.R., Watts, R., MacAskill, M.R., Pearson, J.F., Rueger, S., Pitcher, T.L., Livingston, L., Graham, C., Keenan, R., Shankaranarayanan, A., Alsop, D.C., Dalrymple-Alford, J.C., Anderson, T.J., 2011. Arterial spin labelling reveals an abnormal cerebral perfusion pattern in Parkinson's disease. Brain 134, 845-855.

Mito, Y., Yoshida, K., Yabe, I., Makino, K., Tashiro, K., Kikuchi, S., Sasaki, H., 2006. Brain SPECT analysis by 3D-SSP and phenotype of Parkinson's disease. J Neurol Sci 241, 67-72.

Morley, J.F., Duda, J.E., 2012. Parkinson's disease and the risk of cerebrovascular pathology. Mov Disord 27, 1471-1472.

Muller, M.J., Dragicevic, A., 2003. Standardized rater training for the Hamilton Depression Rating Scale (HAMD-17) in psychiatric novices. J Affect Disord 77, 65-69.

Nobili, F., Frisoni, G., Portet, F., Verhey, F., Rodriguez, G., Caroli, A., Touchon, J., Calvini, P., Morbelli, S., Carli, F., Guerra, U., Pol, L., Visser, P.-J., 2008. Brain SPECT in subtypes of mild cognitive impairment. Journal of Neurology 255, 1344-1353.

O'Sullivan, M., Morris, R.G., Markus, H.S., 2005. Brief cognitive assessment for patients with cerebral small vessel disease. J Neurol Neurosurg Psychiatry 76, 1140-1145.

Paling, D., Thade Petersen, E., Tozer, D.J., Altmann, D.R., Wheeler-Kingshott, C.A., Kapoor, R., Miller, D.H., Golay, X., 2013. Cerebral arterial bolus arrival time is prolonged in multiple sclerosis and associated with disability. J Cereb Blood Flow Metab.

Parkes L.M., B.H., Abernethy L 2012. CBF Quantification in Infants Using Look-Locker ASL and a Single Blood Compartment Model. . Proceedings of the International Society of Magnetic Resonance in Medicine (ISMRM) annual meeting, Melbourne.

Parkes, L.M., Tofts, P.S., 2002. Improved accuracy of human cerebral blood perfusion measurements using arterial spin labeling: accounting for capillary water permeability. Magn Reson Med 48, 27-41.

Petersen, E.T., Zimine, I., Ho, Y.C., Golay, X., 2006. Non-invasive measurement of perfusion: a critical review of arterial spin labelling techniques. Br J Radiol 79, 688-701.

Roberts, D.A., Rizi, R., Lenkinski, R.E., Leigh, J.S., 1996. Magnetic resonance imaging of the Brain:Blood partition coefficient for water: Application to spin-tagging measurement of perfusion. Jmri-Journal of Magnetic Resonance Imaging 6, 363-366.

Sockeel, P., Dujardin, K., Devos, D., Deneve, C., Destee, A., Defebvre, L., 2006. The Lille apathy rating scale (LARS), a new instrument for detecting and quantifying apathy: validation in Parkinson's disease. J Neurol Neurosurg Psychiatry 77, 579-584.

Tomlinson, C.L., Stowe, R., Patel, S., Rick, C., Gray, R., Clarke, C.E., 2010. Systematic review of levodopa dose equivalency reporting in Parkinson's disease. Mov Disord 25, 2649-2653.

Van Den Eeden, S.K., Tanner, C.M., Bernstein, A.L., Fross, R.D., Leimpeter, A., Bloch, D.A., Nelson, L.M., 2003. Incidence of Parkinson's disease: variation by age, gender, and race/ethnicity. Am J Epidemiol 157, 1015-1022.

Vidyasagar, R., Greyling, A., Draijer, R., Corfield, D.R., Parkes, L.M., 2013. The effect of black tea and caffeine on regional cerebral blood flow measured with arterial spin labeling. J Cereb Blood Flow Metab 33, 963-968.

Wahlund, L.O., Barkhof, F., Fazekas, F., Bronge, L., Augustin, M., Sjogren, M., Wallin, A., Ader, H., Leys, D., Pantoni, L., Pasquier, F., Erkinjuntti, T., Scheltens, P., 2001. A new rating scale for age-related white matter changes applicable to MRI and CT. Stroke 32, 1318-1322.

Wang, J., Alsop, D.C., Song, H.K., Maldjian, J.A., Tang, K., Salvucci, A.E., Detre, J.A., 2003. Arterial transit time imaging with flow encoding arterial spin tagging (FEAST). Magn Reson Med 50, 599-607.

Wolk, D.A., Detre, J.A., 2012. Arterial spin labeling MRI: an emerging biomarker for Alzheimer's disease and other neurodegenerative conditions. Curr Opin Neurol 25, 421-428.

Yoon, H.J., Park, K.W., Jeong, Y.J., Kang, D.Y., 2012. Correlation between neuropsychological tests and hypoperfusion in MCI patients: anatomical labeling using xjView and Talairach Daemon software. Ann Nucl Med 26, 656-664.

Zaharchuk, G., 2011. Arterial spin label imaging of acute ischemic stroke and transient ischemic attack. Neuroimaging Clin N Am 21, 285-301, x.

Zappe, A.C., Reichold, J., Burger, C., Weber, B., Buck, A., Pfeuffer, J., Logothetis, N.K., 2007. Quantification of cerebral blood flow in nonhuman primates using arterial spin labeling and a two-compartment model. Magn Reson Imaging 25, 775-783.

Zlokovic, B.V., 2008. The blood-brain barrier in health and chronic neurodegenerative disorders. Neuron 57, 178-201.

Chapter 4

Chapter 3 highlights how our preliminary work demonstrated the utility of MRI ASL techniques as useful probes for assessing NVS in the clinical setting in IPD. This led onto the main study design devised by Drs Emsley, Parkes and myself. The plan was for 20 participants in each of 4 groups (PIGD, TD, CP, CN) to undergo a similar MRI imaging protocol and clinical scales. Data from both preliminary work and the larger study were combined where possible. The key improvements were:-

- With greater numbers, a phenotypic approach in IPD was made possible and thus PIGD and TD groups were recruited separately.
- The importance of a control positive group to investigate whether changes in NVS were due to comorbid CVD was realised and a CP group recruited.
- The imaging protocol was modified. Using a hypercapnic challenge in the pilot study raised several issues, including (1) logistical difficulties, (2) limitation of participant recruitment, (3) its exploratory nature impacting interpretation, and on balance, it was decided not to include a hypercapnic challenge in the main study. This allowed time to add MRI susceptibility weighted imaging (SWI) (microbleeds) and diffusion tensor imaging (DTI) (tissue integrity) to the protocol. These were felt to be more useful in this setting, but as mentioned above, do go beyond the scope of this thesis. The ASL and DCE protocols were shortened by reducing the number of dynamic scans to allow a more efficient acquisition.
- A new scanner was installed at the WTCRF, where it was felt the study would be more appropriately based
- The clinical scales were changed in line with the large multi-centre study PRoBaND as recruitment of patients from PRoBaND was anticipated however due to the demands of the PRoBaND study (on participants) it was later felt not suitable to recruit to a further imaging study.

I initially applied for a major amendment to the ethics approval of the preliminary work to allow for this larger study, but this was rejected, prompting a successful new ethics application. I recruited all the participants, obtained informed consent, arranged their sessions at the WTCRF and coordinated the visits on the day. I performed all the clinical scales and took a blood sample for each patient. I analysed all the results under the supervision and guidance of, and using MATLAB codes devised by, Dr Laura Parkes. I wrote the paper with help from Dr Parkes for the MRI methodology section. Dr Emsley also supervised. The paper has been submitted to the Journal of Cerebral Blood Flow and Metabolism.

Structural and Physiological Neurovascular Changes in Idiopathic Parkinson's Disease and it's Clinical Phenotypes

Sarah Al-Bachari[1,2,3] , Rishma Vidyasagar[2,4,5], Hedley C.A. Emsley[6,7], Laura M. Parkes [2,8]

[1]Department of Neurology, Salford Royal NHS Foundation Trust, Salford , UK; [2]Division of Informatics, Imaging and Data Sciences, School of Health Sciences, Faculty of Biology, Medicine and Health, University of Manchester, UK; [3]Faculty of Health and Medicine, Lancaster University, UK; [4]Anatomy and Neuroscience Department, University of Melbourne, Australia; [5]Florey Institute of Neuroscience and Mental Health, Heidelberg, Melbourne, Australia; [6]Department of Neurology, Royal Preston Hospital, Preston, UK; [7]Faculty of Biology, Medicine and Health, University of Manchester, UK; [8]Division of Neuroscience and Experimental Psychology, School of Biological Sciences, Faculty of Biology, Medicine and Health, University of Manchester, UK

Corresponding author: Dr Sarah Al-Bachari

Address: Imaging and Data Sciences, University of Manchester, Stopford Building, Oxford Road, Manchester M13 9PT

Telephone: 0161 306 6000 Email: sarahalbachari@yahoo.co.uk

Support:

Sydney Driscoll Neuroscience Foundation; University of Manchester (Biomedical Imaging Institute) and Medical Research Council Studentship; Lancashire Teaching Hospitals NHS Foundation Trust & Lancaster University.

Running headline:

MRI neurovascular changes in IPD and its phenotypes

Abbreviations:

ASL - arterial spin labelling, AAT - arterial arrival time, AD - Alzheimer's disease, BBB – blood brain barrier, CBF - cerebral blood flow, CN – control negative, CP - control positive, CVD - cerebrovascular disease, DWMH - deep white matter hyperintensity, EPI - echo planar imaging, FA - flip angle, FLAIR - fluid attenuation inversion recovery, GM-grey matter, IPD - idiopathic Parkinson's disease, L-dopa - levodopa, LEDD - Levodopa equivalent dose, LL - Look-Locker, LTH – Lancashire teaching hospitals, MAP – mean arterial pressure, NVS – neurovascular status, PET - positron emission tomography, PIGD - Postural instability and gait disorder, PVH - peri ventricular hyperintensity, ROI - region of interest, SPECT - single positron emission computed tomography, SPM - statistical

parametric mapping, SRFT- Salford Royal Foundation Trust, STAR - signal targeting with alternating radiofrequency, SVD – small vessel disease, TD - tremor dominant, TE - echo time, 3T - 3 Tesla, TIA – transient ischaemic attach, UKPDS BB - United Kingdom Parkinson's Disease Society Brain Bank, UPDRS - Unified Parkinson's Disease Rating Scale, VBM - volume based morphometry, WTCRF - Wellcome Trust Clinical Research Facility, WML - white matter lesion

Unstructured abstract

Neurovascular changes are likely to interact importantly with the neurodegenerative process in idiopathic Parkinson's disease (IPD). Markers of neurovascular status (NVS) include white matter lesion (WML) burden and arterial spin labelling (ASL) measurements of cerebral blood flow (CBF) and arterial arrival time (AAT). We investigated NVS in IPD, including an analysis of IPD clinical phenotypes, by comparison with two control groups, one with a history of clinical cerebrovascular disease (CVD) (control positive, CP) and one without CVD (control negative, CN).

Fifty-one patients with IPD (mean age 69.0 ± 7.7 years) (21 tremor dominant [TD], 24 postural instability and gait disorder [PIGD] and 6 intermediates), 18 CP (mean age 70.1 ± 8.0 years), and 34 CN subjects (mean age 67.4 ± 7.6 years) completed a 3T MRI scan protocol including T2-weighted fluid-attenuated inversion recovery (FLAIR) and ASL.

IPD patients showed diffuse regions of significantly prolonged AAT, small regions of lower CBF by comparison with CN subjects, and a few regions of prolonged AAT by comparison with CP subjects. In the most part both motor phenotypes revealed a similar pattern of NVS. These data provide evidence of altered NVS in IPD, without significant IPD phenotype specific differences.

Keywords

MRI, ASL, Cerebral blood flow, Parkinson's disease, cerebrovascular disease

4.1 Introduction

Idiopathic Parkinson's disease (IPD) is the second most common neurodegenerative disorder, for which there are no effective disease modifying or neuroprotective agents. What drives the selective and progressive neuronal dysfunction and loss, the hallmark of neurodegeneration, remains elusive. Neurodegeneration is understood to result from a number of insults or key factors that act and interact over time leading to selective neuronal loss (Bourdenx et al., 2015; Collins et al., 2012). Any of these factors found to be potentially modifiable may point to therapeutic opportunities.

The 'vascular' hypothesis has recently gained much momentum, proposing a key role for neurovascular changes in neuronal dysfunction and loss (Collins et al., 2012; Grammas et al., 2011; Nelson et al., 2015; Sagare et al., 2013b; Zhao et al., 2015; Zlokovic, 2008). A number of preclinical studies have identified vascular changes as contributors to the neurodegenerative process, but clinical studies in this area remain equivocal (Nanhoe-Mahabier et al., 2009; Patel et al., 2011b). The nature and relevance of vascular changes may also differ between IPD clinical phenotypes perhaps reflecting pathophysiological differences (Thenganatt and Jankovic, 2014). Clinical studies often use markers of conventional cerebrovascular disease (CVD), whether clinical (stroke, transient ischaemic attack [TIA]) or imaging (white matter lesion [WML]) which may be insensitive to more subtle neurovascular alterations. Herein we have used the term 'neurovascular status' (NVS) to encompass the various structural and physiological neurovascular markers.

Magnetic resonance imaging (MRI) arterial spin labelling (ASL) is a non-invasive tool which allows quantitative measures of cerebral blood flow (CBF) and arterial arrival time (AAT), the time taken for blood to travel from the labelling slab to the tissue of interest (Wang et al., 2003; Zappe et al., 2007). CBF changes have been noted in IPD (Fernandez-Seara et al., 2012; Melzer et al., 2011). How and why these occur in the setting of IPD is poorly understood, as is the temporal relationship of CBF changes with neuronal loss. Whether, for instance, atrophic regions merely exhibit secondary hypoperfusion remains debatable (Borghammer, 2012). Therefore measurements of atrophy in addition to CBF are important to determine whether CBF alterations are simply reflective of areas of atrophy or not. AAT is longest in distal branches, especially in border zone (or watershed) areas (Hendrikse et al., 2008; Petersen et al., 2006). Alterations in AAT are considered likely to reflect chronic arteriolar vasodilatation, collateral flow and/or increased tortuosity of vessels (Derdeyn et al., 2002; Farkas and Luiten, 2001).

Neurovascular alterations have previously been reported in MRI studies of IPD, including our own finding of prolonged AAT (Al-Bachari et al., 2014). However, little is known about

how such changes might vary between clinical IPD phenotypes. In addition, the extent to which such alterations in NVS might either reflect comorbid conventional CVD, or could contribute to, or be a secondary effect of, the neurodegenerative process, is largely unknown.

In this study we sought to (1) confirm and extend our previous finding of AAT prolongation in IPD, (2) investigate other markers of NVS including WML burden and also measures of brain volume changes (to determine the extent and location of any atrophy) and (3) make comparison between phenotypes and with relevant control groups, including both subjects with and without clinical CVD.

4.2 Materials and Methods

4.21 Approvals, recruitment, eligibility and consent

Relevant approvals were obtained including ethics (North West – Preston Research Ethics Committee), research governance and local university approvals. Recruitment of IPD patients was from Lancashire Teaching Hospitals (LTH) and Salford Royal Foundation Trust (SRFT). Eligibility criteria for IPD participants were a clinical diagnosis of IPD fulfilling UK Parkinson's disease society (UKPDS) brain bank (BB) criteria (http://www.ncbi.nlm.nih.gov/projects) without known clinical CVD (no history of TIA or stroke) or dementia (Emre et al., 2007). Participants with CVD were recruited from patients at LTH with a clinical diagnosis of stroke or TIA within the previous 2 years (at least 3 months post onset) supported by relevant brain imaging (control positive, CP). Controls without a history of either IPD or clinical CVD were also recruited (control negative, CN). All groups were matched for age. All participants were required to provide written informed consent and had capacity to do so.

4.22 Clinical assessments and phenotyping

IPD phenotype was assessed using the Unified Parkinson's Disease Rating Scale (UPDRS) (http://www.mdvu.org/library/ratingscales/pd/updrs.pdf) during the scan visit. Participants with IPD were classified into three subtypes (tremor dominant [TD], postural instability and gait disorder [PIGD], intermediate) by Jankovic's method (Jankovic et al., 1990). Disease severity was measured using the Hoehn and Yahr rating scale (Hoehn and Yahr, 1967). No alterations were made to the participants' medications for the study

protocol. Routine clinical baseline data were also recorded and the levodopa equivalent doses (LEDD) calculated (Tomlinson et al., 2010). A battery of clinical scales was also administered, including the Montreal Cognitive Assessment (MoCA) (www.MoCAtest.org), details of which are beyond the scope of this paper. Data from participants in an earlier study were included to provide sufficient numbers for phenotypic comparison, comprising 14 patients with IPD and 14 controls scanned on a 3T Philips Achieva MRI system using an 8 channel coil at Salford Royal Hospital (Al-Bachari et al., 2014). Demographics and clinical data were compared between IPD and control participants using unpaired Student t-test with p-value set at < 0.05.

4.23 MRI protocol

All participants underwent an approximately 1 hour long imaging protocol, on a 3T Philips Achieva MRI system. Twenty-eight participants (14 IPD and 14 CN) were scanned using an 8 channel 8 head coil at Salford Royal Hospital and the remaining participants using a 32 channel head coil at the Wellcome Trust Clinical Research Facility (WTCRF) in Manchester. Involuntary movements in participants were minimised using padding within the head coil. A T2-weighted FLAIR image was acquired with the following parameters: TR 11s, TI 2.8s, TE 120 ms, in-plane resolution of 0.45mm, 30 axial slices of 4mm thickness with 1mm gap covering the whole brain. A Look-Locker (LL) ASL sequence was used (Gunther et al., 2001), with STAR labelling (Edelman et al., 1994) and 4 readout times of 800, 1400, 2000, 2600 ms, TR: 3500 ms; TE 22ms; flip angle 40 degrees; 3.5 x3.5 x 6 mm voxels with 1mm gap between slices; 15 slices covering the cerebrum but not the cerebellum with bipolar 'vascular crusher' gradients (added to dephase fast flowing spins and so remove large vessel signal). Sixty pairs of label and control images were collected with acquisition time of 7 minutes. The labelling slab was 15 cm with a 10 mm gap between labelling and imaging regions. To allow quantification of CBF an additional scan was acquired with TR = 10s and 15 read-out times (from 800 to 9200 ms) in order to estimate the equilibrium magnetisation of the brain. A 3D T1-weighted image with 1mm isotropic resolution was also collected.

4.24 Data analysis

All the data analyses were performed to consider differences between the IPD group as a whole and the CN group (with no history of IPD or clinical CVD), between the IPD group

as a whole and the CP group (no history of IPD, but with history of clinical CVD) and between the PIGD and TD groups. These comparisons were selected to establish whether IPD is associated with vascular changes different from those seen in CVD, and whether any such differences vary between clinical IPD phenotypes. In addition voxel-wise analyses included comparisons between PIGD and CN, and TD and CN, to further investigate regional differences between phenotypes.

ASL data were analysed using in-house MATLAB (Mathworks, MA, USA) routines using a single blood compartment model, adapted for LL readout (Al-Bachari et al., 2014). CBF and AAT maps were calculated and CBF maps were corrected for atrophy using the same method as Johnson et al., according to the proportion of grey matter (GM) and white matter in each voxel obtained from the segmented T1-weighted image (Johnson et al., 2005). Whole brain values for CBF and AAT were calculated using a simple threshold mask based on the ASL control images on an individual basis.

Voxel-wise analysis was also performed using the SPM8 PET toolbox (http://www.fil.ion.ucl.ac.uk/spm/) to determine any regionally specific differences between the groups. The groups were age, but not gender matched, therefore gender was included as a regressor. In addition all the data was reanalysed using a gender matched control group. Image pre-processing in SPM included (1) motion correction, (2) registration and normalisation of the control ASL image to the EPI template within SPM, and application of this procedure to the CBF and AAT images, and (3) spatial smoothing of the normalised images using an 8mm full-width-half-maximum kernel. Voxel-wise comparisons of CBF and AAT between the groups were carried out using a two-sample unpaired t-test (unequal variances). Regions were considered significant at a p value < 0.001 uncorrected, with a minimum cluster size of 50 voxels. Further analysis using Family-Wise Error (FWE) correction for multiple comparisons at the cluster level was performed. The MNI coordinates were used to locate areas of difference using xjview V 8.14 (http://www.alivelearn.net/xjview8/). In addition, to assess the association and impact of potential confounding variables, voxel-wise linear regression of IPD perfusion measures (AAT and CBF) with LEDD score, mean arterial pressure (MAP) and UPDRS 111 were performed.

Voxel-based morphometry (VBM) was performed on the T1-weighted images in SPM8 following standard procedures (http://www.fil.ion.ucl.ac.uk/~john/misc/VBMclass10.pdf), including modulation to allow comparisons of volumes, proportional scaling to individual intracranial volume and smoothing using an 8mm FWHM kernel.

WML burden was assessed semi-quantitatively using visual rating scales (Fazekas et al., 1993; Wahlund et al., 2001). WML volume was also calculated using the lesion segmentation toolbox (LST) in SPM8 with a threshold of 0.3. This threshold was chosen as it gave the most accurate estimates in a sub-study comparing WML volume estimates from LST with those from semi-automated lesion-growing methods on a subset of the data (n=51, including representation from all groups) (Schmidt et al., 2012b). Differences between IPD and CN and CP groups for WML burden were measured using the Fazekas periventricular hyperintensity (PVH) and deep white matter hyperintensity (DWMH) and the Wahlund rating scales. Wahlund and Fazekas scores were stratified into 3 groups: mild (Wahlund score of 0-4; Fazekas 0-1); moderate (Wahlund: 5-10; Fazekas:2); and severe (Wahlund: >10; Fazekas: 3) (Leonards et al., 2012). Fazekas scores were combined into categories (0-1) and 2 where appropriate since the majority of patients scored 1 or 2. The scales were tested using Pearson's Chi squared in SPSS 22, WML volume was compared between the groups using the Mann-Whitney U test in SPSS 22; taking into account the non-parametric nature of the results. Differences were considered significant if $p < 0.05$.

4.3 Results

4.31 Participants

Fifty one IPD patients were recruited (21 TD, 24 PIGD and 6 intermediates), 18 CP subjects with CVD (14 with ischaemic stroke, 4 with single or multiple TIAs) (mean time, in years, since diagnosis 1.1±0.7) and 34 CN subjects (Table 4.1). All groups were matched for age; a difference in gender between the CN group and the other groups was included as a regressor in the ASL analyses. IPD severity and LEDD score varied between the IPD phenotypes, as expected.

	Control (CN) (n=34)	**CP (n=18)**	**All IPD (n=51)**	**p value (IPD Vs. CN)**	**p value (IPD Vs. CP)**	**PIGD (n=24)**	**TD (n=21)**	**p value (PIGD Vs. TD)**
n (F:M)	18:16	4:14	12:39	n/a	n/a	5:19	7:15	n/a
Age, years: (SD) [range]	67.4 (7.6); [52-85]	70.1 (8.0); [53-84]	69.0 (7.7); [52-85]	0.46	0.5	70.0 (7.6); [58-89]	67.9 (7.2); [52-80]	0.33
No. of CV RF: mean (SD)	1.4 (1.1)	3.1 (1.1)	1.7 (1.5)	0.38	0.0001	1.6 (1.4)	1.8 (1.6)	0.7
RF (%):								
Hypertension	32.4	77.8	37.3	n/a	n/a	29.2	33.3	n/a
DM	5.9	5.6	3.9			0	9.5	
FH	44.1	44.4	31.4			20.8	38.1	
Smoker	29.4	66.7	37.2			35.7	19.0	
Hypercholesterolemia	42.9	77.8	29.4			33.3	23.8	
IHD	5.9	27.8	15.6			20.8	14.3	
AF	0	22.2	2			0	0	
Disease Duration: mean (SD)	n/a	1.1 (0.7)	7.2 (4.4)	n/a	n/a	9.1 (4.5)	5.1 (3.5)	0.07
Hoehn&Yahr Score: mean(SD)	n/a	n/a	2.6 (1.0)	n/a	n/a	3.2 (0.8)	1.8 (0.7)	<0.0001
UPDRS 111 Score: mean(SD)	n/a	n/a	30.2 (11.8)	n/a	n/a	29.9 (21.1)	26.3 (10.8)	0.05
PIGD Score: mean (SD)	n/a	n/a	6.8 (4.8)	n/a	n/a	9.2 (4.6)	1.8 (1.5)	n/a
Tremor Score: mean (SD)	n/a	n/a	6.2 (5.2)	n/a	n/a	2.8 (3.0)	9.2 (4.6)	n/a
LEDD Score (mg): mean (SD)	n/a	n/a	586.4 (336.7)	n/a	n/a	785.9 (310.1)	370.0 (247.8)	<0.0001
Whole brain CBF (ml/min/100ml)	46.7±8.8	43.4±7.0	47.5±11.5	1.0	0.06	49.6±13.4	46.7±8.9	0.7
Whole brain AAT (ms)	1375.7±156.5	1463.7±133.6	1524.6±168.0	<0.0001	0.04	1507.1±128.7	1526.8±209.2	0.7

Table 4.1 Demographics, clinical characteristics and whole brain perfusion measures. RF %- percent of group with the risk factor.AF – atrial fibrillation DM – diabetes mellitus, FH – family history, IHD – ischaemic heart disease

4.32 CBF

Whole brain CBF did not differ significantly between the IPD and CN groups, IPD and CP groups nor between the IPD phenotypes (Figure 4.1, Table 4.1). The voxel-wise analyses did reveal areas of lower CBF in the IPD group by comparison with the CN group, which were predominantly posterior with a few frontal regions (Figure 4.2, Table 4.2). There was only one area of higher CBF in the IPD group compared to the CN group, in the right lateral globus pallidus (MNI coordinates [20 -2 4], cluster size 85 voxels, peak t-value 3.7, peak p-value 0.001). Voxel-wise analysis of the IPD group against the CP group revealed one area of higher CBF, in the left superior temporal gyrus (MNI coordinates [-48 -48 -10], cluster size 132 voxels, peak t-value 4.26, peak p-value <0.001). The TD and PIGD groups, when compared to the CN group, revealed phenotype specific patterns of hypoperfusion, with only the PIGD group showing areas of hyperperfusion compared to the CN group (in the right lateral globus pallidus). A direct comparison of the PIGD and TD groups however did not reveal any significant difference in CBF. In summary, we found modest reductions in CBF in IPD in comparison to CN, and little difference compared to CP. There were minimal significant phenotypic differences.

Figure 4.1a *Figure 4.1b*

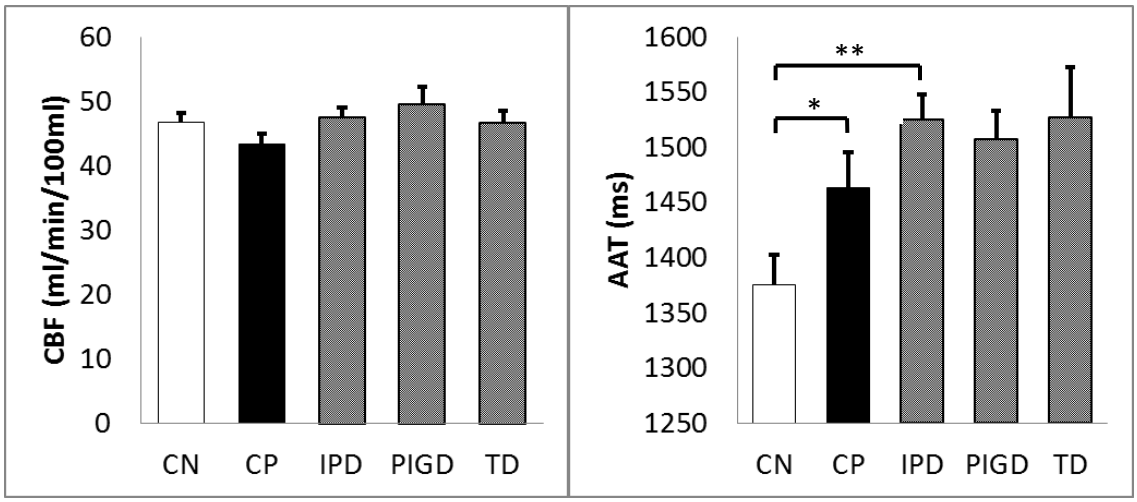

Figure 4.1 a and b: Mean and standard error of whole brain CBF (a) and AAT (b). Error bars show the standard error in the mean. ***** indicates a statistically significant difference at p<0.005.

Below Table 4.2 Regions of CBF differences between groups at p<0.001, cluster size 50 voxels.

Comparison	Region	Cluster Size	Cluster p (FWE Cor.)	Peak t value	Peak p (uncor.)	Peak MNI Coordinates
IPD < CN	R middle frontal gyrus	176	0.3	4.6	<0.0001	44 54 12
	L cuneus extending to calcarine region	201	0.2	4.4 3.8 3.3	<0.0001 0.0001 0.0008	-18 -96 2 2 -94 4 -8 -98 -4
	L mid temporal gyrus extending to inferior gyrus and occipital region	215	0.2	4.3 3.9 3.7	<0.0001 <0.0001 0.0002	-66 -58 4 -66 -54 -4 -60 -66 2
	R mid temporal extending to mid occipital gyrus	96	0.5	4.2	<0.0001	50 -66 24
	R post central gyrus	61	0.6	4.0	<0.0001	32 -36 42
	L precuneus extending to cuneus	358	0.08	4.0 3.9 3.6	<0.0001 0.0001 0.0003	-6 -64 58 0 -68 48 -2 -82 40
	L frontal superior medial region	57	0.7	3.9	0.0001	-4 66 12
	L inferior to superior parietal lobule	68	0.6	3.6 3.5 3.4	0.0003 0.0004 0.0005	-30 -72 44 -54 -66 30 -46 -64 42
IPD > CN	R lateral globus pallidus	85	0.5	3.9	0.0001	20 -2 4
IPD > CP	L subgyral region	132	0.4	4.3	0.0000	-48 -48 -10
PIGD < CN	Large region extending most of occipital lobes bilaterally	1540	0.0002	5.9 4.6 4.0	<0.0001	22 -98 0 -8 -100 0 -40 -90 18
	L mid temporal to occipital gyrus	102	0.5	4.5	<0.0001	-64 -62 6
	L inferior occipital region	74	0.6	3.9	0.0001	-52 -74 -8
	L superior temporal gyrus	51	0.7	3.7 3.6	0.0002 0.0003	-50 12 -6 -48 16 -14
	R inferior temporal to inferior occipital region	102	0.5	3.7 3.8	0.0002 0.0002	50 -76 -2 54 -68 -4
	R mid occipital region	60	0.7	3.7	0.0002	50 -68 26
PIGD > CN	Lentiform nucleus, lateral globus pallidus, putamen and limbic lobe	276	0.1	4.6 4.0 3.9	<0.0001 0.0001 0.0001	20 -12 -12 20 -6 0 30 -18 14
TD < CN	R temporal to mid occipital region extending to parietal lobe	276	0.1	4.8 3.7 3.6	<0.0001 0.0002 0.0003	52 -72 24 40 -78 34 38 -84 26
	R mid frontal lobe	192	0.3	4.7 3.8 3.4	<0.0001 0.0002 0.0002	46 54 6 44 52 22 36 62 14
	Transverse temporal area	76	0.6	4.6	<0.0001	70 -26 -6
	L frontal sub gyral region	53	0.7	4.4	<0.0001	-30 -2 32
	L angular region extending to inferior temporal lobule and middle temporal gyrus	364	0.07	4.2 4.0 3.6	<0.0001 <0.0001 0.0003	-52 -64 40 -46 -72 26 -42 -78 38
	R mid temporal gyrus	149	0.4	3.6 3.3	0.0004 0.0008	60 -52 0 56 -66 0
	L middle temporal gyrus	105	0.5	3.8 3.3	0.0002 0.0008	-64 -60 2 -66 -52 -2
	L inferior parietal lobule	111	0.5	3.7	0.0001 0.0003	-58 -38 50 -46 -46 50
	R subgyral/post central gyrus	75	0.6	3.9	0.0001	26 -42 42

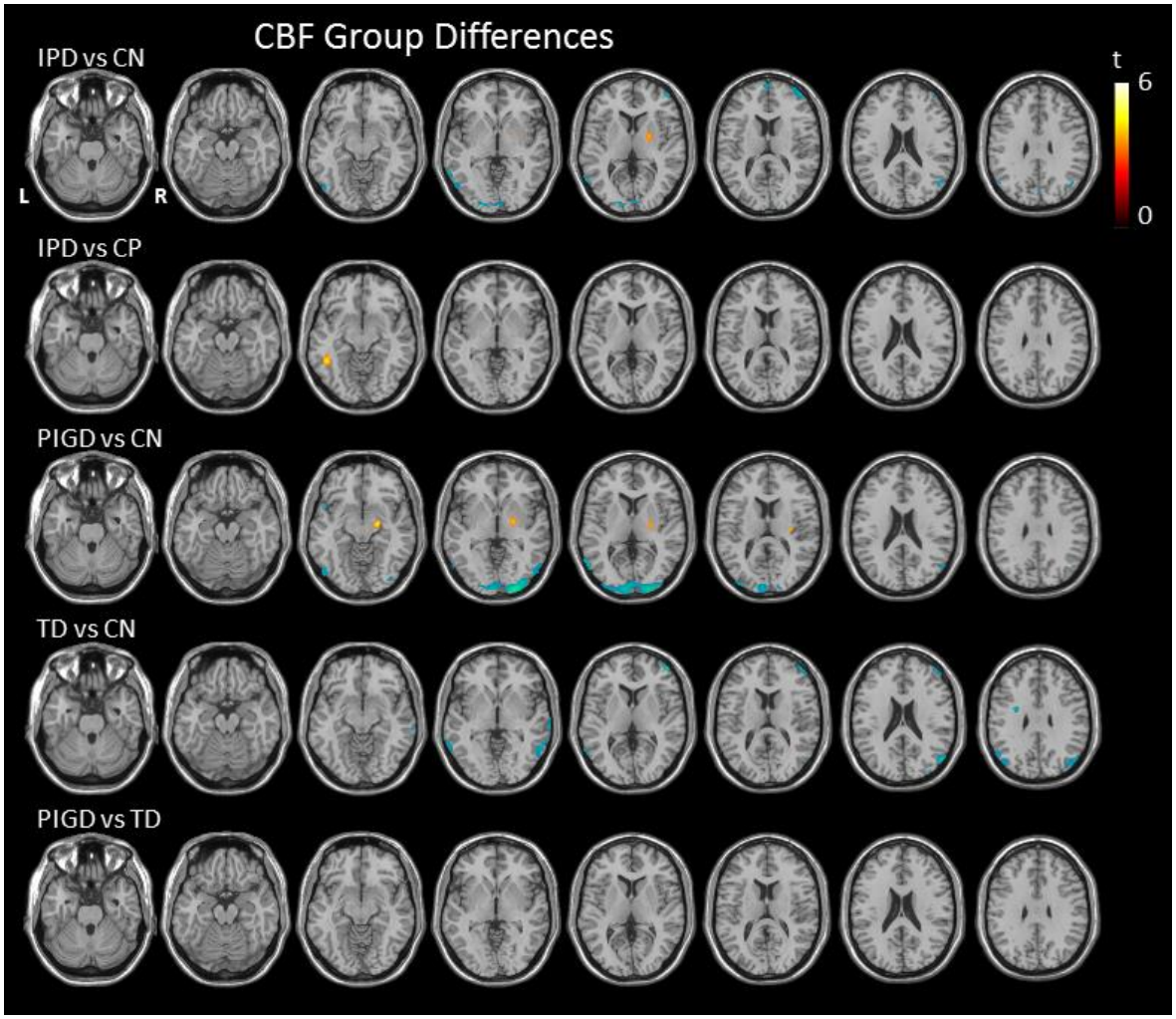

Figure 4.2: Hypoperfusion (blue) and hyperperfusion (red) in the IPD group compared to CN. T statistic maps obtained by comparison of CBF between various groups, thresholded to $p < 0.001$ uncorrected, minimum cluster size 50 voxels.

4.33 AAT

Whole brain AAT revealed significantly longer AAT in the IPD group as a whole compared to both the CN group ($p < 0.005$) and the CP group ($p < 0.05$) (Figure 4.1, Table 4.1). No significant differences were observed between IPD phenotypes.

Voxel-wise analyses revealed widespread regions of significantly increased AAT in the IPD group compared to the CN group (Figure 4.3, Table 4.3). There were no regions in the brain where AAT was significantly shorter in the IPD group compared to the CN group. Voxel-wise analysis of the IPD group against the CP group revealed a few areas of scattered prolonged AAT in the IPD group compared to the CP group, predominantly in posterior regions. The TD group revealed a more diffuse pattern of prolonged AAT than

the PIGD group when compared to the CN group, with a few of these regions reaching significance when directly comparing the TD and PIGD groups.

Comparison	Region	Cluster Size	Cluster p (FWE Cor.)	Peak t value	Peak p (uncor.)	Peak MNI Coordinates
IPD Vs CN	Large region L cerebrum most temporal lobe extending to the insula, parietal and frontal lobes including basal ganglia	7811	*<0.0001	5.4 5.2 4.6	<0.0001	16 -74 6 -26 -64 4 -34 18 8
	R cerebrum extending to most temporal lobe, insula, parietal and frontal lobes Inc. BG	2515	0.0009	4.3 4.1 4.1	<0.0001	36 -12 12 50 -32 12 40 -24 -2
	R cerebrum –limbic and anterior cingulate	410	0.3	4.3	<0.0001 0.0001	10 44 8 -2 44 6
	R middle and inferior frontal lobe	213	0.6	3.9	<0.0001	10 40 42 -4 38 34
	L amygdala	52	0.9	3.7	0.0002	-12 -16 -4
IPD Vs CP	L inferior frontal gyrus extending into insula region	193	0.6	4.4	<0.0001	-32 18 -12
	R medial frontal gyrus	85	0.9	4.2	<0.0001	16 52 6
	R medial frontal extending to superior frontal and cingulate gyrus	130	0.8	4.2 3.4	<0.0001 0.0005	14 46 30 12 38 36
	R superior temporal gyrus extending to middle temporal gyrus	251	0.5	4.1 4.0 3.8	<0.0001 <0.0001 0.0001	44 16 -26 48 -6 -20 50 4 -22
	L transverse temporal gyrus	94	0.8	3.8	0.0002	-68 -16 12
PIGD Vs CN	L superior to middle temporal gyrus	234	0.5	4.6	<0.0001	-26 -62 2
	L precuneus	190	0.6	4.0	<0.0001	-22 -74 18
	R lentiform nucleus and putamen	110	0.8	4.0 3.7 3.3	0.0001 0.0003 0.0009	18 6 4 26 -6 0 32 -12 -2
	R sup. Temporal gyrus	222	0.5	3.9	0.0001	62 -32 12
	L angular gyrus	59	0.9	3.9	0.0002	-38 -56 26
	Sup. & L subgyral Temporal lobe	153	0.7	3.8 3.4	0.0002 0.0006	-36 -40 0 -38 -46 16
	L supramarginal	51	0.9	3.7	0.0002	-50 -46 28
	R calcarine	65	0.9	3.7	0.0002	14 -76 6
	L sup temporal gyrus	131	0.8	3.7 3.5	0.0003 0.0004	-62 -34 10 -54 -44 8
	R calcarine	88	0.9	3.7	0.0003	6 -68 18
TD Vs CN	L post. Central gyrus extending to frontal lobe, L insula and superior temporal gyrus, includes L caudate	3386	*<0.0001	5.7 5.3 5.0	<0.0001	-52 -18 16 -16 14 12 -34 -4 14
	R insula extends to R precentral gyrus includes R putamen	1709	0.002	5.5 5.0 4.2	<0.0001	42 -8 12 58 -4 10 32 6 10
	R occipital and calcarine extends to R lingual region	976	0.02	4.6 4.1 4.0	<0.0001	0 -50 12 16 -86 2 16 -74 2
	L middle temporal gyrus extending to inferior temporal gyrus	708	0.07	4.5 4.5	<0.0001	-62 -30 -8 -64 -38 -14
	L lingual	67	0.9	3.8	0.0002	-6 -80 2
	L sup. occipital to L cuneus	135	0.7	3.8 3.5	0.0002 0.0004	-18 -64 26 -12 -76 18
	R medial frontal gyrus	74	0.9	3.6 3.6	0.0004 0.0004	12 38 36 10 46 32
TD Vs PIGD	R calcarine extending to cuneus	91	0.8	4.1	<0.0001	16 -86 2
	L frontal extending to caudate and limbic region	99	0.8	4.1	<0.0001	-14 16 -10
	L inferior frontal gyrus	53	0.9	4.1	<0.0001	-62 18 6
	L mid occipital and calcarine region	68	0.9	4.0	0.0001	-8 -112 -4
	R fronto- superior orbital region extending to R middle frontal gyrus	74	0.9	3.9	0.0002	20 26 -24
	R middle occipital gyrus extending to calcarine region	52	0.9	3.8	0.0002	26 -102 0
	L mid occipital region	61	0.9	3.7	0.0003	-34 -106 6

Table 4.3: Regions of AAT differences between groups at p<0.001, cluster size 50 voxels.

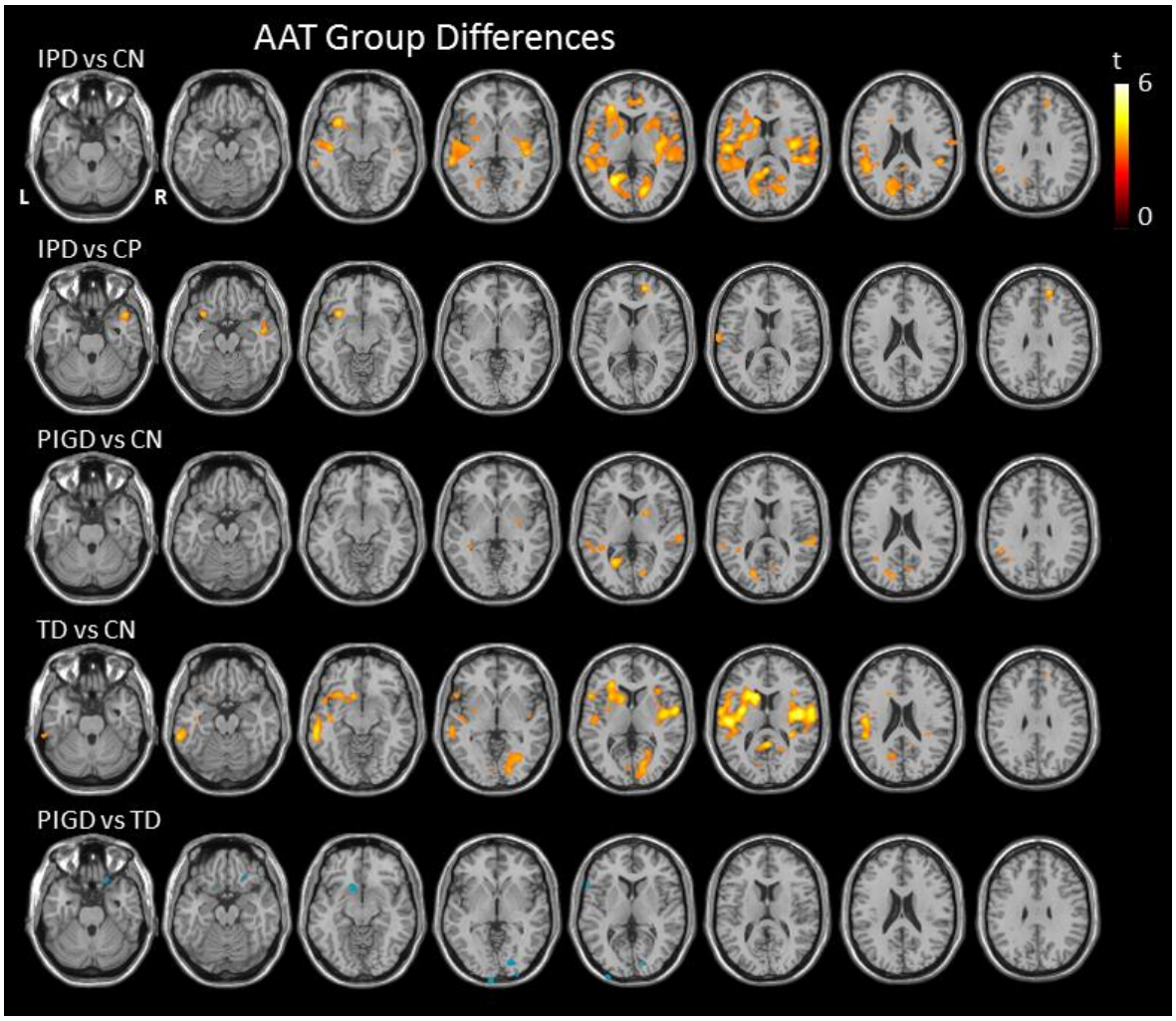

Figure 4.3: Prolonged AAT in IPD compared to controls. T statistic maps obtained by comparison of AAT between various groups, thresholded to $p < 0.001$ uncorrected, minimum cluster size 50 voxels.

4.34 Correlations with Potential Confounding Variables

Voxel-wise linear regression of perfusion measures (AAT and CBF) in the IPD group as a whole with LEDD score, disease duration and MAP respectively (considered potential confounding variables) revealed no association with perfusion measures. However an inverse correlation was noted between UPDRS 111 motor score and AAT (i.e. greater disease severity correlating with shorter AAT) predominantly in the temporal regions (mid to inferior temporal and fusiform gyrus). The same test was performed on the PIGD and TD groups, revealing the association to be only in the PIGD group. No association between UPDRS 111 and CBF measures was revealed.

Re-analysis of the data with the gender matched control group and re-analysis with the removal of the preliminary data (obtained from our earlier study) yielded similar results to those discussed in the above sections.

4.35 VBM analysis

The voxel-wise analysis did reveal areas of reduced GM volume in the IPD group as a whole compared to the CN group, predominantly in the temporal lobes (Figure 4.4). Voxel-wise analysis of the IPD group against the CP group revealed one area of reduced GM in the middle temporal gyrus (MNI coordinates [-48 -48 -10], cluster size 154 voxels, peak t-value 4.02, peak p-value <0.001). Comparison of TD to PIGD revealed one region of lower GM volume in the TD group in the frontal cortex.

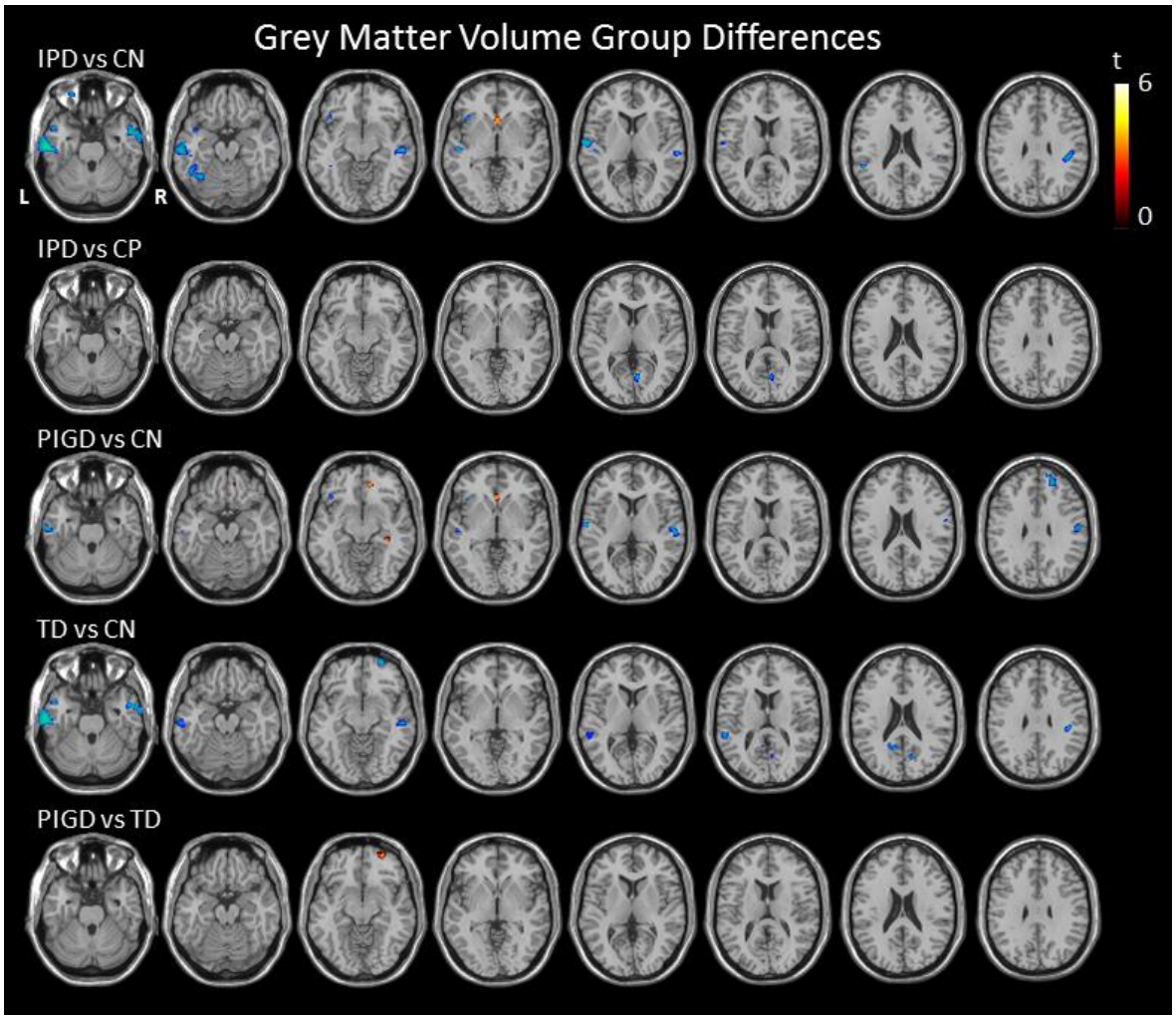

Figure 4.4: T statistic maps obtained by comparison of GM volume between various groups, thresholded to p < 0.001 uncorrected, minimum cluster size 50 voxels.

4.36 WML burden

All the WML scores were significantly higher in the IPD group as a whole compared to the CN group, with no significant differences between the IPD and CP groups or between the IPD phenotypes. These findings differ to that of the pilot study (Chapter 3; 14 IPD patients Vs 14 controls) which revealed no significant differences, this may highlight the fact that when using rating scales a larger sample size is needed to tease out any potential differences.

A trend towards greater WML volume was seen in the IPD group compared to the CN group (p=0.08). WML volume was significantly higher in the CP group when compared with the IPD group and significantly higher in the PIGD group by comparison with the TD group (Table 4.4).

	Control (CN) (n=34)	**CP (n=18)**	**All IPD (n=51)**	**p value (IPD Vs. CN)**	**p value (IPD Vs. CP)**	**PIGD (n=24)**	**TD (n=21)**	**p value (PIGD Vs. TD)**
Wahlund Score: N (%)								
Mild	23 (67.6)	3 (16.7%)	17 (33.3)	0.005	0.296	6 (25.0%)	8 (38.1%)	0.59
Moderate	9 (26.5)	12 (66.7%)	23 (45.1)			13 (54.2%)	8 (38.1%)	
Severe	2 (5.9)	3 (16.7%)	11 (21.6)			5 (20.8%)	5 (23.8%)	
Fazekas PVH: N (%)	25 (73.5)	5 (27.8%)	22 (43.1)	0.020	0.445	8 (33.3%)	11 (52.4%)	0.48
(0-1) Mild	6 (17.6%)	10 (55.6%)	20 (39.2)			12 (50%)	7 (33.3%)	
(2) Moderate	3 (8.8%)	3 (16.7%)	9 (17.6)			4 (16.7%)	3 (14.3%)	
(3) Severe								
Fazekas DWMH: N (%)								
(0-1) Mild	28 (82.4%)	11 (61.1%)	27 (52.9)	0.021	0.858	10 (41.7%)	14 (66.7%)	0.246
(2) Moderate	4 (11.8%)	5 (27.8%)	18 (35.3)			11 (45.8%)	5 (23.8%)	
(3) Severe	2 (5.9%)	2 (11.1%)	6 (11.8)			3 (12.5%)	2 (9.5%)	
WML Volume: (ml) Median (IR)	1.41 (3)	10.44 (15)	4 (9)	0.08	0.00	8.03 (15)	1 (4)	0.00

Table 4.4: WML rating scales and volumes (p value Pearson's Chi squared for rating scales and Mann Whitney for WML volume). PVH, periventricular hyperintensity; DWMH, deep white matter hyperintensity

4.4 Discussion

This study used a multi-modal MRI approach in a clinical study to better understand NVS in IPD and revealed key differences in NVS namely AAT prolongation, reduced CBF and differences in WML burden in IPD patients by comparison with age matched controls with and without CVD. Within the IPD group phenotype specific differences were minimal.

This study confirmed our previous findings of diffuse prolonged AAT in IPD patients compared to controls; whole brain and voxel wise analysis revealed this prolongation to be greater in IPD patients than in controls without CVD and in more areas than the CVD group. As the IPD group had significantly fewer vascular risk factors than the CP group, this raises the interesting possibility that mechanisms of AAT prolongation might be independent of, or at the least driven by factors other than, conventional CVD.

As far back as 2003 Markus et al. described the potential benefit of ASL techniques as a method to evaluate cerebral blood flow in CVD (Markus, 2004). It has developed potential as a non contrast measure of perfusion changes, with reduced CBF found in areas of ischaemia (as would be expected). It has proved particularly helpful in the situation where a contrast agent would be contraindicated (such as in renal failure) (Bokkers et al., 2008; Zaharchuk, 2011, 2014).Indeed AAT has been measured in acute stroke and studies of CVD revealing areas of prolonged AAT generally reflecting preserved perfusion, lack of progression to infarct and more minor symptoms (Chalela et al., 2000; MacIntosh et al., 2010b; Wolf et al., 2014) . Prolonged AAT has been postulated to be reflective of recruitment of collaterals or secondary to altered vasculature causing a decrease in the flow velocity, for example, increased tortuosity, altered vascular wall diameter/compliance and chronic vasodilation (Detre et al., 1999; Liu et al., 2012; MacIntosh et al., 2015; Paling et al., 2013; Zaharchuk, 2011).

WML burden, as measured by visual rating scales, was higher in the IPD patients than in the CN subjects – in keeping with our earlier work (Patel et al., 2011b). WML rating scales also revealed a greater burden in CP than IPD which is to be expected yet also suggests conventional CVD may not be driving AAT prolongation. Of note WML volume (arguably a more accurate measure of WML burden as rating scales do not take into account the size/volume of the lesions) was significantly higher in the PIGD than in the TD group, indeed PIGD WML volumes were comparable to control subjects with CVD.

CBF differences were revealed between the IPD group and CN in keeping with other imaging studies (Fernandez-Seara et al., 2012; Kamagata et al., 2011; Melzer et al., 2011; Nobili et al., 2011)

This study does not really suggest a difference between the PIGD and TD phenotypes with respect to AAT or CBF as any potential differences seen when comparing each phenotype separately to the CN did , in the most part, not survive head to head phenotype comparisons.

Some would argue that perfusion changes are simply secondary to neuronal loss. If that were the case then one would expect a similar anatomical distribution of GM loss demonstrated by VBM to that of the reduction in perfusion, yet they are clearly distinct, with GM loss restricted to the temporal lobes. In addition the perfusion patterns did not differ greatly to that of known CVD and one would not expect a similar pattern of atrophy in IPD to CVD. Interestingly studies in AD at the preclinical stages and even in relatives of those with AD have revealed early perfusion changes (Okonkwo et al., 2014; Wierenga et al., 2014); this may suggest that some changes in perfusion in neurodegenerative states occur before neuronal loss. This raises an interesting hypothesis to be tested in IPD – that perfusion changes are a forerunner to, rather than a sequel of, neuronal loss. There is a need for prodromal studies (for example, in specific individuals with genetic predisposition) and longitudinal studies temporally mapping vascular and neuronal changes.

The main limitations to this study are that certain variables could not be controlled for including LEDD, disease duration, disease severity and MAP. To evaluate their potential impact they were included as correlation tests/coefficients with AAT and CBF respectively, yet no correlation was found except UPDRS correlated with shortened AAT in the PIGD group only, with a pattern completely different to prolonged AAT seen between group comparisons. Therefore it was not felt appropriate to include the above variables as covariates in the group comparisons.

4.5 Conclusion

This study has confirmed and added to our previous findings; namely, there is diffuse prolongation of AAT and reduced CBF in IPD patients by comparison with normal control subjects, with a few regions of prolonged AAT in IPD patients by comparison with controls

subjects with CVD, despite significantly fewer vascular risk factors. We also observed differentially distributed GM loss and reduced perfusion. These data thus provide evidence of altered NVS in IPD, with IPD phenotype comparisons revealing similar patterns of altered NVS. Further studies are needed, likely longitudinal, to further investigate possible differences in the neurovascular contribution to the pathophysiology of particular IPD phenotypes, and to establish whether neurovascular changes partly drive, or are secondary to, the neurodegenerative process.

Acknowledgements

We are grateful to all participants without whom the work would not have been possible. We are also grateful to the following groups of people and individuals for their help with various parts of the work: MRI radiographers at Salford Royal Hospital and at the Wellcome Trust Clinical Research Facility, Parkinson's disease nurse specialists at Lancashire Teaching Hospitals NHS Foundation Trust, Drs Martha Hanby and Monty Silverdale, Dan Cox, Helen Beaumont, Laura Howell and Wenge Wu.

Funding acknowledgements

Salary (Dr Al-Bachari) and research costs for this work were provided through support from: Sydney Driscoll Neuroscience Foundation; University of Manchester (Biomedical Imaging Institute) and Medical Research Council Studentship; Lancashire Teaching Hospitals NHS Foundation Trust & Lancaster University. Dr Vidyasagar is supported by the University of Melbourne. Dr Emsley is supported by Lancashire Teaching Hospitals NHS Foundation Trust. Dr Parkes is supported by the University of Manchester.

Author Contribution statement

All authors made a substantial contribution to the concept and design, acquisition of data and analysis and interpretation of data. SAB, HE and LP drafted the article and revised it critically for important intellectual content, and all authors approved the version to be published.

Disclosure/Conflict of Interest

The authors have no relevant disclosures or conflicts of interest to declare.

References

Al-Bachari, S., Parkes, L.M., Vidyasagar, R., Hanby, M.F., Tharaken, V., Leroi, I., Emsley, H.C., 2014. Arterial spin labelling reveals prolonged arterial arrival time in idiopathic Parkinson's disease. Neuroimage Clin 6, 1-8.

Borghammer, P., 2012. Perfusion and metabolism imaging studies in Parkinson's disease. Dan Med J 59, B4466.

Bourdenx, M., Dovero, S., Engeln, M., Bido, S., Bastide, M.F., Dutheil, N., Vollenweider, I., Baud, L., Piron, C., Grouthier, V., Boraud, T., Porras, G., Li, Q., Baekelandt, V., Scheller, D., Michel, A., Fernagut, P.O., Georges, F., Courtine, G., Bezard, E., Dehay, B., 2015. Lack of additive role of ageing in nigrostriatal neurodegeneration triggered by alpha-synuclein overexpression. Acta Neuropathol Commun 3, 46.

Chalela, J.A., Alsop, D.C., Gonzalez-Atavales, J.B., Maldjian, J.A., Kasner, S.E., Detre, J.A., 2000. Magnetic resonance perfusion imaging in acute ischemic stroke using continuous arterial spin labeling. Stroke 31, 680-687.

Collins, L.M., Toulouse, A., Connor, T.J., Nolan, Y.M., 2012. Contributions of central and systemic inflammation to the pathophysiology of Parkinson's disease. Neuropharmacology 62, 2154-2168.

Derdeyn, C.P., Videen, T.O., Yundt, K.D., Fritsch, S.M., Carpenter, D.A., Grubb, R.L., Powers, W.J., 2002. Variability of cerebral blood volume and oxygen extraction: stages of cerebral haemodynamic impairment revisited. Brain 125, 595-607.

Detre, J.A., Samuels, O.B., Alsop, D.C., Gonzalez-At, J.B., Kasner, S.E., Raps, E.C., 1999. Noninvasive magnetic resonance imaging evaluation of cerebral blood flow with acetazolamide challenge in patients with cerebrovascular stenosis. J Magn Reson Imaging 10, 870-875.

Edelman, R.R., Siewert, B., Darby, D.G., Thangaraj, V., Nobre, A.C., Mesulam, M.M., Warach, S., 1994. Qualitative mapping of cerebral blood flow and functional localization with echo-planar MR imaging and signal targeting with alternating radio frequency. Radiology 192, 513-520.

Emre, M., Aarsland, D., Brown, R., Burn, D.J., Duyckaerts, C., Mizuno, Y., Broe, G.A., Cummings, J., Dickson, D.W., Gauthier, S., Goldman, J., Goetz, C., Korczyn, A., Lees, A., Levy, R., Litvan, I., McKeith, I., Olanow, W., Poewe, W., Quinn, N., Sampaio, C., Tolosa, E., Dubois, B., 2007. Clinical diagnostic criteria for dementia associated with Parkinson's disease. Mov Disord 22, 1689-1707; quiz 1837.

Farkas, E., Luiten, P.G., 2001. Cerebral microvascular pathology in aging and Alzheimer's disease. Prog Neurobiol 64, 575-611.

Fazekas, F., Kleinert, R., Offenbacher, H., Schmidt, R., Kleinert, G., Payer, F., Radner, H., Lechner, H., 1993. Pathologic correlates of incidental MRI white matter signal hyperintensities. Neurology 43, 1683-1689.

Fernandez-Seara, M.A., Mengual, E., Vidorreta, M., Aznarez-Sanado, M., Loayza, F.R., Villagra, F., Irigoyen, J., Pastor, M.A., 2012. Cortical hypoperfusion in Parkinson's disease assessed using arterial spin labeled perfusion MRI. NeuroImage 59, 2743-2750.

Grammas, P., Martinez, J., Miller, B., 2011. Cerebral microvascular endothelium and the pathogenesis of neurodegenerative diseases. Expert Rev Mol Med 13, e19.

Gunther, M., Bock, M., Schad, L.R., 2001. Arterial spin labeling in combination with a look-locker sampling strategy: inflow turbo-sampling EPI-FAIR (ITS-FAIR). Magn Reson Med 46, 974-984.

Hendrikse, J., Petersen, E.T., van Laar, P.J., Golay, X., 2008. Cerebral border zones between distal end branches of intracranial arteries: MR imaging. Radiology 246, 572-580.

Hoehn, M.M., Yahr, M.D., 1967. Parkinsonism: onset, progression and mortality. Neurology 17, 427-442.

Jankovic, J., McDermott, M., Carter, J., Gauthier, S., Goetz, C., Golbe, L., Huber, S., Koller, W., Olanow, C., Shoulson, I., et al., 1990. Variable expression of Parkinson's disease: a base-line analysis of the DATATOP cohort. The Parkinson Study Group. Neurology 40, 1529-1534.

Johnson, N.A., Jahng, G.H., Weiner, M.W., Miller, B.L., Chui, H.C., Jagust, W.J., Gorno-Tempini, M.L., Schuff, N., 2005. Pattern of cerebral hypoperfusion in Alzheimer disease and mild cognitive impairment measured with arterial spin-labeling MR imaging: initial experience. Radiology 234, 851-859.

Kamagata, K., Motoi, Y., Hori, M., Suzuki, M., Nakanishi, A., Shimoji, K., Kyougoku, S., Kuwatsuru, R., Sasai, K., Abe, O., Mizuno, Y., Aoki, S., Hattori, N., 2011. Posterior hypoperfusion in Parkinson's disease with and without dementia measured with arterial spin labeling MRI. J Magn Reson Imaging 33, 803-807.

Leonards, C.O., Ipsen, N., Malzahn, U., Fiebach, J.B., Endres, M., Ebinger, M., 2012. White matter lesion severity in mild acute ischemic stroke patients and functional outcome after 1 year. Stroke 43, 3046-3051.

Liu, Y., Zhu, X., Feinberg, D., Guenther, M., Gregori, J., Weiner, M.W., Schuff, N., 2012. Arterial spin labeling MRI study of age and gender effects on brain perfusion hemodynamics. Magn Reson Med 68, 912-922.

MacIntosh, B.J., Lindsay, A.C., Kylintireas, I., Kuker, W., Gunther, M., Robson, M.D., Kennedy, J., Choudhury, R.P., Jezzard, P., 2010. Multiple inflow pulsed arterial spin-labeling reveals delays in the arterial arrival time in minor stroke and transient ischemic attack. AJNR Am J Neuroradiol 31, 1892-1894.

MacIntosh, B.J., Swardfager, W., Robertson, A.D., Tchistiakova, E., Saleem, M., Oh, P.I., Herrmann, N., Stefanovic, B., Lanctot, K.L., 2015. Regional cerebral arterial transit time hemodynamics correlate with vascular risk factors and cognitive function in men with coronary artery disease. AJNR Am J Neuroradiol 36, 295-301.

Melzer, T.R., Watts, R., MacAskill, M.R., Pearson, J.F., Rueger, S., Pitcher, T.L., Livingston, L., Graham, C., Keenan, R., Shankaranarayanan, A., Alsop, D.C., Dalrymple-Alford, J.C., Anderson, T.J., 2011. Arterial spin labelling reveals an abnormal cerebral perfusion pattern in Parkinson's disease. Brain 134, 845-855.

Mure, H., Hirano, S., Tang, C.C., Isaias, I.U., Antonini, A., Ma, Y., Dhawan, V., Eidelberg, D., 2011. Parkinson's disease tremor-related metabolic network: characterization, progression, and treatment effects. NeuroImage 54, 1244-1253.

Nanhoe-Mahabier, W., de Laat, K.F., Visser, J.E., Zijlmans, J., de Leeuw, F.E., Bloem, B.R., 2009. Parkinson disease and comorbid cerebrovascular disease. Nat Rev Neurol 5, 533-541.

Nelson, A.R., Sweeney, M.D., Sagare, A.P., Zlokovic, B.V., 2015. Neurovascular dysfunction and neurodegeneration in dementia and Alzheimer's disease. Biochim Biophys Acta.

Nobili, F., Arnaldi, D., Campus, C., Ferrara, M., De Carli, F., Brugnolo, A., Dessi, B., Girtler, N., Morbelli, S., Abruzzese, G., Sambuceti, G., Rodriguez, G., 2011. Brain perfusion correlates of cognitive and nigrostriatal functions in de novo Parkinson's disease. Eur J Nucl Med Mol Imaging 38, 2209-2218.

Okonkwo, O.C., Xu, G., Oh, J.M., Dowling, N.M., Carlsson, C.M., Gallagher, C.L., Birdsill, A.C., Palotti, M., Wharton, W., Hermann, B.P., LaRue, A., Bendlin, B.B., Rowley, H.A., Asthana, S., Sager, M.A., Johnson, S.C., 2014. Cerebral blood flow is diminished in asymptomatic middle-aged adults with maternal history of Alzheimer's disease. Cereb Cortex 24, 978-988.

Paling, D., Thade Petersen, E., Tozer, D.J., Altmann, D.R., Wheeler-Kingshott, C.A., Kapoor, R., Miller, D.H., Golay, X., 2013. Cerebral arterial bolus arrival time is prolonged in multiple sclerosis and associated with disability. J Cereb Blood Flow Metab.

Patel, M., Coutinho, C., Emsley, H.C., 2011. Prevalence of radiological and clinical cerebrovascular disease in idiopathic Parkinson's disease. Clin Neurol Neurosurg 113, 830-834.

Petersen, E.T., Zimine, I., Ho, Y.C., Golay, X., 2006. Non-invasive measurement of perfusion: a critical review of arterial spin labelling techniques. Br J Radiol 79, 688-701.

Sagare, A.P., Bell, R.D., Zlokovic, B.V., 2013. Neurovascular defects and faulty amyloid-beta vascular clearance in Alzheimer's disease. J Alzheimers Dis 33 Suppl 1, S87-100.

Schmidt, R., Berghold, A., Jokinen, H., Gouw, A.A., van der Flier, W.M., Barkhof, F., Scheltens, P., Petrovic, K., Madureira, S., Verdelho, A., Ferro, J.M., Waldemar, G., Wallin, A., Wahlund, L.O., Poggesi, A., Pantoni, L., Inzitari, D., Fazekas, F., Erkinjuntti, T., 2012. White matter lesion progression in LADIS: frequency, clinical effects, and sample size calculations. Stroke 43, 2643-2647.

Thenganatt, M.A., Jankovic, J., 2014. Parkinson disease subtypes. JAMA Neurol 71, 499-504.

Tomlinson, C.L., Stowe, R., Patel, S., Rick, C., Gray, R., Clarke, C.E., 2010. Systematic review of levodopa dose equivalency reporting in Parkinson's disease. Mov Disord 25, 2649-2653.

Wahlund, L.O., Barkhof, F., Fazekas, F., Bronge, L., Augustin, M., Sjogren, M., Wallin, A., Ader, H., Leys, D., Pantoni, L., Pasquier, F., Erkinjuntti, T., Scheltens, P., 2001. A new rating scale for age-related white matter changes applicable to MRI and CT. Stroke 32, 1318-1322.

Wang, J., Alsop, D.C., Song, H.K., Maldjian, J.A., Tang, K., Salvucci, A.E., Detre, J.A., 2003. Arterial transit time imaging with flow encoding arterial spin tagging (FEAST). Magn Reson Med 50, 599-607.

Wierenga, C.E., Hays, C.C., Zlatar, Z.Z., 2014. Cerebral blood flow measured by arterial spin labeling MRI as a preclinical marker of Alzheimer's disease. J Alzheimers Dis 42 Suppl 4, S411-419.

Wolf, M.E., Layer, V., Gregori, J., Griebe, M., Szabo, K., Gass, A., Hennerici, M.G., Matthias, G., Rolf, K., 2014. Assessment of perfusion deficits in ischemic stroke using 3D-GRASE arterial spin labeling magnetic resonance imaging with multiple inflow times. J Neuroimaging 24, 453-459.

Zaharchuk, G., 2011. Arterial spin label imaging of acute ischemic stroke and transient ischemic attack. Neuroimaging Clin N Am 21, 285-301, x.

Zappe, A.C., Reichold, J., Burger, C., Weber, B., Buck, A., Pfeuffer, J., Logothetis, N.K., 2007. Quantification of cerebral blood flow in nonhuman primates using arterial spin labeling and a two-compartment model. Magn Reson Imaging 25, 775-783.

Zhao, Z., Nelson, A.R., Betsholtz, C., Zlokovic, B.V., 2015. Establishment and Dysfunction of the Blood-Brain Barrier. Cell 163, 1064-1078.

Zlokovic, B.V., 2008. The blood-brain barrier in health and chronic neurodegenerative disorders. Neuron 57, 178-201.

Chapter 5

Chapter 5 outlines the DCE MRI section of the study combining both preliminary data and data from the main study. The chapter is written in the form of a paper with the intention to submit it in the near future.

I was involved in the design of the study, I acquired all the data, performed the DCE analysis under the supervision, guidance and using MATLAB codes devised by Dr Parkes and Dr Naish. Professor Parker set up the imaging protocol and gave general advice throughout. Dr Parkes wrote the MRI parts of the methodology section of the paper and provided significant help with the results section. I wrote the remainder of the paper by myself. Dr Emsley provided guidance throughout.

Dynamic Contrast Enhanced MRI Reveals Blood Brain Barrier Breakdown in the Basal Ganglia Nuclei in Idiopathic Parkinson's Disease Phenotypes

Title page:

DCE MRI measures of BBB disruption in IPD

Sarah Al-Bachari[1,2]

Josephine Naish[2]

Geoff JM Parker[2]

Hedley CA Emsley[3,4]

Laura M Parkes[2]

[1]Department of Neurology, Salford Royal NHS Foundation Trust, Salford , UK; [2]Centre for Imaging Science, Institute of Population Health, University of Manchester, UK; [3]Department of Neurology, Royal Preston Hospital, Preston, UK; [4]Faculty of Medical and Human Sciences, University of Manchester, UK.

Corresponding author: Dr Sarah Al-Bachari

Address: Imaging and Data Sciences, University of Manchester, Stopford Building, Oxford Road, Manchester M13 9PT

Telephone: 0161 306 6000 Email: sarahalbachari@yahoo.co.uk

Support:

Sydney Driscoll Neuroscience Foundation; University of Manchester (Biomedical Imaging Institute) and Medical Research Council Studentship; Lancashire Teaching Hospitals NHS Foundation Trust & Lancaster University.

Headline:

DCE MRI measures of BBB disruption in IPD

Abbreviations:

AD - Alzheimer's disease, Arterial Input Function – arterial input function, ASL – arterial spin labelling, BBB – blood brain barrier, BG – Basal ganglia, CBF – cerebral blood flow, CN – control negative, CP - control positive, CVD - cerebrovascular disease, DCE MRI – dynamic contrast enhanced magnetic resonance imaging, DWMH - deep white matter hyperintensity, EPI - echo planar imaging, FA - flip angle, FLAIR - fluid attenuation inversion recovery, GM- grey matter, Hct- hematocrit IPD - idiopathic Parkinson's disease, k^{Tran} – transfer constant, L-dopa - levodopa, LEDD - Levodopa equivalent dose, LTH – Lancashire teaching hospitals, MoCA – Montreal cognitive assessment tool, NVU – neurovascular unit, PET - positron emission tomography, PIGD - Postural instability and gait disorder, PVH - peri ventricular hyperintensity, ROI - region of interest, SN – substantia nigra, SPM - statistical parametric mapping, SRFT- Salford Royal Foundation Trust, STAR - signal targeting with alternating radiofrequency, STN – subthalamic nucleus, SVD – small vessel disease, TD - tremor dominant, TE - echo time, 3T - 3 Tesla, TIA – transient ischaemic attack, TR – repetition time, UKPDS BB - United Kingdom Parkinson's Disease Society Brain Bank, UPDRS - Unified Parkinson's Disease Rating Scale, Vp – blood volume, WTCRF - Wellcome Trust Clinical Research Facility, WML - white matter lesion

Unstructured abstract:

Blood-brain barrier disruption has been noted in the context of idiopathic Parkinson's disease (IPD) and forms the basis of the vascular hypothesis of neurodegeneration. It is possible to detect subtle blood-brain barrier breakdown using quantitative DCE MRI measures, yet studies in IPD are lacking.

Forty-five IPD patients were recruited (19 tremor dominant [TD], 22 postural instability and gait dominant [PIGD] and 4 intermediate), 18 control positive (CP) subjects with cerebrovascular disease (CVD) (14 with ischaemic stroke, 4 with single or multiple TIAs) (mean time, in years, since diagnosis 1.1±0.7) and 33 control negative (CN) subjects. Imaging was performed using Philips Achieva 3.0 Tesla whole body MRI scanner with a 32 channel head coil. Dynamic T_1-weighted MR images were acquired prior to and for 20 minutes following gadolinium contrast injection. Voxel-wise fitting to a Patlak model was performed to produce maps of the gadolinium transfer constant across the BBB (K^{Trans}) and blood plasma volume (Vp). ROI analysis was performed on basal ganglia (BG) nuclei

and compared between groups. T_2-weighted FLAIR images were also collected for white matter lesion (WML) volume estimation.

Results revealed higher K^{Trans} throughout all BG nuclei (except the caudate) in the IPD group in a similar pattern to CP, when compared to CN. No differences in Vp were found between the IPD group and CN, yet Vp was significantly higher than the CP group (except in the caudate). The 2 motor phenotypes of IPD revealed similar alterations in K^{Trans} yet Vp was significantly higher in the PIGD group compared to the TD in the putamen and thalamus. No correlations between K^{Trans} and Vp with WML volume were found.

Collectively these results show how DCE MRI has revealed BBB disruption in IPD in the BG, in a pattern which is similar to yet distinct from CVD, with phenotype specific differences in Vp, warranting further attention.

Five key words:
BBB, CVD, DCE MRI, Parkinson's disease, Phenotypes

5.1 Introduction

The blood-brain barrier (BBB) consists of highly specialised, metabolically active and synthetic cells producing a selectively permeable, highly electrically resistant barrier to diffusion of blood products (Pardridge, 2005). It is closely intertwined with glial cells (i.e. microglia, oligodendroglia, and astrocyte end-feet), all in close proximity to a neuron; collectively termed the neurovascular unit (NVU) (Alvarez et al., 2013). The NVU controls BBB permeability and cerebral blood flow (CBF), it also maintains the neuronal 'milieu' which is required for proper functioning of neuronal circuits and ensures the metabolic needs of the neurons are met (Zlokovic, 2008, 2011).

NVU dysfunction, unsurprisingly, has deleterious effects on the neurons contributing to neuronal dysfunction and death; which forms the basis of the 'vascular model of neurodegeneration' (Andreone et al., 2015; Grammas et al., 2011; Nelson et al., 2015; Zhao et al., 2015; Zlokovic, 2011). Neurodegeneration is now understood to be the consequence of multiple factors acting and interacting over time to lead to neuronal dysfunction and death (Collins et al., 2012). For example, NVU dysfunction has been attributed to impairment of filtering of inflammatory factors increased nitric oxide production and oxidative stress, hypoxia and mitochondrial dysfunction (Sagare et al., 2013b; Stanimirovic and Friedman, 2012).

BBB disruption has been reported in the setting of idiopathic Parkinson's disease (IPD). A relatively small PET study in IPD patients revealed dysfunction of the BBB transporter system (Kortekaas et al., 2005). An in vivo histological study revealed significantly increased permeability of the BBB in the post commissural putamen of IPD patients (Gray and Woulfe, 2015). Work in animal models has revealed areas of BBB disruption in Parkinson's models expressing angiogenic factors (Carvey et al., 2005). Studies remain few and predominantly preclinical.

Advances in neuroimaging techniques, in particular quantitative MRI techniques such as arterial spin labelling (ASL) and dynamic contrast enhanced (DCE) MRI, have paved the way for exciting insights into probing the microcirculation in the clinical setting, with DCE MRI specifically exploring BBB integrity. Though traditionally DCE MRI has been applied to brain pathologies known to cause significant opening of the BBB (such as tumours and acute ischaemic stroke), recently it has been applied in multiple settings including small vessel disease (SVD), AD, mild cognitive impairment, normal ageing and diabetes to probe subtle and chronic BBB disruption (Montagne et al., 2015; Starr et al., 2009; Starr et al., 2003; Taheri et al., 2011; Wardlaw et al., 2008). A recent systematic review of

DCE MRI measurements of subtle BBB disruption suggested DCE MRI provides valuable information in this setting (Heye et al., 2014). Indeed Wardlaw et al. revealed greater BBB disruption in lacunar stroke than in cortical stroke, demonstrating the benefit of quantitative DCE MRI for the measurement of subtle BBB disruption (Wardlaw, 2010). To the author's knowledge published work on DCE MRI measures in IPD is completely lacking.

To better understand the potential microvascular changes in IPD, the importance of the heterogeneity of clinical features within the umbrella term of IPD has to be recognised. Large longitudinal studies have led to the recognition of 2 key motor phenotypes namely, postural instability and gait disorder (PIGD) and tremor dominant (TD), based on the predominant motor features (Hu et al., 2014b; Malek et al., 2015; Williams-Gray et al., 2013). Indeed the PIGD phenotype has been felt to have a poorer prognosis, to be less responsive to levodopa (L-dopa), more often associated with cognitive and neuropsychiatric and other non-motor features when compared to TD, with postulations of varying underlying pathophysiologies (Aarsland et al., 2007; Leroi et al., 2012; Malek et al., 2015).

This study aims to use high resolution DCE MRI to investigate subtle, regional alterations in BBB permeability in the context of IPD, more specifically the PIGD and TD phenotypes, compared to two control groups. A control positive (CP) group with known cerebrovascular disease (CVD) and a control negative (CN) group without known CVD or IPD. This is to investigate whether potential changes are simply attributable to co-existing CVD in an aging population or if an IPD specific pattern is revealed. The region of interest selected was the basal ganglia nuclei based on preclinical and pathological studies. In addition, a more traditional measure of small vessel disease, namely white matter lesion (WML) volume has been included to give an estimation of the burden of cerebrovascular disease in the groups.

5.2 Materials and Methods

5.21 Approvals, recruitment, eligibility and consent

Relevant approvals were obtained including ethics (North West – Preston Research Ethics Committee), research governance and local university approvals. Recruitment of IPD patients was from Lancashire Teaching Hospitals (LTH) and Salford Royal Foundation Trust (SRFT). Eligibility criteria for IPD participants were a clinical diagnosis of IPD

fulfilling UK Parkinson's disease society brain bank criteria (http://www.ncbi.nlm.nih.gov/projects) without known clinical CVD (no history of TIA or stroke) or dementia (Emre et al., 2007). Participants with CVD were recruited from patients at LTH with a clinical diagnosis of stroke or TIA within the previous 2 years (at least 3 months post onset) supported by relevant brain imaging (control positives, CP). Controls without a history of either IPD or clinical CVD were also recruited (control negatives, CN). All groups were matched for age. All participants were required to provide written informed consent and had capacity to do so.

5.22 Clinical assessments and phenotyping

IPD phenotype was assessed using the Unified Parkinson's Disease Rating Scale (UPDRS) (http://www.mdvu.org/library/ratingscales/pd/updrs.pdf) during the scan visit. Participants with IPD were classified into three subtypes (TD, PIGD, intermediate) by Jankovic's method (Jankovic et al., 1990). Disease severity was measured using the Hoehn and Yahr rating scale (Hoehn and Yahr, 1967). No alterations were made to the participants' medications for the study protocol. Routine clinical baseline data were also recorded and the levodopa equivalent daily dose (LEDD) calculated (Tomlinson et al., 2010). A battery of clinical scales was also administered, including the Montreal Cognitive Assessment (MoCA) (www.MoCAtest.org). Data from participants in an earlier study were included to provide sufficient numbers for phenotypic comparison, comprising 13 patients with IPD (6 TD, 5 PIGD and 2 intermediates) and 14 controls (14 CN) scanned on a 3T Philips Achieva MRI system using an 8 channel head coil at Salford Royal Hospital (Al-Bachari et al., 2014). Demographics and clinical data were compared between IPD and control participants using unpaired Student t-test with p-value set at < 0.05.

5.23 MRI protocol

A dynamic series of 3D spoiled gradient echo images were acquired with the following scan parameters: Field of view 192 mm x 192 mm and matrix size of 128 giving in-plane resolution of 1.5 x 1.5 mm; 32 contiguous axial slices of 4mm thickness; TE = 0.8ms, TR=2.4ms, flip angle 10 degrees and image acquisition time of 7.6 seconds. 160 images were acquired over approximately 20 minutes. On the 8th dynamic, a gadolinium (Dotarem) bolus was administered using a power injector. The volume administered was proportional to the weight of the subject with a dose ratio of 0.1mmol/kg.

Prior to the dynamic scan, a series of additional 3D spoiled gradient echo images were acquired at 3 flip angles (2, 5 and 10 degrees) in order to calculate a pre-contrast T_1 map. The acquisition parameters were the same as for the dynamic series except only 8 dynamics were collected (from which a mean image was created), giving an acquisition time of 60 s per flip angle. In order to correct for B_1 field inhomogeneities, a B_1 mapping sequence was also acquired with the same voxel size and coverage as for the variable flip angle images. This consisted of a pair of 3D spoiled gradient echo images with TR1 = 25 ms and TR2 = 125 ms, flip angle 60 degrees, TE 5 ms, acquisition time 117 seconds.

In addition, a T_2-weighted FLAIR image was acquired with the following parameters: TR 10 s, TI 2.75 s, TE 140 ms, in-plane resolution of 0.69 mm, and 100 contiguous axial slices of 1.3 mm thickness with an acquisition time of 450 seconds. A 3D T_1-weighted image was also collected with scan parameters: TR 8.4 ms, TE 3.9 ms, flip angle 8 degrees. Data was reconstructed with a resolution of 0.94 x 0.94 x 1mm, acquisition time 311 seconds.

5.24 MRI analysis

The dynamic series of 160 images was first corrected for motion using the 'realignment' option in SPM8 (http://www.fil.ion.ucl.ac.uk/spm/), which aligned all DCE MRI images to the first image in the time-series. An 'Arterial Input Function' (AIF) was derived from the sagittal sinus (Lavini and Verhoeff, 2010) which was delineated using MRIcro on the final, registered dynamic image. The sagittal sinus showed clear signal enhancement on this image and a region could be easily selected using the 3D intensity threshold tool in MRIcro. Regions of 50 voxels were selected. A voxel-by-voxel fit of the dynamic data for both the transfer constant (K^{Trans}) and blood volume (Vp) was performed using the uptake or 'Patlak' model assuming unidirectional transport of the tracer from the blood plasma to the extravascular, extracellular space (Heye et al., 2014).

$$C_t(t) = K^{trans} \int_0^t C_p(t')dt' + v_p C_p(t) \qquad [1]$$

Where $C_t(t)$ is the tissue concentration of the contrast agent and $C_p(t)$ is the plasma concentration at time t after contrast agent injection at t=0.

The tissue concentration $C_t(t)$ is calculated from the signal in the dynamic images $S_t(t)$ according to:

$$C_{t,b}(t) = \frac{R_1(t) - R_{10}}{r_1} \quad [2]$$

Where $R_1(t)$ is calculated from $S_t(t)$ as described subsequently in equation 5. Where r_1 is the longitudinal relativity of the contrast agent, which was assumed to be 3.4 s–1mM^{-1}. R_{10} is the baseline longitudinal relaxation rate, taken from the pre-contrast T_1 map using $R_{10} = 1/T_{10}$. This pre-contrast T_1 map was calculated by fitting the variable flip angle images on a voxel-by-voxel basis for T_{10} and A_0 using equation [3] (Fram et al., 1987).

$$S = \frac{A_0 \sin\theta (1 - e^{\frac{-TR}{T10}})}{1 - \cos\theta e^{\frac{-TR}{T10}}} \quad [3]$$

In order to correct for inaccuracies in the specified flip angles, θ_S, due to B_1 inhomogeneities, the ratio of the image intensities in the B_1 mapping sequence (r) was used to estimate the true flip angle θ_T on a voxel-by-voxel basis (Pohmann and Scheffler, 2013) , using:

$$\theta_T = \arccos\left(\frac{r.n - 1}{n - r}\right) \quad \text{where n=TR1/TR2.} \quad [4]$$

The deviation of the true flip angle from the specified flip angle (θ_S) is given by θ_T/θ_S and θ in equation [3] is multiplied by this factor on a voxel wise basis when calculating T_1. Prior to multiplication, the θ_T/θ_S image was smoothed using a convolution kernel of 3 voxels.

$R_1(t)$ was calculated using equation [5] below, derived from equation [3], considering S_t as the signal in the post-contrast dynamic images and S_0 as the mean signal from 5 pre-contrast dynamics, ignoring the first image due to equilibrium effects.

$$R_1(t) = -\frac{1}{TR}\ln\left[\frac{1 - B\cos\theta + \frac{S_t(t)}{S_0}(B-1)}{1 - B\cos\theta + \frac{S_t(t)}{S_0}\cos\theta(B-1)}\right] \quad \text{where B=exp(-R}_{10}\text{.TR).} \quad [5]$$

Finally, the plasma concentration $C_p(t)$, is derived from the blood concentration $C_b(t)$ which is also calculated using equations [2] and [5] with S_t the mean signal from the

sagittal sinus region, S_0 the mean signal from 5 pre-contrast dynamics within this region (again, neglecting the first one to avoid inflow effects), and T_{10} equal to the mean pre-contrast T_1 from the sagittal sinus region. $C_p(t)$ is derived from the measured blood concentration by correcting for hematocrit according to: $C_p(t) = C_b(t)/ (1\text{-Hct})$ where Hct of 0.40 was used for a female and 0.45 for male (Cirillo et al., 1992).

Equation [1] was then fit to $C_t(t)$ and $C_p(t)$ using constrained least squares minimisation (lsqcurvefit in Matlab) on a voxel-wise basis for 3 parameters: K^{Trans}, Vp and T_0, where T_0 is the offset time between $C_t(t)$ and $C_p(t)$. K^{Trans} was constrained to be between 0 and 0.1 min^{-1}, Vp between 0 and (1-Hct) and T_0 between 0 and 20 s (i.e. assuming the sagittal sinus signal always lagged the tissue signal but by a maximum of 20 s). In order to avoid local minima, minimisation was performed twice, using the fitted parameters of the first minimisation as starting parameters for the second minimisation, except for one parameter which was kept as the original value.

5.25 Extracting Region of Interest Measurements

The general approach was to normalise the K^{Trans} and Vp images to MNI space in order to extract signal from key regions based on established brain atlases. SPM8 was used to co-register the K^{Trans} and Vp maps to the high resolution 3D T_1-weighted image. The first dynamic of the DCE series was used to compute the registration parameters which were then applied to the other images. The T_1-weighted images were normalised to MNI space and the transformation applied to the DCE MRI parameter maps.

Regions of interest (ROI) in the subthalamic nucleus (STN), globus pallidus, thalamus, caudate and putamen were obtained from MNI atlases (Prodoehl et al., 2008; Tzourio-Mazoyer et al., 2002). The substantia nigra (SN) region was manually drawn on the T_2-weighted template image from SPM by an experienced researcher. Median K^{Trans} and Vp values were extracted from each of these regions for each subject, along with whole brain values. Unpaired two-tailed t-tests assuming unequal variances were performed to determine group differences between: CN and IPD, TD, PIGD and CP and phenotype differences between TD and PIGD.

The concentration time course in the whole brain region and the sagittal sinus region (i.e. the AIF) were extracted in order to consider group differences in this raw data prior to fitting.

5.26 White matter lesion volume estimation

White matter lesion (WML) volume was also calculated using the lesion segmentation toolbox (LST) (Schmidt et al., 2012a) in SPM8 with a threshold of 0.3. This threshold was chosen as it gave the most accurate estimates in a sub-study comparing WML volume estimates from LST with those from semi-automated lesion-growing methods on a subset of the data (n=51, including representation from all groups, unpublished).

In order to determine if there is a relationship between cerebrovascular disease and the DCE MRI parameters, a comparison was made between the whole brain DCE MRI parameters and WML volume and number of CVD risk factors. Finally, to determine if medication had any effect on the DCE MRI parameters, the correlation between LEDD dose and whole brain DCE MRI parameters was tested for significance.

5.3 Results

Forty-five IPD patients were recruited (19 TD, 22 PIGD and 4 intermediate), 18 CP subjects with CVD (14 with ischemic stroke, 4 with single or multiple TIAs) (mean time, in years, since diagnosis 1.1±0.7) and 33 CN subjects.

Imaging was performed at Salford Royal Hospital (n=5 PIGD, n=5 TD, n=13 CN and no CP) and the Wellcome Trust Clinical Research Facility (WTCRF) (n=19 PIGD, n=16 TD, n=20 CN and n=18 CP), both using a Philips Achieva 3.0 Tesla whole body MRI scanner, with an 8 channel head coil at Salford Royal Hospital and 32 channel at WTCRF.

Data from 10 participants could not be analysed due to i) failure to tolerate the full scan procedure (n=5), ii) failure of the contrast agent injection (n=3), iii) error in image transfer (n=2), leaving data from 86 participants (n=29, CN, n=16 CP, n=19 TD, n=21 PIGD). Summary demographic information from these patients is given in Table 5.1, along with the WML volume measurements. The IPD group had significantly higher mean WML volume compared to the CN group, but is not significantly different from the CP group. There are no significant phenotypic differences.

	CN (n=29)	**CP (n=16)**	**IPD (n=40)**	**p value IPD v CN**	**p value IPD v CP**	**PIGD (n=19)**	**TD (n=17)**	**p value PIGD v TD**
n (F:M)	14:15	4:12	8:32	n/a	n/a	4:15	4:13	n/a
Age: years [range]	66.8 (52-81)	68.7 (53-84)	68.5 (53-85)	0.35	0.94	69.9 (53-85)	66.9 (52-77)	0.34
No. of CV RF: mean (SD)	1.52 (1.15)	3.00 (1.33)	1.65 (1.48)	0.68	0.0005	1.63 (1.30)	1.53 (1.54)	0.23
RF (%): Hypertension	37	75	30			42	29.4	
DM	3.3	6.25	2.5	n/a		0	0	n/a
FH	44.1	43.8	25			31.5	29.4	
Smoker	29.4	62.5	32.5			36.8	35.3	
Hypercholesterolemia	40.0	75.0	25.0			31.6	23.5	
IHD	5.9	18.8	12.5			15.8	11.7	
AF	0	25.0	2.5			0	5.9	
Disease Duration: mean (SD)	n/a	1.1 (0.7)	7.49 (4.27)	n/a	n/a	9.29 (4.40)	5.87 (3.82)	0.02
Hoehn & Yahr Score: mean (SD)	n/a	n/a	2.59 (1.02)	n/a	n/a	3.18 (0.71)	2.05 (0.96)	0.0003
PIGD Score: mean (SD)	n/a	n/a	7.00 (5.13)	n/a	n/a	10.81 (3.61)	1.89 (1.45)	<0.0001
Tremor Score: mean (SD)	n/a	n\a	6.2 (4.95)	n/a	n/a	2.96 (2.96)	10.2 (4.79)	<0.0001
LEDD (mg): mean (SD)	n/a	n/a	560.9 (348.4)	n/a	n/a	788.5 (304.3)	361.4 (267.3)	<0.0001
WML volume (ml) : mean (SD)	5.4 (1.7)	11.7 (2.7)	10.3 (1.7)	0.05	0.7	12.4 (2.4)	8.1 (2.2)	0.2

Table 5.1: Demographics and clinical characteristics of the study group with white matter lesion (WML) volume measurements. Values are given as mean ± SD. RF %- percent of group with the CV risk factor. AF – atrial fibrillation DM – diabetes mellitus, FH – family history, IHD – ischaemic heart disease

Figure 5.1 shows example maps of K^{Trans} and Vp in both a healthy control and a PIGD patient, both chosen to have ROI values close to the mean for the group. It can be seen that white matter has higher K^{Trans} in general than grey matter, as seen in all images.

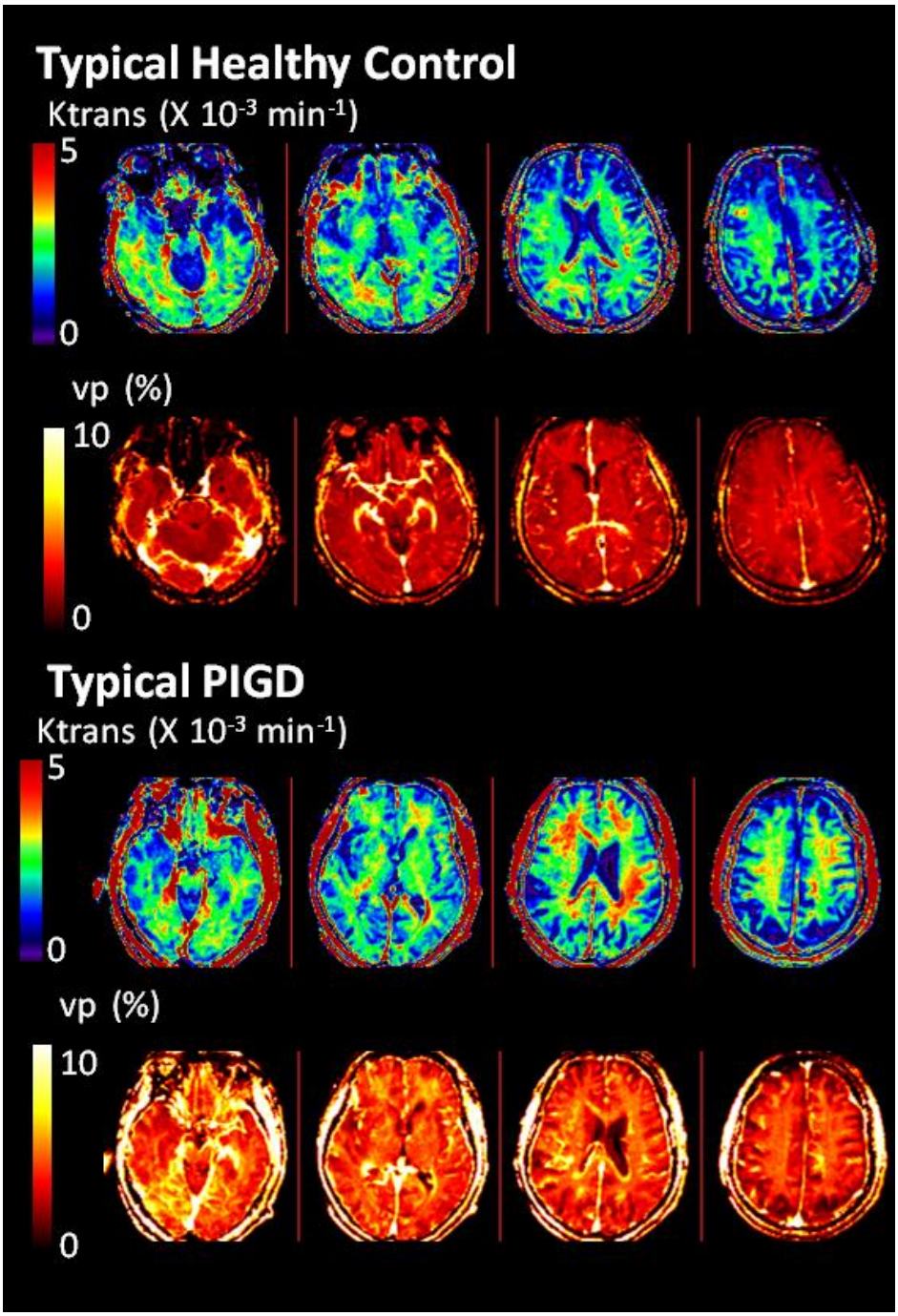

Figure 5.1: K^{Trans} and Vp maps from typical subjects

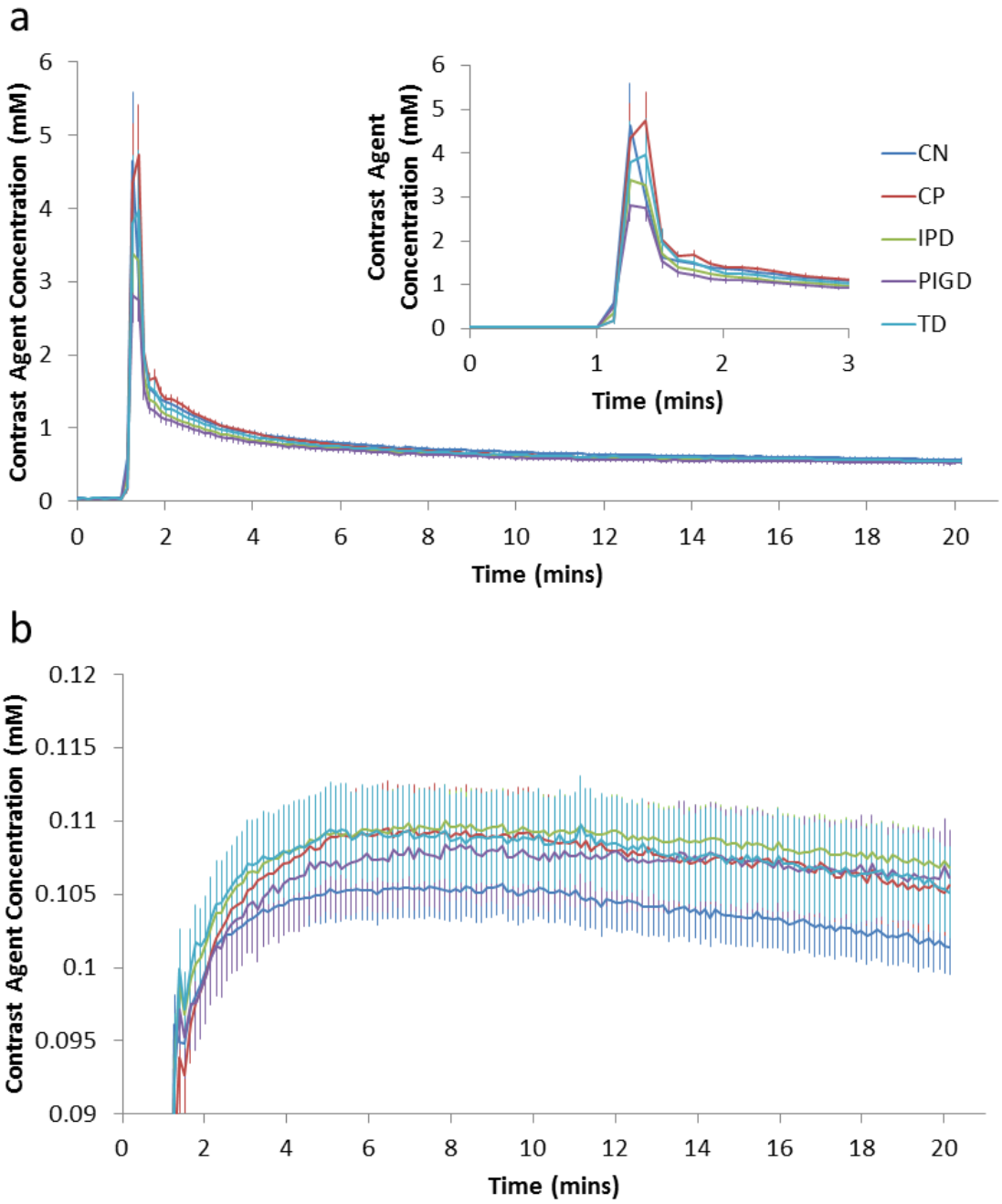

Figure 5.2: AIF (a) and whole brain (b) concentration time course for each group

Figure 5.2 shows the (a) mean arterial and (b) whole brain concentration time course for each group. The arterial input functions are very similar, but the tissue curves begin to diverge, particularly between the CN and patient groups. This difference is reflected as a difference in the fitted parameters (Table 5.2) which show significantly increased K^{Trans} values for the patient groups compared to CN. Blood plasma volume, Vp, is lower, particularly in the CP group by comparison with both the CN and IPD groups. There is a

trend (p = 0.07) to higher Vp for the PIGD group compared to the TD group. Baseline blood T_1 values are also given in Table 5.2, for which there were no significant group differences.

	CN (n=29)	**CP (n=16)**	**IPD (n=40)**	**p value IPD Vs CN**	**p value IPD Vs CP**	**PIGD (n=19)**	**TD (n=17)**	**p value PIGD Vs TD**
Blood T_1 (s)	1.71 ± 0.04	1.77 ± 0.04	1.77 ± 0.04	0.2	0.9	1.81 ± 0.05	1.74 ± 0.06	0.4
K^{Trans} (x 10^{-3} min^{-1})	3.43 ± 0.11	4.23 ± 0.18	4.06 ± 0.17	0.004	0.5	4.09 ± 0.27	3.92 ± 0.23	0.6
Vp (%)	3.77 ± 0.31	2.65 ± 0.27	3.98 ± 0.23	0.6	0.0005	4.36 ± 0.31	3.48 ± 0.34	0.07

Table 5.2: Blood T_1 values and mean values of fitted parameters from the whole brain tissue curves. Mean ± SE over subjects are given.

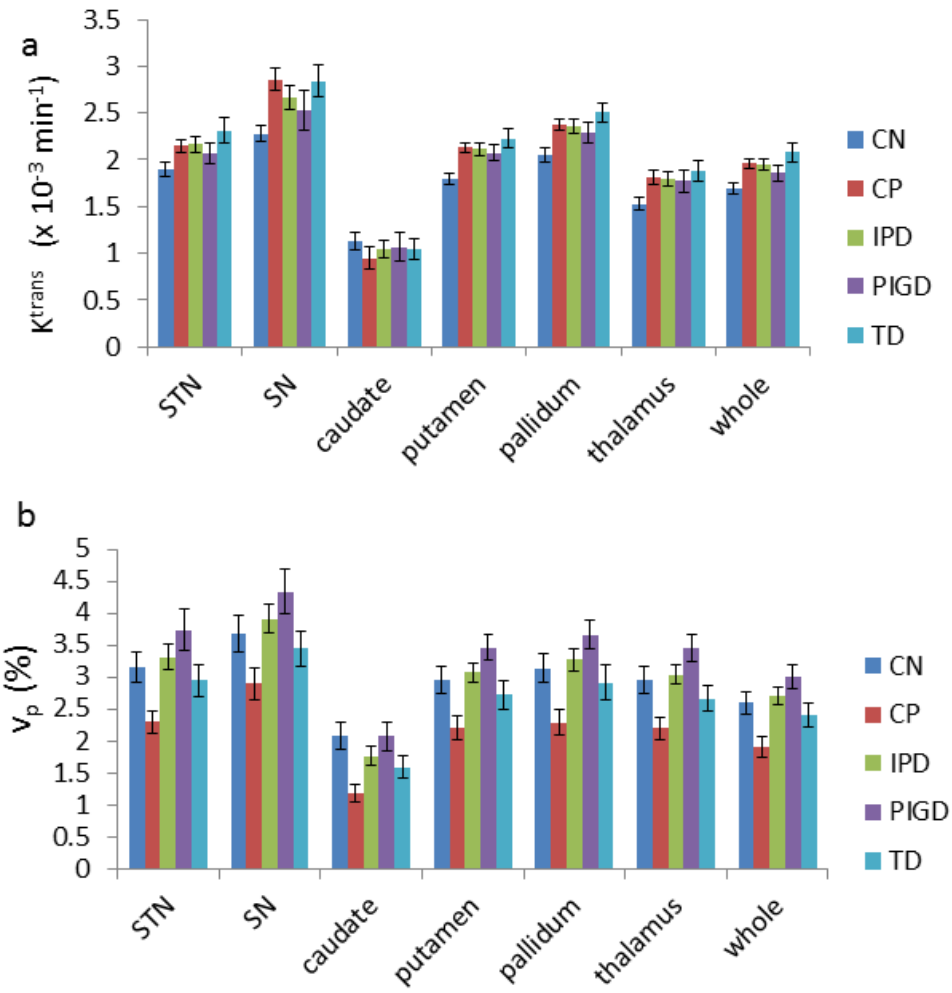

Figure 5.3: Median ROI values for (a) K^{Trans} and (b) Vp. Error bars show the standard error in the mean.

	CN (n=29)	CP (n=16)	IPD (n=40)	p value IPD Vs CN	p value IPD Vs CP	PIGD (n=19)	TD (n=17)	p value PIGD Vs TD
STN	1.90 ± 0.07	2.15 ± 0.07	2.16 ± 0.09	0.03	0.9	2.07 ± 0.12	2.31 ± 0.13	0.2
SN	2.28 ± 0.09	2.86 ± 0.12	2.67 ± 0.13	0.02	0.3	2.53 ± 0.22	2.84 ± 0.17	0.3
caudate	1.12 ± 0.09	0.95 ± 0.12	1.03 ± 0.09	0.5	0.6	1.06 ± 0.15	1.05 ± 0.11	0.9
Putamen	1.79 ± 0.06	2.13 ± 0.05	2.11 ± 0.07	0.002	0.9	2.07 ± 0.09	2.22 ± 0.10	0.3
Pallidum	2.05 ± 0.07	2.38 ± 0.07	2.36 ± 0.08	0.007	0.9	2.29 ± 0.11	2.50 ± 0.11	0.2
Thalamus	1.53 ± 0.06	1.81 ± 0.08	1.79 ± 0.08	0.02	0.9	1.77 ± 0.12	1.89 ± 0.11	0.5
Whole brain	1.69 ± 0.05	1.96 ± 0.05	1.95 ± 0.06	0.005	0.9	1.86 ± 0.08	2.08 ± 0.10	0.1

Table 5.3: K^{Trans} ROI values x 10^{-3} min^{-1} (mean ± SE)

	CN (n=29)	CP (n=16)	IPD (n=40)	p value IPD Vs CN	p value IPD Vs CP	PIGD (n=19)	TD (n=17)	p value PIGD Vs TD
STN	3.16 ± 0.23	2.30 ± 0.18	3.31 ± 0.2	0.6	0.0006	3.74 ± 0.32	2.94 ± 0.26	0.08
SN	3.68 ± 0.28	2.89 ± 0.25	3.91 ± 0.22	0.5	0.005	4.34 ± 0.35	3.44 ± 0.28	0.07
Caudate	2.08 ± 0.20	1.19 ± 0.13	1.77 ± 0.14	0.2	0.005	2.07 ± 0.23	1.59 ± 0.17	0.1
Putamen	2.96 ± 0.21	2.20 ± 0.19	3.07 ± 0.15	0.7	0.001	3.46 ± 0.20	2.72 ± 0.22	0.02
Pallidum	3.13 ± 0.23	2.29 ± 0.2	3.27 ± 0.17	0.7	0.0007	3.66 ± 0.23	2.91 ± 0.27	0.05
Thalamus	2.95 ± 0.21	2.20 ± 0.18	3.03 ± 0.15	0.8	0.001	3.45 ± 0.22	2.66 ± 0.20	0.02
Whole brain	2.60 ± 0.18	1.91 ± 0.16	2.70 ± 0.13	0.7	0.0006	3.00 ± 0.18	2.41 ± 0.20	0.04

Table 5.4: Vp ROI values % (mean ± SE)

Figure 5.3 and Tables 5.3 and 5.4 show values for K^{Trans} and Vp that are in broad agreement with previous studies (Montagne et al., 2015). A significantly higher K^{Trans} is seen for CP compared with CN. This is seen in all regions with the noticeable exception of the caudate nucleus which also shows markedly lower K^{Trans} values in general than other regions. The IPD group shows similar results to CP with significantly higher K^{Trans} compared to CN, reaching significance in all regions except for the caudate nucleus. There are no significant phenotypic differences in K^{Trans}.

Blood plasma volume, Vp is significantly lower in CP in comparison to CN and IPD in all regions. However, the same reduction compared to CN is not seen in IPD. Phenotypic differences are present with PIGD showing higher Vp compared to TD, reaching significance in the putamen, thalamus and whole brain regions.

Results remained broadly the same on re-analysis including only the data from the scanner at the WTCRF (see supplementary information). Differences in the K^{Trans} parameter were accentuated (they were larger and became more significant); however the lower Vp noted in the CP group compared to the CN group was no longer present. Vp of the IPD group remained significantly greater than the CP group in all regions and phenotypic difference in Vp remained. Due to the gender imbalance in the groups (see Table 5.1), additional analysis considered data from men only, revealing similar results to those displayed.

In terms of the relationship between DCE MRI parameters and CVD, Table 5.5 shows the mean values of WML volume, and whole brain parameters for K^{Trans} and Vp over all participants grouped according to cerebrovascular risk factors. K^{Trans} and WML volume do not appear to relate to CVD risk factors, and there is a lot of variability within each group. There is a trend (p=0.06) to reduced Vp with increased CVD risk factors.

CVD risk factors	K^{Trans} x 10^{-3} min^{-1}	Vp (%)	WML vol (ml)
0	2.01 ± 0.13	2.91 ± 0.22	10.9 ± 2.8
1	1.79 ± 0.09	2.43 ± 0.24	6.4 ± 2.1
2	1.88 ± 0.06	2.51 ± 0.20	5.5 ± 1.3
>2	1.83 ± 0.06	2.36 ± 0.18	12.5 ± 2.6
P value: 0 vs >2	0.2	0.06	0.7

Table 5.5: Relationship between DCE MRI parameters and cerebrovascular risk factors.

Linear regression revealed no significant relationship between WML volume and whole brain K^{Trans} or Vp values (r=0.17, p=0.15 for K^{Trans} and r=-0.11, p=0.3 for Vp). There was no significant relationship between whole brain K^{Trans} and LEDD (r=0.21, p=0.2), but

there was a weak positive correlation between whole brain Vp and LEDD (r=0.34, p=0.05).

5.4 Discussion

The aim of this study was to apply dynamic contrast enhanced MRI in the clinical setting in an IPD population to probe BBB integrity. The results reveal DCE MRI is sensitive enough to detect higher K^{Trans}, reflecting BBB leakiness, in the IPD population compared to controls, which is comparable with patients with known CVD. However Vp, a measure of plasma volume, was globally lower in the CVD group compared to the IPD group with results in the IPD group more in keeping with healthy controls. This mismatch would suggest alterations in BBB disruption in the BG nuclei of patients with IPD occur but perhaps due to a differing pathophysiology to cerebrovascular disease. The 2 motor phenotypes of IPD did reveal the same pattern of BBB changes, yet differing patterns of Vp. Collectively these data demonstrate BBB disruption in IPD and its phenotypes in the clinical setting in keeping with suggestions from preclinical studies.

This study revealed BBB disruption in the BG nuclei of IPD patients, in a pattern comparable to patients with CVD. This BBB disruption has been noted in animal models of parkinsonism, in a postmortem study of IPD patients and one small clinical study (Carvey et al., 2005; Gray and Woulfe, 2015; Kortekaas et al., 2005; Patel et al., 2011a; Pisani et al., 2012). Multiple stroke studies have utilized DCE MRI to demonstrate increased BBB leakiness in the setting of stroke. Therefore this study is in keeping with current stroke and CVD literature that suggest there is a link to BBB breakdown (Wardlaw et al., 2009; Wardlaw et al., 2013a; Wardlaw et al., 2008). However these studies tend to use whole grey matter, white matter and CSF as regions of interest and to the author's knowledge the pattern of altered BBB disruption across the BG nuclei, sparing the caudate is a unique finding. Why the caudate region is spared in both groups is difficult to understand, but in keeping with preclinical work in IPD (Gray and Woulfe, 2015). Altered BBB function in the BG may be explained by the fact the BG nuclei are supplied by deep perforating arteries, many of which are at border zone regions and so particularly prone to ischemia. Although ischemia secondary to atherosclerosis is understandable it seems difficult to attribute the similar pattern of altered BBB disruption in the IPD group simply to CVD.

Blood plasma volume, Vp, was significantly lower in the CP in comparison to CN and IPD groups, in all regions apart from the caudate, with a trend (p=0.06) towards reduced Vp with increasing number of CVD risk factors. Regional cerebral blood flow changes have

been noted in stroke and IPD studies, with hypoperfusion mainly in the peri-infarct regions following stroke (Chalela et al., 2000; Richardson et al., 2011; Rodriguez et al., 1993). IPD studies have consistently revealed a pattern of hypoperfusion in the posterior cortices (not the BG) and therefore our finding of normal Vp in the BG, is in keeping with such studies (Borghammer et al., 2010; Fernandez-Seara et al., 2012; Melzer et al., 2011) . What is noteworthy is the mismatch of high K^{Trans} and low Vp in the CVD group and high K^{Trans} with higher Vp in the IPD group, pointing towards differing pathophysiologies between the two groups. Indeed much work by Carvey et al. in the preclinical setting have suggested that altered BBB in neurodegeneration is related to increased expression of angiogenic markers that co-localised with punctate areas of leakage in animal models of PD, suggesting BBB disruption and angiogenesis are associated; indeed newly formed angiogenic vessels are leaky (Brown and Thore, 2011; Carvey et al., 2005; Patel et al., 2011a). Thus neovasculisation in PD may explain the increased Vp compared to the CP group.

The 2 motor phenotypes of IPD did reveal a similar pattern of BBB changes, but differing pattern of Vp. There is some suggestion of a trend of higher K^{Trans} in the TD than in the PIGD group, though this did not reach statistical significance. In terms of plasma volume there was almost global (bar the caudate) increased Vp in the PIGD group compared to TD, reaching statistical significance in the putamen, thalamus and whole brain regions. This is in line with quantitative perfusion measures using ASL and PET that have revealed hyperperfusion in the basal ganglia nuclei, with our previous work (Chapter 4) suggesting this to be predominantly in the PIGD group (Borghammer, 2012; Melzer et al., 2011). The similar patterns of K^{Trans} between the phenotypes would suggest that BBB dysfunction occurs in both phenotypes. Yet the differing patterns in Vp between the phenotypes are in keeping with current evidence to suggest differing pathophysiologies (Aarsland et al., 2007; Malek et al., 2015).

This study revealed no correlation between global WML volume and values of K^{Trans} or Vp. Armitage et al., used DCE MRI in 2 groups of mild stroke patients differentiated by Fazekas white matter lesion rating score. The work revealed no significant differences between high or low white matter lesion scores attributing the lack of difference to acquisition noise, drift and intrinsic tissue parameters (Armitage et al., 2011). Therefore the lack of association noted in this study may be multi-factorial and is perhaps understandable as the ROI in this study was BG nuclei and not WML.

This study is not without its limitations. Regions of interest were extracted using an atlas-based automated approach involving the normalization of the maps to MNI space. A manual approach on the unwarped individual images maybe favorable due to the size of

the structures. The Patlak model assumes negligible flow of tracer from the tissue back into the blood, however the tissue enhancement curves show some evidence of this, suggesting that inclusion of the volume of the extravascular, extracellular space in the model may be warranted.

In conclusion, this study has shown that DCE MRI is sensitive to detecting subtle BBB disruption in the clinical setting of IPD, at least in the BG nuclei. Increased BBB leakiness in IPD is comparable to CVD, with differing patterns of Vp. Vp patterns vary between phenotypes also. These data add further weight to there being BBB disruption in IPD and the huge need for greater attention to be paid to this pathology on the path to finding neuroprotective/disease modifying agents for this disorder.

Acknowledgements

We are grateful to all participants without whom the work would not have been possible. We are also grateful to the following groups of people and individuals for their help with various parts of the work: MRI radiographers at Salford Royal Hospital and at the Wellcome Trust Clinical Research Facility, Parkinson's disease nurse specialists at Lancashire Teaching Hospitals NHS Foundation Trust, Drs Martha Hanby and Monty Silverdale,

Funding acknowledgements

Salary (Dr Al-Bachari) and research costs for this work were provided through support from: Sydney Driscoll Neuroscience Foundation; University of Manchester (Biomedical Imaging Institute) and Medical Research Council Studentship; Lancashire Teaching Hospitals NHS Foundation Trust & Lancaster University Dr Emsley is supported by Lancashire Teaching Hospitals NHS Foundation Trust. Dr Parkes is supported by the University of Manchester.

Author Contribution statement

All authors made a substantial contribution to the concept and design, acquisition of data and analysis and interpretation of data. SAB, HE and LP drafted the article and revised it critically for important intellectual content, and all authors approved the version to be published.

Disclosure/Conflict of Interest

The authors have no relevant disclosures or conflicts of interest to declare.

Supplementary Information:

A second analysis was performed using only the data collected at the WRTCRF, in order to avoid any erroneous results due to scanner differences.
Table 5.1S shows the new demographic data for this subset of participants and including WML volume measurements.

	CN (n=18)	**CP (n=16)**	**IPD (n=31)**	**p value IPD v CN**	**p value IPD v CP**	**PIGD (n=15)**	**TD (n=12)**	**p value PIGD v TD**
n (F:M)	11:7	4:12	6:25	n/a	n/a	2:13	4:8	n/a
Age, years [range]	68.6 [52-81]	68.7 [53-84]	69.7 [52-83]	0.65	0.67	70.6 [58-85]	68.6 [58-80]	0.49
No. of CV RF: mean (SD)	1.8 (1.1)	3 (1.2)	1.8 (1.5)	0.86	0.003	1.7 (1.3)	1.8 (1.4)	0.81
Disease Duration	n/a	n/a	7.0 (3.9)	n/a	n/a	8.2 (4.0)	5.8 (4.0)	0.1
Hoehn & Yahr Score	n/a	n/a	2.5 (0.9)	n/a	n/a	3.1 (0.7)	2.0 (0.9)	0.0001
PIGD Score	n/a	n/a	7.5 (4.7)	n/a	n/a	10.2 (3.5)	4.5 (5.0)	0.002
Tremor Score	n/a	n/a	9 (4.6)	n/a	n/a	2.9 (2.5)	9 (4.6)	0.0005
LEDD dose (mg)	n/a	n/a	601.5 (318.9)	n/a	n/a	831.5 (249.4)	345.5 (328.1)	<0.0001
WML volume (ml)	7.4 ± 2.7	11.7 ± 2.7	12.5 ± 2.0	0.1	0.8	14.3 ± 2.8	10.3 ± 2.8	0.3

Table 5.1S: Demographics and clinical characteristics of the study group with white matter lesion (WML) volume measurements. Values are given as mean ± SD.
LEDD, levodopa equivalent daily dose.

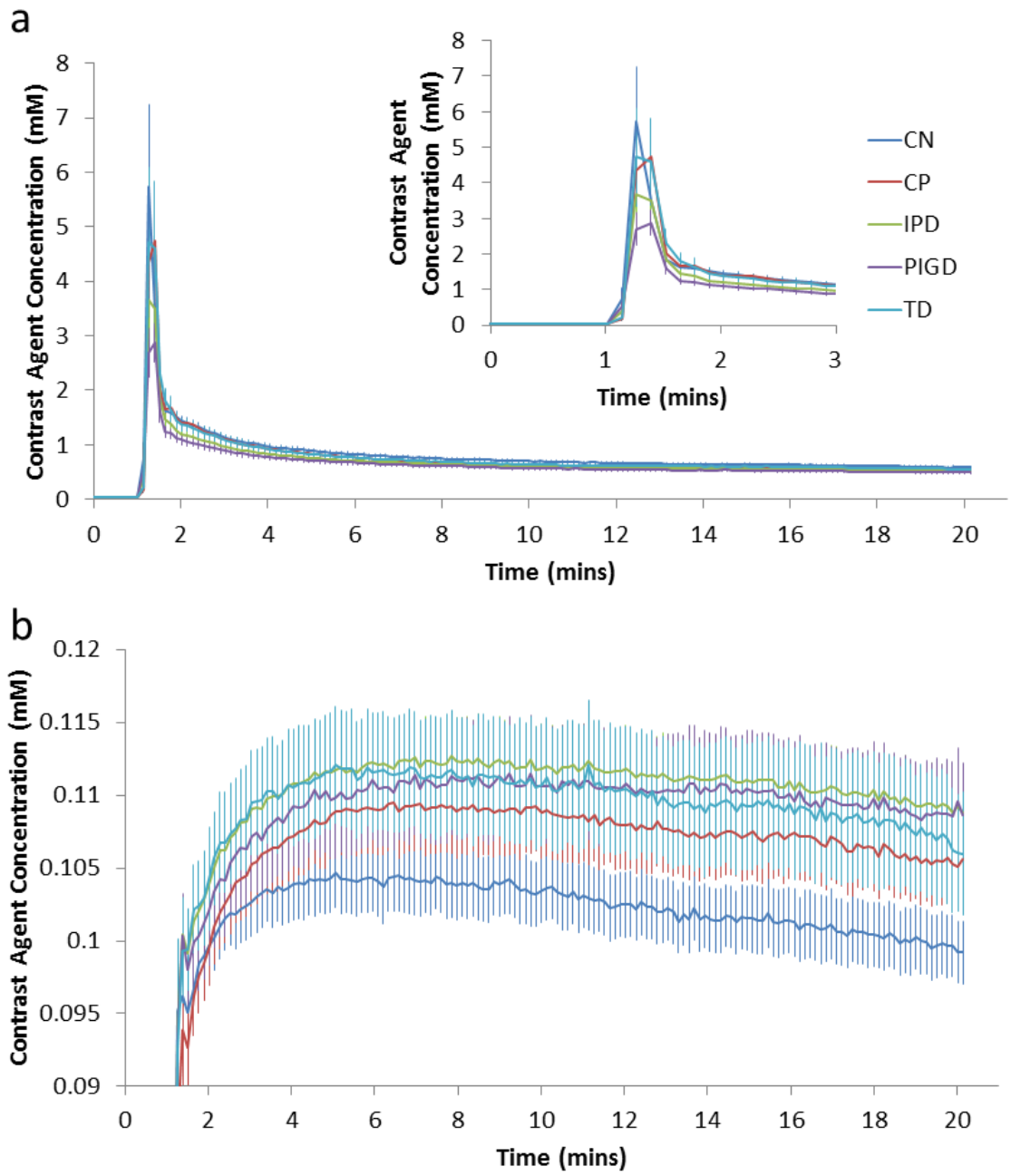

Figure 5.1S: AIF (a) and whole brain (b) concentration time course for each sub-group

	CN (n=18)	CP (n=16)	IPD (n=31)	p value IPD v CN	p value IPD v CP	PIGD (n=15)	TD (n=12)	p value PIGD v TD
Blood T_1 (s)	1.70 ± 0.04	1.77 ± 0.04	1.82 ± 0.04	0.04	0.4	1.85 ± 0.05	1.80 ± 0.06	0.6
K^{Trans} (x 10^{-3} min^{-1})	3.39 ± 0.12	4.23 ± 0.18	4.29 ± 0.20	0.0004	0.8	4.40 ± 0.29	4.09 ± 0.30	0.5
Vp (%)	3.15 ± 0.37	2.65 ± 0.27	3.86 ± 0.28	0.1	0.004	4.43 ± 0.38	2.90 ± 0.39	0.01

Table 5.2S: Blood T1 values and mean values of fitted parameters from the whole brain tissue curves. Mean ± SE over subjects are given.

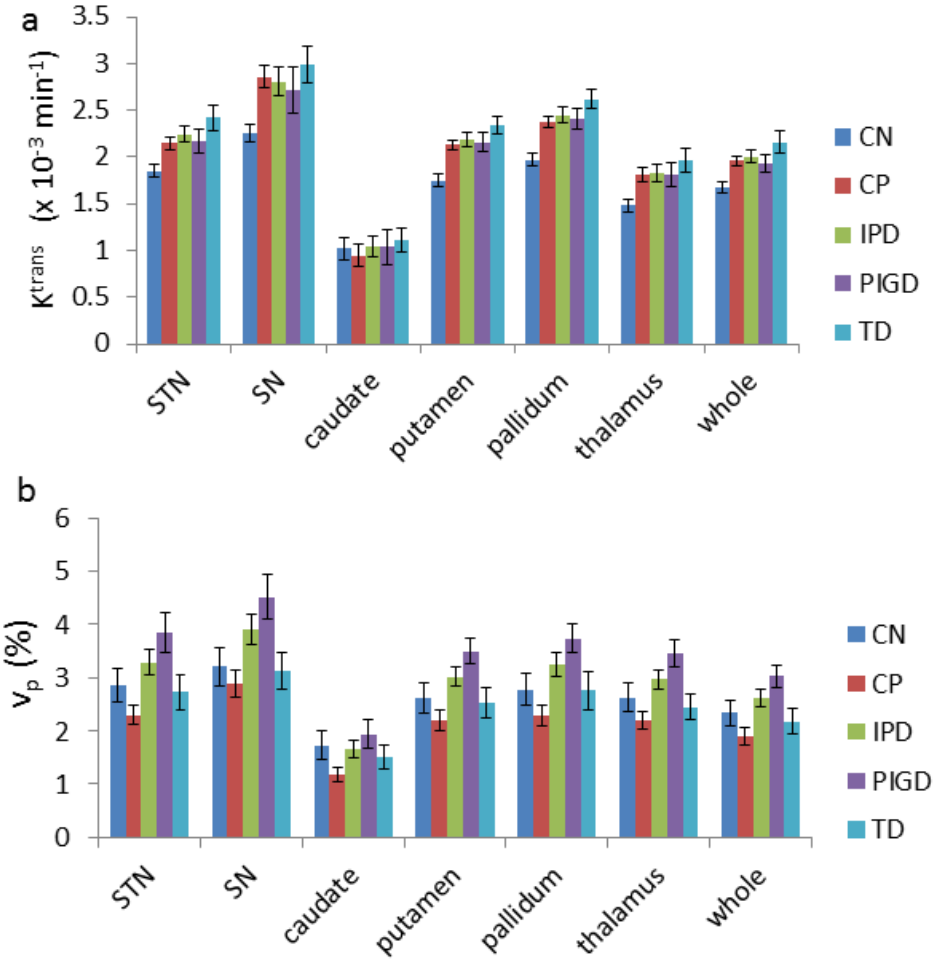

Figure 5.2S: Median ROI values for (a) KT^{rans} and (b) v_p. Error bars show the standard error in the mean.

	CN (n=18)	CP (n=16)	IPD (n=31)	p value IPD v CN	p value IPD v CP	PIGD (n=15)	TD (n=12)	p value PIGD v TD
STN	1.85 ± 0.07	2.15 ± 0.07	2.24 ± 0.09	0.002	0.4	2.17 ± 0.12	2.42 ± 0.14	0.2
SN	2.26 ± 0.09	2.86 ± 0.12	2.81 ± 0.15	0.004	0.8	2.72 ± 0.24	2.99 ± 0.20	0.4
Caudate	1.02 ± 0.12	0.95 ± 0.12	1.04 ± 0.12	0.9	0.6	1.04 ± 0.19	1.11 ± 0.13	0.8
Putamen	1.75 ± 0.07	2.13 ± 0.05	2.19 ± 0.07	0.0002	0.5	2.16 ± 0.10	2.34 ± 0.10	0.2
Pallidum	1.97 ± 0.07	2.38 ± 0.07	2.45 ± 0.08	0.00009	0.5	2.41 ± 0.12	2.62 ± 0.11	0.2
Thalamus	1.48 ± 0.07	1.81 ± 0.08	1.83 ± 0.09	0.006	0.8	1.81 ± 0.13	1.97 ± 0.13	0.4
Whole brain	1.68 ± 0.06	1.96 ± 0.05	2.00 ± 0.07	0.002	0.7	1.93 ± 0.09	2.16 ± 0.12	0.2

Table 5.3S: K^{Trans} ROI values x 10^{-3} min^{-1} (mean ± SE).

	CN (n=18)	CP (n=16)	IPD (n=31)	p value IPD v CN	p value IPD v CP	PIGD (n=15)	TD (n=12)	p value PIGD v TD
STN	2.87 ± 0.32	2.30 ± 0.18	3.29 ± 0.25	0.3	0.004	3.85 ± 0.39	2.73 ± 0.33	0.05
SN	3.20 ± 0.36	2.89 ± 0.25	3.90 ± 0.28	0.1	0.01	4.52 ± 0.41	3.14 ± 0.35	0.02
Caudate	1.73 ± 0.28	1.19 ± 0.13	1.66 ± 0.16	0.8	0.04	1.94 ± 0.27	1.51 ± 0.22	0.3
Putamen	2.28 ± 0.21	2.20 ± 0.19	3.02 ± 0.18	0.2	0.005	3.49 ± 0.23	2.52 ± 0.28	0.02
Pallidum	2.77 ± 0.30	2.29 ± 0.20	3.25 ± 0.21	0.2	0.003	3.73 ± 0.27	2.75 ± 0.36	0.05
Thalamus	2.63 ± 0.27	2.20 ± 0.18	2.97 ± 0.18	0.3	0.005	3.47 ± 0.25	2.45 ± 0.25	0.01
Whole brain	2.34 ± 0.24	1.91 ± 0.16	2.63 ± 0.16	0.3	0.004	3.02 ± 0.22	2.17 ± 0.24	0.02

Table 5.4S: Vp ROI values x 10^{-3} min^{-1} (mean ± SE).

References:

Aarsland, D., Bronnick, K., Ehrt, U., De Deyn, P.P., Tekin, S., Emre, M., Cummings, J.L., 2007. Neuropsychiatric symptoms in patients with Parkinson's disease and dementia: frequency, profile and associated care giver stress. J Neurol Neurosurg Psychiatry 78, 36-42.

Alvarez, J.I., Katayama, T., Prat, A., 2013. Glial influence on the blood brain barrier. Glia 61, 1939-1958.

Andreone, B.J., Lacoste, B., Gu, C., 2015. Neuronal and vascular interactions. Annu Rev Neurosci 38, 25-46.

Armitage, P.A., Farrall, A.J., Carpenter, T.K., Doubal, F.N., Wardlaw, J.M., 2011. Use of dynamic contrast-enhanced MRI to measure subtle blood-brain barrier abnormalities. Magn Reson Imaging 29, 305-314.

Borghammer, P., 2012. Perfusion and metabolism imaging studies in Parkinson's disease. Dan Med J 59, B4466.

Borghammer, P., Chakravarty, M., Jonsdottir, K.Y., Sato, N., Matsuda, H., Ito, K., Arahata, Y., Kato, T., Gjedde, A., 2010. Cortical hypometabolism and hypoperfusion in Parkinson's disease is extensive: probably even at early disease stages. Brain Struct Funct 214, 303-317.

Brown, W.R., Thore, C.R., 2011. Review: cerebral microvascular pathology in ageing and neurodegeneration. Neuropathol Appl Neurobiol 37, 56-74.

Carvey, P.M., Zhao, C.H., Hendey, B., Lum, H., Trachtenberg, J., Desai, B.S., Snyder, J., Zhu, Y.G., Ling, Z.D., 2005. 6-Hydroxydopamine-induced alterations in blood-brain barrier permeability. Eur J Neurosci 22, 1158-1168.

Chalela, J.A., Alsop, D.C., Gonzalez-Atavales, J.B., Maldjian, J.A., Kasner, S.E., Detre, J.A., 2000. Magnetic resonance perfusion imaging in acute ischemic stroke using continuous arterial spin labeling. Stroke 31, 680-687.

Cirillo, M., Laurenzi, M., Trevisan, M., Stamler, J., 1992. Hematocrit, blood pressure, and hypertension. The Gubbio Population Study. Hypertension 20, 319-326.

Collins, L.M., Toulouse, A., Connor, T.J., Nolan, Y.M., 2012. Contributions of central and systemic inflammation to the pathophysiology of Parkinson's disease. Neuropharmacology 62, 2154-2168.

Emre, M., Aarsland, D., Brown, R., Burn, D.J., Duyckaerts, C., Mizuno, Y., Broe, G.A., Cummings, J., Dickson, D.W., Gauthier, S., Goldman, J., Goetz, C., Korczyn, A., Lees, A., Levy, R., Litvan, I., McKeith, I., Olanow, W., Poewe, W., Quinn, N., Sampaio, C., Tolosa, E., Dubois, B., 2007. Clinical diagnostic criteria for dementia associated with Parkinson's disease. Mov Disord 22, 1689-1707; quiz 1837.

Fernandez-Seara, M.A., Mengual, E., Vidorreta, M., Aznarez-Sanado, M., Loayza, F.R., Villagra, F., Irigoyen, J., Pastor, M.A., 2012. Cortical hypoperfusion in Parkinson's disease assessed using arterial spin labeled perfusion MRI. NeuroImage 59, 2743-2750.

Fram, E.K., Herfkens, R.J., Johnson, G.A., Glover, G.H., Karis, J.P., Shimakawa, A., Perkins, T.G., Pelc, N.J., 1987. Rapid calculation of T1 using variable flip angle gradient refocused imaging. Magn Reson Imaging 5, 201-208.

Grammas, P., Martinez, J., Miller, B., 2011. Cerebral microvascular endothelium and the pathogenesis of neurodegenerative diseases. Expert Rev Mol Med 13, e19.

Gray, M.T., Woulfe, J.M., 2015. Striatal blood-brain barrier permeability in Parkinson's disease. J Cereb Blood Flow Metab 35, 747-750.

Heye, A.K., Culling, R.D., Valdes Hernandez Mdel, C., Thrippleton, M.J., Wardlaw, J.M., 2014. Assessment of blood-brain barrier disruption using dynamic contrast-enhanced MRI. A systematic review. Neuroimage Clin 6, 262-274.

Hoehn, M.M., Yahr, M.D., 1967. Parkinsonism: onset, progression and mortality. Neurology 17, 427-442.

Hu, M.T., Szewczyk-Krolikowski, K., Tomlinson, P., Nithi, K., Rolinski, M., Murray, C., Talbot, K., Ebmeier, K.P., Mackay, C.E., Ben-Shlomo, Y., 2014. Predictors of cognitive impairment in an early stage Parkinson's disease cohort. Mov Disord.

Jankovic, J., McDermott, M., Carter, J., Gauthier, S., Goetz, C., Golbe, L., Huber, S., Koller, W., Olanow, C., Shoulson, I., et al., 1990. Variable expression of Parkinson's disease: a base-line analysis of the DATATOP cohort. The Parkinson Study Group. Neurology 40, 1529-1534.

Kortekaas, R., Leenders, K.L., van Oostrom, J.C., Vaalburg, W., Bart, J., Willemsen, A.T., Hendrikse, N.H., 2005. Blood-brain barrier dysfunction in parkinsonian midbrain in vivo. Ann Neurol 57, 176-179.

Lavini, C., Verhoeff, J.J., 2010. Reproducibility of the gadolinium concentration measurements and of the fitting parameters of the vascular input function in the superior sagittal sinus in a patient population. Magn Reson Imaging 28, 1420-1430.

Leroi, I., Pantula, H., McDonald, K., Harbishettar, V., 2012. Neuropsychiatric symptoms in Parkinson's disease with mild cognitive impairment and dementia. Parkinsons Dis 2012, 308097.

Malek, N., Swallow, D.M., Grosset, K.A., Lawton, M.A., Marrinan, S.L., Lehn, A.C., Bresner, C., Bajaj, N., Barker, R.A., Ben-Shlomo, Y., Burn, D.J., Foltynie, T., Hardy, J., Morris, H.R., Williams, N.M., Wood, N., Grosset, D.G., 2015. Tracking Parkinson's: Study Design and Baseline Patient Data. J Parkinsons Dis 5, 947-959.

Melzer, T.R., Watts, R., MacAskill, M.R., Pearson, J.F., Rueger, S., Pitcher, T.L., Livingston, L., Graham, C., Keenan, R., Shankaranarayanan, A., Alsop, D.C., Dalrymple-Alford, J.C., Anderson, T.J., 2011. Arterial spin labelling reveals an abnormal cerebral perfusion pattern in Parkinson's disease. Brain 134, 845-855.

Montagne, A., Barnes, S.R., Sweeney, M.D., Halliday, M.R., Sagare, A.P., Zhao, Z., Toga, A.W., Jacobs, R.E., Liu, C.Y., Amezcua, L., Harrington, M.G., Chui, H.C., Law, M., Zlokovic, B.V., 2015. Blood-brain barrier breakdown in the aging human hippocampus. Neuron 85, 296-302.

Nelson, A.R., Sweeney, M.D., Sagare, A.P., Zlokovic, B.V., 2015. Neurovascular dysfunction and neurodegeneration in dementia and Alzheimer's disease. Biochim Biophys Acta.

Pardridge, W.M., 2005. Molecular biology of the blood-brain barrier. Mol Biotechnol 30, 57-70.

Patel, A., Toia, G.V., Colletta, K., Bradaric, B.D., Carvey, P.M., Hendey, B., 2011. An angiogenic inhibitor, cyclic RGDfV, attenuates MPTP-induced dopamine neuron toxicity. Exp Neurol 231, 160-170.

Pisani, V., Stefani, A., Pierantozzi, M., Natoli, S., Stanzione, P., Franciotta, D., Pisani, A., 2012. Increased blood-cerebrospinal fluid transfer of albumin in advanced Parkinson's disease. J Neuroinflammation 9, 188.

Pohmann, R., Scheffler, K., 2013. A theoretical and experimental comparison of different techniques for B(1) mapping at very high fields. NMR Biomed 26, 265-275.

Prodoehl, J., Yu, H., Little, D.M., Abraham, I., Vaillancourt, D.E., 2008. Region of interest template for the human basal ganglia: comparing EPI and standardized space approaches. NeuroImage 39, 956-965.

Richardson, J.D., Baker, J.M., Morgan, P.S., Rorden, C., Bonilha, L., Fridriksson, J., 2011. Cerebral perfusion in chronic stroke: implications for lesion-symptom mapping and functional MRI. Behav Neurol 24, 117-122.

Rodriguez, G., Nobili, F., De Carli, F., Francione, S., Marenco, S., Celestino, M.A., Hassan, K., Rosadini, G., 1993. Regional cerebral blood flow in chronic stroke patients. Stroke 24, 94-99.

Sagare, A.P., Bell, R.D., Zlokovic, B.V., 2013. Neurovascular defects and faulty amyloid-beta vascular clearance in Alzheimer's disease. J Alzheimers Dis 33 Suppl 1, S87-100.

Schmidt, P., Gaser, C., Arsic, M., Buck, D., Forschler, A., Berthele, A., Hoshi, M., Ilg, R., Schmid, V.J., Zimmer, C., Hemmer, B., Muhlau, M., 2012. An automated tool for detection of FLAIR-hyperintense white-matter lesions in Multiple Sclerosis. NeuroImage 59, 3774-3783.

Stanimirovic, D.B., Friedman, A., 2012. Pathophysiology of the neurovascular unit: disease cause or consequence? J Cereb Blood Flow Metab 32, 1207-1221.

Starr, J.M., Farrall, A.J., Armitage, P., McGurn, B., Wardlaw, J., 2009. Blood-brain barrier permeability in Alzheimer's disease: a case-control MRI study. Psychiatry Res 171, 232-241.

Starr, J.M., Wardlaw, J., Ferguson, K., MacLullich, A., Deary, I.J., Marshall, I., 2003. Increased blood-brain barrier permeability in type II diabetes demonstrated by gadolinium magnetic resonance imaging. J Neurol Neurosurg Psychiatry 74, 70-76.

Taheri, S., Gasparovic, C., Huisa, B.N., Adair, J.C., Edmonds, E., Prestopnik, J., Grossetete, M., Shah, N.J., Wills, J., Qualls, C., Rosenberg, G.A., 2011. Blood-brain barrier permeability abnormalities in vascular cognitive impairment. Stroke 42, 2158-2163.

Tomlinson, C.L., Stowe, R., Patel, S., Rick, C., Gray, R., Clarke, C.E., 2010. Systematic review of levodopa dose equivalency reporting in Parkinson's disease. Mov Disord 25, 2649-2653.

Tzourio-Mazoyer, N., Landeau, B., Papathanassiou, D., Crivello, F., Etard, O., Delcroix, N., Mazoyer, B., Joliot, M., 2002. Automated anatomical labeling of activations in SPM using a macroscopic anatomical parcellation of the MNI MRI single-subject brain. NeuroImage 15, 273-289.

Wardlaw, J.M., 2010. Blood-brain barrier and cerebral small vessel disease. J Neurol Sci 299, 66-71.

Wardlaw, J.M., Doubal, F., Armitage, P., Chappell, F., Carpenter, T., Munoz Maniega, S., Farrall, A., Sudlow, C., Dennis, M., Dhillon, B., 2009. Lacunar stroke is associated with diffuse blood-brain barrier dysfunction. Ann Neurol 65, 194-202.

Wardlaw, J.M., Doubal, F.N., Valdes-Hernandez, M., Wang, X., Chappell, F.M., Shuler, K., Armitage, P.A., Carpenter, T.C., Dennis, M.S., 2013. Blood-brain barrier permeability and long-term clinical and imaging outcomes in cerebral small vessel disease. Stroke 44, 525-527.

Wardlaw, J.M., Farrall, A., Armitage, P.A., Carpenter, T., Chappell, F., Doubal, F., Chowdhury, D., Cvoro, V., Dennis, M.S., 2008. Changes in background blood-brain barrier integrity between lacunar and cortical ischemic stroke subtypes. Stroke 39, 1327-1332.

Williams-Gray, C.H., Mason, S.L., Evans, J.R., Foltynie, T., Brayne, C., Robbins, T.W., Barker, R.A., 2013. The CamPaIGN study of Parkinson's disease: 10-year outlook in an incident population-based cohort. J Neurol Neurosurg Psychiatry 84, 1258-1264.

Zhao, Z., Nelson, A.R., Betsholtz, C., Zlokovic, B.V., 2015. Establishment and Dysfunction of the Blood-Brain Barrier. Cell 163, 1064-1078.

Zlokovic, B.V., 2008. The blood-brain barrier in health and chronic neurodegenerative disorders. Neuron 57, 178-201.

Zlokovic, B.V., 2011. Neurovascular pathways to neurodegeneration in Alzheimer's disease and other disorders. Nat Rev Neurosci 12, 723-738.

Chapter 6: Discussion

This chapter starts by elaborating on the practicalities of the PhD that have only been touched upon in previous chapters. This is important in terms of understanding the difficulties of conducting clinical research, how this could be improved, and how to maximise the benefit in terms of translation into clinical practice. This will lead onto a summary of all the key findings and their collective interpretation. This will be followed by a reflection and critique of the extent to which the final results meet the aims and objectives of the study. After establishing where we have reached and our current standpoint, a reflection on future perspectives followed by concluding remarks will complete the chapter.

6.1 Conducting the Clinical Study

Clinical research is a collaborative process and this PhD in particular involved the collective work of a cross-disciplinary team including neurologists, physicists and specialist nurses, also drawing in colleagues in vascular surgery and clinical laboratory science. As such it has been challenging to bring the project together from a practical perspective and has necessitated learning a wealth of information.

Familiarisation with the study design and the MRI methodology began by virtue of working on preliminary data for a sister study into late-onset epilepsy (Hanby et al., 2015). This highlighted the challenge of learning image acquisition and analysis and also the fact that with the methods being so novel, re-analysis of data was an ongoing process. Completing this initial study, leading onto the pilot study, enabled me to work with greater confidence, knowledge and autonomy on the PhD study.

Opportunities to expand the scope of the main clinical study by adding sub-studies using novel ultrasound measures, as well as blood markers of inflammation and endothelial activation/dysfunction (data from the sub-studies to be reported separately), meant forming new collaborations with various groups including Professor McCollum (Vascular Surgeon) and Dr Stephen Hopkins (Clinical Scientist).

6.11 Ethical Approvals

The first hurdle to starting the main study was to gain the necessary ethical and regulatory approvals for the work, including LREC and R&D as well as relevant university processes. This exercise gave me considerable insight into the complexities, including the setting and process for a major amendment and not least because more than one site was ultimately required for patient recruitment.

6.12 Recruitment

I selected, recruited and made all the arrangements for the participants to attend the WTCRF. I led the process on their day of attendance including pre scan preparations, taking the blood samples, performing the clinical scales and arranging transport and reimbursements. The challenges on the day of attendance were rather few in comparison to the challenges of recruitment yet both have been summarised below.

6.121 IPD Recruitment

As soon as the necessary approvals had been received, the first round of recruitment began. Approximately 600-700 notes of IPD patients of the PD nurse database at LTH were searched, 222 patients shortlisted, 64 were removed as they no longer fulfilled the inclusion/exclusion criteria or were not deemed well enough to tolerate an hour long MRI scan. Of the remainder, a total of 25 were interested in taking part (the rest were not interested or after further questioning did not fulfil the criteria or had no contact details). Of these 25, 9 patients were booked, who then had to be cancelled due to illness/change of mind. One patient fainted and so was rebooked; one patient was unable to go ahead with the scan because of claustrophobia. Three scan cancellations occurred on the day due to problems with the scanner. A total of 13 patients and 6 controls had completed the study by the end of the second year of the PhD.

By the start of the third year of the PhD the second round of recruitment began. After discussions with consultants at SRFT, additional avenues for recruitment were explored. One such avenue was recruitment via PRoBaND, a longitudinal study. This was later rejected as it was decided to be too burdensome for the participants in addition to the requirements of the PRoBaND study. Instead patients were to be recruited from PD clinics at SRFT, with 80 patients from an elderly care IPD clinic considered. Of these, only 19 were suitable, most being unsuitable due to multiple comorbidities that would make them unable to tolerate the hour long scanning protocol; 3 accepted and completed the scanning protocol. I attended the Neurology clinic at Macclesfield and recruited one patient and liaised with their IPD nurses; 33 potential IPD patients were selected, and 3 participants recruited. One participant recruited from another list of IPD patients that was kindly selected by a consultant at SRFT. A further 14 IPD patients were recruited from LTH by going through IPD nurse lists a year on (June 2014) and through re-reviewing

clinic lists of Neurologists based at LTH. One suitable patient was found via a colleague. A further 19 potential PIGD patients were selected with help from IPD nurses based at Blackpool; 3 recruited.

In terms of set-backs during this second round, the radiographers were unable to position the head of one PIGD patient correctly into the scanner therefore no scan information could be obtained. 1 TD and 2 PIGD participants did not complete the final ~10 min of the DCE protocol as they could no longer tolerate the scan after around 50 minutes of scanning. 2 TD and 2 PIGD fell into the intermediate category (i.e. neither TD nor PIGD) but full data were acquired.

In order to be recruited a potential participant had to be willing, able to give written informed consent, fulfil the IPD subgroup inclusion criteria, lack the exclusion criteria, and be able to lie flat and withstand an hour long MRI scan, and be well enough to participate. The willingness of participants was not usually such a limiting factor. The inclusion/exclusion criteria was made more complicated by additional factors such as the blood test for inflammatory markers which meant participants who had been ill in the previous 6 weeks or who had inflammatory conditions had to be excluded. Another factor that came into play was that LTH covers a large region in Lancashire, with no research 3T MRI facility in Lancashire, so the distance from the patient's home to the WTCRF understandably acted as a barrier for some potential participants. This was a common problem throughout all groups.

Within the IPD group, at least 7 scans had to be rearranged due to problems with the scanner either a few days before or on the day of scanning, leading to the loss of 3 potential participants who did not wish to be rebooked.

There was also difficulty identifying suitable patients as the new computer record systems at LTH did not allow patients to be identified based on disease (from 2012). A potential method of overcoming this limitation would be to create computer systems with coded information which would allow for effective searches for research purposes.

6.122 Control Negative

The plan for the recruitment of the control negative group was to encourage spouses/friends of the IPD/CP groups to participate. Although this was helpful it proved insufficient, so a further 8 participants were booked from a list kindly provided by a colleague (of participants of a previous study in which consent had been taken for

agreement to be contacted for further studies). One CN participant cancelled on the day due to difficulties getting to the scanner because of adverse weather conditions.

This method of recruitment of controls did lead to a practical error on my behalf. I had not appreciated that overwhelmingly the IPD and CP groups would consist of males and so recruiting their spouses resulted in significant gender differences between the groups and therefore a gender imbalance between the control negative and other groups. In the future this should be avoided by having multiple avenues of recruitment of controls and matching genders throughout the recruitment process.

6.123 Cerebrovascular Disease Recruitment

Various methods of recruitment involved retrospectively reviewing notes of patients who attended Dr Emsley's TIA clinic from Jan 2012-2013, and stroke physicians at RPH from Jan 2012 onwards. I also liaised with the stroke coordinator at RPH who provided lists of inpatients to the stroke ward at the Royal Preston Hospital (RPH) from Jan 2013-June 2014 (around 250 were reviewed). One CP participant did not tolerate the complete scan so had incomplete DCE data, one CP patient could not be successfully cannulated so incomplete DCE data acquired.

In summary, both the ethical review process and recruitment were very time-consuming. The emergence of clinical research networks with project managers dedicated to gaining ethical approval and recruitment are important to ensure the delivery of clinical research. Establishing a database of local cohorts of patients would also be very valuable.

6.2 A Summary of the Key Findings

	IPD Vs CP	IPD Vs CN	PIGD Vs CN	TD Vs CN	PIGD Vs TD
ASL					
CBF	Minimal difference	IPD < CN Posteriorly	PIGD < CN Posteriorly PIGD > CN	TD < CN Posteriorly	Nil
AAT	IPD > CP	IPD > CN	PIGD > CN	TD > CN	TD > PIGD
DCE (BG)					
k^{Trans}	Nil	IPD > CN	PIGD > CN	TD > CN	Nil
Vp	IPD > CP	Nil	PIGD > CN	TD > CN	PIGD > TD
WML Vol.	IPD < CP	Nil	PIGD > CN	Nil	PIGD > TD
Atrophy	Minimal IPD > CP	IPD > CN Temporal	PIGD > CN	TD > CN	Minimal difference
MoCA	Nil	IPD > CN	PIGD < CN	Nil	TD > PIGD

Table 6.1: A table to demonstrate the differences in NVS between IPD and CN and CP groups. The pattern of change has some overlap with known CVD, yet also clear differences. Phenotypic differences can also be appreciated.

We have validated the use of MRI perfusion and DCE techniques in the clinical setting in IPD, showing that such a study is feasible, including the mobilisation of a multidisciplinary team.

ASL appears to be a robust method for quantifying CBF. Our ASL findings are in keeping with PET studies and consistent with other ASL studies (Borghammer, 2012; Borghammer et al., 2010; Borghammer et al., 2012; Fernandez-Seara et al., 2012; Ma et al., 2010; Melzer et al., 2011). Considering both our results and those from previous studies, clear perfusion patterns have come to light, in particular posterior hypoperfusion in IPD compared to CN. In the PIGD group this is located in occipital regions and in the TD group more in temporal regions. It is less clear from this study alone why this specific pattern of change occurs, however in general studies seem to attribute posterior hypoperfusion to loss of corticostriatal pathways (Borghammer, 2012). One must note these perfusion patterns differed to patterns of atrophy therefore not favouring the idea that perfusion changes simply reflect atrophy, if this were the case the perfusion changes would have been expected to occur in the same areas as atrophy.

Our results also show a striking diffuse pattern of prolonged AAT in IPD compared to CN. To the author's knowledge, in the context of IPD, AAT has not been measured, yet our

findings of striking differences between the groups demonstrates that it as an exciting prospect to further our understanding of NVS in IPD. Of note, AAT differences in the IPD group compared to CN were more striking than the CBF differences perhaps suggesting they precede CBF changes, yet using our data alone, we can only speculate.

In preclinical studies a range of vascular pathologies, namely tortuosity of vessels, string vessels, and loss of capillaries have been demonstrated but not, to the author's knowledge, reflected in clinical studies (Brown and Thore, 2011; Farkas et al., 2000b). Although there is no way of knowing for sure if our findings of prolonged AAT reflect such pathology or increased collaterals, on balance it would seem to be in keeping with these morphological changes seen in pathological studies. Although prolonged AAT has mostly been attributed to microvascular pathology at the arteriole level (Yang et al., 2000), the contribution of macrovascular disease is difficult to quantify.

Whether these changes are causally related to, or are an effect of, the neurodegenerative process – or indeed protective, unfortunately, I don't think can be answered by this cross sectional study alone. Yet what can be said is that it is a step forward in confirming altered NVS in the clinical setting of IPD and provides validation for the application of ASL measures of CBF and AAT in future studies. To understand the changes better, ideally these ASL techniques would need to be applied in longitudinal studies and prodromal studies to track the sequence of events and pattern of changes. These measures could also be used in clinical trials to track changes in NVS with treatments and measuring the impact of NV modifying agents; a very exciting prospect. What would aid our knowledge further and may truly bridge the gap between clinical and preclinical studies is to work alongside preclinical studies in animal models of PD to track such changes and better understand them accordingly. So at the very least this work should help to alleviate scepticism surrounding the topic of altered NVS in IPD and provide an impetus to move forwards towards more studies utilising these techniques.

DCE MRI techniques revealed subtle BBB disruptions, in the BG structures, in IPD and CVD groups. The increased k^{Trans} in BG regions, seen in the IPD group, would be more in keeping with the hypothesis that NVS drives or at least plays a role in the neurodegenerative process as these areas are characteristically affected in IPD. The differences in k^{Trans} across the regions are interesting, warranting further investigation in this field. Equally the sparing of the caudate nucleus was clear yet difficult to decipher. Despite difficulties in mapping the BG structures and the fact that traditionally DCE has been used to look at much more significant levels of BBB disruption, our study demonstrates how DCE MRI is a promising tool to better understand the pathophysiology of neurodegenerative disorders. Of note the k^{Trans} whole brain values are significantly

higher in IPD compared to CN. Further analysis, such as voxel-based comparisons of the k^{Trans} maps would be required to understand more fully the global/regional nature of the k^{Trans} differences. What is interesting is the regional increase in CBF in the BG structures in the PIGD group, as demonstrated by ASL techniques, is also reflected by increased Vp in these areas in this group only, helping to validate these results.

The phenotype specific differences have been outlined in Table 6.1. Of note, not all head to head PIGD Vs TD differences in NVS measures reach significance, despite different patterns when comparing each group against CN, therefore there must be some overlap in the measurements between the PIGD and TD groups. Table 6.1 demonstrates how both phenotypes show diffuse prolonged AAT and posterior hypoperfusion with increased BBB leakiness in the BG nuclei. Table 6.1 also highlights some, but mostly marginal, differences between the groups. Only few imaging studies have taken a phenotypic approach. In order to better understand any potential differences, longitudinal, prodromal studies are required in addition to working alongside our preclinical colleagues. In particular, this may allow us to understand why hyperperfusion is seen in the BG in the PIGD group only, and whether greater AAT is neuroprotective.

The role of a control positive group in the form of CVD has been demonstrated. The rationale was that this is a group with expected alteration in NVS, with more CV risk factors than the IPD group. Indeed, such a group would be expected to show more pronounced changes in NVS compared to the IPD group. Yet in some ways we found that the IPD and CP groups exhibited similar changes; both showing posterior hypoperfusion, prolonged AAT and increased k^{Trans} in the BG structures. Contrary to expectations we found that hypoperfusion and prolonged AAT was *greatest* in the IPD group compared to the CP group and although k^{Trans} changes were similar, Vp changes were in opposite directions, with Vp lower in CP than CN, yet higher in IPD. Equally a similar cognitive profile was revealed between the 2 groups (Chapter 2, Table 2.1). However, taken together, the CP pattern of perfusion changes did not match that of IPD, where there was overlap it was difficult to attribute to comorbid CVD alone as the IPD group had fewer CV risk factors so what would be the driving force behind these changes?

All-the-same having a CP group did add its own layer of complexity as the chronic perfusion changes in CVD have not been well quantified and are arguably poorly understood (Richardson et al., 2011; Rodriguez et al., 1993). In addition the heterogeneity of the CP sample (comprising patients with TIAs and infarcts in various locations, and a combination of small vessel and large vessel disease) meant there may have also been heterogeneity in the results obtained, therefore it would seem the CP findings in their own right are interesting and warrant further investigation. Clearly this is

also a limitation of the work as the heterogeneity of the CP sample may, for example, have limited the findings in the group-wise voxel-based analysis. What remains is that the collective pattern of NVS changes in the IPD and CP groups show both similarities and differences. Altered NVS in IPD should therefore be appreciated in its own right and not simply attributed to comorbid CVD. Studies investigating NVS in IPD should not focus purely on stroke and TIA measures, but include more subtle measures of CVD, including markers of the small vessel disease. Future studies would need to make comparison with more homogenous cerebrovascular disease control groups.

WML burden assessed using visual rating scores has been used as a more traditional and accepted method of measuring vascular disease in the field of IPD as demonstrated by Table 1.1 in the introduction. In this work we consider the use of both visual rating scores and WML volume estimation, and the results appear a little conflicted. WML scores and volumes are clearly highest in the CP group as would be expected. Yet WML scores (not volumes) are significantly higher in the IPD group compared to CN, with no differences emerging between the phenotypes using the WML scores alone, but significant differences using WML volumes. This would be in keeping with a recent study highlighting the importance of distinguishing the distribution and size of WML to truly understand the burden (Rost et al., 2014). The increased WML volumes in PIGD would perhaps be more expected as SVD is already known to cause gait abnormalities (Schmidt et al., 2012b). What may be surprising, is the lack of correlation between k^{Trans} measures and WML burden, as at least theoretically Wardlaw et al. would argue they are on the same spectrum and suggestive of similar pathologies of SVD (Wardlaw et al., 2013a). Yet this would not be the first study to demonstrate a lack of correlation, with some attributing this to methodological reasons as outlined in the discussion section (5.5) of Chapter 5 (Armitage et al., 2011). Perhaps most importantly in our study is that the ROI was hypothesis driven (BG regions) which traditionally are spared of WMLs, so there could be no direct confound of WMLs themselves having altered k^{Trans}.

In terms of the non motor features of IPD a greater burden of non-motor features was found in the PIGD compared to the TD group. There were inevitable confounders of higher LEDD scores and longer disease durations in the PIGD group. All-the-same our work reflects a very similar pattern of differences to that which has been found in large prospective studies of newly diagnosed patients (PRoBaND) (Malek et al., 2015). Of note our study recruited far fewer numbers than those of traditional epidemiological studies, yet yielded similar results perhaps suggesting these differences are more pronounced than previously appreciated.

6.3 So Where Do we Stand Now?

To summarise our data is in keeping with our hypotheses:-

1. MRI techniques can be utilised as feasible structural and physiological measures of NVS. The physiological markers of NVS include cerebral perfusion (CBF and AAT), cerebrovascular reactivity (CVR) and DCE MRI measures of subtle BBB dysfunction.

2. Differences in structural and physiological measures of NVS exist between idiopathic Parkinson's disease patients and controls.

3. NVS varies according to the clinical phenotype of IPD and may modify the clinical features including non motor features.

Since embarking on the PhD, studies at the intersection of CVD and IPD began to emerge. An initiative in 2012, referred to *'an ambitious international effort to create expert consensus on the terminology and definitions used to describe vascular pathology on neuroimaging…… (which) should serve as a catalyst for research to establish the role of vascular factors in cognitive decline, dementia, and neurodegeneration'* (Editorial,(2012)). These studies are probably a consequence of preclinical studies implicating altered BBB function and hypoperfusion in neurodegenerative states. The role of MRI ASL and DCE techniques in the context of neurodegenerative states has been minimally explored and measurements of AAT non-existent. Therefore our findings of altered NVS in IPD have confirmed our hypotheses (which are outlined above) and have shown such measures to be exciting prospects for future studies.

Perhaps what hasn't been demonstrated is the benefit of CVR measurements in this context as this proved to be logistically challenging and difficult to interpret. The concept of CVR measurements remains in its infancy, but perhaps once it is better understood it may have applications in IPD. Equally through this study alone, perhaps one cannot go as far as to suggest NVS may modify the clinical features including non motor features but at the least it demonstrates that it varies according to the clinical phenotype of IPD.

So the question that remains is what does this mean in terms of understanding the vascular processes of IPD, i.e. what has this work added? Firstly our results have

demonstrated in the clinical setting that altered NVS occurs in IPD, with comparable patterns to CVD, despite the IPD patients having fewer vascular risk factors, so perhaps warranting a move away from assumptions that it is the association with vascular risk factors alone that drives these changes (de la Torre, 2012; Di Marco et al., 2015). Indeed there are differences in measurements of NVS between the IPD and CP groups, therefore suggesting altered NVS in IPD should not be viewed simply as a comorbidity with CVD. In addition, the NV changes did not match the regions showing atrophy so scepticism suggesting vascular changes are simply reflective of atrophy should also be reconsidered.

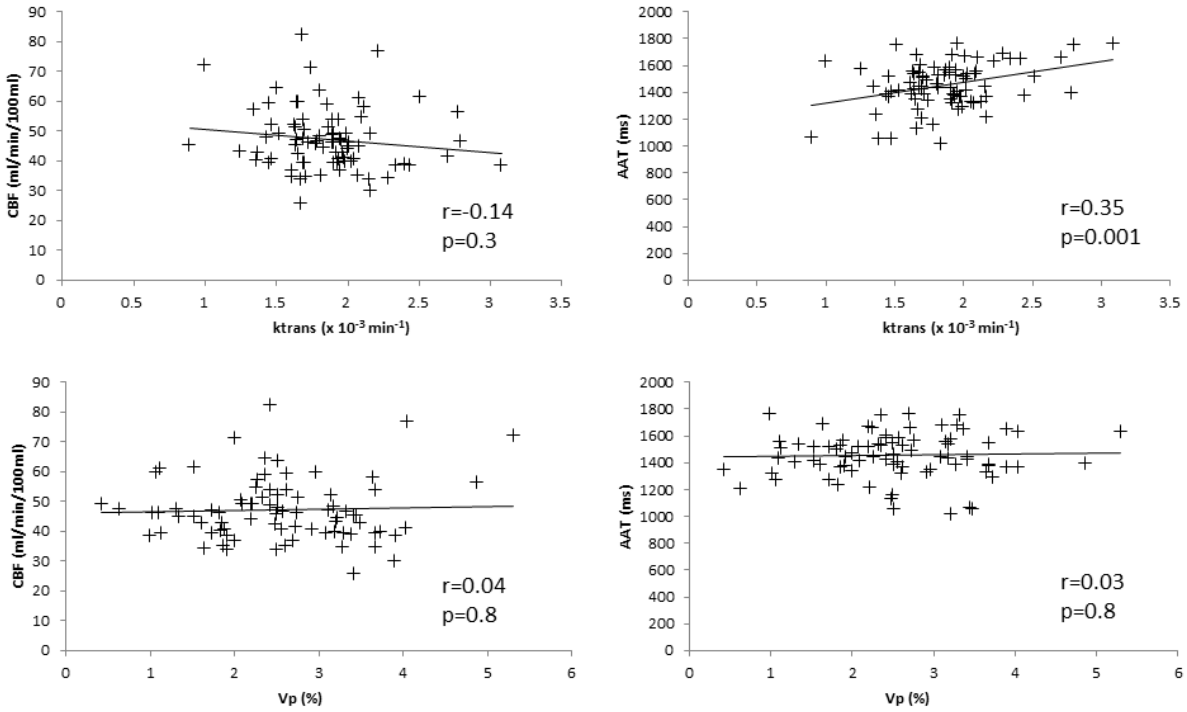

Figure 6.1: Linear Regression between whole brain perfusion and DCE imaging parameters across all individuals.

Figure 6.1 shows the associations between the key imaging parameters, which may help to advance our understanding of the underlying vascular processes. It can be seen that the only significant association is between k^{Trans} and AAT. The vascular hypothesis of neurodegeneration, would suggest that chronic hypoperfusion has a deleterious effect on the functioning of the BBB and vice versa (Stanimirovic and Friedman, 2012; Zlokovic, 2008, 2011). Yet, as demonstrated in Figure 6.1, in our study there were no correlations between global CBF measures and k^{Trans}. Indeed increased BBB leakage was observed in the BG nuclei, which would be in direct keeping with this hypothesis, yet hypoperfusion was minimal in these regions and more confined to the posterior cortices. Adding in the

extra dimension of diffusely prolonged AAT (which we have demonstrated) would suggest that perhaps there are some missing steps in our understanding of the process. As pathological studies have shown alteration in vasculature (string vessels etc. occur in the context of IPD) this would conceivably increase the AAT, yet perhaps not directly cause an alteration in CBF, hence the correlation between k^{Trans} and AAT, but not CBF (see Figure 6.1). This may also help explain why reduced CBF (and indeed metabolism) are restricted to posterior cortical regions (perhaps corticostriatal connections) and not directly at the site of the altered BBB. Ostergaard et al., are performing interesting work into understanding capillary dysfunction and have identified the complexity of the situation; they describe *'as capillary dysfunction results in heterogeneity of capillary blood flow pattern, elevated CBF ensues in order to maintain adequate oxygenation. However, with progressive increases in heterogeneity, the resulting low tissue oxygen tension will require a suppression of CBF in order to maintain tissue metabolism. The observed biphasic nature of CBF responses in preclinical AD and AD is therefore consistent with progressive disturbances of capillary flow patterns'* (Ostergaard et al., 2013).Thus one could postulate that BBB dysfunction can be implicated in the vicious cycle of neuronal death, as can hypoperfusion, yet perhaps not linked directly with each other. Equally it can be argued that subtle CBF changes at the BBB level may not be appreciated using ASL due to the low signal to noise ratio, yet one would still wonder why posterior hypoperfusion predominates. Ostergaard's et al., work may however help explain the hyperperfusion seen in IPD in the BG. What remains, is that it is paramount that further work be performed in this very exciting field.

6.4 Limitations of the Case-control Design

A brief critique of the case control approach has been included in Section 1.6, what follows is a more in-depth look into potential confounders. As NVS was the outcome measure in this study, the number of cerebrovascular risk factors in each group (apart from the CVD group) was matched. A not dissimilar distribution of risk factors was seen between the CN and IPD groups apart from perhaps IHD and smoking. A sub analysis was performed with greater matching of cases of IHD and smoking history between the CN and IPD groups (IHD; IPD 5.8%, CN 5.9% and smoking IPD 31.3 %, CN 29.4 %) 34 CN Vs 46 IPD, they remained matched for age, which yielded similar ASL results as described in chapter 4, the ASL AAT data has been demonstrated in Figure 6.2.

Similarly in the DCE group, a more matched group for IHD and smoking was selected (IHD; IPD 7.5%, CN 5.9 % and smoking IPD 31.6 %, CN 29.4%) with a total of 34 CN Vs 38 IPD, again remaining age matched, revealing larger SE yet similar results, as demonstrated in Figure 6.3. Ultimately a method of strengthening the power of the results would be to recruit more than one control for every case (Lewallen and Courtright, 1998) or to consider further analysis with logical regression in the future to adjust for differences in specific vascular risk factors.

Additionally there will be inevitable differences between the groups in terms of other comorbidities, protective factors such as diet and exercise, regular medications and so on. Therefore some of the between group differences may (at least in part) be accounted for by a measured or unmeasured confounding factor that might also differ between the groups. Interestingly clearly the burden of all CV RF was much greater in the CVD group yet NVS outcomes were similar between the IPD and CVD groups.

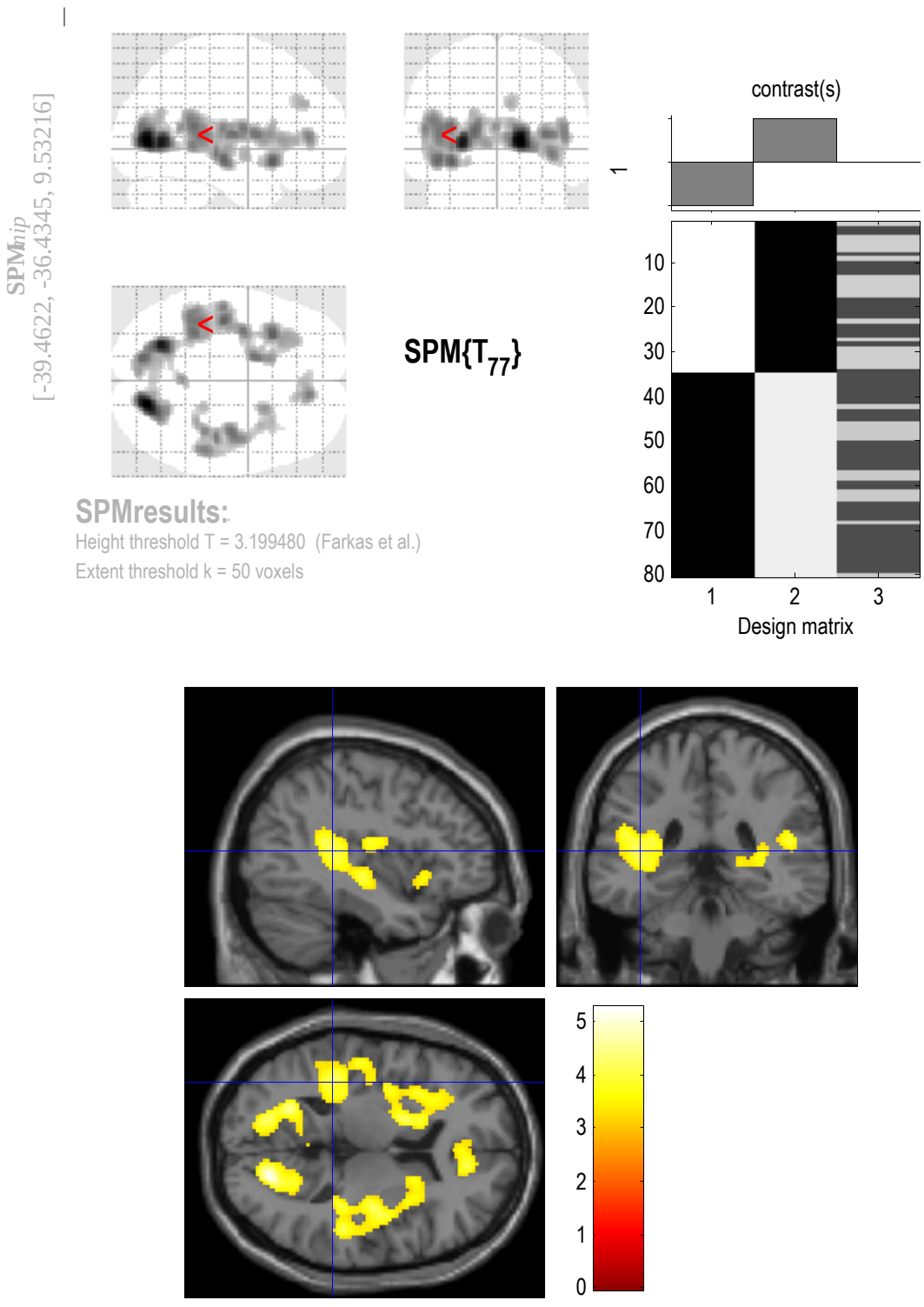

Figure 6.2: T Statistic maps revealing areas of prolonged AAT in the IPD group compared to controls (greater matching for CV RF).

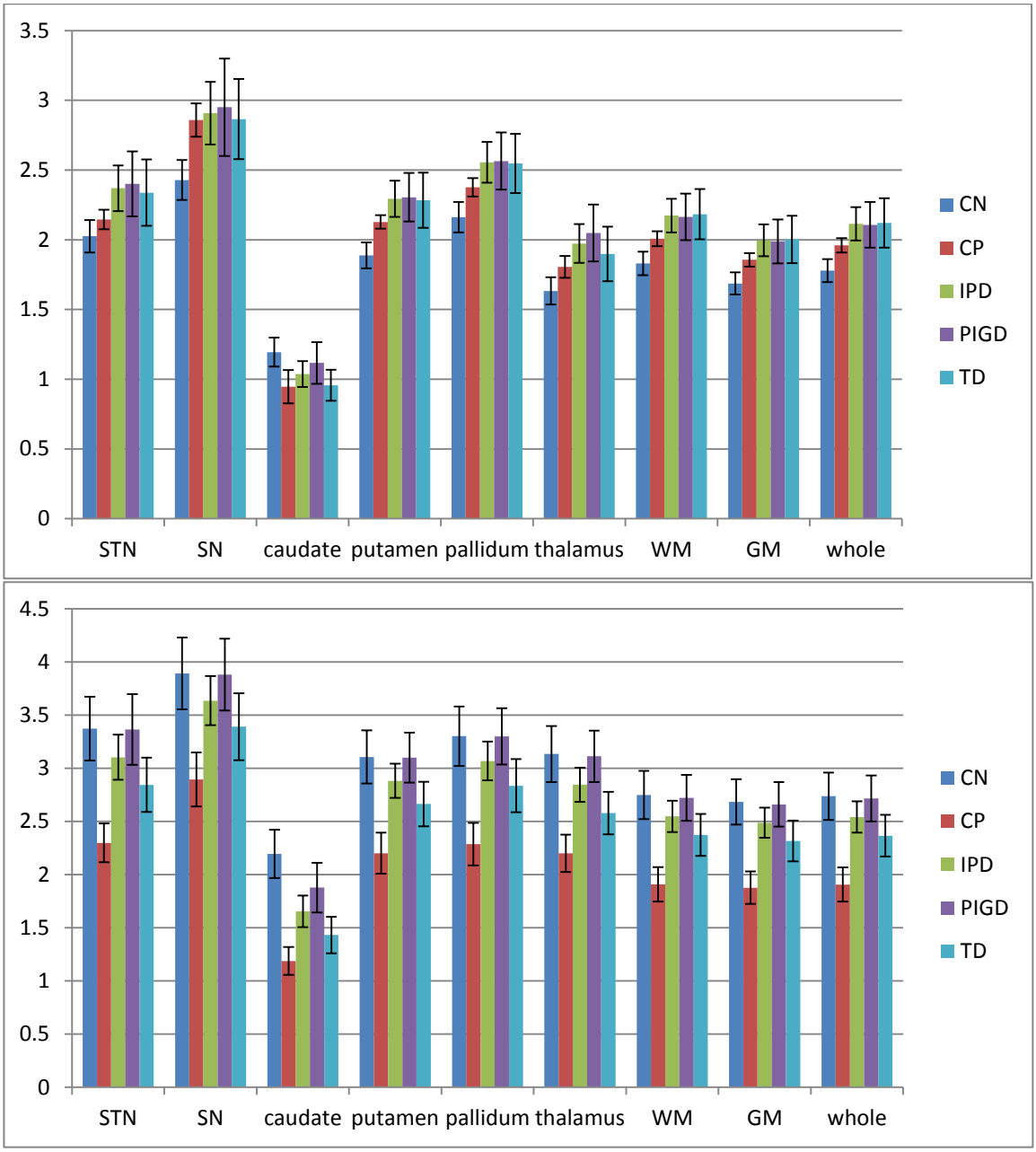

Figure 6.3: Median ROI values for (a) K^{Trans} and (b) Vp. Error bars show the standard error in the mean (.greater matching for CV RF)

6.5 Future Perspectives

There are many exciting future perspectives for our work. In the short term our work is not complete in terms of further analysis including the blood samples, DTI, SWI,

measurements of microbleeds etc. Looking to the future, incorporating other measures of altered NVS, as outlined in the recent progress report, such as DWI should be considered (Wardlaw et al., 2013c).

Our work would advocate a systems biology approach to understanding and unpicking the many factors that act and interact in the clearly dynamic and complicated process of neurodegeneration. For example it will likely be necessary to combine markers of neuroinflammation with markers of BBB breakdown in clinical and preclinical studies.

There is a clear need to take advantage of the longitudinal studies underway adding in measures of NVS into the imaging protocol, indeed such studies claim they want to 'provide a platform for imaging studies', which I think needs to be exploited in the future (Malek et al., 2015). Equally imaging studies can be extended to studies in the prodromal stages of the disease and prospective studies as outlined in the previous section. Indeed this can also be extended to clinical trials using imaging of NVS as a surrogate end point.

The ultimate aim would be to move away from 'an observed *association* to a verdict of *causation*'(Hill, 1965). The Austin Bradford Hill criterion for causation is dependent upon the 9 principles of: - strength of association, consistency, specificity, temporality, biological gradient, plausibility, coherence, experiment and analogy. Can our data alongside our current understanding of NVS in IPD fulfil such criteria? In brief one would argue no because even collectively the preclinical and clinical work to date, although observing associations cannot define the temporal association i.e. altered NVS in IPD as a cause or effect or even both of the neurodegenerative process. Inevitably preclinical and clinical studies working in conjunction and prodromal studies are needed to tease out the temporal association. All-the-same looking at our data, quite striking differences in AAT and BBB were revealed between the IPD group and controls. As table 1.2 illustrates, with accurate molecular measurements of NVS in IPD, greater consistency in demonstrating an association between NVS and IPD is emerging. It could be argued that specificity (i.e. altered NVS specifically causing neurodegeneration in IPD) would not necessarily apply in the case of neurodegenerative states due to the complexity of the process as neurodegeneration is now known to be multi-factorial requiring may factors to act and interact over time. Equally NVS will inevitably have multiple implications not just neurodegeneration.

In summary the Austin Bradford Hill criterion for causality of NVS in IPD is yet to be met, yet that can tempered by the fact that developments in molecular and imaging techniques will potentially increase our 'analytical capabilities for exploring potential cause-and-effect

relationships, and have resulted in a greater understanding of the complexity behind human disease onset and progression' (Fedak et al., 2015).

6.6 Concluding Remarks

In summary, this thesis has provided evidence for phenotypic-specific alterations in NVS in IPD. The nature and spatial distribution of the changes differ from those in pure CVD, suggesting that altered NVS in IPD is more than simply a reflection of co-morbid CVD. Novel microvascular imaging methods provide us with a window on these alterations. This work has been, but a stepping stone in the direction of better understanding altered NVS in IPD with the intention of directing future work in this exciting and incredibly important field on the path to finding effective neuroprotective and disease modifying treatments.

References

Editorial, 2012. A united approach to vascular disease and neurodegeneration. Lancet Neurol 11, 293.

Armitage, P.A., Farrall, A.J., Carpenter, T.K., Doubal, F.N., Wardlaw, J.M., 2011. Use of dynamic contrast-enhanced MRI to measure subtle blood-brain barrier abnormalities. Magn Reson Imaging 29, 305-314.

Borghammer, P., 2012. Perfusion and metabolism imaging studies in Parkinson's disease. Dan Med J 59, B4466.

Borghammer, P., Chakravarty, M., Jonsdottir, K.Y., Sato, N., Matsuda, H., Ito, K., Arahata, Y., Kato, T., Gjedde, A., 2010. Cortical hypometabolism and hypoperfusion in Parkinson's disease is extensive: probably even at early disease stages. Brain Struct Funct 214, 303-317.

Borghammer, P., Cumming, P., Ostergaard, K., Gjedde, A., Rodell, A., Bailey, C.J., Vafaee, M.S., 2012. Cerebral oxygen metabolism in patients with early Parkinson's disease. J Neurol Sci 313, 123-128.

Brown, W.R., Thore, C.R., 2011. Review: cerebral microvascular pathology in ageing and neurodegeneration. Neuropathol Appl Neurobiol 37, 56-74.

de la Torre, J.C., 2012. Cerebral hemodynamics and vascular risk factors: setting the stage for Alzheimer's disease. J Alzheimers Dis 32, 553-567.

Di Marco, L.Y., Venneri, A., Farkas, E., Evans, P.C., Marzo, A., Frangi, A.F., 2015. Vascular dysfunction in the pathogenesis of Alzheimer's disease--A review of endothelium-mediated mechanisms and ensuing vicious circles. Neurobiol Dis 82, 593-606.

Farkas, E., De Jong, G.I., de Vos, R.A., Jansen Steur, E.N., Luiten, P.G., 2000. Pathological features of cerebral cortical capillaries are doubled in Alzheimer's disease and Parkinson's disease. Acta Neuropathol 100, 395-402.

Fernandez-Seara, M.A., Mengual, E., Vidorreta, M., Aznarez-Sanado, M., Loayza, F.R., Villagra, F., Irigoyen, J., Pastor, M.A., 2012. Cortical hypoperfusion in Parkinson's disease assessed using arterial spin labeled perfusion MRI. NeuroImage 59, 2743-2750.

Hanby, M.F., Al-Bachari, S., Makin, F., Vidyasagar, R., Parkes, L.M., Emsley, H.C., 2015. Structural and physiological MRI correlates of occult cerebrovascular disease in late-onset epilepsy. Neuroimage Clin 9, 128-133.

Ma, Y., Huang, C., Dyke, J.P., Pan, H., Alsop, D., Feigin, A., Eidelberg, D., 2010. Parkinson's disease spatial covariance pattern: noninvasive quantification with perfusion MRI. J Cereb Blood Flow Metab 30, 505-509.

Malek, N., Swallow, D.M., Grosset, K.A., Lawton, M.A., Marrinan, S.L., Lehn, A.C., Bresner, C., Bajaj, N., Barker, R.A., Ben-Shlomo, Y., Burn, D.J., Foltynie, T., Hardy, J., Morris, H.R., Williams, N.M., Wood, N., Grosset, D.G., 2015. Tracking Parkinson's: Study Design and Baseline Patient Data. J Parkinsons Dis 5, 947-959.

Melzer, T.R., Watts, R., MacAskill, M.R., Pearson, J.F., Rueger, S., Pitcher, T.L., Livingston, L., Graham, C., Keenan, R., Shankaranarayanan, A., Alsop, D.C., Dalrymple-Alford, J.C., Anderson, T.J., 2011. Arterial spin labelling reveals an abnormal cerebral perfusion pattern in Parkinson's disease. Brain 134, 845-855.

Ostergaard, L., Aamand, R., Gutierrez-Jimenez, E., Ho, Y.C., Blicher, J.U., Madsen, S.M., Nagenthiraja, K., Dalby, R.B., Drasbek, K.R., Moller, A., Braendgaard, H., Mouridsen, K., Jespersen, S.N., Jensen, M.S., West, M.J., 2013. The capillary dysfunction hypothesis of Alzheimer's disease. Neurobiol Aging 34, 1018-1031.

Richardson, J.D., Baker, J.M., Morgan, P.S., Rorden, C., Bonilha, L., Fridriksson, J., 2011. Cerebral perfusion in chronic stroke: implications for lesion-symptom mapping and functional MRI. Behav Neurol 24, 117-122.

Rodriguez, G., Nobili, F., De Carli, F., Francione, S., Marenco, S., Celestino, M.A., Hassan, K., Rosadini, G., 1993. Regional cerebral blood flow in chronic stroke patients. Stroke 24, 94-99.

Rost, N.S., Sadaghiani, S., Biffi, A., Fitzpatrick, K.M., Cloonan, L., Rosand, J., Shibata, D.K., Mosley, T.H., Jr., 2014. Setting a gold standard for quantification of leukoaraiosis burden in patients with ischemic stroke: the Atherosclerosis Risk in Communities Study. J Neurosci Methods 221, 196-201.

Schmidt, R., Berghold, A., Jokinen, H., Gouw, A.A., van der Flier, W.M., Barkhof, F., Scheltens, P., Petrovic, K., Madureira, S., Verdelho, A., Ferro, J.M., Waldemar, G., Wallin, A., Wahlund, L.O., Poggesi, A., Pantoni, L., Inzitari, D., Fazekas, F., Erkinjuntti, T., 2012. White matter lesion progression in LADIS: frequency, clinical effects, and sample size calculations. Stroke 43, 2643-2647.

Stanimirovic, D.B., Friedman, A., 2012. Pathophysiology of the neurovascular unit: disease cause or consequence? J Cereb Blood Flow Metab 32, 1207-1221.

Szewczyk-Krolikowski, K., Tomlinson, P., Nithi, K., Wade-Martins, R., Talbot, K., Ben-Shlomo, Y., Hu, M.T., 2014. The influence of age and gender on motor and non-motor features of early Parkinson's disease: initial findings from the Oxford Parkinson Disease Center (OPDC) discovery cohort. Parkinsonism Relat Disord 20, 99-105.

Wardlaw, J.M., Doubal, F.N., Valdes-Hernandez, M., Wang, X., Chappell, F.M., Shuler, K., Armitage, P.A., Carpenter, T.C., Dennis, M.S., 2013a. Blood-brain barrier permeability and long-term clinical and imaging outcomes in cerebral small vessel disease. Stroke 44, 525-527.

Wardlaw, J.M., Smith, E.E., Biessels, G.J., Cordonnier, C., Fazekas, F., Frayne, R., Lindley, R.I., O'Brien, J.T., Barkhof, F., Benavente, O.R., Black, S.E., Brayne, C., Breteler, M., Chabriat, H., Decarli, C., de Leeuw, F.E., Doubal, F., Duering, M., Fox, N.C., Greenberg, S., Hachinski, V., Kilimann, I., Mok, V., Oostenbrugge, R., Pantoni, L., Speck, O., Stephan, B.C., Teipel, S., Viswanathan, A., Werring, D., Chen, C., Smith, C., van Buchem, M., Norrving, B., Gorelick, P.B., Dichgans, M., 2013b. Neuroimaging standards for research into small vessel disease and its contribution to ageing and neurodegeneration. Lancet Neurol 12, 822-838.

Yang, Y., Engelien, W., Xu, S., Gu, H., Silbersweig, D.A., Stern, E., 2000. Transit time, trailing time, and cerebral blood flow during brain activation: measurement using multislice, pulsed spin-labeling perfusion imaging. Magn Reson Med 44, 680-685.

Zlokovic, B.V., 2008. The blood-brain barrier in health and chronic neurodegenerative disorders. Neuron 57, 178-201.

Zlokovic, B.V., 2011. Neurovascular pathways to neurodegeneration in Alzheimer's disease and other disorders. Nat Rev Neurosci 12, 723-738.

References (Complete)

Editorial 2012. A united approach to vascular disease and neurodegeneration. Lancet Neurol 11, 293.

Aarsland, D., Bronnick, K., Ehrt, U., De Deyn, P.P., Tekin, S., Emre, M., Cummings, J.L., 2007. Neuropsychiatric symptoms in patients with Parkinson's disease and dementia: frequency, profile and associated care giver stress. J Neurol Neurosurg Psychiatry 78, 36-42.

Aarsland, D., Kurz, M.W., 2010. The epidemiology of dementia associated with Parkinson disease. J Neurol Sci 289, 18-22.

Aarsland, D., Larsen, J.P., Lim, N.G., Janvin, C., Karlsen, K., Tandberg, E., Cummings, J.L., 1999. Range of neuropsychiatric disturbances in patients with Parkinson's disease. J Neurol Neurosurg Psychiatry 67, 492-496.

Al-Bachari, S., Parkes, L.M., Vidyasagar, R., Hanby, M.F., Tharaken, V., Leroi, I., Emsley, H.C., 2014. Arterial spin labelling reveals prolonged arterial arrival time in idiopathic Parkinson's disease. Neuroimage Clin 6, 1-8.

Alsop, D.C., Detre, J.A., 1996. Reduced transit-time sensitivity in noninvasive magnetic resonance imaging of human cerebral blood flow. J Cereb Blood Flow Metab 16, 1236-1249.

Alvarez, J.I., Katayama, T., Prat, A., 2013. Glial influence on the blood brain barrier. Glia 61, 1939-1958.

Alves, G., Kurz, M., Lie, S.A., Larsen, J.P., 2004. Cigarette smoking in Parkinson's disease: influence on disease progression. Mov Disord 19, 1087-1092.

Anderson, C.M., Nedergaard, M., 2003. Astrocyte-mediated control of cerebral microcirculation. Trends Neurosci 26, 340-344; author reply 344-345.

Andreone, B.J., Lacoste, B., Gu, C., 2015. Neuronal and vascular interactions. Annu Rev Neurosci 38, 25-46.

Arai, H., Furuya, T., Mizuno, Y., Mochizuki, H., 2006. Inflammation and infection in Parkinson's disease. Histol Histopathol 21, 673-678.

Armitage, P.A., Farrall, A.J., Carpenter, T.K., Doubal, F.N., Wardlaw, J.M., 2011. Use of dynamic contrast-enhanced MRI to measure subtle blood-brain barrier abnormalities. Magn Reson Imaging 29, 305-314.

Armulik, A., Genove, G., Mae, M., Nisancioglu, M.H., Wallgard, E., Niaudet, C., He, L., Norlin, J., Lindblom, P., Strittmatter, K., Johansson, B.R., Betsholtz, C., 2010. Pericytes regulate the blood-brain barrier. Nature 468, 557-561.

Attwell, D., Buchan, A.M., Charpak, S., Lauritzen, M., Macvicar, B.A., Newman, E.A., 2010. Glial and neuronal control of brain blood flow. Nature 468, 232-243.

Ba, F., Obaid, M., Wieler, M., Camicioli, R., Martin, W.R., 2016. Parkinson Disease: The Relationship Between Non-motor Symptoms and Motor Phenotype. Can J Neurol Sci 43, 261-267.

Barcia, C., Bautista, V., Sanchez-Bahillo, A., Fernandez-Villalba, E., Faucheux, B., Poza y Poza, M., Fernandez Barreiro, A., Hirsch, E.C., Herrero, M.T., 2005. Changes in vascularization in substantia nigra pars compacta of monkeys rendered parkinsonian. J Neural Transm (Vienna) 112, 1237-1248.

Becker, C., Jick, S.S., Meier, C.R., 2010. Risk of stroke in patients with idiopathic Parkinson disease. Parkinsonism Relat Disord 16, 31-35.

Bell, R.D., Zlokovic, B.V., 2009. Neurovascular mechanisms and blood-brain barrier disorder in Alzheimer's disease. Acta Neuropathol 118, 103-113.

Ben-Shlomo, Y., Marmot, M.G., 1995. Survival and cause of death in a cohort of patients with parkinsonism: possible clues to aetiology? J Neurol Neurosurg Psychiatry 58, 293-299.

Bohnen, N.I., Muller, M.L., Zarzhevsky, N., Koeppe, R.A., Bogan, C.W., Kilbourn, M.R., Frey, K.A., Albin, R.L., 2011. Leucoaraiosis, nigrostriatal denervation and motor symptoms in Parkinson's disease. Brain 134, 2358-2365.

Bokkers, R.P., van Laar, P.J., van de Ven, K.C., Kapelle, L.J., Klijn, C.J., Hendrikse, J., 2008. Arterial spin-labeling MR imaging measurements of timing parameters in patients with a carotid artery occlusion. AJNR Am J Neuroradiol 29, 1698-1703.

Borghammer, P., 2012. Perfusion and metabolism imaging studies in Parkinson's disease. Dan Med J 59, B4466.

Borghammer, P., Chakravarty, M., Jonsdottir, K.Y., Sato, N., Matsuda, H., Ito, K., Arahata, Y., Kato, T., Gjedde, A., 2010. Cortical hypometabolism and hypoperfusion in Parkinson's disease is extensive: probably even at early disease stages. Brain Struct Funct 214, 303-317.

Borghammer, P., Cumming, P., Ostergaard, K., Gjedde, A., Rodell, A., Bailey, C.J., Vafaee, M.S., 2012. Cerebral oxygen metabolism in patients with early Parkinson's disease. J Neurol Sci 313, 123-128.

Bourdenx, M., Dovero, S., Engeln, M., Bido, S., Bastide, M.F., Dutheil, N., Vollenweider, I., Baud, L., Piron, C., Grouthier, V., Boraud, T., Porras, G., Li, Q., Baekelandt, V., Scheller, D., Michel, A., Fernagut, P.O., Georges, F., Courtine, G., Bezard, E., Dehay, B., 2015. Lack of additive role of ageing in nigrostriatal neurodegeneration triggered by alpha-synuclein overexpression. Acta Neuropathol Commun 3, 46.

Braak, H., Del Tredici, K., Rub, U., de Vos, R.A., Jansen Steur, E.N., Braak, E., 2003. Staging of brain pathology related to sporadic Parkinson's disease. Neurobiol Aging 24, 197-211.

Brown, W.R., 2010. A review of string vessels or collapsed, empty basement membrane tubes. J Alzheimers Dis 21, 725-739.

Brown, W.R., Thore, C.R., 2011. Review: cerebral microvascular pathology in ageing and neurodegeneration. Neuropathol Appl Neurobiol 37, 56-74.

Calamante, F., 2013. Arterial input function in perfusion MRI: a comprehensive review. Prog Nucl Magn Reson Spectrosc 74, 1-32.

Cantin, S., Villien, M., Moreaud, O., Tropres, I., Keignart, S., Chipon, E., Le Bas, J.F., Warnking, J., Krainik, A., 2011. Impaired cerebral vasoreactivity to CO2 in Alzheimer's disease using BOLD fMRI. NeuroImage 58, 579-587.

Carvey, P.M., Zhao, C.H., Hendey, B., Lum, H., Trachtenberg, J., Desai, B.S., Snyder, J., Zhu, Y.G., Ling, Z.D., 2005. 6-Hydroxydopamine-induced alterations in blood-brain barrier permeability. Eur J Neurosci 22, 1158-1168.

Chalela, J.A., Alsop, D.C., Gonzalez-Atavales, J.B., Maldjian, J.A., Kasner, S.E., Detre, J.A., 2000. Magnetic resonance perfusion imaging in acute ischemic stroke using continuous arterial spin labeling. Stroke 31, 680-687.

Chao, L.L., Buckley, S.T., Kornak, J., Schuff, N., Madison, C., Yaffe, K., Miller, B.L., Kramer, J.H., Weiner, M.W., 2010. ASL perfusion MRI predicts cognitive decline and conversion from MCI to dementia. Alzheimer Dis Assoc Disord 24, 19-27.

Chao, Y.X., He, B.P., Tay, S.S., 2009. Mesenchymal stem cell transplantation attenuates blood brain barrier damage and neuroinflammation and protects dopaminergic neurons against MPTP toxicity in the substantia nigra in a model of Parkinson's disease. J Neuroimmunol 216, 39-50.

Chaudhuri, K.R., Healy, D.G., Schapira, A.H., 2006. Non-motor symptoms of Parkinson's disease: diagnosis and management. Lancet Neurol 5, 235-245.

Chen, X., Lan, X., Roche, I., Liu, R., Geiger, J.D., 2008. Caffeine protects against MPTP-induced blood-brain barrier dysfunction in mouse striatum. J Neurochem 107, 1147-1157.

Chen, Y., Liu, L., 2012. Modern methods for delivery of drugs across the blood-brain barrier. Adv Drug Deliv Rev 64, 640-665.

Chen, Y., Wang, D.J., Detre, J.A., 2012. Comparison of arterial transit times estimated using arterial spin labeling. MAGMA 25, 135-144.

Chen, Y., Wolk, D.A., Reddin, J.S., Korczykowski, M., Martinez, P.M., Musiek, E.S., Newberg, A.B., Julin, P., Arnold, S.E., Greenberg, J.H., Detre, J.A., 2011. Voxel-level comparison of arterial spin-labeled perfusion MRI and FDG-PET in Alzheimer disease. Neurology 77, 1977-1985.

Choonara, Y.E., Pillay, V., du Toit, L.C., Modi, G., Naidoo, D., Ndesendo, V.M., Sibambo, S.R., 2009. Trends in the molecular pathogenesis and clinical therapeutics of common neurodegenerative disorders. Int J Mol Sci 10, 2510-2557.

Chung, Y.C., Ko, H.W., Bok, E., Park, E.S., Huh, S.H., Nam, J.H., Jin, B.K., 2010. The role of neuroinflammation on the pathogenesis of Parkinson's disease. BMB Rep 43, 225-232.

Cirillo, M., Laurenzi, M., Trevisan, M., Stamler, J., 1992. Hematocrit, blood pressure, and hypertension. The Gubbio Population Study. Hypertension 20, 319-326.

Collins, L.M., Toulouse, A., Connor, T.J., Nolan, Y.M., 2012. Contributions of central and systemic inflammation to the pathophysiology of Parkinson's disease. Neuropharmacology 62, 2154-2168.

Cooney, J.W., Stacy, M., 2016. Neuropsychiatric Issues in Parkinson's Disease. Curr Neurol Neurosci Rep 16, 49.

Cummings, J.L., 1997. The Neuropsychiatric Inventory: assessing psychopathology in dementia patients. Neurology 48, S10-16.

Cummings, J.L., Mega, M., Gray, K., Rosenberg-Thompson, S., Carusi, D.A., Gornbein, J., 1994. The Neuropsychiatric Inventory: comprehensive assessment of psychopathology in dementia. Neurology 44, 2308-2314.

Dai, W., Lopez, O.L., Carmichael, O.T., Becker, J.T., Kuller, L.H., Gach, H.M., 2009. Mild cognitive impairment and alzheimer disease: patterns of altered cerebral blood flow at MR imaging. Radiology 250, 856-866.

Danbolt, N.C., 2001. Glutamate uptake. Prog Neurobiol 65, 1-105.

Darbin, O., 2012. The aging striatal dopamine function. Parkinsonism Relat Disord 18, 426-432.

de la Torre, J.C., 2004. Alzheimer's disease is a vasocognopathy: a new term to describe its nature. Neurol Res 26, 517-524.

de la Torre, J.C., 2012. Cerebral hemodynamics and vascular risk factors: setting the stage for Alzheimer's disease. J Alzheimers Dis 32, 553-567.

de Lau, L.M., Verbaan, D., van Rooden, S.M., Marinus, J., van Hilten, J.J., 2014. Relation of clinical subtypes in Parkinson's disease with survival. Mov Disord 29, 150-151.

Derdeyn, C.P., Videen, T.O., Yundt, K.D., Fritsch, S.M., Carpenter, D.A., Grubb, R.L., Powers, W.J., 2002. Variability of cerebral blood volume and oxygen extraction: stages of cerebral haemodynamic impairment revisited. Brain 125, 595-607.

Derejko, M., Slawek, J., Wieczorek, D., Brockhuis, B., Dubaniewicz, M., Lass, P., 2006. Regional cerebral blood flow in Parkinson's disease as an indicator of cognitive impairment. Nucl Med Commun 27, 945-951.

Desai Bradaric, B., Patel, A., Schneider, J.A., Carvey, P.M., Hendey, B., 2012. Evidence for angiogenesis in Parkinson's disease, incidental Lewy body disease, and progressive supranuclear palsy. J Neural Transm (Vienna) 119, 59-71.

Detre, J.A., Alsop, D.C., Vives, L.R., Maccotta, L., Teener, J.W., Raps, E.C., 1998. Noninvasive MRI evaluation of cerebral blood flow in cerebrovascular disease. Neurology 50, 633-641.

Detre, J.A., Samuels, O.B., Alsop, D.C., Gonzalez-At, J.B., Kasner, S.E., Raps, E.C., 1999. Noninvasive magnetic resonance imaging evaluation of cerebral blood flow with acetazolamide challenge in patients with cerebrovascular stenosis. J Magn Reson Imaging 10, 870-875.

Di Marco, L.Y., Venneri, A., Farkas, E., Evans, P.C., Marzo, A., Frangi, A.F., 2015. Vascular dysfunction in the pathogenesis of Alzheimer's disease--A review of endothelium-mediated mechanisms and ensuing vicious circles. Neurobiol Dis 82, 593-606.

Djulejic, V., Marinkovic, S., Milic, V., Georgievski, B., Rasic, M., Aksic, M., Puskas, L., 2015. Common features of the cerebral perforating arteries and their clinical significance. Acta Neurochir (Wien) 157, 1393.

Dore-Duffy, P., LaManna, J.C., 2007. Physiologic angiodynamics in the brain. Antioxid Redox Signal 9, 1363-1371.

Drake, C.T., Iadecola, C., 2007. The role of neuronal signaling in controlling cerebral blood flow. Brain Lang 102, 141-152.

Edelman, R.R., Siewert, B., Darby, D.G., Thangaraj, V., Nobre, A.C., Mesulam, M.M., Warach, S., 1994. Qualitative mapping of cerebral blood flow and functional localization with echo-planar MR imaging and signal targeting with alternating radio frequency. Radiology 192, 513-520.

Eggers, C., Pedrosa, D.J., Kahraman, D., Maier, F., Lewis, C.J., Fink, G.R., Schmidt, M., Timmermann, L., 2012. Parkinson subtypes progress differently in clinical course and imaging pattern. PLoS One 7, e46813.

Emre, M., Aarsland, D., Brown, R., Burn, D.J., Duyckaerts, C., Mizuno, Y., Broe, G.A., Cummings, J., Dickson, D.W., Gauthier, S., Goldman, J., Goetz, C., Korczyn, A., Lees, A., Levy, R., Litvan, I., McKeith, I., Olanow, W., Poewe, W., Quinn, N., Sampaio, C., Tolosa, E., Dubois, B., 2007. Clinical diagnostic criteria for dementia associated with Parkinson's disease. Mov Disord 22, 1689-1707; quiz 1837.

Fahn, S., Cohen, G., 1992. The oxidant stress hypothesis in Parkinson's disease: evidence supporting it. Ann Neurol 32, 804-812.

Farkas, E., De Jong, G.I., Apro, E., De Vos, R.A., Steur, E.N., Luiten, P.G., 2000a. Similar ultrastructural breakdown of cerebrocortical capillaries in Alzheimer's disease, Parkinson's disease, and experimental hypertension. What is the functional link? Ann N Y Acad Sci 903, 72-82.

Farkas, E., De Jong, G.I., de Vos, R.A., Jansen Steur, E.N., Luiten, P.G., 2000b. Pathological features of cerebral cortical capillaries are doubled in Alzheimer's disease and Parkinson's disease. Acta Neuropathol 100, 395-402.

Farkas, E., Luiten, P.G., 2001. Cerebral microvascular pathology in aging and Alzheimer's disease. Prog Neurobiol 64, 575-611.

Farkas, E., Luiten, P.G., Bari, F., 2007. Permanent, bilateral common carotid artery occlusion in the rat: a model for chronic cerebral hypoperfusion-related neurodegenerative diseases. Brain Res Rev 54, 162-180.

Farooqui, T., Farooqui, A.A., 2009. Aging: an important factor for the pathogenesis of neurodegenerative diseases. Mech Ageing Dev 130, 203-215.

Faucheux, B.A., Bonnet, A.M., Agid, Y., Hirsch, E.C., 1999. Blood vessels change in the mesencephalon of patients with Parkinson's disease. Lancet 353, 981-982.

Fazekas, F., Kleinert, R., Offenbacher, H., Schmidt, R., Kleinert, G., Payer, F., Radner, H., Lechner, H., 1993. Pathologic correlates of incidental MRI white matter signal hyperintensities. Neurology 43, 1683-1689.

Fedak, K.M., Bernal, A., Capshaw, Z.A., Gross, S., 2015. Applying the Bradford Hill criteria in the 21st century: how data integration has changed causal inference in molecular epidemiology. Emerg Themes Epidemiol 12, 14.

Feinstein, A.R., 1970. The pre-therapeutic classification of co-morbidity in chronic disease. Journal of Chronic Diseases 23, 455-468.

Fenn, W.O., Craig, A.B., Jr., 1963. Effect of CO2 on respiration using a new method of administering CO2. J Appl Physiol 18, 1023-1024.

Fernandez-Seara, M.A., Mengual, E., Vidorreta, M., Aznarez-Sanado, M., Loayza, F.R., Villagra, F., Irigoyen, J., Pastor, M.A., 2012. Cortical hypoperfusion in Parkinson's disease assessed using arterial spin labeled perfusion MRI. NeuroImage 59, 2743-2750.

Fernandez, H.H., Aarsland, D., Fenelon, G., Friedman, J.H., Marsh, L., Troster, A.I., Poewe, W., Rascol, O., Sampaio, C., Stebbins, G.T., Goetz, C.G., 2008. Scales to assess psychosis in Parkinson's disease: Critique and recommendations. Mov Disord 23, 484-500.

Ferro, J.M., Caeiro, L., Figueira, M.L., 2016. Neuropsychiatric sequelae of stroke. Nat Rev Neurol 12, 269-280.

Firbank, M.J., Colloby, S.J., Burn, D.J., McKeith, I.G., O'Brien, J.T., 2003. Regional cerebral blood flow in Parkinson's disease with and without dementia. NeuroImage 20, 1309-1319.

Fisher, C.M., 1968. The arterial lesions underlying lacunes. Acta Neuropathol 12, 1-15.

Fisher, C.M., 2011. Lacunes: Small, deep cerebral infarcts. Neurology 77, 2104.

Florey, 1966. The endothelial cell. Br Med J 2, 487-490.

Foltynie, T., Kahan, J., 2013. Parkinson's disease: an update on pathogenesis and treatment. Journal of Neurology 260, 1433-1440.

Fram, E.K., Herfkens, R.J., Johnson, G.A., Glover, G.H., Karis, J.P., Shimakawa, A., Perkins, T.G., Pelc, N.J., 1987. Rapid calculation of T1 using variable flip angle gradient refocused imaging. Magn Reson Imaging 5, 201-208.

Freeman, L.R., Keller, J.N., 2012. Oxidative stress and cerebral endothelial cells: regulation of the blood-brain-barrier and antioxidant based interventions. Biochim Biophys Acta 1822, 822-829.

Ghebremedhin, E., Rosenberger, A., Rub, U., Vuksic, M., Berhe, T., Bickeboller, H., de Vos, R.A., Thal, D.R., Deller, T., 2010. Inverse relationship between cerebrovascular lesions and severity of lewy body pathology in patients with lewy body diseases. J Neuropathol Exp Neurol 69, 442-448.

Girouard, H., Iadecola, C., 2006. Neurovascular coupling in the normal brain and in hypertension, stroke, and Alzheimer disease. J Appl Physiol (1985) 100, 328-335.

Glass, C.K., Saijo, K., Winner, B., Marchetto, M.C., Gage, F.H., 2010. Mechanisms underlying inflammation in neurodegeneration. Cell 140, 918-934.

Goedert, M., Spillantini, M.G., Del Tredici, K., Braak, H., 2013. 100 years of Lewy pathology. Nat Rev Neurol 9, 13-24.

Golpich, M., Amini, E., Mohamed, Z., Azman Ali, R., Mohamed Ibrahim, N., Ahmadiani, A., 2016. Mitochondrial Dysfunction and Biogenesis in Neurodegenerative diseases: Pathogenesis and Treatment. CNS Neurosci Ther.

Gorell, J.M., Johnson, C.C., Rybicki, B.A., 1994. Parkinson's disease and its comorbid disorders: an analysis of Michigan mortality data, 1970 to 1990. Neurology 44, 1865-1868.

Grammas, P., Martinez, J., Miller, B., 2011. Cerebral microvascular endothelium and the pathogenesis of neurodegenerative diseases. Expert Rev Mol Med 13, e19.

Gray, M.T., Woulfe, J.M., 2015. Striatal blood-brain barrier permeability in Parkinson's disease. J Cereb Blood Flow Metab 35, 747-750.

Grimes, D.A., Schulz, K.F., 2002. An overview of clinical research: the lay of the land. Lancet 359, 57-61.

Grimes, D.A., Schulz, K.F., 2005. Compared to what? Finding controls for case-control studies. Lancet 365, 1429-1433.

Guan, J., Pavlovic, D., Dalkie, N., Waldvogel, H.J., O'Carroll, S.J., Green, C.R., Nicholson, L.F., 2013. Vascular degeneration in Parkinson's disease. Brain Pathol 23, 154-164.

Gunther, M., Bock, M., Schad, L.R., 2001. Arterial spin labeling in combination with a look-locker sampling strategy: inflow turbo-sampling EPI-FAIR (ITS-FAIR). Magn Reson Med 46, 974-984.

Hachinski, V.C., Potter, P., Merskey, H., 1987. Leuko-araiosis. Arch Neurol 44, 21-23.

Hajjar, I., Zhao, P., Alsop, D., Novak, V., 2010. Hypertension and cerebral vasoreactivity: a continuous arterial spin labeling magnetic resonance imaging study. Hypertension 56, 859-864.

Hanby, M.F., Al-Bachari, S., Makin, F., Vidyasagar, R., Parkes, L.M., Emsley, H.C., 2015. Structural and physiological MRI correlates of occult cerebrovascular disease in late-onset epilepsy. Neuroimage Clin 9, 128-133.

Harley, C.B., 1991. Telomere loss: mitotic clock or genetic time bomb? Mutat Res 256, 271-282.

Harman, D., 1981. The aging process. Proc Natl Acad Sci U S A 78, 7124-7128.

Hely, M.A., Reid, W.G., Adena, M.A., Halliday, G.M., Morris, J.G., 2008. The Sydney multicenter study of Parkinson's disease: the inevitability of dementia at 20 years. Mov Disord 23, 837-844.

Hemmer, B., Cepok, S., Zhou, D., Sommer, N., 2004. Multiple sclerosis -- a coordinated immune attack across the blood brain barrier. Curr Neurovasc Res 1, 141-150.

Hendrikse, J., Petersen, E.T., van Laar, P.J., Golay, X., 2008. Cerebral border zones between distal end branches of intracranial arteries: MR imaging. Radiology 246, 572-580.

Herman, T., Rosenberg-Katz, K., Jacob, Y., Auriel, E., Gurevich, T., Giladi, N., Hausdorff, J.M., 2013. White matter hyperintensities in Parkinson's disease: do they explain the disparity between the postural instability gait difficulty and tremor dominant subtypes? PLoS One 8, e55193.

Herman, T., Weiss, A., Brozgol, M., Wilf-Yarkoni, A., Giladi, N., Hausdorff, J.M., 2015. Cognitive function and other non-motor features in non-demented Parkinson's disease motor subtypes. J Neural Transm (Vienna) 122, 1115-1124.

Hershey, T., Black, K.J., Carl, J.L., McGee-Minnich, L., Snyder, A.Z., Perlmutter, J.S., 2003. Long term treatment and disease severity change brain responses to levodopa in Parkinson's disease. J Neurol Neurosurg Psychiatry 74, 844-851.

Heye, A.K., Culling, R.D., Valdes Hernandez Mdel, C., Thrippleton, M.J., Wardlaw, J.M., 2014. Assessment of blood-brain barrier disruption using dynamic contrast-enhanced MRI. A systematic review. Neuroimage Clin 6, 262-274.

Heye, A.K., Thrippleton, M.J., Armitage, P.A., Valdes Hernandez Mdel, C., Makin, S.D., Glatz, A., Sakka, E., Wardlaw, J.M., 2016. Tracer kinetic modelling for DCE-MRI quantification of subtle blood-brain barrier permeability. NeuroImage 125, 446-455.

Hill, A.B., 1965. THE ENVIRONMENT AND DISEASE: ASSOCIATION OR CAUSATION? Proc R Soc Med 58, 295-300.

Hirano, S., Asanuma, K., Ma, Y., Tang, C., Feigin, A., Dhawan, V., Carbon, M., Eidelberg, D., 2008. Dissociation of metabolic and neurovascular responses to levodopa in the treatment of Parkinson's disease. J Neurosci 28, 4201-4209.

Hoehn, M.M., Yahr, M.D., 1967. Parkinsonism: onset, progression and mortality. Neurology 17, 427-442.

Hu, M.T., Szewczyk-Krolikowski, K., Tomlinson, P., Nithi, K., Rolinski, M., Murray, C., Talbot, K., Ebmeier, K.P., Mackay, C.E., Ben-Shlomo, Y., 2014a. Predictors of cognitive impairment in an early stage Parkinson's disease cohort. Mov Disord 29, 351-359.

Hu, M.T., Szewczyk-Krolikowski, K., Tomlinson, P., Nithi, K., Rolinski, M., Murray, C., Talbot, K., Ebmeier, K.P., Mackay, C.E., Ben-Shlomo, Y., 2014b. Predictors of cognitive impairment in an early stage Parkinson's disease cohort. Mov Disord.

Hurn, P.D., Traystman, R.J., 1997. Overview of cerebrovascular hemodynamics. Primer on Cardiovascular Diseases, 42-44.

Iadecola, C., 2004. Neurovascular regulation in the normal brain and in Alzheimer's disease. Nat Rev Neurosci 5, 347-360.

Jangula, A., Murphy, E.J., 2013. Lipopolysaccharide-induced blood brain barrier permeability is enhanced by alpha-synuclein expression. Neurosci Lett 551, 23-27.

Jankovic, J., McDermott, M., Carter, J., Gauthier, S., Goetz, C., Golbe, L., Huber, S., Koller, W., Olanow, C., Shoulson, I., et al., 1990. Variable expression of Parkinson's disease: a base-line analysis of the DATATOP cohort. The Parkinson Study Group. Neurology 40, 1529-1534.

Jellinger, K.A., 2003. Prevalence of cerebrovascular lesions in Parkinson's disease. A postmortem study. Acta Neuropathol 105, 415-419.

Johnson, N.A., Jahng, G.H., Weiner, M.W., Miller, B.L., Chui, H.C., Jagust, W.J., Gorno-Tempini, M.L., Schuff, N., 2005. Pattern of cerebral hypoperfusion in Alzheimer disease and mild cognitive impairment measured with arterial spin-labeling MR imaging: initial experience. Radiology 234, 851-859.

Kalaria, R.N., 1996. Cerebral vessels in ageing and Alzheimer's disease. Pharmacol Ther 72, 193-214.

Kamagata, K., Motoi, Y., Hori, M., Suzuki, M., Nakanishi, A., Shimoji, K., Kyougoku, S., Kuwatsuru, R., Sasai, K., Abe, O., Mizuno, Y., Aoki, S., Hattori, N., 2011. Posterior hypoperfusion in Parkinson's disease with and without dementia measured with arterial spin labeling MRI. J Magn Reson Imaging 33, 803-807.

Kelleher, R.J., Soiza, R.L., 2013. Evidence of endothelial dysfunction in the development of Alzheimer's disease: Is Alzheimer's a vascular disorder? Am J Cardiovasc Dis 3, 197-226.

Kimura, Y., Oku, N., Kajimoto, K., Katoh, H., Tanaka, M.R., Takasawa, M., Imaizumi, M., Kitagawa, K., Hori, M., Hatazawa, J., 2006. Diastolic blood pressure influences cerebrovascular reactivity measured by means of 123I-iodoamphetamine brain single photon emission computed tomography in medically treated patients with occlusive carotid or middle cerebral artery disease. Ann Nucl Med 20, 209-215.

Kish, S.J., Shannak, K., Rajput, A., Deck, J.H., Hornykiewicz, O., 1992. Aging produces a specific pattern of striatal dopamine loss: implications for the etiology of idiopathic Parkinson's disease. J Neurochem 58, 642-648.

Kloppenborg, R.P., Nederkoorn, P.J., Geerlings, M.I., van den Berg, E., 2014. Presence and progression of white matter hyperintensities and cognition: a meta-analysis. Neurology 82, 2127-2138.

Knottnerus, I.L., Ten Cate, H., Lodder, J., Kessels, F., van Oostenbrugge, R.J., 2009. Endothelial dysfunction in lacunar stroke: a systematic review. Cerebrovasc Dis 27, 519-526.

Kobari, M., Fukuuchi, Y., Shinohara, T., Obara, K., Nogawa, S., 1995. Levodopa-induced local cerebral blood flow changes in Parkinson's disease and related disorders. J Neurol Sci 128, 212-218.

Kohler, C.A., Magalhaes, T.F., Oliveira, J.M., Alves, G.S., Knochel, C., Oertel-Knochel, V., Pantel, J., Carvalho, A.F., 2016. Neuropsychiatric Disturbances in Mild Cognitive Impairment (MCI): a Systematic Review of Population-Based Studies. Curr Alzheimer Res.

Kortekaas, R., Leenders, K.L., van Oostrom, J.C., Vaalburg, W., Bart, J., Willemsen, A.T., Hendrikse, N.H., 2005. Blood-brain barrier dysfunction in parkinsonian midbrain in vivo. Ann Neurol 57, 176-179.

Kurtis, M.M., Rodriguez-Blazquez, C., Martinez-Martin, P., 2013. Relationship between sleep disorders and other non-motor symptoms in Parkinson's disease. Parkinsonism Relat Disord 19, 1152-1155.

Kuter, K., Kratochwil, M., Marx, S.H., Hartwig, S., Lehr, S., Sugawa, M.D., Dencher, N.A., 2016. Native DIGE proteomic analysis of mitochondria from substantia nigra and striatum during neuronal degeneration and its compensation in an animal model of early Parkinson's disease. Arch Physiol Biochem 122, 238-256.

L'Episcopo, F., Tirolo, C., Testa, N., Caniglia, S., Morale, M.C., Impagnatiello, F., Marchetti, B., 2011. Switching the microglial harmful phenotype promotes lifelong restoration of subtantia nigra dopaminergic neurons from inflammatory neurodegeneration in aged mice. Rejuvenation Res 14, 411-424.

Lavini, C., Verhoeff, J.J., 2010. Reproducibility of the gadolinium concentration measurements and of the fitting parameters of the vascular input function in the superior sagittal sinus in a patient population. Magn Reson Imaging 28, 1420-1430.

Lawton, M., Baig, F., Rolinski, M., Ruffman, C., Nithi, K., May, M.T., Ben-Shlomo, Y., Hu, M.T., 2015. Parkinson's Disease Subtypes in the Oxford Parkinson Disease Centre (OPDC) Discovery Cohort. J Parkinsons Dis 5, 269-279.

Lee, S.J., Kim, J.S., Lee, K.S., An, J.Y., Kim, W., Kim, Y.I., Kim, B.S., Jung, S.L., 2009. The severity of leukoaraiosis correlates with the clinical phenotype of Parkinson's disease. Arch Gerontol Geriatr 49, 255-259.

Leonards, C.O., Ipsen, N., Malzahn, U., Fiebach, J.B., Endres, M., Ebinger, M., 2012. White matter lesion severity in mild acute ischemic stroke patients and functional outcome after 1 year. Stroke 43, 3046-3051.

Leroi, I., Pantula, H., McDonald, K., Harbishettar, V., 2012. Neuropsychiatric symptoms in Parkinson's disease with mild cognitive impairment and dementia. Parkinsons Dis 2012, 308097.

Lesage, S., Brice, A., 2009. Parkinson's disease: from monogenic forms to genetic susceptibility factors. Hum Mol Genet 18, R48-59.

Levine, R.L., Stadtman, E.R., 2001. Oxidative modification of proteins during aging. Exp Gerontol 36, 1495-1502.

Lewallen, S., Courtright, P., 1998. Epidemiology in practice: case-control studies. Community Eye Health 11, 57-58.

Lezi, E., Swerdlow, R.H., 2012. Mitochondria in neurodegeneration. Adv Exp Med Biol 942, 269-286.

Lieberman, M.D., Cunningham, W.A., 2009. Type I and Type II error concerns in fMRI research: re-balancing the scale. Soc Cogn Affect Neurosci 4, 423-428.

Lill, C.M., Roehr, J.T., McQueen, M.B., Kavvoura, F.K., Bagade, S., Schjeide, B.M., Schjeide, L.M., Meissner, E., Zauft, U., Allen, N.C., Liu, T., Schilling, M., Anderson, K.J., Beecham, G., Berg, D., Biernacka, J.M., Brice, A., DeStefano, A.L., Do, C.B., Eriksson, N., Factor, S.A., Farrer, M.J., Foroud, T., Gasser, T., Hamza, T., Hardy, J.A., Heutink, P., Hill-Burns, E.M., Klein, C., Latourelle, J.C., Maraganore, D.M., Martin, E.R., Martinez, M., Myers, R.H., Nalls, M.A., Pankratz, N., Payami, H., Satake, W., Scott, W.K., Sharma, M., Singleton, A.B., Stefansson, K., Toda, T., Tung, J.Y., Vance, J., Wood, N.W., Zabetian, C.P., Young, P., Tanzi, R.E., Khoury, M.J., Zipp, F., Lehrach, H., Ioannidis, J.P., Bertram, L., 2012. Comprehensive research synopsis and systematic meta-analyses in Parkinson's disease genetics: The PDGene database. PLoS Genet 8, e1002548.

Lipton, S.A., 2005. The molecular basis of memantine action in Alzheimer's disease and other neurologic disorders: low-affinity, uncompetitive antagonism. Curr Alzheimer Res 2, 155-165.

Litvan, I., Aarsland, D., Adler, C.H., Goldman, J.G., Kulisevsky, J., Mollenhauer, B., Rodriguez-Oroz, M.C., Troster, A.I., Weintraub, D., 2011. MDS Task Force on mild cognitive impairment in Parkinson's disease: critical review of PD-MCI. Mov Disord 26, 1814-1824.

Liu, Y., Zhu, X., Feinberg, D., Guenther, M., Gregori, J., Weiner, M.W., Schuff, N., 2012. Arterial spin labeling MRI study of age and gender effects on brain perfusion hemodynamics. Magn Reson Med 68, 912-922.

Longstreth, W.T., Jr., Arnold, A.M., Manolio, T.A., Burke, G.L., Bryan, N., Jungreis, C.A., O'Leary, D., Enright, P.L., Fried, L., 2000. Clinical correlates of ventricular and sulcal size on cranial magnetic resonance imaging of 3,301 elderly people. The Cardiovascular Health Study. Collaborative Research Group. Neuroepidemiology 19, 30-42.

Lu, H.Z., Clingman, C., Golay, X., van Zijl, P.C.M., 2004. Determining the longitudinal relaxation time (T-1) of blood at 3.0 tesla. Magnetic Resonance in Medicine 52, 679-682.

Luk, K.C., Kehm, V., Carroll, J., Zhang, B., O'Brien, P., Trojanowski, J.Q., Lee, V.M., 2012. Pathological alpha-synuclein transmission initiates Parkinson-like neurodegeneration in nontransgenic mice. Science 338, 949-953.

Ma, Y., Huang, C., Dyke, J.P., Pan, H., Alsop, D., Feigin, A., Eidelberg, D., 2010. Parkinson's disease spatial covariance pattern: noninvasive quantification with perfusion MRI. J Cereb Blood Flow Metab 30, 505-509.

Machado, A., Herrera, A.J., Venero, J.L., Santiago, M., de Pablos, R.M., Villaran, R.F., Espinosa-Oliva, A.M., Arguelles, S., Sarmiento, M., Delgado-Cortes, M.J., Maurino, R., Cano, J., 2011. Inflammatory Animal Model for Parkinson's Disease: The Intranigral Injection of LPS Induced the Inflammatory Process along with the Selective Degeneration of Nigrostriatal Dopaminergic Neurons. ISRN Neurol 2011, 476158.

MacIntosh, B.J., Filippini, N., Chappell, M.A., Woolrich, M.W., Mackay, C.E., Jezzard, P., 2010a. Assessment of arterial arrival times derived from multiple inversion time pulsed arterial spin labeling MRI. Magn Reson Med 63, 641-647.

MacIntosh, B.J., Lindsay, A.C., Kylintireas, I., Kuker, W., Gunther, M., Robson, M.D., Kennedy, J., Choudhury, R.P., Jezzard, P., 2010b. Multiple inflow pulsed arterial spin-labeling reveals delays in the arterial arrival time in minor stroke and transient ischemic attack. AJNR Am J Neuroradiol 31, 1892-1894.

MacIntosh, B.J., Swardfager, W., Robertson, A.D., Tchistiakova, E., Saleem, M., Oh, P.I., Herrmann, N., Stefanovic, B., Lanctot, K.L., 2015. Regional cerebral arterial transit time hemodynamics correlate with vascular risk factors and cognitive function in men with coronary artery disease. AJNR Am J Neuroradiol 36, 295-301.

Mai, V.M., Berr, S.S., 1999. MR perfusion imaging of pulmonary parenchyma using pulsed arterial spin labeling techniques: FAIRER and FAIR. J Magn Reson Imaging 9, 483-487.

Mak, H.K., Chan, Q., Zhang, Z., Petersen, E.T., Qiu, D., Zhang, L., Yau, K.K., Chu, L.W., Golay, X., 2012. Quantitative assessment of cerebral hemodynamic parameters by QUASAR arterial spin labeling in Alzheimer's disease and cognitively normal Elderly adults at 3-tesla. J Alzheimers Dis 31, 33-44.

Malek, N., Swallow, D.M., Grosset, K.A., Lawton, M.A., Marrinan, S.L., Lehn, A.C., Bresner, C., Bajaj, N., Barker, R.A., Ben-Shlomo, Y., Burn, D.J., Foltynie, T., Hardy, J., Morris, H.R., Williams, N.M., Wood, N., Grosset, D.G., 2015. Tracking Parkinson's: Study Design and Baseline Patient Data. J Parkinsons Dis 5, 947-959.

Markus, H.S., 2004. Cerebral perfusion and stroke. J Neurol Neurosurg Psychiatry 75, 353-361.

Marras, C., Chaudhuri, K.R., 2016. Nonmotor features of Parkinson's disease subtypes. Mov Disord.

Mastaglia, F.L., Johnsen, R.D., Kakulas, B.A., 2002. Prevalence of stroke in Parkinson's disease: a postmortem study. Mov Disord 17, 772-774.

McGeer, P.L., Itagaki, S., Boyes, B.E., McGeer, E.G., 1988. Reactive microglia are positive for HLA-DR in the substantia nigra of Parkinson's and Alzheimer's disease brains. Neurology 38, 1285-1291.

Meissner, W.G., Frasier, M., Gasser, T., Goetz, C.G., Lozano, A., Piccini, P., Obeso, J.A., Rascol, O., Schapira, A., Voon, V., Weiner, D.M., Tison, F., Bezard, E., 2011. Priorities in Parkinson's disease research. Nat Rev Drug Discov 10, 377-393.

Melo, T.Q., van Zomeren, K.C., Ferrari, M.F., Boddeke, H.W., Copray, J.C., 2016. Impairment of mitochondria dynamics by human A53T alpha-synuclein and rescue by NAP (davunetide) in a cell model for Parkinson's disease. Exp Brain Res.

Melzer, T.R., Watts, R., MacAskill, M.R., Pearson, J.F., Rueger, S., Pitcher, T.L., Livingston, L., Graham, C., Keenan, R., Shankaranarayanan, A., Alsop, D.C., Dalrymple-Alford, J.C., Anderson, T.J., 2011. Arterial spin labelling reveals an abnormal cerebral perfusion pattern in Parkinson's disease. Brain 134, 845-855.

Meredith, G.E., Sonsalla, P.K., Chesselet, M.F., 2008. Animal models of Parkinson's disease progression. Acta Neuropathol 115, 385-398.

Mito, Y., Yoshida, K., Yabe, I., Makino, K., Hirotani, M., Tashiro, K., Kikuchi, S., Sasaki, H., 2005. Brain 3D-SSP SPECT analysis in dementia with Lewy bodies, Parkinson's disease with and without dementia, and Alzheimer's disease. Clin Neurol Neurosurg 107, 396-403.

Mito, Y., Yoshida, K., Yabe, I., Makino, K., Tashiro, K., Kikuchi, S., Sasaki, H., 2006. Brain SPECT analysis by 3D-SSP and phenotype of Parkinson's disease. J Neurol Sci 241, 67-72.

Montagne, A., Barnes, S.R., Sweeney, M.D., Halliday, M.R., Sagare, A.P., Zhao, Z., Toga, A.W., Jacobs, R.E., Liu, C.Y., Amezcua, L., Harrington, M.G., Chui, H.C., Law, M., Zlokovic, B.V., 2015. Blood-brain barrier breakdown in the aging human hippocampus. Neuron 85, 296-302.

Moody, D.M., Bell, M.A., Challa, V.R., 1990. Features of the cerebral vascular pattern that predict vulnerability to perfusion or oxygenation deficiency: an anatomic study. AJNR Am J Neuroradiol 11, 431-439.

Moody, D.M., Santamore, W.P., Bell, M.A., 1991. Does tortuosity in cerebral arterioles impair down-autoregulation in hypertensives and elderly normotensives? A hypothesis and computer model. Clin Neurosurg 37, 372-387.

Morale, M.C., Serra, P.A., L'Episcopo, F., Tirolo, C., Caniglia, S., Testa, N., Gennuso, F., Giaquinta, G., Rocchitta, G., Desole, M.S., Miele, E., Marchetti, B., 2006. Estrogen, neuroinflammation and neuroprotection in Parkinson's disease: glia dictates resistance versus vulnerability to neurodegeneration. Neuroscience 138, 869-878.

Morley, J.F., Duda, J.E., 2012. Parkinson's disease and the risk of cerebrovascular pathology. Mov Disord 27, 1471-1472.

Mueggler, T., Sturchler-Pierrat, C., Baumann, D., Rausch, M., Staufenbiel, M., Rudin, M., 2002. Compromised hemodynamic response in amyloid precursor protein transgenic mice. J Neurosci 22, 7218-7224.

Muller, M.J., Dragicevic, A., 2003. Standardized rater training for the Hamilton Depression Rating Scale (HAMD-17) in psychiatric novices. J Affect Disord 77, 65-69.

Mure, H., Hirano, S., Tang, C.C., Isaias, I.U., Antonini, A., Ma, Y., Dhawan, V., Eidelberg, D., 2011. Parkinson's disease tremor-related metabolic network: characterization, progression, and treatment effects. NeuroImage 54, 1244-1253.

Murphy, K., Harris, A.D., Diukova, A., Evans, C.J., Lythgoe, D.J., Zelaya, F., Wise, R.G., 2011. Pulsed arterial spin labeling perfusion imaging at 3 T: estimating the number of subjects required in common designs of clinical trials. Magn Reson Imaging 29, 1382-1389.

Nalls, M.A., Plagnol, V., Hernandez, D.G., Sharma, M., Sheerin, U.M., Saad, M., Simon-Sanchez, J., Schulte, C., Lesage, S., Sveinbjornsdottir, S., Stefansson, K., Martinez, M., Hardy, J., Heutink, P., Brice, A., Gasser, T., Singleton, A.B., Wood, N.W., 2011. Imputation of sequence variants for identification of genetic risks for Parkinson's disease: a meta-analysis of genome-wide association studies. Lancet 377, 641-649.

Nanhoe-Mahabier, W., de Laat, K.F., Visser, J.E., Zijlmans, J., de Leeuw, F.E., Bloem, B.R., 2009. Parkinson disease and comorbid cerebrovascular disease. Nat Rev Neurol 5, 533-541.

Nataraj, A., Rajput, A.H., 2005. Parkinson's disease, stroke, and related epidemiology. Mov Disord 20, 1476-1480.

Nelson, A.R., Sweeney, M.D., Sagare, A.P., Zlokovic, B.V., 2015. Neurovascular dysfunction and neurodegeneration in dementia and Alzheimer's disease. Biochim Biophys Acta.

Nishimura, N., Schaffer, C.B., Friedman, B., Lyden, P.D., Kleinfeld, D., 2007. Penetrating arterioles are a bottleneck in the perfusion of neocortex. Proc Natl Acad Sci U S A 104, 365-370.

Nobili, F., Arnaldi, D., Campus, C., Ferrara, M., De Carli, F., Brugnolo, A., Dessi, B., Girtler, N., Morbelli, S., Abruzzese, G., Sambuceti, G., Rodriguez, G., 2011. Brain perfusion correlates of cognitive and nigrostriatal functions in de novo Parkinson's disease. Eur J Nucl Med Mol Imaging 38, 2209-2218.

Nobili, F., Frisoni, G., Portet, F., Verhey, F., Rodriguez, G., Caroli, A., Touchon, J., Calvini, P., Morbelli, S., Carli, F., Guerra, U., Pol, L., Visser, P.-J., 2008. Brain SPECT in subtypes of mild cognitive impairment. Journal of Neurology 255, 1344-1353.

O'Kane, R.L., Vina, J.R., Simpson, I., Hawkins, R.A., 2004. Na+ -dependent neutral amino acid transporters A, ASC, and N of the blood-brain barrier: mechanisms for neutral amino acid removal. Am J Physiol Endocrinol Metab 287, E622-629.

O'Sullivan, M., 2010. Imaging small vessel disease: lesion topography, networks, and cognitive deficits investigated with MRI. Stroke 41, S154-158.

O'Sullivan, M., Morris, R.G., Markus, H.S., 2005. Brief cognitive assessment for patients with cerebral small vessel disease. J Neurol Neurosurg Psychiatry 76, 1140-1145.

O'Sullivan, M., 2008. Leukoaraiosis. Practical Neurology 8, 26-38.

Ochudlo, S., Opala, G., Jasinska-Myga, B., Siuda, J., Nowak, S., 2003. [Inferior frontal region hypoperfusion in Parkinson disease with dementia]. Neurol Neurochir Pol 37 Suppl 5, 133-144.

Ogawa, S., Lee, T.M., Nayak, A.S., Glynn, P., 1990. Oxygenation-sensitive contrast in magnetic resonance image of rodent brain at high magnetic fields. Magn Reson Med 14, 68-78.

Okonkwo, O.C., Xu, G., Oh, J.M., Dowling, N.M., Carlsson, C.M., Gallagher, C.L., Birdsill, A.C., Palotti, M., Wharton, W., Hermann, B.P., LaRue, A., Bendlin, B.B., Rowley, H.A., Asthana, S., Sager, M.A., Johnson, S.C., 2014. Cerebral blood flow is diminished in asymptomatic middle-aged adults with maternal history of Alzheimer's disease. Cereb Cortex 24, 978-988.

Onyango, I.G., Khan, S.M., Bennett, J.P., Jr., 2017. Mitochondria in the pathophysiology of Alzheimer's and Parkinson's diseases. Front Biosci (Landmark Ed) 22, 854-872.

Ostergaard, L., Aamand, R., Gutierrez-Jimenez, E., Ho, Y.C., Blicher, J.U., Madsen, S.M., Nagenthiraja, K., Dalby, R.B., Drasbek, K.R., Moller, A., Braendgaard, H., Mouridsen, K., Jespersen, S.N., Jensen, M.S., West, M.J., 2013. The capillary dysfunction hypothesis of Alzheimer's disease. Neurobiol Aging 34, 1018-1031.

Ostergaard, L., Engedal, T.S., Moreton, F., Hansen, M.B., Wardlaw, J.M., Dalkara, T., Markus, H.S., Muir, K.W., 2016. Cerebral small vessel disease: Capillary pathways to stroke and cognitive decline. J Cereb Blood Flow Metab 36, 302-325.

Owen, A.M., James, M., Leigh, P.N., Summers, B.A., Marsden, C.D., Quinn, N.P., Lange, K.W., Robbins, T.W., 1992. Fronto-striatal cognitive deficits at different stages of Parkinson's disease. Brain 115 (Pt 6), 1727-1751.

Paling, D., Thade Petersen, E., Tozer, D.J., Altmann, D.R., Wheeler-Kingshott, C.A., Kapoor, R., Miller, D.H., Golay, X., 2013. Cerebral arterial bolus arrival time is prolonged in multiple sclerosis and associated with disability. J Cereb Blood Flow Metab.

Pantoni, L., Garcia, J.H., 1997. Pathogenesis of leukoaraiosis: a review. Stroke 28, 652-659.

Pardridge, W.M., 2005. Molecular biology of the blood-brain barrier. Mol Biotechnol 30, 57-70.

Parkes L.M., B.H., Abernethy L 2012. CBF Quantification in Infants Using Look-Locker ASL and a Single Blood Compartment Model. . Proceedings of the International Society of Magnetic Resonance in Medicine (ISMRM) annual meeting, Melbourne.

Parkes, L.M., Tofts, P.S., 2002. Improved accuracy of human cerebral blood perfusion measurements using arterial spin labeling: accounting for capillary water permeability. Magn Reson Med 48, 27-41.

Patel, A., Toia, G.V., Colletta, K., Bradaric, B.D., Carvey, P.M., Hendey, B., 2011a. An angiogenic inhibitor, cyclic RGDfV, attenuates MPTP-induced dopamine neuron toxicity. Exp Neurol 231, 160-170.

Patel, M., Coutinho, C., Emsley, H.C., 2011b. Prevalence of radiological and clinical cerebrovascular disease in idiopathic Parkinson's disease. Clin Neurol Neurosurg 113, 830-834.

Paula, J.J., Miranda, D.M., Moraes, E.N., Malloy-Diniz, L.F., 2013. Mapping the clockworks: what does the Clock Drawing Test assess in normal and pathological aging? Arq Neuropsiquiatr 71, 763-768.

Perry, G., Nunomura, A., Hirai, K., Takeda, A., Aliev, G., Smith, M.A., 2000. Oxidative damage in Alzheimer's disease: the metabolic dimension. Int J Dev Neurosci 18, 417-421.

Petersen, E.T., Zimine, I., Ho, Y.C., Golay, X., 2006. Non-invasive measurement of perfusion: a critical review of arterial spin labelling techniques. Br J Radiol 79, 688-701.

Piccini, P., Pavese, N., Canapicchi, R., Paoli, C., Del Dotto, P., Puglioli, M., Rossi, G., Bonuccelli, U., 1995. White matter hyperintensities in Parkinson's disease. Clinical correlations. Arch Neurol 52, 191-194.

Pillai, J.J., Zaca, D., 2012. Comparison of BOLD cerebrovascular reactivity mapping and DSC MR perfusion imaging for prediction of neurovascular uncoupling potential in brain tumors. Technol Cancer Res Treat 11, 361-374.

Pisani, V., Stefani, A., Pierantozzi, M., Natoli, S., Stanzione, P., Franciotta, D., Pisani, A., 2012. Increased blood-cerebrospinal fluid transfer of albumin in advanced Parkinson's disease. J Neuroinflammation 9, 188.

Pohmann, R., Scheffler, K., 2013. A theoretical and experimental comparison of different techniques for B(1) mapping at very high fields. NMR Biomed 26, 265-275.

Popescu, B.O., Toescu, E.C., Popescu, L.M., Bajenaru, O., Muresanu, D.F., Schultzberg, M., Bogdanovic, N., 2009. Blood-brain barrier alterations in ageing and dementia. J Neurol Sci 283, 99-106.

Postuma, R.B., Dagher, A., 2006. Basal ganglia functional connectivity based on a meta-analysis of 126 positron emission tomography and functional magnetic resonance imaging publications. Cereb Cortex 16, 1508-1521.

Powers, W.J., Zazulia, A.R., 2010. PET in Cerebrovascular Disease. PET Clin 5, 83106.

Princz-Kranz, F.L., Mueggler, T., Knobloch, M., Nitsch, R.M., Rudin, M., 2010. Vascular response to acetazolamide decreases as a function of age in the arcA beta mouse model of cerebral amyloidosis. Neurobiol Dis 40, 284-292.

Prodoehl, J., Yu, H., Little, D.M., Abraham, I., Vaillancourt, D.E., 2008. Region of interest template for the human basal ganglia: comparing EPI and standardized space approaches. NeuroImage 39, 956-965.

Przedborski, S., Vila, M., Jackson-Lewis, V., 2003. Neurodegeneration: what is it and where are we? J Clin Invest 111, 3-10.

Reid, W.G., Hely, M.A., Morris, J.G., Loy, C., Halliday, G.M., 2011. Dementia in Parkinson's disease: a 20-year neuropsychological study (Sydney Multicentre Study). J Neurol Neurosurg Psychiatry 82, 1033-1037.

Rektor, I., Goldemund, D., Sheardova, K., Rektorova, I., Michalkova, Z., Dufek, M., 2009. Vascular pathology in patients with idiopathic Parkinson's disease. Parkinsonism Relat Disord 15, 24-29.

Richardson, J.D., Baker, J.M., Morgan, P.S., Rorden, C., Bonilha, L., Fridriksson, J., 2011. Cerebral perfusion in chronic stroke: implications for lesion-symptom mapping and functional MRI. Behav Neurol 24, 117-122.

Riess, O., Kruger, R., 1999. Parkinson's disease--a multifactorial neurodegenerative disorder. J Neural Transm Suppl 56, 113-125.

Roberts, D.A., Rizi, R., Lenkinski, R.E., Leigh, J.S., 1996. Magnetic resonance imaging of the Brain:Blood partition coefficient for water: Application to spin-tagging measurement of perfusion. Jmri-Journal of Magnetic Resonance Imaging 6, 363-366.

Rodriguez, G., Nobili, F., De Carli, F., Francione, S., Marenco, S., Celestino, M.A., Hassan, K., Rosadini, G., 1993. Regional cerebral blood flow in chronic stroke patients. Stroke 24, 94-99.

Rost, N.S., Sadaghiani, S., Biffi, A., Fitzpatrick, K.M., Cloonan, L., Rosand, J., Shibata, D.K., Mosley, T.H., Jr., 2014. Setting a gold standard for quantification of leukoaraiosis burden in patients with ischemic stroke: the Atherosclerosis Risk in Communities Study. J Neurosci Methods 221, 196-201.

Sagare, A.P., Bell, R.D., Zhao, Z., Ma, Q., Winkler, E.A., Ramanathan, A., Zlokovic, B.V., 2013a. Pericyte loss influences Alzheimer-like neurodegeneration in mice. Nat Commun 4, 2932.

Sagare, A.P., Bell, R.D., Zlokovic, B.V., 2012. Neurovascular dysfunction and faulty amyloid beta-peptide clearance in Alzheimer disease. Cold Spring Harb Perspect Med 2.

Sagare, A.P., Bell, R.D., Zlokovic, B.V., 2013b. Neurovascular defects and faulty amyloid-beta vascular clearance in Alzheimer's disease. J Alzheimers Dis 33 Suppl 1, S87-100.

Sandhu, J.K., Gardaneh, M., Iwasiow, R., Lanthier, P., Gangaraju, S., Ribecco-Lutkiewicz, M., Tremblay, R., Kiuchi, K., Sikorska, M., 2009. Astrocyte-secreted GDNF and glutathione antioxidant system protect neurons against 6OHDA cytotoxicity. Neurobiol Dis 33, 405-414.

Sarkar, S., Raymick, J., Mann, D., Bowyer, J.F., Hanig, J.P., Schmued, L.C., Paule, M.G., Chigurupati, S., 2014. Neurovascular changes in acute, sub-acute and chronic mouse models of Parkinson's disease. Curr Neurovasc Res 11, 48-61.

Savitt, J.M., Dawson, V.L., Dawson, T.M., 2006. Diagnosis and treatment of Parkinson disease: molecules to medicine. J Clin Invest 116, 1744-1754.

Sawada, H., Hishida, R., Hirata, Y., Ono, K., Suzuki, H., Muramatsu, S., Nakano, I., Nagatsu, T., Sawada, M., 2007. Activated microglia affect the nigro-striatal dopamine neurons differently in neonatal and aged mice treated with 1-methyl-4-phenyl-1,2,3,6-tetrahydropyridine. J Neurosci Res 85, 1752-1761.

Schmidt, P., Gaser, C., Arsic, M., Buck, D., Forschler, A., Berthele, A., Hoshi, M., Ilg, R., Schmid, V.J., Zimmer, C., Hemmer, B., Muhlau, M., 2012a. An automated tool for detection of FLAIR-hyperintense white-matter lesions in Multiple Sclerosis. NeuroImage 59, 3774-3783.

Schmidt, R., Berghold, A., Jokinen, H., Gouw, A.A., van der Flier, W.M., Barkhof, F., Scheltens, P., Petrovic, K., Madureira, S., Verdelho, A., Ferro, J.M., Waldemar, G., Wallin, A., Wahlund, L.O., Poggesi, A., Pantoni, L., Inzitari, D., Fazekas, F., Erkinjuntti, T., 2012b. White matter lesion progression in LADIS: frequency, clinical effects, and sample size calculations. Stroke 43, 2643-2647.

Schuff, N., 2009. Potential role of high-field MRI for studies in Parkinson's disease. Mov Disord 24 Suppl 2, S684-690.

Schulz, K.F., Grimes, D.A., Case-control studies: research in reverse. The Lancet 359, 431-434.

Schulz, K.F., Grimes, D.A., 2002. Case-control studies: research in reverse. Lancet 359, 431-434.

Schwartz, R.S., Halliday, G.M., Cordato, D.J., Kril, J.J., 2012. Small-vessel disease in patients with Parkinson's disease: a clinicopathological study. Mov Disord 27, 1506-1512.

Scigliano, G., Ronchetti, G., Girotti, F., Musicco, M., 2008. Levodopa reduces risk factors for vascular disease in parkinsonian patients. Journal of Neurology 255, 1266-1267.

Scigliano, G., Ronchetti, G., Girotti, F., Musicco, M., 2009. Sympathetic modulation by levodopa reduces vascular risk factors in Parkinson disease. Parkinsonism Relat Disord 15, 138-143.

Shah, K., Desilva, S., Abbruscato, T., 2012. The role of glucose transporters in brain disease: diabetes and Alzheimer's Disease. Int J Mol Sci 13, 12629-12655.

Shimizu, H., Watanabe, E., Hiyama, T.Y., Nagakura, A., Fujikawa, A., Okado, H., Yanagawa, Y., Obata, K., Noda, M., 2007. Glial Nax channels control lactate signaling to neurons for brain [Na+] sensing. Neuron 54, 59-72.

Sockeel, P., Dujardin, K., Devos, D., Deneve, C., Destee, A., Defebvre, L., 2006. The Lille apathy rating scale (LARS), a new instrument for detecting and quantifying apathy: validation in Parkinson's disease. J Neurol Neurosurg Psychiatry 77, 579-584.

Sohn, Y.H., Kim, J.S., 1998. The influence of white matter hyperintensities on the clinical features of Parkinson's disease. Yonsei Med J 39, 50-55.

Stanimirovic, D.B., Friedman, A., 2012. Pathophysiology of the neurovascular unit: disease cause or consequence? J Cereb Blood Flow Metab 32, 1207-1221.

Starr, J.M., Farrall, A.J., Armitage, P., McGurn, B., Wardlaw, J., 2009. Blood-brain barrier permeability in Alzheimer's disease: a case-control MRI study. Psychiatry Res 171, 232-241.

Starr, J.M., Wardlaw, J., Ferguson, K., MacLullich, A., Deary, I.J., Marshall, I., 2003. Increased blood-brain barrier permeability in type II diabetes demonstrated by gadolinium magnetic resonance imaging. J Neurol Neurosurg Psychiatry 74, 70-76.

Stebbins, G.T., Goetz, C.G., Burn, D.J., Jankovic, J., Khoo, T.K., Tilley, B.C., 2013. How to identify tremor dominant and postural instability/gait difficulty groups with the movement disorder society unified Parkinson's disease rating scale: comparison with the unified Parkinson's disease rating scale. Mov Disord 28, 668-670.

Stevenson, S.F., Doubal, F.N., Shuler, K., Wardlaw, J.M., 2010. A systematic review of dynamic cerebral and peripheral endothelial function in lacunar stroke versus controls. Stroke 41, e434-442.

Stolp, H.B., Dziegielewska, K.M., 2009. Review: Role of developmental inflammation and blood-brain barrier dysfunction in neurodevelopmental and neurodegenerative diseases. Neuropathol Appl Neurobiol 35, 132-146.

Storkebaum, E., Quaegebeur, A., Vikkula, M., Carmeliet, P., 2011. Cerebrovascular disorders: molecular insights and therapeutic opportunities. Nat Neurosci 14, 1390-1397.

Struck, L.K., Rodnitzky, R.L., Dobson, J.K., 1990. Stroke and its modification in Parkinson's disease. Stroke 21, 1395-1399.

Sulzer, D., 2007. Multiple hit hypotheses for dopamine neuron loss in Parkinson's disease. Trends Neurosci 30, 244-250.

Szewczyk-Krolikowski, K., Tomlinson, P., Nithi, K., Wade-Martins, R., Talbot, K., Ben-Shlomo, Y., Hu, M.T., 2014. The influence of age and gender on motor and non-motor features of early Parkinson's disease: initial findings from the Oxford Parkinson Disease Center (OPDC) discovery cohort. Parkinsonism Relat Disord 20, 99-105.

Taheri, S., Gasparovic, C., Huisa, B.N., Adair, J.C., Edmonds, E., Prestopnik, J., Grossetete, M., Shah, N.J., Wills, J., Qualls, C., Rosenberg, G.A., 2011. Blood-brain barrier permeability abnormalities in vascular cognitive impairment. Stroke 42, 2158-2163.

Tang, C.C., Poston, K.L., Dhawan, V., Eidelberg, D., 2010. Abnormalities in metabolic network activity precede the onset of motor symptoms in Parkinson's disease. J Neurosci 30, 1049-1056.

Tansey, M.G., Goldberg, M.S., 2010. Neuroinflammation in Parkinson's disease: its role in neuronal death and implications for therapeutic intervention. Neurobiol Dis 37, 510-518.

Teune, L.K., Renken, R.J., de Jong, B.M., Willemsen, A.T., van Osch, M.J., Roerdink, J.B., Dierckx, R.A., Leenders, K.L., 2014. Parkinson's disease-related perfusion and glucose metabolic brain patterns identified with PCASL-MRI and FDG-PET imaging. Neuroimage Clin 5, 240-244.

Thenganatt, M.A., Jankovic, J., 2014. Parkinson disease subtypes. JAMA Neurol 71, 499-504.

Todorova, A., Jenner, P., Ray Chaudhuri, K., 2014. Non-motor Parkinson's: integral to motor Parkinson's, yet often neglected. Practical Neurology 14, 310-322.

Tomlinson, C.L., Stowe, R., Patel, S., Rick, C., Gray, R., Clarke, C.E., 2010. Systematic review of levodopa dose equivalency reporting in Parkinson's disease. Mov Disord 25, 2649-2653.

Tzourio-Mazoyer, N., Landeau, B., Papathanassiou, D., Crivello, F., Etard, O., Delcroix, N., Mazoyer, B., Joliot, M., 2002. Automated anatomical labeling of activations in SPM using a macroscopic anatomical parcellation of the MNI MRI single-subject brain. NeuroImage 15, 273-289.

Ursino, M., 1991. Mechanisms of cerebral blood flow regulation. Crit Rev Biomed Eng 18, 255-288.

Van Den Eeden, S.K., Tanner, C.M., Bernstein, A.L., Fross, R.D., Leimpeter, A., Bloch, D.A., Nelson, L.M., 2003. Incidence of Parkinson's disease: variation by age, gender, and race/ethnicity. Am J Epidemiol 157, 1015-1022.

van Rooden, S.M., Colas, F., Martinez-Martin, P., Visser, M., Verbaan, D., Marinus, J., Chaudhuri, R.K., Kok, J.N., van Hilten, J.J., 2011. Clinical subtypes of Parkinson's disease. Mov Disord 26, 51-58.

Vidyasagar, R., Greyling, A., Draijer, R., Corfield, D.R., Parkes, L.M., 2013. The effect of black tea and caffeine on regional cerebral blood flow measured with arterial spin labeling. J Cereb Blood Flow Metab 33, 963-968.

Visser, M., Marinus, J., Stiggelbout, A.M., Van Hilten, J.J., 2004. Assessment of autonomic dysfunction in Parkinson's disease: the SCOPA-AUT. Mov Disord 19, 1306-1312.

Vitosevic, Z., Cetkovic, M., Vitosevic, B., Jovic, D., Rajkovic, N., Millisavljevic, M., 2005. [Blood supply of the internal capsule and basal nuclei]. Srp Arh Celok Lek 133, 41-45.

Volpicelli-Daley, L.A., Luk, K.C., Patel, T.P., Tanik, S.A., Riddle, D.M., Stieber, A., Meaney, D.F., Trojanowski, J.Q., Lee, V.M., 2011. Exogenous alpha-synuclein fibrils induce Lewy body pathology leading to synaptic dysfunction and neuron death. Neuron 72, 57-71.

Wada, K., Arai, H., Takanashi, M., Fukae, J., Oizumi, H., Yasuda, T., Mizuno, Y., Mochizuki, H., 2006. Expression levels of vascular endothelial growth factor and its receptors in Parkinson's disease. Neuroreport 17, 705-709.

Wahlund, L.O., Barkhof, F., Fazekas, F., Bronge, L., Augustin, M., Sjogren, M., Wallin, A., Ader, H., Leys, D., Pantoni, L., Pasquier, F., Erkinjuntti, T., Scheltens, P., 2001. A new rating scale for age-related white matter changes applicable to MRI and CT. Stroke 32, 1318-1322.

Wang, J., Alsop, D.C., Song, H.K., Maldjian, J.A., Tang, K., Salvucci, A.E., Detre, J.A., 2003. Arterial transit time imaging with flow encoding arterial spin tagging (FEAST). Magn Reson Med 50, 599-607.

Wardlaw, J.M., 2010. Blood-brain barrier and cerebral small vessel disease. J Neurol Sci 299, 66-71.

Wardlaw, J.M., Doubal, F., Armitage, P., Chappell, F., Carpenter, T., Munoz Maniega, S., Farrall, A., Sudlow, C., Dennis, M., Dhillon, B., 2009. Lacunar stroke is associated with diffuse blood-brain barrier dysfunction. Ann Neurol 65, 194-202.

Wardlaw, J.M., Doubal, F.N., Valdes-Hernandez, M., Wang, X., Chappell, F.M., Shuler, K., Armitage, P.A., Carpenter, T.C., Dennis, M.S., 2013a. Blood-brain barrier permeability and long-term clinical and imaging outcomes in cerebral small vessel disease. Stroke 44, 525-527.

Wardlaw, J.M., Farrall, A., Armitage, P.A., Carpenter, T., Chappell, F., Doubal, F., Chowdhury, D., Cvoro, V., Dennis, M.S., 2008. Changes in background blood-brain barrier integrity between lacunar and cortical ischemic stroke subtypes. Stroke 39, 1327-1332.

Wardlaw, J.M., Smith, C., Dichgans, M., 2013b. Mechanisms of sporadic cerebral small vessel disease: insights from neuroimaging. Lancet Neurol 12, 483-497.

Wardlaw, J.M., Smith, E.E., Biessels, G.J., Cordonnier, C., Fazekas, F., Frayne, R., Lindley, R.I., O'Brien, J.T., Barkhof, F., Benavente, O.R., Black, S.E., Brayne, C., Breteler, M., Chabriat, H., Decarli, C., de Leeuw, F.E., Doubal, F., Duering, M., Fox, N.C., Greenberg, S., Hachinski, V., Kilimann, I., Mok, V., Oostenbrugge, R., Pantoni, L., Speck, O., Stephan, B.C., Teipel, S., Viswanathan, A., Werring, D., Chen, C., Smith, C., van Buchem, M., Norrving, B., Gorelick, P.B., Dichgans, M., 2013c. Neuroimaging standards for research into small vessel disease and its contribution to ageing and neurodegeneration. Lancet Neurol 12, 822-838.

Wardlaw, J.M., Valdes Hernandez, M.C., Munoz-Maniega, S., 2015. What are white matter hyperintensities made of? Relevance to vascular cognitive impairment. J Am Heart Assoc 4, 001140.

Weintraub, D., Mamikonyan, E., Papay, K., Shea, J.A., Xie, S.X., Siderowf, A., 2012. Questionnaire for Impulsive-Compulsive Disorders in Parkinson's Disease-Rating Scale. Mov Disord 27, 242-247.

Whiteside, D.M., Kealey, T., Semla, M., Luu, H., Rice, L., Basso, M.R., Roper, B., 2016. Verbal Fluency: Language or Executive Function Measure? Appl Neuropsychol Adult 23, 29-34.

Wierenga, C.E., Hays, C.C., Zlatar, Z.Z., 2014. Cerebral blood flow measured by arterial spin labeling MRI as a preclinical marker of Alzheimer's disease. J Alzheimers Dis 42 Suppl 4, S411-419.

Wijsman, E.M., Daw, E.W., Yu, X., Steinbart, E.J., Nochlin, D., Bird, T.D., Schellenberg, G.D., 2005. APOE and other loci affect age-at-onset in Alzheimer's disease families with PS2 mutation. Am J Med Genet B Neuropsychiatr Genet 132B, 14-20.

Williams-Gray, C.H., Evans, J.R., Goris, A., Foltynie, T., Ban, M., Robbins, T.W., Brayne, C., Kolachana, B.S., Weinberger, D.R., Sawcer, S.J., Barker, R.A., 2009. The distinct cognitive syndromes of Parkinson's disease: 5 year follow-up of the CamPaIGN cohort. Brain 132, 2958-2969.

Williams-Gray, C.H., Mason, S.L., Evans, J.R., Foltynie, T., Brayne, C., Robbins, T.W., Barker, R.A., 2013. The CamPaIGN study of Parkinson's disease: 10-year outlook in an incident population-based cohort. J Neurol Neurosurg Psychiatry 84, 1258-1264.

Williams, A., 2002. Defining neurodegenerative diseases. BMJ 324, 1465-1466.

Winkler, E.A., Bell, R.D., Zlokovic, B.V., 2011. Central nervous system pericytes in health and disease. Nat Neurosci 14, 1398-1405.

Winkler, E.A., Sagare, A.P., Zlokovic, B.V., 2014. The pericyte: a forgotten cell type with important implications for Alzheimer's disease? Brain Pathol 24, 371-386.

Wolf, M.E., Layer, V., Gregori, J., Griebe, M., Szabo, K., Gass, A., Hennerici, M.G., Matthias, G., Rolf, K., 2014. Assessment of perfusion deficits in ischemic stroke using 3D-GRASE arterial spin labeling magnetic resonance imaging with multiple inflow times. J Neuroimaging 24, 453-459.

Wolf, R.L., Alsop, D.C., McGarvey, M.L., Maldjian, J.A., Wang, J., Detre, J.A., 2003. Susceptibility contrast and arterial spin labeled perfusion MRI in cerebrovascular disease. J Neuroimaging 13, 17-27.

Wolf, R.L., Detre, J.A., 2007. Clinical neuroimaging using arterial spin-labeled perfusion magnetic resonance imaging. Neurotherapeutics 4, 346-359.

Wolk, D.A., Detre, J.A., 2012. Arterial spin labeling MRI: an emerging biomarker for Alzheimer's disease and other neurodegenerative conditions. Curr Opin Neurol 25, 421-428.

Wu, Y., Guo, X.Y., Wei, Q.Q., Ou, R.W., Song, W., Cao, B., Zhao, B., Shang, H.F., 2016. Non-motor symptoms and quality of life in tremor dominant vs postural instability gait disorder Parkinson's disease patients. Acta Neurol Scand 133, 330-337.

Yamagata, K., Tagami, M., Takenaga, F., Yamori, Y., Itoh, S., 2004. Hypoxia-induced changes in tight junction permeability of brain capillary endothelial cells are associated with IL-1beta and nitric oxide. Neurobiol Dis 17, 491-499.

Yang, P., Pavlovic, D., Waldvogel, H., Dragunow, M., Synek, B., Turner, C., Faull, R., Guan, J., 2015. String Vessel Formation is Increased in the Brain of Parkinson Disease. J Parkinsons Dis 5, 821-836.

Yang, Y., Engelien, W., Xu, S., Gu, H., Silbersweig, D.A., Stern, E., 2000. Transit time, trailing time, and cerebral blood flow during brain activation: measurement using multislice, pulsed spin-labeling perfusion imaging. Magn Reson Med 44, 680-685.

Yasuda, T., Fukuda-Tani, M., Nihira, T., Wada, K., Hattori, N., Mizuno, Y., Mochizuki, H., 2007. Correlation between levels of pigment epithelium-derived factor and vascular endothelial growth factor in the striatum of patients with Parkinson's disease. Exp Neurol 206, 308-317.

Yezhuvath, U.S., Lewis-Amezcua, K., Varghese, R., Xiao, G., Lu, H., 2009. On the assessment of cerebrovascular reactivity using hypercapnia BOLD MRI. NMR Biomed 22, 779-786.

Yoon, H.J., Park, K.W., Jeong, Y.J., Kang, D.Y., 2012. Correlation between neuropsychological tests and hypoperfusion in MCI patients: anatomical labeling using xjView and Talairach Daemon software. Ann Nucl Med 26, 656-664.

Zaharchuk, G., 2011. Arterial spin label imaging of acute ischemic stroke and transient ischemic attack. Neuroimaging Clin N Am 21, 285-301, x.

Zaharchuk, G., 2014. Arterial spin-labeled perfusion imaging in acute ischemic stroke. Stroke 45, 1202-1207.

Zappe, A.C., Reichold, J., Burger, C., Weber, B., Buck, A., Pfeuffer, J., Logothetis, N.K., 2007. Quantification of cerebral blood flow in nonhuman primates using arterial spin labeling and a two-compartment model. Magn Reson Imaging 25, 775-783.

Zhao, C., Ling, Z., Newman, M.B., Bhatia, A., Carvey, P.M., 2007. TNF-alpha knockout and minocycline treatment attenuates blood-brain barrier leakage in MPTP-treated mice. Neurobiol Dis 26, 36-46.

Zhao, Z., Nelson, A.R., Betsholtz, C., Zlokovic, B.V., 2015. Establishment and Dysfunction of the Blood-Brain Barrier. Cell 163, 1064-1078.

Zlokovic, B.V., 2005. Neurovascular mechanisms of Alzheimer's neurodegeneration. Trends Neurosci 28, 202-208.

Zlokovic, B.V., 2008. The blood-brain barrier in health and chronic neurodegenerative disorders. Neuron 57, 178-201.

Zlokovic, B.V., 2011. Neurovascular pathways to neurodegeneration in Alzheimer's disease and other disorders. Nat Rev Neurosci 12, 723-738.